doi : 10.17596/0002683

MR18-04 Leg.1

(19 Jul : Shimizu - 10 Aug 2018: Chuuk)

Preliminary Cruise Report

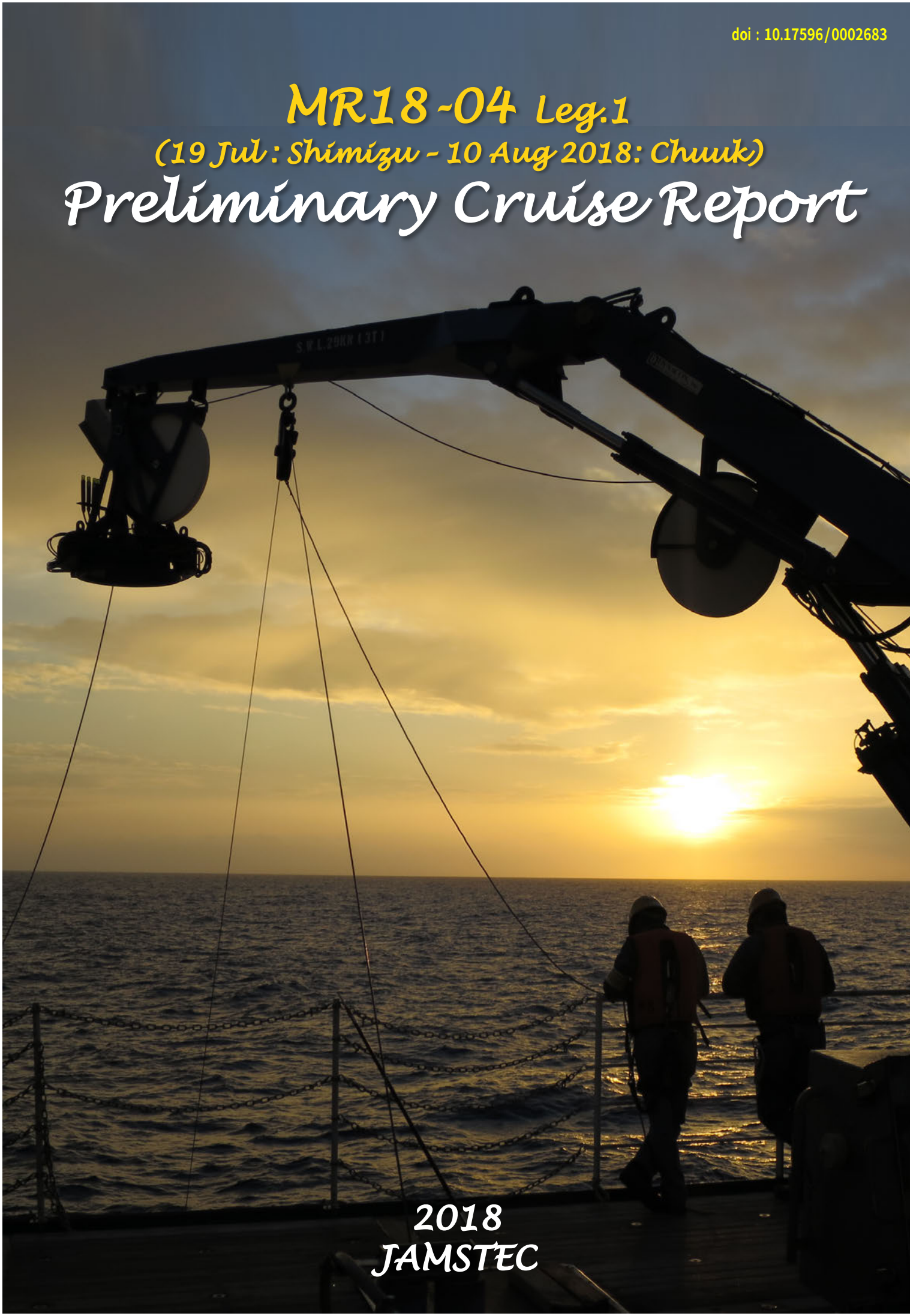

2018

JAMSTEC

Note

This cruise report is a preliminary documentation as of the end of cruise. This report is not necessarily corrected even if there is any inaccurate description. This report is subject to be revised without notice. Some data on this report may be raw or unprocessed. If you are going to use or refer the data on this report, it is recommended to ask the Chief Scientist for latest status. Users of information on this report are requested to submit Publication Report to JAMSTEC.

Acknowledgments

We are grateful to the captain and crew of the R/V MIRAI for their support during the cruise.

Chief Scientist of MR18-04 Leg. 1

Tetsuichi Fujiki
JAMSTEC

Contents of MR18-04 Leg. 1 Preliminary Cruise Report

1. Outline of MR18-04 Leg. 1

1.1 Cruise information

Cruise ID: MR18-04 Leg.1

Research vessel: MIRAI

Cruise title: The observational study to construct and to extend the "western Pacific super site network

Cruise period (port call):

19 July (Shimizu, Shizuoka, Japan) – 10 August 2018 (Chuuk, FSM)

Research area: The western North Pacific

Ship Captain: Toshihisa Akutagawa (Nippon Marine Enterprises, Ltd.)

Chief Scientist:

Tetsuichi Fujiki (Research and Development Center for Global Change, JAMSTEC)

Deputy Chief Scientist:

Fumikazu Taketani (Research and Development Center for Global Change, JAMSTEC)

Representative of the Science Party:

Masaki Katsumata (Research and Development Center for Global Change, JAMSTEC)

1.2 Cruise participants

Scientists

Tetsuichi Fujiki	JAMSTEC
Fumikazu Taketani	JAMSTEC
Makio Honda	JAMSTEC
Kazuhiko Matsumoto	JAMSTEC
Katsunori Kimoto	JAMSTEC
Minoru Kitamura	JAMSTEC
Hiroshi Uchida	JAMSTEC
Masahito Shigemitsu	JAMSTEC
Hajime Kimura	JAMSTEC
Masahide Wakita	JAMSTEC
Taichi Yokokawa	JAMSTEC
Akinori Yabuki	JAMSTEC
Takashi Shiratori	JAMSTEC
Yoshiyuki Nakano	JAMSTEC
Kensuke Watari	JAMSTEC
Masahiro Kaku	JAMSTEC
Yoshihisa Mino	Nagoya University

Yoshiyuki Ishitani	University of Tsukuba
Yuki Yazaki	University of Tsukuba
Tatsuki Toda	Soka University
Noriaki Natori	Soka University
Satoshi Tsubone	Interlink Inc.

Research Engineers

Katsunori Sagishima	Marine Works Japan, Ltd.
Shinsuke Toyoda	Marine Works Japan, Ltd.
Rio Kobayashi	Marine Works Japan, Ltd.
Tomokazu Chiba	Marine Works Japan, Ltd.
Shinichiro Yokogawa	Marine Works Japan, Ltd.
Nagisa Fujiki	Marine Works Japan, Ltd.
Atsushi Ono	Marine Works Japan, Ltd.
Haruka Tamada	Marine Works Japan, Ltd.
Tomohide Noguchi	Marine Works Japan, Ltd.
Kenichi Katayama	Marine Works Japan, Ltd.
Hiroki Ushiromura	Marine Works Japan, Ltd.
Keisuke Takeda	Marine Works Japan, Ltd.
Jun Matsuoka	Marine Works Japan, Ltd.
Masanori Enoki	Marine Works Japan, Ltd.
Hiroshi Hoshino	Marine Works Japan, Ltd.
Masahiro Orui	Marine Works Japan, Ltd.
Elena Hayashi	Marine Works Japan, Ltd.
Keitaro Matsumoto	Marine Works Japan, Ltd.
Tomomi Sone	Marine Works Japan, Ltd.
Erii Irie	Marine Works Japan, Ltd.
Yoshiaki Sato	Marine Works Japan, Ltd.
Ryo Oyama	Nippon Marine Enterprises, Ltd.
Masanori Murakami	Nippon Marine Enterprises, Ltd.

1.3 Research brief

1.3(a) Study of "Nutrient Missing Source" in the oligotrophic region

Based on the comparison study of biogeochemistry in the northwestern North Pacific eutrophic subarctic region and oligotrophic subtropical region (K2S1 project), it was clarified that

biological activity in the subtropical region is comparable to or slightly larger than that in the subarctic region. In order to verify the support mechanism of biological activity, that is the mechanism of nutrient supply, time-series sediment trap experiment was initiated in 2014 at about 4900 m of the station KEO. This station is the time-series station maintained by National Ocean and Atmosphere Administration (NOAA) Pacific Marine Environmental Laboratory (PMEL). Surface buoy with meteorological sensors and physical oceanographic sensors have been deployed at station KEO since 2004. Therefore, these time-series data of meteorology and physical oceanography can be utilized to interpret time-series variability in sediment trap data. Owing to simultaneous analysis of time-series data obtained by NOAA surface buoy and JAMSTEC sediment trap between 2014 and 2016, it was verified that mesoscale cyclonic eddy potentially plays a role in nutrient supplier. In order to evaluate other potential mechanisms such as typhoon and aeolian dust input, sediment trap experiment has been continued at station KEO. During this cruise, KEO sediment trap was recovered and re-deployed. Time-series sediment trap sample since middle November 2017 was successfully collected. Preliminary result showed that total mass flux peaked in April 2018 and its seasonal variability is typical at station KEO.

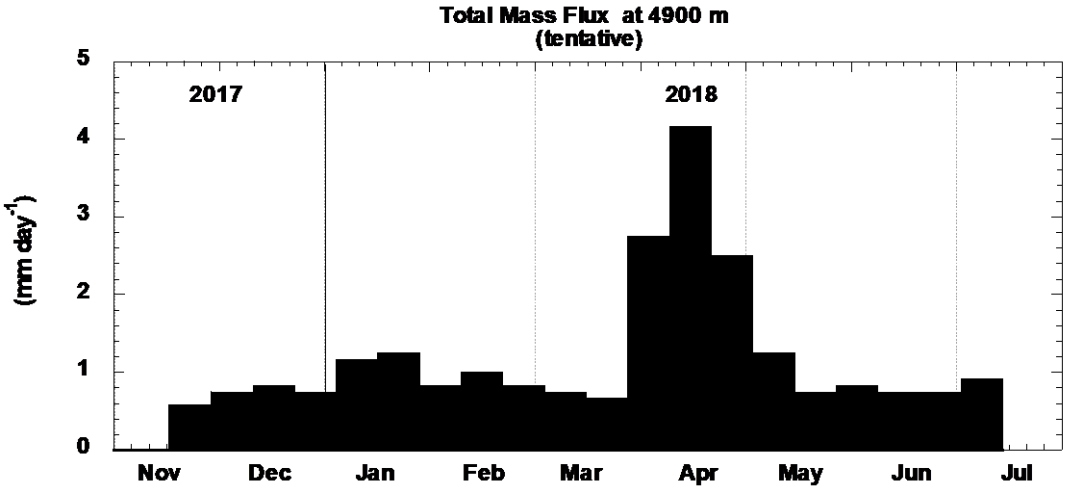

Figure 1.3.1. Seasonal variability in quantitative total mass flux (height day^{-1}) during November 2017 and July 2018.

1.3(b) Time-series observations for marine ecosystem dynamics research in the subarctic western North Pacific

The subarctic western North Pacific is a cyclonic upwelling gyre (western subarctic gyre; WSG) that extends from the northeast of Japan to near the international dateline. To investigate the

spatial and temporal variability of biogeochemical processes in the WSG, time-series observations have been carried out since 1997 at stations KNOT (44°N, 155°E) and /or K2 (47°N, 160°E) in the WSG, indicating that ocean acidification was rapidly progressing in this gyre. However, the effect of ocean acidification on lower trophic levels in this region is not well understood. To better understand the response of lower trophic level ecosystem to multiple environmental stressors (e.g., warming, acidification and deoxygenation), we conducted the following observations and operations at stations K2 and S1-6 during this cruise

(1) Recovery and deployment of hybrid profiling buoy system
(2) CTD cast and water sampling/biochemical analysis
(3) Assessment of phytoplankton productivity by fast repetition rate fluorometry
(4) Zooplankton sampling by using the VMPS, ORI and NORPAC nets
(5) Particle collection by using in situ filtration system
(6) On-deck incubation experiments
(7) Measurements of shortwave and longwave radiation
(8) Upper ocean current measurements by shipboard ADCP
(9) Sea surface water sampling
(10) Deployment of profiling floats
(11) Multi observation glider observation
(12) Gas and particles observation at the marine atmosphere

1.4 Cruise track and log

Cruise track:

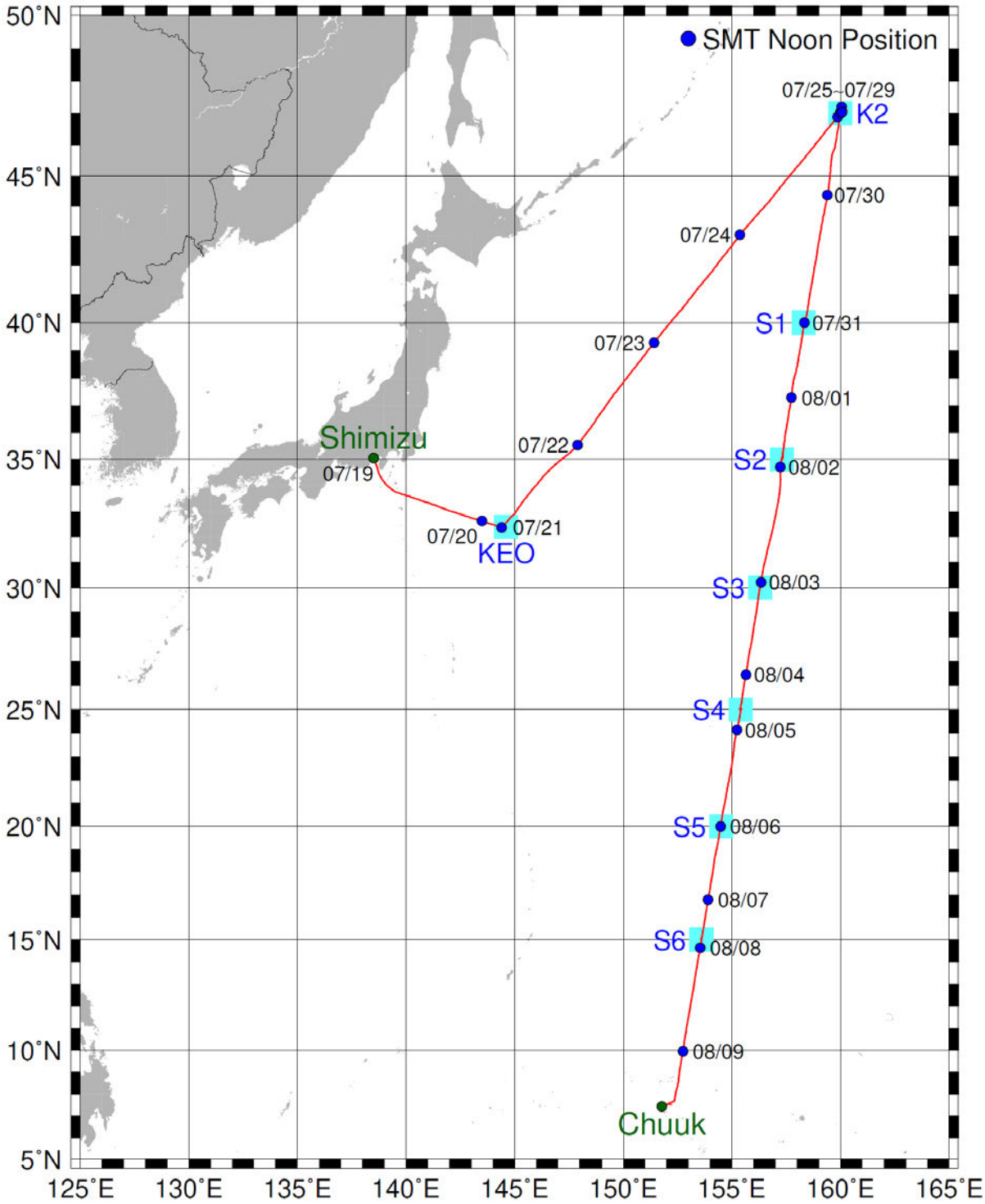

Cruise log:

U.T.C.		S.M.T.		Position		Event logs
Date	Time	Date	Time	Lat.	Lon.	
7.19	4:40	7.19	13:40	35-02.34N	138-30.59E	Departure from Shimizu
	6:05		15:05	34-52.26N	138-35.77E	Sea water pump start
	6:17		15:17	34-49.37N	138-36.44E	MBES observation start
	7:05		16:05	34-38.99N	138-40.91E	EPCS observation start
	19:00	7.20	4:00	33-14.69N	141-18.79E	Doppler Rader Start
7.20	6:33		15:33	32-22.42N	144-23.47E	XCTD
	6:48		15:48	32-22.16N	144-24.50E	Arrival at KEO
	6:49		15:49	32-22.16N	144-24.51E	CTD cast #01 (150 m)
	8:49		17:49	32-21.82N	144-24.17E	Mooring system recovery
	10:26		19:26	32-21.17N	144-24.35E	CTD cast #02 (5780 m)
	14:57		23:57	32-22.11N	144-24.08E	NORPAC net #01-01 (300 m)
	15:18	7.21	0:18	32-22.14N	144-24.01E	NORPAC net #01-02 (300 m)
	15:42		0:42	32-22.19N	144-23.94E	NORPAC net #01-03 (300 m)
	16:00		1:00	32-22.23N	144-23.98E	Surface water sampling
	16:05		1:05	32-22.27N	144-23.93E	NORPAC net #01-04 (300 m)
	16:27		1:27	32-22.34N	144-23.90E	NORPAC net #01-05 (300 m)
	17:00		2:00	32-22.34N	144-24.31E	CTD cast #03 (300 m)
	18:09		3:09	32-22.37N	144-24.36E	FRRF #01 (200 m)
	18:54		3:54	32-22.27N	144-24.41E	VMPS net #01-01 (500m)
	19:02		4:02	32-22.29N	144-24.44E	Surface water sampling
	19:38		4:38	32-22.34N	144-24.49E	VMPS net #01-02 (200m)
	20:02		5:02	32-22.33N	144-24.55E	VMPS net #01-03 (50m)
	20:30		5:30	32-22.25N	144-24.52E	NORPAC net #02-01 (150 m)
	20:45		5:45	32-22.22N	144-24.50E	NORPAC net #02-02 (150 m)
	20:59		5:59	32-22.14N	144-24.49E	NORPAC net #02-03 (150 m)
	21:13		6:13	32-22.05N	144-24.47E	NORPAC net #02-04 (150 m)
	21:27		6:27	32-21.96N	144-24.44E	NORPAC net #02-05 (150 m)
	22:06		7:06	32-19.93N	144-24.97E	Surface water sampling
	23:12		8:12	32-18.37N	144-25.64E	Mooring system deployment
7.21	1:40		10:40	32-21.84N	144-25.33E	Surface water sampling
	2:20		11:20	32-21.99N	144-24.97E	Mooring calibration (sinker fixed position)
	2:43		11:43	32-21.99N	144-24.57E	CTD cast #04 (150 m)
	3:41		12:41	32-21.99N	144-24.14E	VMPS net #02-01 (75m)
	4:04		13:04	32-22.01N	144-24.10E	VMPS net #02-02 (950m)
	4:26		13:26	32-22.03N	144-24.08E	Surface water sampling
	5:12		14:12	32-21.97N	144-24.04E	VMPS net #02-03 (300m)
	5:54		14:54	32-21.96N	144-24.00E	Departure from KEO
7.23	13:00	7.23	22:00	-	-	Time adjustment +1 hour (SMT=UTC+10h)
7.24	12:00	7.24	22:00	-	-	Time adjustment +1 hour (SMT=UTC+11h)
7.25	1:48	7.25	12:48	46-59.94N	160-00.33E	Arrival at K2
	1:55		12:55	47-00.00N	160-00.42E	CTD cast #05 (5,183 m)
	6:17		17:17	47-01.08N	160-01.94E	MOG deployment#1
	7:11		18:11	47-01.01N	160-02.41E	ARGO float (deep) deployment #1
	7:17		18:17	47-01.01N	160-02.35E	ARGO float (BGC) deployment #1
	7:44		18:44	47-01.06N	160-02.56E	MOG deployment#2
	8:34		19:34	47-00.11N	160-00.14E	NORPAC net #03-01 (150 m)

	8:49		19:49	47-00.24N	160-00.18E	NORPAC net #03-02 (150 m)
	9:03		20:03	47-00.30N	160-00.26E	NORPAC net #03-03 (50 m)
	9:11		20:11	47-00.36N	160-00.29E	NORPAC net #03-04 (50 m)
	9:18		20:18	47-00.42N	160-00.33E	NORPAC net #03-05 (50 m)
	9:26		20:26	47-00.48N	160-00.40E	NORPAC net #03-06 (50 m)
	9:37		20:37	47-00.57N	160-00.44E	NORPAC net #04-01 (600 m)
	21:02	7.26	8:02	47-01.56N	159-59.14E	CTD cast #06 (3,000 m)
	23:24		10:24	47-02.24N	159-59.77E	VMPS net #03-01 (950m)
	23:45		10:45	47-02.34N	159-59.81E	VMPS net #03-02 (300m)
7.26	0:12		11:12	47-02.39N	159-59.65E	VMPS net #03-03 (950m)
	1:16		12:16	47-02.22N	159-59.46E	CTD cast #07-01/02 (250 m)
	4:33		15:33	47-00.73N	159-58.15E	Mooring system recovery
	16:01	7.27	3:01	47-00.48N	160-00.63E	CTD cast #08 (300 m)
	16:59		3:59	47-00.54N	160-00.86E	FRRF #02 (150 m)
	18:27		5:27	47-01.55N	16-00.44E	Surface water sampling
	19:26		6:26	47-00.53N	160-00.03E	Calibration for magnetometer #01
	21:24		8:24	47-00.14N	159-59.82E	Sampling suspension particle #1
	21:36		8:36	47-00.12N	159-59.85E	Surface water sampling
7.27	0:27		11:27	47-00.04N	159-59.85E	Surface water sampling
	3:29		14:29	46-59.79N	160-00.15E	Surface water sampling
	4:02		15:02	46-59.86N	160-00.24E	FRRF #03 (150 m)
	4:40		15:40	46-59.93N	160-00.29E	ORI net #01-01 (800 m)
	5:33		16:33	46-58.98N	160-00.51E	ORI net #01-02 (100 m)
	6:26		17:26	47-00.42N	160-00.41E	Surface water sampling
	7:00		18:00	47-00.29N	159-59.82E	FRRF #04 (150 m)
	7:34		18:34	47-00.53N	159-59.95E	NORPAC net #05-01 (150 m)
	7:46		18:46	47-00.63N	159-59.99E	NORPAC net #05-02 (150 m)
	7:59		18:59	47-00.69N	160-00.04E	NORPAC net #05-03 (150 m)
	8:12		19:12	47-00.76N	160-00.10E	NORPAC net #05-04 (150 m)
	11:01		22:01	47-01.03N	159-59.60E	ORI net #02-01 (800 m)
	11:46		22:46	47-00.35N	159-59.92E	ORI net #02-02 (100 m)
	12:30		23:30	47-00.40N	160-00.14E	Surface water sampling
	15:55	7.28	2:55	47-00.24N	159-59.98E	Sampling suspension particle #2
	22:50		9:50	47-19.79N	160-02.03E	MOG recovery#1
7.28	0:03		11:03	47-18.45N	160-03.92E	MOG recovery#2
	2:17		13:17	47-00.28N	160-00.12E	ORI net #03-01 (800 m)
	3:01		14:01	46-59.97N	159-58.87E	ORI net #03-02 (100 m)
	3:40		14:40	46-59.96N	159-58.87E	CTD cast #09 (500 m)
	5:30		16:30	47-00.32N	159-59.74E	CTD cast #10 (5175 m)
	8:24		19:24	47-00.20N	159-59.93E	Surface water sampling
	21:12	7.29	8:12	47-05.74N	160-13.39E	Mooring system deployment
7.29	3:50		14:50	47-00.46N	159-58.40E	Mooring calibration (sinker fixed position)
	4:17		15:17	47-00.72N	159-58.56E	Mooring system check
	6:20		17:20	47-00.15N	160-00.40E	CTD cast #11 (1200 m)
	8:18		19:18	47-00.59N	160-00.77E	CTD cast #12 (1200 m)
	9:28		20:28	47-00.51N	160-00.52E	VMPS net #04-01 (500m)
	9:57		20:57	47-00.34N	160-00.44E	VMPS net #04-02 (150m)
	10:18		21:18	47-00.27N	160-00.40E	NORPAC net #06-01 (600 m)
	10:57		21:57	47-00.40N	160-00.60E	NORPAC net #06-02 (150 m)
	11:12		22:12	47-00.48N	160-00.67E	Departure from K2

7.30	23:30	7.31	10:30	40-00.50N	158-19.92E	Arrival at S1
	23:45		10:45	40-00.06N	158-19.86E	CTD cast #13 (5446 m)
7.31	4:06		15:06	40-00.40N	158-20.64E	VMPS net #05-01 (1350m)
	5:03		16:03	39-59.98N	158-20.54E	VMPS net #05-02 (800m)
	5:39		16:39	39-59.75N	158-20.41E	VMPS net #05-03 (520m)
	6:13		17:13	39-59.56N	158-20.36E	VMPS net #05-04 (470m)
	7:59		18:59	39-59.99N	158-20.01E	NORPAC net #07-01 (600 m)
	8:38		19:38	40-00.01N	158-20.15E	NORPAC net #07-02 (150 m)
	9:00		20:00	39-59.29N	158-20.12E	Departure from S1
8.1	15:42	8.2	2:42	35-00.25N	157-19.34E	Arrival at S2
	15:44		2:44	35-00.21N	157-19.33E	CTD cast #14 (2000 m)
	17:54		4:54	35-02.17N	157-20.30E	FRRF #05 (150 m)
	18:33		5:33	35-03.08N	157-20.49E	VMPS net #06-01 (1000m)
	19:33		6:33	35-03.83N	157-20.30E	VMPS net #06-02 (690m)
	20:28		7:28	35-04.81N	157-19.94E	VMPS net #06-03 (610m)
	21:18		8:18	35-05.54N	157-19.49E	VMPS net #06-04 (410m)
	22:00		9:00	35-06.27N	157-19.16E	CTD cast #15 (150 m)
	22:18		9:18	25-06.69N	157-19.08E	Departure from S2
8.3	2:06	8.3	13:06	30-00.07N	156-19.75E	Arrival at S3
	2:09		13:09	30-00.01N	156-19.78E	CTD cast #16 (5786 m)
	6:30		17:30	29-59.61N	156-18.78E	VMPS net #07-01 (300m)
	6:55		17:55	29-59.56N	156-18.49E	VMPS net #07-02 (1000m)
	7:55		18:55	29-59.21N	156-17.94E	NORPAC net #08-01 (300 m)
	8:17		19:17	29-59.04N	156-17.74E	NORPAC net #08-02 (150 m)
	8:30		19:30	29-58.94N	156-17.66E	NORPAC net #08-03 (150 m)
	8:43		19:43	29-58.84N	156-17.47E	NORPAC net #08-04 (300 m)
	9:04		20:04	29-58.63N	156-17.22E	NORPAC net #08-05 (300 m)
	9:26		20:26	29-58.43N	156-16.99E	NORPAC net #08-06 (150 m)
	9:42		20:42	29-58.25N	156-16.85E	NORPAC net #08-07 (150 m)
	9:54		20:54	29-58.15N	156-16.72E	Departure from S3
8.4	7:12	8.4	18:12	25-00.48N	155-23.02E	Arrival at S4
	7:21		18:21	25-00.07N	155-22.93E	VMPS net #08-01 (1000m)
	8:14		19:14	24-59.97N	155-22.90E	VMPS net #08-02 (300m)
	8:57		19:57	25-00.11N	155-23.20E	NORPAC net #09-01 (600 m)
	9:36		20:36	25-00.30N	155-23.52E	NORPAC net #09-02 (150 m)
	9:48		20:48	25-00.38N	155-23.71E	NORPAC net #09-03 (150 m)
	10:03		21:03	25-00.45N	155-23.95E	NORPAC net #09-04 (300 m)
	10:16		21:16	25-00.48N	155-24.18E	NORPAC net #09-05 (300 m)
	10:29		21:29	25-00.54N	155-24.42E	NORPAC net #09-06 (150 m)
	10:44		21:44	25-00.62N	155-24.67E	NORPAC net #09-07 (150 m)
	10:58		21:58	25-00.67N	155-24.90E	NORPAC net #09-08 (150 m)
	13:01	8.5	0:01	25-00.00N	155-23.51E	CTD cast #17 (2000 m)
	15:16		2:16	25-00.34N	155-25.25E	FRRF #06 (200 m)
	17:08		4:08	24-59.78N	155-23.67E	Sampling suspension particle #3
	19:43		6:43	24-58.88N	155-24.52E	CTD cast #18 (150 m)
	20:12		7:12	24-57.75N	155-24.54E	Departure from S4
8.5	23:36	8.6	10:36	20-00.52N	154-28.77E	Arrival at S5
	23:44		10:44	20-00.03N	154-28.80E	CTD cast #19 (5851 m)
8.6	4:19		15:19	20-01.90N	154-29.11E	VMPS net #09-01 (1000m)
	5:11		16:11	20-01.92N	154-29.12E	VMPS net #09-02 (300m)

	5:36		16:36	20-01.97N	154-29.09E	VMPS net #09-03 (1000m)
	6:32		17:32	20-02.02N	154-28.96E	VMPS net #09-04 (610m)
	7:14		18:14	20-01.98N	154-28.81E	VMPS net #09-05 (190m)
	7:44		18:44	20-01.95N	154-28.74E	NORPAC net #10-01 (200 m)
	7:59		18:59	20-02.06N	154-28.80E	NORPAC net #10-02 (50 m)
	8:05		19:05	20-02.11N	154-28.82E	NORPAC net #10-03 (50 m)
	8:15		19:15	20-02.17N	154-28.85E	NORPAC net #10-04 (150 m)
	8:28		19:28	20-02.26N	154-28.85E	NORPAC net #10-05 (150 m)
	8:48		19:48	20-01.36N	154-28.64E	Departure from S5
8.7	9:54	8.7	20:54	15-00.16N	153-36.00E	Arrival at S6
	9:57		20:57	15-00.03N	153-36.05E	CTD cast #20 (2000 m)
	12:07		23:07	15-01.08N	153-35.90E	FRRF #07 (200 m)
	12:53		23:53	15-01.26N	153-35.78E	VMPS net #10-01 (1000m)
	13:48	8.8	0:48	15-00.81N	153-35.77E	VMPS net #10-02 (1000m)
	14:27		1:27	15-00.52N	153-35.89E	NORPAC net #11-01 (150 m)
	14:39		1:39	15-00.54N	153-35.89E	NORPAC net #11-02 (150 m)
	14:55		1:55	15-00.60N	153-35.87E	NORPAC net #11-03 (150 m)
	15:08		2:08	15-00.68N	153-35.89E	NORPAC net #11-04 (150 m)
	18:03		5:03	14-59.29N	153-35.75E	Calibration for magnetometer #02
	19:00		6:00	15-00.04N	153-35.98E	CTD cast #21 (500 m)
	22:38		9:38	14-59.92N	153-36.27E	CTD cast #22 (150 m)
	23:06		10:06	14-59.96N	153-36.21E	Departure from S6
8.8	11:00		22:00	-	-	Time adjustment -1 hour (SMT=UTC+10h)
8.9	3:56	8.9	13:56	9-36.94N	152-40.81E	EPCS observation finish
	4:00		14:00	9-36.22N	152-40.70E	Sea water pump finish
	5:00		15:00	9-25.29N	152-39.16E	Doppler Rader finish
	8:15		18:15	8-47.99N	152-33.64E	MBES observation finish
	23:10	8.10	9:10	7-26.66N	151-50.35E	Arrival at Chuuk

2. Ship observations and measurements

2.1 Meteorological observations

2.1(a) Surface meteorological observations

Tetsuichi FUJIKI (JAMSTEC RCGC)
Ryo OYAMA (NME)
Masanori MURAKAMI (NME)
Takehito HATTORI (MIRAI crew)

(1) Objectives

Surface meteorological parameters are observed as a basic dataset of the meteorology. These parameters provide the temporal variation of the meteorological condition surrounding the ship.

(2) Methods

Surface meteorological parameters were observed during this cruise. In this cruise, we used two systems for the observation.

i MIRAI Surface Meteorological observation (SMet) system

Instruments of SMet system are listed in Table 2.1(a).1 and measured parameters are listed in Table 2.1(a).2 Data were collected and processed by KOAC-7800 weather data processor made by Koshin-Denki, Japan. The data set consists of 6 seconds averaged data.

ii Shipboard Oceanographic and Atmospheric Radiation (SOAR) measurement system

SOAR system designed by BNL (Brookhaven National Laboratory, USA) consists of major five parts.

a) Portable Radiation Package (PRP) designed by BNL - short and long wave downward radiation.
b) Analog meteorological data sampling with CR1000 logger manufactured by Campbell Inc. Canada - wind, pressure, and rainfall (by a capacitive rain gauge) measurement.
c) Digital meteorological data sampling from individual sensors - air temperature, relative humidity and rainfall (by optical rain gauge) measurement.
d) Photosynthetically Available Radiation (PAR) sensor manufactured by Biospherical Instruments Inc. (USA) - PAR measurement.
e) Scientific Computer System (SCS) developed by NOAA (National Oceanic and Atmospheric Administration, USA) - centralized data acquisition and logging of all data sets.

SCS recorded PRP data every 6 seconds, CR1000 data every second, air temperature and relative humidity data every 2 seconds and ORG data every 6 seconds. SCS composed Event data (JamMet) from these data and ship's navigation data. Instruments and their locations are listed in Table2.1(a).3 and measured parameters are listed in Table2.1(a).4.

For the quality control as post processing, we checked the following sensors, before and after the

cruise.

i) Young rain gauge (SMet and SOAR)

Inspect of the linearity of output value from the rain gauge sensor to change input value by adding fixed quantity of test water.

ii) Barometer (SMet and SOAR)

Comparison with the portable barometer value, PTB220, VAISALA

iii) Thermometer (air temperature and relative humidity) (SMet and SOAR)

Comparison with the portable thermometer value, HMP75, VAISALA

(3) Preliminary results

Fig.2.1(a).1 shows the time series of the following parameters;

Wind (SOAR)
Air temperature (SMet)
Relative humidity (SMet)
Precipitation (SOAR, ORG)
Short/long wave radiation (SOAR)
Barometric Pressure (SMet)
Sea surface temperature (SMet)
Significant wave height (SMet)

(4) Data archives

All data obtained during this cruise will be submitted to the Data Management Group (DMG) in JAMSTEC, and will be archived there.

(5) Remarks (Times in UTC)

i) The following periods, sea surface temperature of SMet data was available.
06:05 19 Jul. 2018 - 04:00 09 Aug. 2018

Table2.1(a).1. Instruments and installation locations of MIRAI Surface Meteorological observation system.

Sensors	Type	Manufacturer	Location (altitude from surface)
Anemometer	KS-5900	Koshin Denki, Japan	foremast (25 m)
Tair/RH	HMP155	Vaisala, Finland	
with 43408 Gill aspirated radiation shield			
		R.M. Young, USA	compass deck (21 m)
			starboard side and port side
Thermometer: SST	RFN2-0	Koshin Denki, Japan	4th deck (-1m, inlet -5m)
Barometer	Model-370	Setra System, USA	captain deck (13 m)
			weather observation room
Capacitive rain gauge	50202	R. M. Young, USA	compass deck (19 m)
Optical rain gauge	ORG-815DS	Osi, USA	compass deck (19 m)
Radiometer (short wave)		MS-802	Eko Seiki, Japan radar mast (28 m)
Radiometer (long wave)	MS-202	Eko Seiki, Japan	radar mast (28 m)
Wave height meter	WM-2	Tsurumi-seiki, Japan	bow (10 m)

Table2.1(a).2. Parameters of MIRAI Surface Meteorological observation system.

Parameter	Units	Remarks
1 Latitude	degree	
2 Longitude	degree	
3 Ship's log speed	knot	Log, DS-30, Furuno
4 Ship's heading	degree	Gyro,TG-8000,TOKYO-KEIKI
5 Relative wind speed	m/s	6sec. averaged
6 Relative wind direction	degree	6sec. averaged
7 True wind speed	m/s	6sec. averaged
8 True wind direction	degree	6sec. averaged
9 Barometric pressure	hPa	adjusted to sea surface level
		6sec. averaged
10 Air temperature (starboard)	degC	6sec. averaged
11 Air temperature (port side)	degC	6sec. averaged
12 Dewpoint temperature (starboard)	degC	6sec. averaged
13 Dewpoint temperature (port side)	degC	6sec. averaged
14 Relative humidity (starboard)	%	6sec. averaged
15 Relative humidity (port side)	%	6sec. averaged
16 Sea surface temperature	degC	6sec. averaged
17 Rain rate (optical rain gauge)	mm/hr	hourly accumulation
18 Rain rate (capacitive rain gauge)	mm/hr	hourly accumulation
19 Down welling shortwave radiation	W/m^2	6sec. averaged
20 Down welling infra-red radiation	W/m^2	6sec. averaged
21 Significant wave height (bow)	m	hourly
22 Significant wave height (aft)	m	hourly
23 Significant wave period (bow)	second	hourly
24 Significant wave period (aft)	second	hourly

Table2.1(a).3. Instruments and installation locations of SOAR system.

Sensors	Type	Manufacturer	Location (altitude from surface)
Anemometer	05106	R.M. Young, USA	foremast (26 m)
Barometer	PTB210	Vaisala, Finland	
with 61002 Gill pressure port		R.M. Young, USA	foremast (23 m)
Capacitive rain gauge	50202	R.M. Young, USA	foremast (25 m)
Tair/RH	HMP155	Vaisala, Finland	
with 43408 Gill aspirated radiation shield			
		R.M. Young, USA	foremast (23 m)
Optical rain gauge	ORG-815DR	Osi, USA	foremast (25 m)

Sensors (PRP)	Type	Manufacturer	Location (altitude from surface)
Radiometer (short wave)	PSP	Epply Labs, USA	foremast (25 m)
Radiometer (long wave)	PIR	Epply Labs, USA	foremast (25 m)
Fast rotating shadowband radiometer		Yankee, USA	foremast (25 m)

Table2.1(a).4. Parameters of SOAR system (JamMet).

	Parameter	Units	Remarks
1	Latitude	degree	
2	Longitude	degree	
3	SOG	knot	
4	COG	degree	
5	Relative wind speed	m/s	
6	Relative wind direction	degree	
7	Barometric pressure	hPa	
8	Air temperature	degC	
9	Relative humidity	%	
10	Rain rate (optical rain gauge)	mm/hr	
11	Precipitation (capacitive rain gauge)	mm	reset at 50 mm
12	Down welling shortwave radiation	W/m^2	
13	Down welling infra-red radiation	W/m^2	
14	Defuse irradiance	W/m^2	

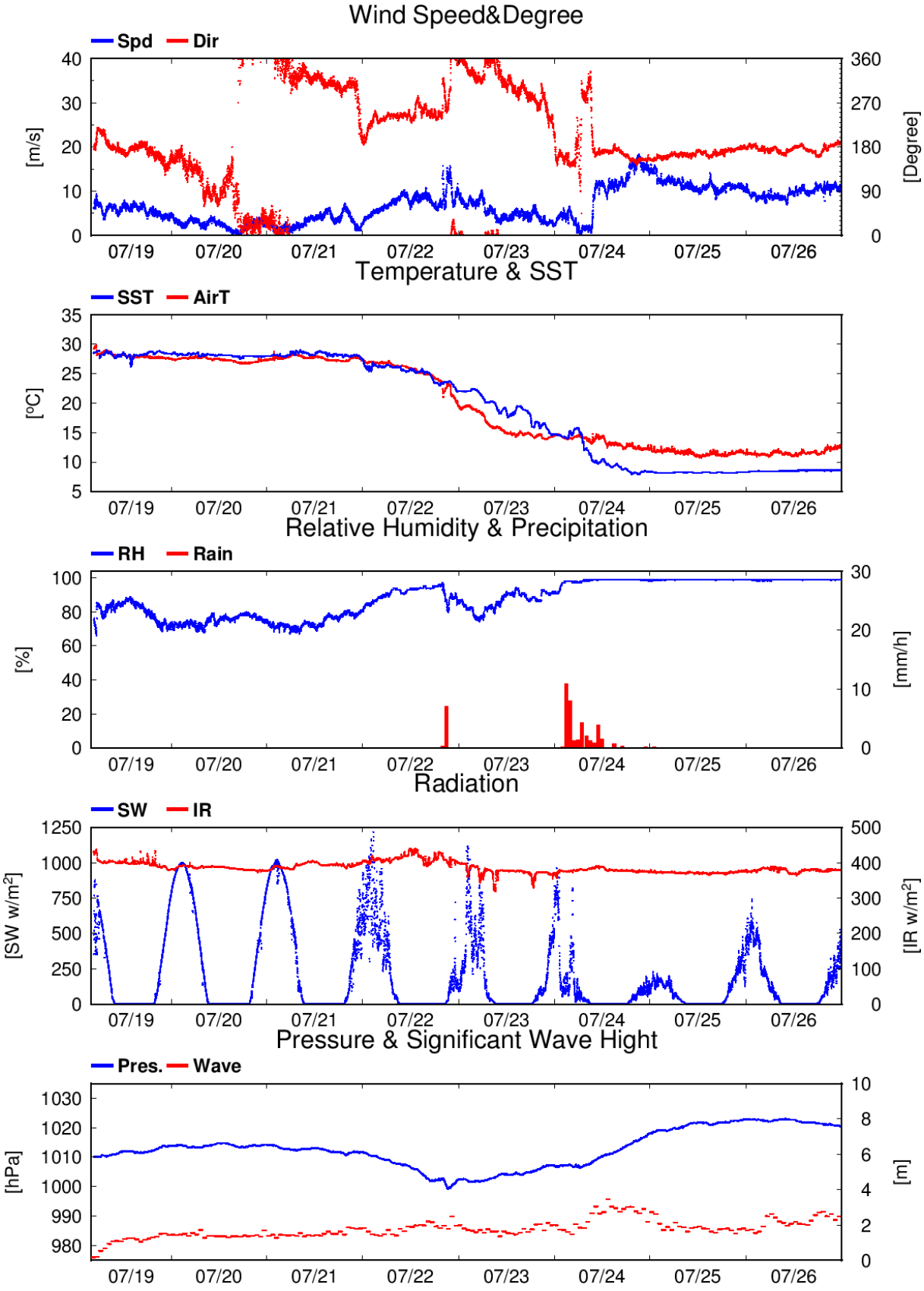

Figure 2.1(a).1. Time series of surface meteorological parameters during the cruise.

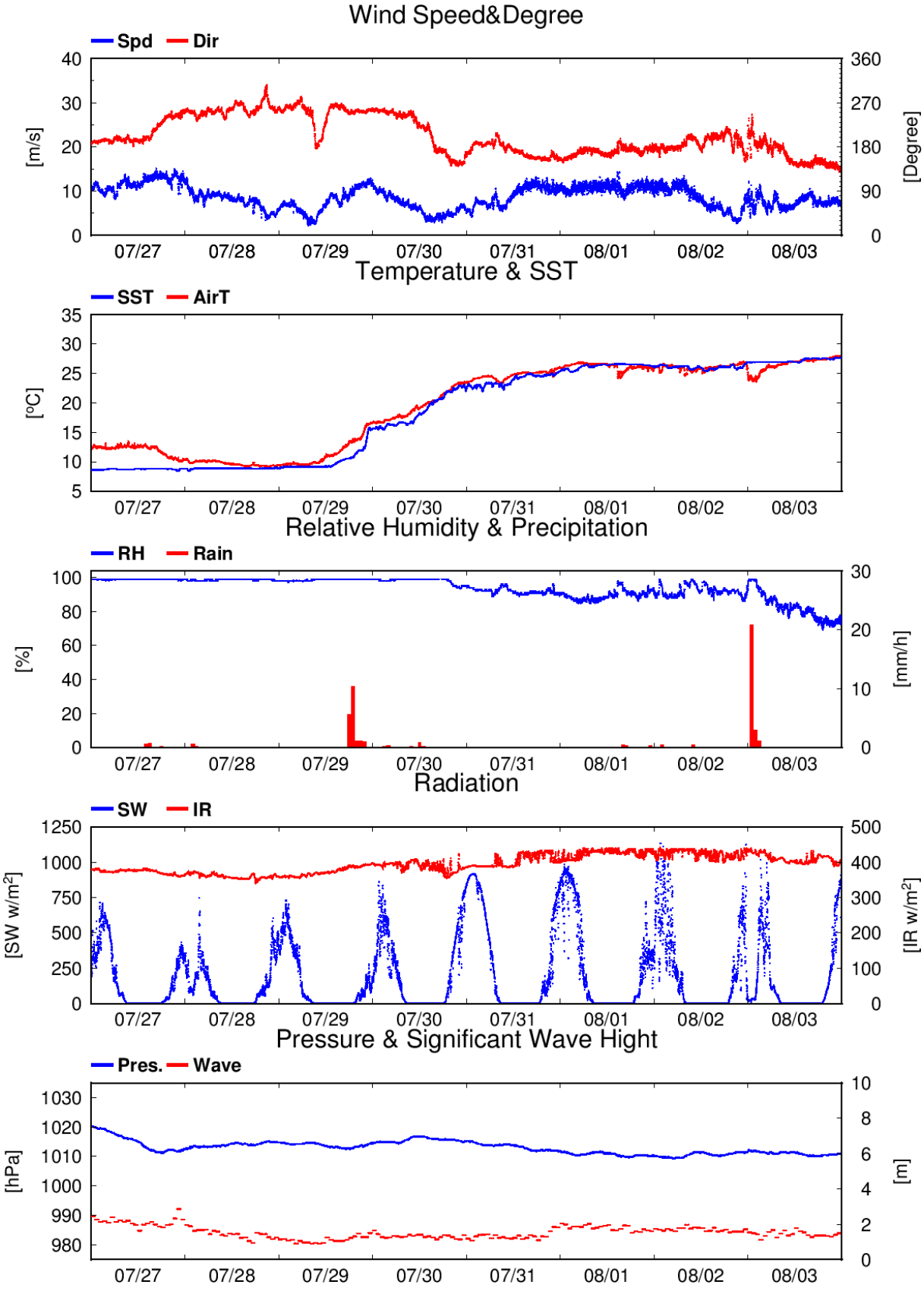

Figure 2.1(a).1. (Continued).

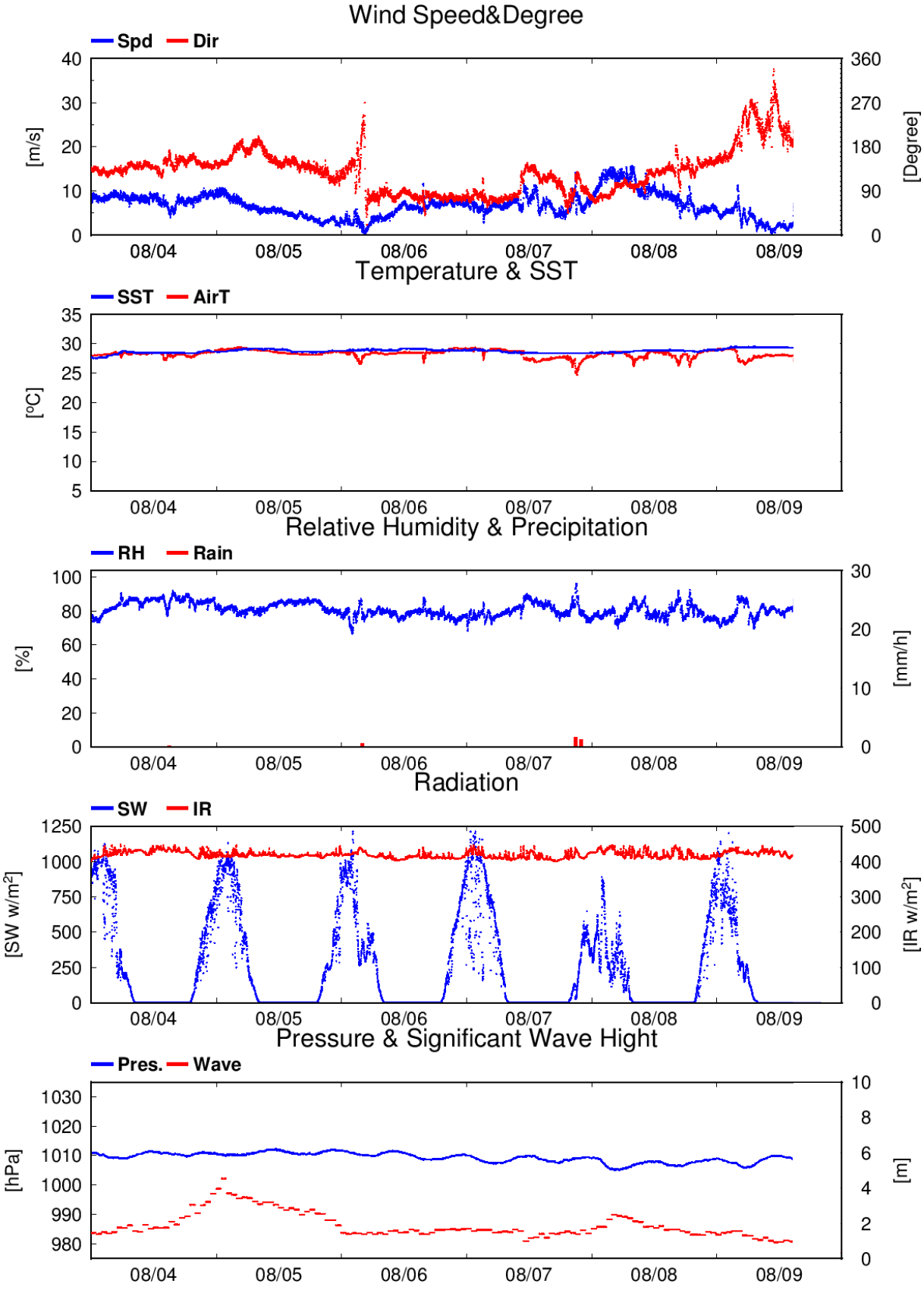

Figure 2.1(a).1. (Continued).

2.1(b) Ceilometer observation

Tetsuichi FUJIKI (JAMSTEC RCGC)
Ryo OYAMA (NME)
Masanori MURAKAMI (NME)
Takehito HATTORI (MIRAI crew)

(1) Objectives

The information of cloud base height and the liquid water amount around cloud base is important to understand the process on formation of the cloud. As one of the methods to measure them, the ceilometer observation was carried out.

(2) Parameters

1. Cloud base height [m].
2. Backscatter profile, sensitivity and range normalized at 10 m resolution.
3. Estimated cloud amount [oktas] and height [m]; Sky Condition Algorithm.

(3) Methods

We measured cloud base height and backscatter profile using ceilometer (CL51, VAISALA, Finland). Major parameters for the measurement configuration are shown in Table2.1(b).1.

Table2.1(b).1. Major parameters.

Laser source:	Indium Gallium Arsenide (InGaAs) Diode
Transmitting center wavelength:	910±10 nm at 25 degC
Transmitting average power:	19.5 mW
Repetition rate:	6.5 kHz
Detector:	Silicon avalanche photodiode (APD)
Responsibility at 905 nm:	65 A/W
Cloud detection range:	0 ~ 13 km
Measurement range:	0 ~ 15 km
Resolution:	10 meter in full range
Sampling rate:	36 sec
Sky Condition:	Cloudiness in octas (0 ~ 9) (0:Sky Clear, 1:Few, 3:Scattered, 5-7:Broken, 8:Overcast, 9:Vertical Visibility)

(4) Preliminary results

Fig. 2.1(b).1 shows the time series plot of the lowest, second and third cloud base height during the cruise.

(5) Data archives

All data obtained during this cruise will be submitted to the Data Management Group (DMG) in JAMSTEC, and will be archived there.

(6) Remarks

1) Window Cleaning

01:52UTC 16 Jul. 2018
00:25UTC 29 Jul. 2018
21:54UTC 06 Aug. 2018

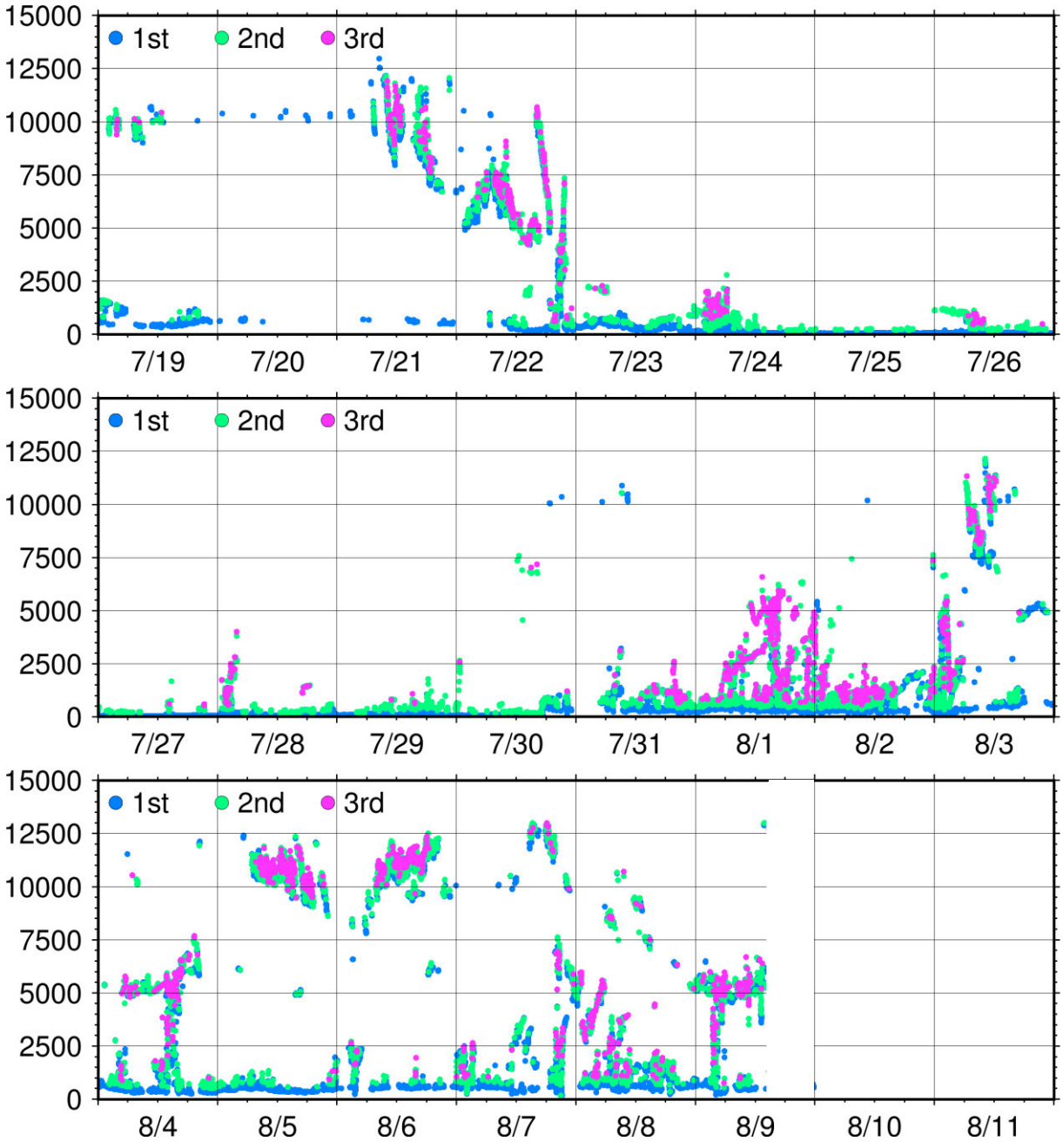

Figure 2.1(b).1. First (Blue), 2nd (Green) and 3rd (Red) lowest cloud base height during the cruise.

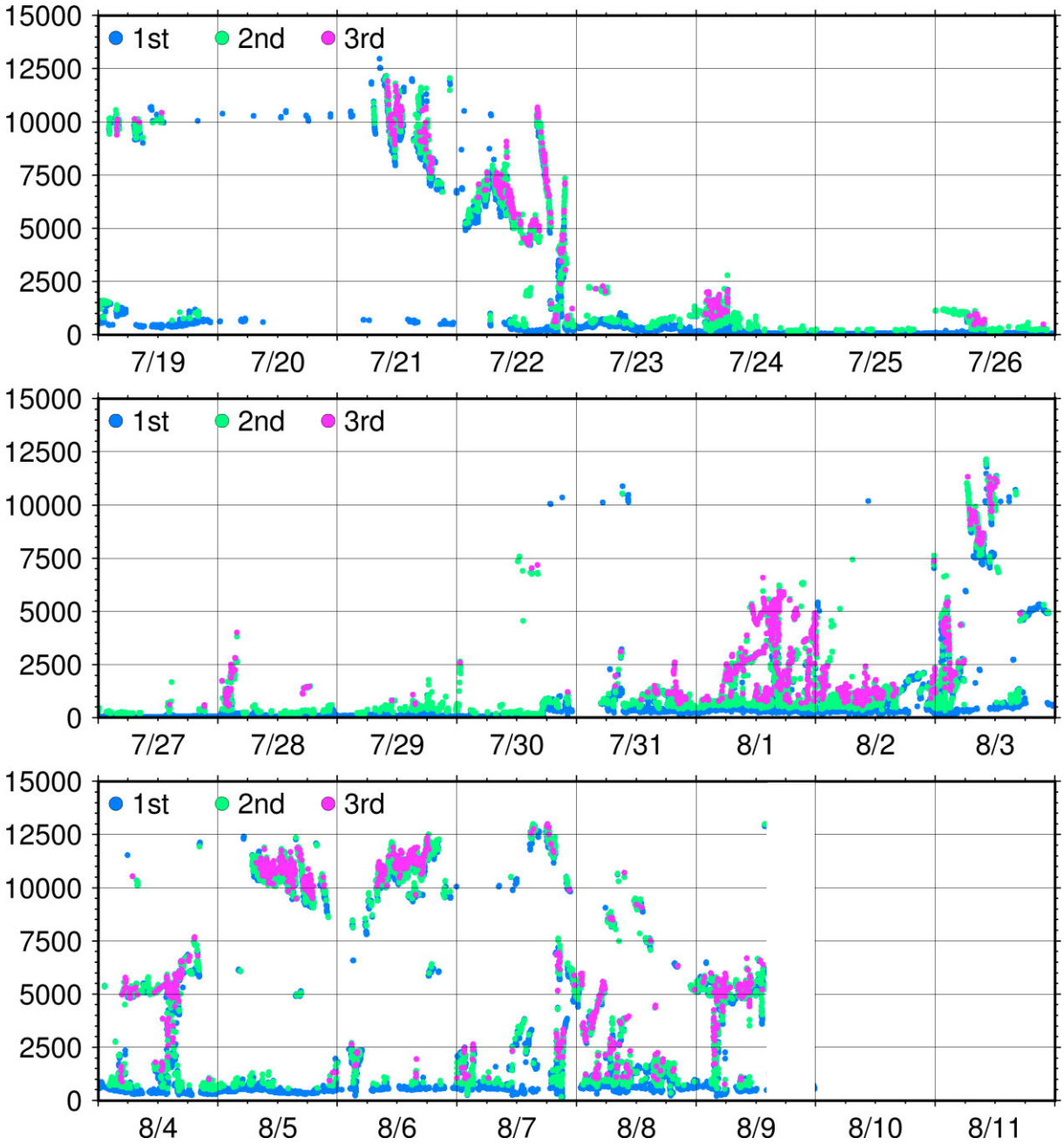

Figure 2.1(b).1. First (Blue), 2nd (Green) and 3rd (Red) lowest cloud base height during the cruise.

2.1(c) Gas and particles observation at the marine atmosphere

Fumikazu TAKETANI (JAMSTEC RCGC)
Yugo KANAYA (JAMSTEC RCGC)
Takuma MIYAKAWA (JAMSTEC RCGC)
Chunmao ZHU (JAMSTEC RCGC)
Takashi SEKIYA (JAMSTEC RCGC)
Kazuma AOKI (Toyama Univ.)

(1) Objectives
• To investigate roles of aerosols in the marine atmosphere in relation to climate change
• To investigate contribution of the rain as a nutrients to the marine ecosystem.

(2) Parameters
• Black carbon(BC)
• Particle size distribution and number concentration
• Composition of ambient particles
• Composition of rain
• Surface ozone(O3), and carbon monoxide(CO) mixing ratios
• Aerosol optical thickness and Single scattering albedo

(3) Instruments and methods
i) Online aerosol observations:

Particle number concentration and size distribution: The number concentration and size distribution of ambient particles was measured by a handheld optical particle counter (OPC) (KR-12A, Rion).

Black carbon (BC): Number and mass BC concentrations were measured by an instrument based on laser-induced incandescence, single particle soot photometer (SP2) (model D, Droplet Measurement Technologies). The laser-induced incandescence technique based on intracavity Nd:YVO_4 laser operating at 1064 nm were used for detection of single particles of BC.

For SP2 instrument, the ambient air was commonly sampled from the compass deck by a 3-m-long conductive tube through the dryer to dry up the particles, and then introduced to each instrument installed at the environmental research room. OPC instrument were installed at the compass deck. The ambient air was directly introduced to the instruments.

ii) Ambient air sampling

Ambient air samplings were carried out by air samplers installed at compass deck. Ambient particles were collected on the filters (ϕ =47mm) along cruise track to analyze their composition and ice nuclei ability using Nile sampler operated at flow rate of 10L/min, respectively. To avoid collecting particles emitted from the funnel of the own vessel, the sampling period was controlled automatically by using a “wind-direction selection system”. These sampling logs are listed in Table 2.1(c).1. All samples are going to be analyzed in laboratory.

iii) Rain sampling

Rain sample was corrected using a hand-made sampler. These sampling logs are listed in Table 2.1(c).2. To investigate the nutrients in the rain, these samples are going to be analyzed in laboratory.

iv) CO and O_3

Ambient air was continuously sampled on the compass deck and drawn through ~20-m-long Teflon tubes connected to a gas filter correlation CO analyzer (Model 48, Thermo Fisher Scientific) and a UV photometric ozone analyzer (Model 49C, Thermo Fisher Scientific), located in the Research Information Center. The data will be used for characterizing air mass origins.

v) Aerosol optical thickness and Single scattering albedo

The sky radiometer measures the direct solar irradiance and the solar aureole radiance distribution with seven interference filters (0.315, 0.4, 0.5, 0.675, 0.87, 0.94, and 1.02 μm). Analysis of these data was performed by SKYRAD.pack version 4.2

(4) Data archive

These obtained data will be submitted to JAMSTEC Data Management Group (DMG).

(5) Observation log

Table 2.1(c).1 Ambient air sampling logs in this cruise.

	date sampling(UTC)			sampling (UTC)		latitude			longtude		
ID	yyyy	mm	dd	art (hh:mm	op (hh:mm	deg	min	N-S	deg	min	E-W
MR1804-NI-002	2018	7	19	7:25		34	33.49	N	138	41	E
	2018	7	20		5:27	32	26.7	N	144	24.17	E
MR1804-NI-003	2018	7	20	8:01		32	21.96	N	144	24.17	E
	2018	7	21		5:50	32	21.96	N	144	24	E
MR1804-NI-004	2018	7	21	6:52		32	29.7	N	144	32.04	E
	2018	7	22		5:00	35	52.08	N	148	12.32	E
MR1804-NI-005	2018	7	22	5:49		35	59.9	N	148	19.8	E
	2018	7	22		23:09	38	53.19	N	151	1.04	E
MR1804-NI-006	2018	7	22	23:35		38	56.95	N	151	4.59	E
	2018	7	23		21:59	42	32.02	N	154	50.89	E
MR1804-NI-007	2018	7	23	22:18		42	35.07	N	154	54.08	E
	2018	7	24		22:07	46	26.03	N	159	19.04	E
MR1804-NI-008	2018	7	24	2:06		47	0	N	160	0.5	E
	2018	7	24		21:32	47	1.56	N	159	59.22	E
MR1804-NI-009	2018	7	25	22:25		47	2.39	N	159	59.57	E
	2018	7	26		21:58	46	0.01	N	159	59.22	E
MR1804-NI-010	2018	7	26	22:27		47	0.1	N	159	59.91	E
	2018	7	27		20:30	46	59.9	N	160	0.4	E
MR1804-NI-011	2018	7	28	1:37		47	6.16	N	160	0.8	E
	2018	7	28		21:56	47	5.5	N	160	12.4	E
MR1804-NI-012	2018	7	28	22:35		47	4.87	N	160	10.15	E
	2018	7	29		21:58	44	57.08	N	159	30.47	E
MR1804-NI-014	2018	7	29	22:20		44	52.35	N	159	29.45	E
	2018	7	30		22:03	40	13.12	N	158	25.63	E
MR1804-NI-015	2018	7	30	22:34		40	13.12	N	158	25.63	E
	2018	7	31		21:58	37	46.71	N	157	48.68	E
MR1804-NI-016	2018	7	31	22:50		37	38.85	N	157	47.28	E
	2018	8	1		21:55	35	6.49	N	157	19.1	E
MR1804-NI-017	2018	8	1	22:18		35	6.49	N	157	19.1	E
	2018	8	2		21:56	30	48.25	N	156	26.09	E
MR1804-NI-018	2018	8	2	22:19		30	43.9	N	156	27.3	E
	2018	8	3		21:56	27	10.02	N	155	45.9	E
MR1804-NI-019	2018	8	3	22:28		27	2.19	N	155	44.64	E
	2018	8	4		21:58	24	38.75	N	155	21.06	E
MR1804-NI-020	2018	8	4	22:23		24	34.42	N	155	20.2	E
	2018	8	5		22:00	20	18.91	N	154	31.83	E
MR1804-NI-021	2018	8	5	22:26		20	13.91	N	154	31.08	E
	2018	8	6		22:05	17	22.68	N	154	0.49	E
MR1804-NI-023	2018	8	6	22:36		17	16.41	N	153	59.42	E
	2018	8	7		21:58	15	0.66	N	153	34.86	E
MR1804-NI-024	2018	8	7	22:27		14	59.97	N	153	36.26	E
	2018	8	8		22:57	10	31.9	N	152	49.95	E

Table 2.1(c).2. Rain sampling logs in this cruise.

	sampling		date sampling(UTC)			latitude			longtude		
Bottle ID	tart (hh:m	top (hh:mn	yyyy	mm	dd	deg	min	N-S	deg	min	E-W
R'001	18:00	21:00	2018	7	22	35	6.43	N	147	12.21	E
R'002	1:00	3:00	2018	7	24	43	20	N	155	45	E
R'003	3:00	4:30	2018	7	24	43	37.09	N	156	2.86	E
R'004	4:30	6:30	2018	7	24	43	56.62	N	156	26	E
R'005	6:30	22:00	2018	7	24	46	31.83	N	159	26.32	E
R'006	22:00	2:10	2018	7	25	47	0	N	160	0.5	E
R'007	2:10	6:30	2018	7	25	47	0.96	N	160	2.22	E
R'008	6:30	22:30	2018	7	25	47	2.5	N	159	59.58	E
R'009	22:30	22:30	2018	7	26	47	0	N	159	59.59	E
R'010	22:30	5:30	2018	7	27	47	0	N	160	0.5	E
R'011	5:30	22:30	2018	7	27	47	10	N	160	10	E
R'012	23:00	6:30	2018	7	28	47	0	N	159	59.87	E
R'013	6:30	22:00	2018	7	29	44	49.52	N	159	28.77	E
R'014	22:00	22:00	2018	7	30	40	6.36	N	158	22.68	E
R'015	22:00	21:00	2018	8	1	35	5.32	N	157	19.6	E
R'016	21:00	2:00	2018	8	2	34	33.3	N	157	13.5	E
R'017	22:00	0:30	2018	8	3	30	14.66	N	156	21.4	E
R'018	0:30	1:00	2018	8	3	30	12.2	N	156	21.1	E
R'019	1:00	1:30	2018	8	3	30	6.2	N	156	20.4	E
R'020	1:30	2:00	2018	8	3	30	0.4	N	156	19.78	E
R'021	2:00	2:30	2018	8	3	30	0.1	N	156	19.72	E
R'022	2:30	3:00	2018	8	3	30	0.1	N	156	19.71	E
R'023	22:00	22:00	2018	8	4	24	34.42	N	156	20.2	E
R'024	22:00	3:50	2018	8	6	20	1.89	N	154	29.11	E
R'025	6:00	21:05	2018	8	7	15	0.35	N	153	35.09	E
R'026	21:05	21:35	2018	8	7	15	0.54	N	153	35.09	E

2.2 Geophysical observation

2.2(a) Swath bathymetry

Tetsuichi FUJIKI (JAMSTEC RCGC)
Ryo OYAMA (NME)
Masanori MURAKAMI (NME)
Takehito HATTORI (MIRAI crew)

(1) Introduction

The objective of Multi-Beam Echo Sounding system (MBES) is collecting continuous bathymetric data along ship's track to contribute to geological and geophysical investigations and global data sets.

(2) Data Acquisition

The "SEABEAM 3012" on R/V MIRAI was used for bathymetry mapping during this cruise. To get accurate sound velocity of water column for ray-path correction of acoustic multibeam, we used Surface Sound Velocimeter (SSV) data to get the sea surface (6.62m) sound velocity, and the deeper depth sound velocity profiles were calculated by temperature and salinity profiles from CTD, XCTD and Argo float data by the equation in Del Grosso (1974) during the cruise.

(3) Preliminary Results

The results will be published after primary processing.

(4) Data Archives

All data obtained during this cruise will be submitted to the Data Management Group (DMG) in JAMSTEC, and will be archived there.

2.2(b) Sea surface gravity

Tetsuichi FUJIKI (JAMSTEC RCGC)
Ryo OYAMA (NME)
Masanori MURAKAMI (NME)
Takehito HATTORI (MIRAI crew)

(1) Introduction

The local gravity is an important parameter in geophysics and geodesy. We collected gravity data at the sea surface.

(2) Parameters

Relative Gravity [CU: Counter Unit]
[mGal] = (coef1: 0.9946) * [CU]

(3) Data Acquisition

We measured relative gravity using LaCoste and Romberg air-sea gravity meter S-116 (Micro-G LaCoste, LLC) during this cruise.

To convert the relative gravity to absolute gravity, we measured gravity, using portable gravity meter (CG-5, Scintrex), at Shimizu as the reference point.

(4) Preliminary Results

Absolute gravity table is shown in Table 2.2(b).1.

Table 2.2(b).1. Absolute gravity table of this cruise.

No.	Date m/d	UTC	Port	Absolute Gravity [mGal]	Sea Level [cm]	Ship Draft [cm]	Gravity at Sensor *1 [mGal]	S-116 Gravity [mGal]
#1	7/19	00:28	Shimizu	979,729.47	176	649	979,730.28	12018.00

*1: Gravity at Sensor = Absolute Gravity + Sea Level*0.3086/100 + (Draft-530)/100*0.2222

(5) Data Archive

All data obtained during this cruise will be submitted to the Data Management Group (DMG) in JAMSTEC, and will be archived there.

2.2(c) Sea surface magnetic field

Tetsuichi FUJIKI (JAMSTEC RCGC)
Ryo OYAMA (NME)
Masanori MURAKAMI (NME)
Takehito HATTORI (MIRAI crew)

(1) Introduction

Measurement of magnetic force on the sea is required for the geophysical investigations of marine magnetic anomaly caused by magnetization in upper crustal structure. We measured geomagnetic field using a three-component magnetometer during this cruise.

(2) Instruments

A shipboard three-component magnetometer system (Tierra Tecnica SFG2018) is equipped on-board R/V MIRAI. Three-axes flux-gate sensors with ring-cored coils are fixed on the fore mast. Outputs from the sensors are sampled at 8 times per second. Ship's heading, pitch, and roll are measured by the Inertial Navigation System (INS) for controlling attitude of a Doppler radar. Ship's position and speed data are taken from LAN every second.

(3) Principle of ship-board geomagnetic vector measurement

The relation between a magnetic-field vector observed on-board, *Hob*, (in the ship's fixed coordinate system) and the geomagnetic field vector, *F*, (in the Earth's fixed coordinate system) is expressed as:

$$Hob = A * R * P * Y * F + Hp \qquad (a)$$

where, *R*, *P* and *Y* are the matrices of rotation due to roll, pitch and heading of a ship, respectively. *A* is a 3 x 3 matrix which represents magnetic susceptibility of the ship, and *Hp* is a magnetic field vector produced by a permanent magnetic moment of the ship's body. Rearrangement of Eq. (a) makes

$$R * Hob + Hbp = R * P * Y * F \qquad (b)$$

where $R = A^{-1}$, and $Hbp = -R * Hp$. The magnetic field, *F*, can be obtained by measuring *R*, *P*, *Y* and *Hob*, if *R* and *Hbp* are known. Twelve constants in *R* and *Hbp* can be determined by measuring variation of *Hob* with *R*, *P* and *Y* at a place where the geomagnetic field, *F*, is known.

(4) Preliminary results

The results will be published after primary processing.

(5) Data Archive

All data obtained during this cruise will be submitted to the Data Management Group (DMG) in JAMSTEC, and will be archived there

(6) Remarks (Times in UTC)

The following periods, we made a “figure-eight” turn (a pair of clockwise and anti-clockwise rotation) for calibration of the ship’s magnetic effect.

19:26 - 19:56 26 Jul. 2018 around 47-00N, 160-00E
18:03 - 18:36 07 Aug. 2018 around 14-59N, 153-36E

2.3 Shipboard ADCP

Tetsuichi FUJIKI (JAMSTEC RCGC)
Ryo OYAMA (NME)
Masanori MURAKAMI (NME)
Takehito HATTORI (MIRAI crew)

(1) Objectives

To obtain continuous measurement data of the current profile along the ship's track.

(2) Instruments and methods

Upper ocean current measurements were made in this cruise, using the hull-mounted Acoustic Doppler Current Profiler (ADCP) system. For most of its operation, the instrument was configured for water-tracking mode. Bottom-tracking mode, interleaved bottom-ping with water-ping, was made to get the calibration data for evaluating transducer misalignment angle in the shallow water. The system consists of following components;

1. R/V MIRAI has installed the Ocean Surveyor for vessel-mount ADCP (frequency 76.8 kHz; Teledyne RD Instruments, USA). It has a phased-array transducer with single ceramic assembly and creates 4 acoustic beams electronically. We mounted the transducer head rotated to a ship-relative angle of 45 degrees azimuth from the keel.
2. For heading source, we use ship's gyro compass (Tokyo Keiki, Japan), continuously providing heading to the ADCP system directory. Additionally, we have Inertial Navigation System (Phins, Ixblue, France) which provide high-precision heading, attitude information, pitch and roll. They are stored in ".N2R" data files with a time stamp.
3. Differential GNSS system (StarPack-D, Fugro, Netherlands) providing precise ship's position.
4. We used VmDas software version 1.49(TRDI) for data acquisition.
5. To synchronize time stamp of ping with Computer time, the clock of the logging computer is adjusted to GPS time server continuously by the application software.
6. Fresh water is charged in the sea chest to prevent bio fouling at transducer face.
7. The sound speed at the transducer does affect the vertical bin mapping and vertical velocity measurement, and that is calculated from temperature, salinity (constant value; 35.0 PSU) and depth (6.5 m; transducer depth) by equation in Medwin (1975).

Data was configured for "8 m" layer intervals starting about 23m below sea surface, and recorded every ping as raw ensemble data (.ENR). Additionally, 10 seconds averaged data were recorded as short-term average (.STA). 300 seconds averaged data were long-term average (.LTA), respectively.

(3) Parameters

Major parameters for the measurement, Direct Command, are shown in Table 2.3.1.

Table 2.3.1. Major parameters.

Bottom-Track Commands

BP = 001	Pings per Ensemble (almost less than 1,300m depth)

Environmental Sensor Commands

EA = 04500	Heading Alignment (1/100 deg)
ED = 00065	Transducer Depth (0 - 65535 dm)
EF = +001	Pitch/Roll Divisor/Multiplier (pos/neg) [1/99 - 99]
EH = 00000	Heading (1/100 deg)
ES = 35	Salinity (0-40 pp thousand)
EX = 00000	Coordinate Transform (Xform:Type; Tilts; 3Bm; Map)
EZ = 10200010	Sensor Source (C; D; H; P; R; S; T; U)

C (1): Sound velocity calculates using ED, ES, ET (temp.)
D (0): Manual ED
H (2): External synchro
P (0), R (0): Manual EP, ER (0 degree)
S (0): Manual ES
T (1): Internal transducer sensor
U (0): Manual EU

EV = 0	Heading Bias(1/100 deg)

Water-Track Commands

WA = 255	False Target Threshold (Max) (0-255 count)
WC = 120	Low Correlation Threshold (0-255)
WD = 111 100 000	Data Out (V; C; A; PG; St; Vsum; Vsum^2; #G; P0)
WE = 1000	Error Velocity Threshold (0-5000 mm/s)
WF = 0800	Blank After Transmit (cm)
WN = 100	Number of depth cells (1-128)
WP = 00001	Pings per Ensemble (0-16384)
WS = 800	Depth Cell Size (cm)
WV = 0390	Mode 1 Ambiguity Velocity (cm/s radial)

(4) Preliminary results

Horizontal velocity along the ship's track is presented in Fig. 2.3.1. In vertical direction, the data are averaged from 35 to 60m.

(5) Data Archives

All data obtained during this cruise will be submitted to the Data Management Group (DMG) in JAMSTEC, and will be archived there.

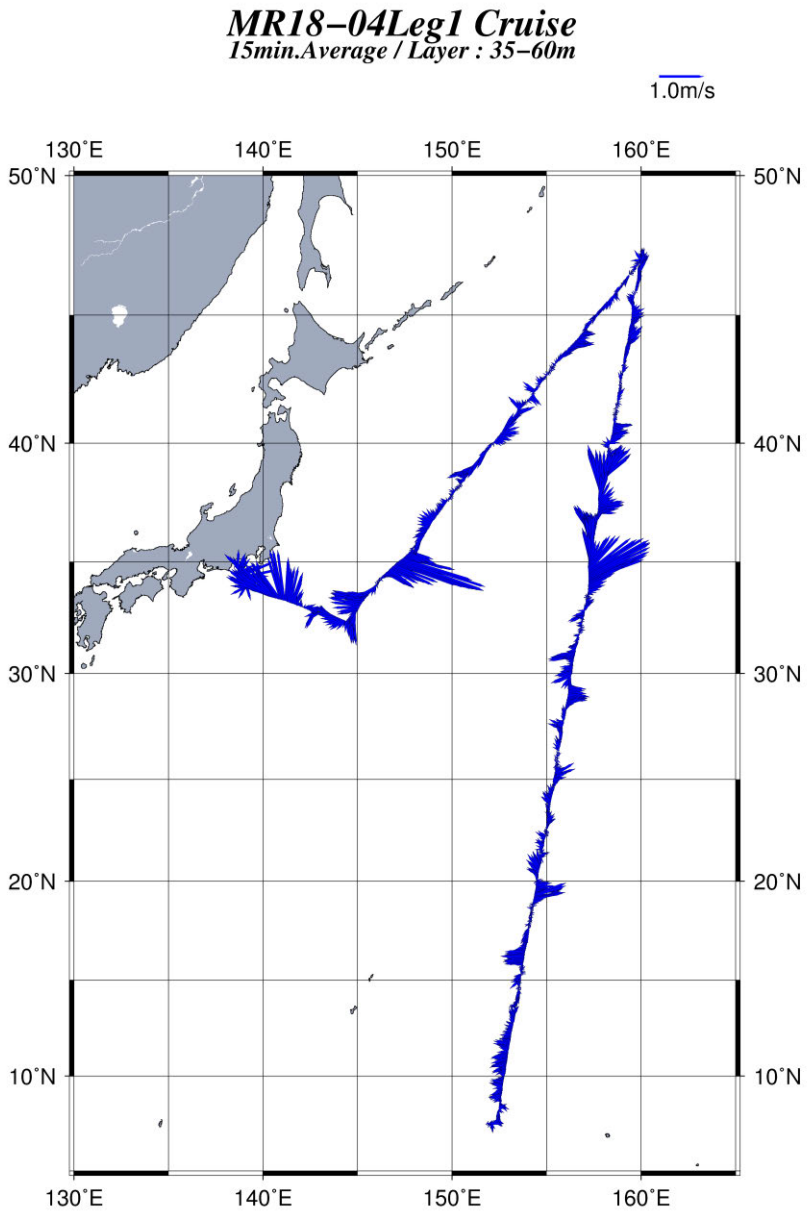

Figure. 2.3.1. Horizontal Velocity along the ship's track.

2.4 CTD cast and water sampling

Hiroshi UCHIDA (JAMSTEC RCGC)
Masahide WAKITA (JAMSTEC MIO)
Shinsuke TOYODA (MWJ)
Tomohide NOGUCHI (MWJ)
Keisuke TAKEDA (MWJ)
Rio KOBAYASHI (MWJ)
Tomokazu CHIBA (MWJ)

(1) Winch arrangements

The CTD package was deployed from starboard side by using 4.5 Ton Traction Winch System (Dynacon, Inc., Bryan, Texas, USA), which was renewed on the R/V Mirai in April 2014 (e.g. Fukasawa et al., 2004). Primary system components include a complete CTD Traction Winch System with a 9.53 mm armored cable (Rochester Wire & Cable, LLC, Culpeper, Virginia, USA).

(2) Overview of the equipment

The CTD system was SBE 911plus system (Sea-Bird Electronics, Inc., Bellevue, Washington, USA). The SBE 911plus system controls 36-position SBE 32 Carousel Water Sampler. The Carousel accepts 12-litre Niskin-X water sample bottles (General Oceanics, Inc., Miami, Florida, USA). The SBE 9plus was mounted horizontally in a 36-position carousel frame. SBE's temperature (SBE 3) and conductivity (SBE 4) sensor modules were used with the SBE 9plus underwater unit. The pressure sensor is mounted in the main housing of the underwater unit and is ported to outside through the oil-filled plastic capillary tube. A modular unit of underwater housing pump (SBE 5T) flushes water through sensor tubing at a constant rate independent of the CTD's motion, and pumping rate (3000 rpm) remain nearly constant over the entire input voltage range of 12-18 volts DC. Flow speed of pumped water in standard TC duct is about 2.4 m/s. Two sets of temperature and conductivity modules were used. An SBE's dissolved oxygen sensor (SBE 43) was placed between the primary conductivity sensor and the pump module. Auxiliary sensors, a Deep Ocean Standards Thermometer (SBE 35), an altimeter (PSA-916T; Teledyne Benthos, Inc., North Falmous, Massachusetts, USA), an oxygen optodes (RINKO-III; JFE Advantech Co., Ltd, Kobe Hyogo, Japan), a fluorometers (Seapoint sensors, Inc., Kingston, New Hampshire, USA), a transmissometer (C-Star Transmissometer; WET Labs, Inc., Philomath, Oregon, USA), a turbidity meter (Seapoint Sensors, Inc., Exeter, New Hampshire, USA), a Photosynthetically Active Radiation (PAR) sensor (Satlantic, LP, Halifax, Nova Scotia, Canada), and a colored dissolved organic matter (Seapoint Sensors, Inc.) were also used with the SBE 9plus underwater unit.

To minimize rotation of the CTD package, a heavy stainless frame (total weight of the CTD package without sea water in the bottles is about 1000 kg) was used with an aluminum plate (54 × 90 cm) and a compact underwater slip ring swivel (Hanayuu Co., Ltd., Shizuoka, Japan). A simple azimuth meter (Hanayuu Co., Ltd.) was attached to the termination (Evergrip, PMI Industries, Cleveland, Ohio, USA) of an armored cable to investigate the effectiveness of the slip ring swivel.

Summary of the system used in this cruise

36-position Carousel system

Deck unit:

SBE 11plus, S/N 11P54451-0872

Under water unit:

SBE 9plus, S/N 09P54451-1027 (117457)

Temperature sensor:

SBE 3, S/N 031525 (primary)

SBE 3, S/N 031524 (secondary)

Conductivity sensor:

SBE 4, S/N 042435 (primary)

SBE 4, S/N 041088 (secondary)

Oxygen sensor:

SBE 43, S/N 430949 (from station KEO_1 to K02_5)

SBE 43, S/N 432211 (from station K02_6 to 006_3)

JFE Advantech RINKO-III, S/N 0287 (foil batch no. 163011BA)

Pump:

SBE 5T, S/N 055816 (primary)

SBE 5T, S/N 054595 (secondary)

Altimeter:

PSA-916T, S/N 1157

Deep Ocean Standards Thermometer:

SBE 35, S/N 0022

Fluorometer:

Seapoint Sensors, Inc., S/N 3618 (measurement range: 0-15 □g/L) (Gain: 10X)

Turbidity meter:

Seapoint Sensors, Inc., S/N 14953 (measurement range: 0-25 FTU) (Gain: 100X)

Transmissometer:

C-Star, S/N CST-1726DR

PAR:

Satlantic LP, S/N 1025

CDOM:

Seapoint Sensors, Inc., S/N 6223 (measurement range: 0-50 QSU) (Gain: 30X)

Carousel Water Sampler:

SBE 32, S/N 3227443-0391

Water sample bottle:

12-litre OTE model 110 (OceanTest Equipment, Inc., Fort Lauderdale, Florida, USA)
(#1-9: Teflon coating, #10-36: non Teflon coating)

Azimuth meter:

Hanayuu Co., Ltd.

(3) Pre-cruise calibration

i. Pressure

The Paroscientific series 4000 Digiquartz high pressure transducer (Model 415K: Paroscientific,

Inc., Redmond, Washington, USA) uses a quartz crystal resonator whose frequency of oscillation varies with pressure induced stress with 0.01 per million of resolution over the absolute pressure range of 0 to 15000 psia (0 to 10332 dbar). Also, a quartz crystal temperature signal is used to compensate for a wide range of temperature changes at the time of an observation. The pressure sensor has a nominal accuracy of 0.015 % FS (1.5 dbar), typical stability of 0.0015 % FS/month (0.15 dbar/month), and resolution of 0.001 % FS (0.1 dbar). Since the pressure sensor measures the absolute value, it inherently includes atmospheric pressure (about 14.7 psi). SEASOFT subtracts 14.7 psi from computed pressure automatically.

Pre-cruise sensor calibrations for linearization were performed at SBE, Inc. The time drift of the pressure sensor is adjusted by periodic recertification corrections against electronic dead-weight testers (Model E-DWT-H, Fluke Co., Phoenix, Arizona, USA) calibrated by Ohte Giken, Inc., Tsukuba, Ibaraki, Japan.

A70 Me-L, S/N 181, 18 January 2018

A200Me-L, S/N 1305, 18 January 2018

The corrections are performed at JAMSTEC, Yokosuka, Kanagawa, Japan by Marine Works Japan Ltd. (MWJ), Yokohama, Kanagawa, Japan, usually once in a year in order to monitor sensor time drift and linearity.

S/N 1027, 26 February 2018

slope = 0.99988702

offset = 01.58819

ii. Temperature (SBE 3)

The temperature sensing element is a glass-coated thermistor bead in a stainless steel tube, providing a pressure-free measurement at depths up to 10500 (6800) m by titanium (aluminum) housing. The SBE 3 thermometer has a nominal accuracy of 1 mK, typical stability of 0.2 mK/month, and resolution of 0.2 mK at 24 samples per second. The premium temperature sensor, SBE 3plus, is a more rigorously tested and calibrated version of standard temperature sensor (SBE 3).

Pre-cruise sensor calibrations were performed at SBE, Inc.

S/N 031525, 22 February 2018

S/N 031524, 27 February 2018

iii. Conductivity (SBE 4)

The flow-through conductivity sensing element is a glass tube (cell) with three platinum electrodes to provide in-situ measurements at depths up to 10500 (6800) m by titanium (aluminum) housing. The SBE 4 has a nominal accuracy of 0.0003 S/m, typical stability of 0.0003 S/m/month, and resolution of 0.00004 S/m at 24 samples per second. The conductivity cells have been replaced to newer style cells for deep ocean measurements.

Pre-cruise sensor calibrations were performed at SBE, Inc.

S/N 042435, 15 February 2018

S/N 041088, 16 February 2018

The value of conductivity at salinity of 35, temperature of 15 °C (IPTS-68) and pressure of 0 dbar is 4.2914 S/m.

iv. Oxygen (SBE 43)

The SBE 43 oxygen sensor uses a Clark polarographic element to provide in-situ measurements at depths up to 7000 m. The range for dissolved oxygen is 120 % of surface saturation in all natural waters, nominal accuracy is 2 % of saturation, and typical stability is 2 % per 1000 hours.

Pre-cruise sensor calibration was performed at SBE, Inc.

S/N 430949, 03 February 2018

S/N 432211, 03 February 2018

v. Deep Ocean Standards Thermometer

Deep Ocean Standards Thermometer (SBE 35) is an accurate, ocean-range temperature sensor that can be standardized against Triple Point of Water and Gallium Melt Point cells and is also capable of measuring temperature in the ocean to depths of 6800 m. The SBE 35 was used to calibrate the SBE 3 temperature sensors in situ (Uchida et al., 2007).

Pre-cruise sensor linearization was performed at SBE, Inc.

S/N 0022, 4 March 2009

Then the SBE 35 is certified by measurements in thermodynamic fixed-point cells of the TPW (0.01 °C) and GaMP (29.7646 °C). The slow time drift of the SBE 35 is adjusted by periodic recertification corrections. Pre-cruise sensor calibration was performed at RCGC/JAMSTEC by using fixed-point cells traceable to NMIJ temperature standards.

S/N 0022, 14 May 2018 (slope and offset correction)

Slope = 1.000014

Offset = 0.000640

The time required per sample = 1.1 × NCYCLES + 2.7 seconds. The 1.1 seconds is total time per an acquisition cycle. NCYCLES is the number of acquisition cycles per sample and was set to 4. The 2.7 seconds is required for converting the measured values to temperature and storing average in EEPROM.

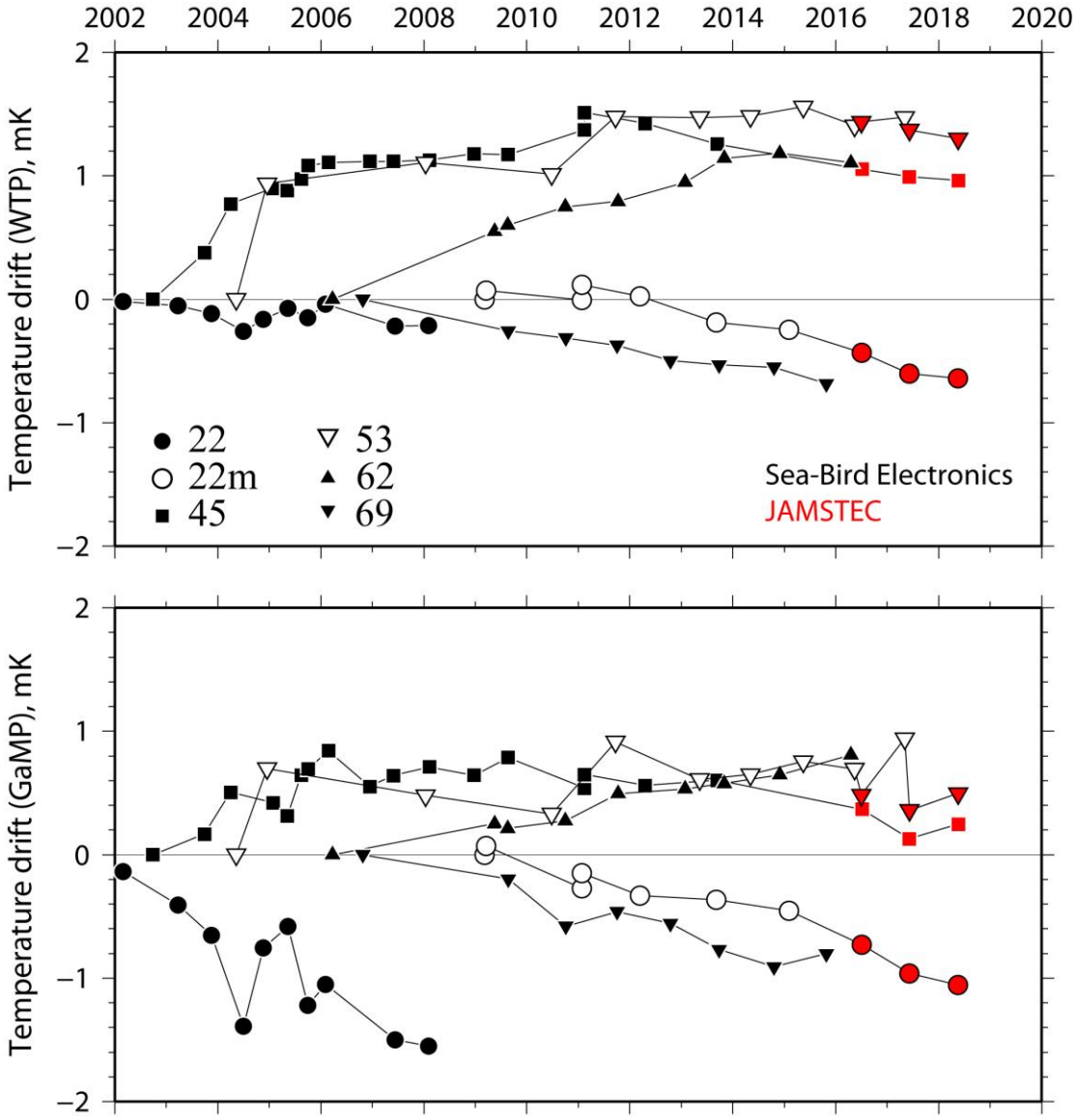

Figure 2.4.1. Time drifts (temperature offsets relative to the first calibration) of six reference thermometers (SBE 35) based on laboratory calibrations in fixed-point cells. Results performed at JAMSTEC are shown in red marks.

vi. Altimeter

Benthos PSA-916T Sonar Altimeter (Teledyne Benthos, Inc.) determines the distance of the target from the unit by generating a narrow beam acoustic pulse and measuring the travel time for the pulse to bounce back from the target surface. It is rated for operation in water depths up to 10000 m. The PSA-916T uses the nominal speed of sound of 1500 m/s.

vii. Oxygen optode (RINKO)

RINKO (JFE Advantech Co., Ltd.) is based on the ability of selected substances to act as dynamic fluorescence quenchers. RINKO model III is designed to use with a CTD system which accept an auxiliary analog sensor, and is designed to operate down to 7000 m.

Data from the RINKO can be corrected for the time-dependent, pressure-induced effect by means of the same method as that developed for the SBE 43 (Edwards et al., 2010). The calibration coefficients, H1 (amplitude of hysteresis correction), H2 (curvature function for hysteresis), and H3 (time constant for hysteresis) were determined empirically as follows.

H1 = 0.0055

H2 = 5000 dbar

H3 = 2000 seconds

Outputs from RINKO are the raw phase shift data. The RINKO can be calibrated by the modified Stern-Volmer equation slightly modified from a method by Uchida et al. (2010):

$$O_2\ (\mu mol/l) = [(V_0 / V)^E - 1] / K_{sv}$$

where V is voltage, V_0 is voltage in the absence of oxygen, K_{sv} is Stern-Volmer constant. The coefficient E corrects nonlinearity of the Stern-Volmer equation. The V_0 and the K_{sv} are assumed to be functions of temperature as follows.

$$K_{sv} = C_0 + C_1 \times T + C_2 \times T^2$$

$$V_0 = 1 + C_3 \times T$$

$$V = C_4 + C_5 \times V_b$$

where T is CTD temperature (°C) and V_b is raw output (volts). V_0 and V are normalized by the output in the absence of oxygen at 0°C. The oxygen concentration is calculated using accurate temperature data from the CTD temperature sensor instead of temperature data from the RINKO. The pressure-compensated oxygen concentration O_{2c} can be calculated as follows.

$$O_{2c} = O_2\ (1 + C_p p / 1000)$$

where p is CTD pressure (dbar) and C_p is the compensation coefficient. Since the sensing foil of the optode is permeable only to gas and not to water, the optode oxygen must be corrected for salinity. The salinity-compensated oxygen can be calculated by multiplying the factor of the effect of salt on the oxygen solubility (Garcia and Gordon, 1992).

Pre-cruise sensor calibrations were performed at RCGC/JAMSTEC.

S/N 0287, 25 June 2018

viii. Fluorometer

The Seapoint Chlorophyll Fluorometer (Seapoint Sensors, Inc., Kingston, New Hampshire, USA) provides in-situ measurements of chlorophyll-a at depths up to 6000 m. The instrument uses modulated blue LED lamps and a blue excitation filter to excite chlorophyll-a. The fluorescent light emitted by the chlorophyll-a passes through a red emission filter and is detected by a silicon photodiode. The low level signal is then processed using synchronous demodulation circuitry, which generates an output voltage proportional to chlorophyll-a concentration.

ix. Transmissometer

The C-Star Transmissometer (WET Labs, Inc., Philomath, Oregon, USA) measures light transmittance at a single wavelength (650 nm) over a know path (25 cm). In general, losses of light propagating through water can be attributed to two primary causes: scattering and absorption. By projecting a collimated beam of light through the water and placing a focused receiver at a known distance away, one can quantify these losses. The ratio of light gathered by the receiver to the amount originating at the source is known as the beam transmittance. Suspended particles, phytoplankton, bacteria and dissolved organic matter contribute to the losses sensed by the instrument. Thus, the

instrument provides information both for an indication of the total concentrations of matter in the water as well as for a value of the water clarity.

Light transmission T_r (in %) and beam attenuation coefficient c_p are calculated from the sensor output (V in volt) as follows.

$$T_r = (c_0 + c_1 V) \times 100$$

$$c_p = -(1 / 0.25) \ln(T_r / 100)$$

x. Turbidity meter

The Seapoint turbidity meter (Seapoint Sensors, Inc., Kingston, New Hampshire, USA) detects light scattered by particles suspended in water at depths up to 6000 m. The sensor generates an output voltage proportional to turbidity or suspended solids. The unique optical design confines the sensing volume to within 5 cm of the sensor.

xi. PAR

Photosynthetically Active Radiation (PAR) sensors (Satlantic, LP, Halifax, Nova Scotia, Canada) provide highly accurate measurements of PAR (400 – 700 nm) for a wide range of aquatic and terrestrial applications. The ideal spectral response for a PAR sensor is one that gives equal emphasis to all photons between 400 – 700 nm. Satlantic PAR sensors use a high quality filtered silicon photodiode to provide a near equal spectral response across the entire wavelength range of the measurement.

Pre-cruise sensor calibration was performed at Satlantic, LP.

S/N 1025, 6 July 2015

xii. CDOM

The Seapoint Ultraviolet Fluorometer (SUVF) is a high-performance, low power instrument for in situ measurement of chromophoric dissolved organic matter (CDOM) at depths up to 6000 m. The SUVF uses modulated ultraviolet LED lamps and optical filter for excitation. The fluorescent light signal passes through a blue emission filter and is detected by a silicon photodiode. The SUFV is operated without a pump and the sensing volume is left open to the surrounding water.

(4) Data collection and processing

i. Data collection

CTD system was powered on at least 20 minutes in advance of the data acquisition to stabilize the pressure sensor and was powered off at least two minutes after the operation in order to acquire pressure data on the ship's deck.

The package was lowered into the water from the starboard side and held 10 m beneath the surface in order to activate the pump. After the pump was activated, the package was lifted to the surface and lowered at a rate of 1.0 m/s to 200 m (or 300 m when significant wave height was high) then the package was stopped to operate the heave compensator of the crane. The package was lowered again at a rate of 1.2 m/s to the bottom. For the up cast, the package was lifted at a rate of 1.1 m/s except for bottle firing stops. As a rule, the bottle was fired after waiting from the stop for more than 30 seconds and the package was stayed at least 5 seconds for measurement of the SBE 35 at each bottle firing stops. For depths where vertical gradient of water properties were expected to be large (from surface to thermocline), the bottle was exceptionally fired after waiting from the stop for 60 seconds to enhance exchanging the water between inside and outside of the bottle. At 200 m (or 300 m) from the surface,

the package was stopped to stop the heave compensator of the crane.

Water samples were collected using a 36-bottle SBE 32 Carousel Water Sampler with 12-litre Niskin-X bottles.

Data acquisition software

SEASAVE-Win32, version 7.23.2

iii. Data processing

SEASOFT consists of modular menu driven routines for acquisition, display, processing, and archiving of oceanographic data acquired with SBE equipment. Raw data are acquired from instruments and are stored as unmodified data. The conversion module DATCNV uses instrument configuration and calibration coefficients to create a converted engineering unit data file that is operated on by all SEASOFT post processing modules. The following are the SEASOFT and original software data processing module sequence and specifications used in the reduction of CTD data in this cruise.

Data processing software

SBEDataProcessing-Win32, version 7.26.7.114

DATCNV converted the raw data to engineering unit data. DATCNV also extracted bottle information where scans were marked with the bottle confirm bit during acquisition. The duration was set to 4.4 seconds, and the offset was set to 0.0 second. The hysteresis correction for the SBE 43 data (voltage) was applied for both profile and bottle information data.

TCORP (original module, version 1.1) corrected the pressure sensitivity of the SBE 3 for both profile and bottle information file.

RINKOCOR (original module, version 1.0) corrected the time-dependent, pressure-induced effect (hysteresis) of the RINKO for both profile data.

RINKOCORROS (original module, version 1.0) corrected the time-dependent, pressure-induced effect (hysteresis) of the RINKO for bottle information data by using the hysteresis-corrected profile data.

BOTTLESUM created a summary of the bottle data. The data were averaged over 4.4 seconds.

ALIGNCTD converted the time-sequence of sensor outputs into the pressure sequence to ensure that all calculations were made using measurements from the same parcel of water. For a SBE 9plus CTD with the ducted temperature and conductivity sensors and a 3000-rpm pump, the typical net advance of the conductivity relative to the temperature is 0.073 seconds. So, the SBE 11plus deck unit was set to advance the primary and the secondary conductivity for 1.73 scans (1.75/24 = 0.073 seconds). Oxygen data are also systematically delayed with respect to depth mainly because of the long time constant of the oxygen sensor and of an additional delay from the transit time of water in the pumped plumbing line. This delay was compensated by 5 seconds advancing the SBE 43 oxygen sensor output (voltage) relative to the temperature data. Delay of the RINKO data was also compensated by 1 second advancing sensor output (voltage) relative to the temperature data. Delay of the transmissometer data was also compensated by 2 seconds advancing sensor output (voltage) relative to the temperature data. Delay of the transmissometer data was also compensated by 2 seconds advancing sensor output (voltage) relative to the temperature data.

WILDEDIT marked extreme outliers in the data files. The first pass of WILDEDIT obtained an accurate estimate of the true standard deviation of the data. The data were read in blocks of 1000 scans. Data greater than 10 standard deviations were flagged. The second pass computed a standard deviation over the same 1000 scans excluding the flagged values. Values greater than 20 standard deviations were

marked bad. This process was applied to pressure, temperature, conductivity, and SBE 43 output.

CELLTM used a recursive filter to remove conductivity cell thermal mass effects from the measured conductivity. Typical values used were thermal anomaly amplitude alpha = 0.03 and the time constant 1/beta = 7.0.

FILTER performed a low pass filter on pressure with a time constant of 0.15 seconds. In order to produce zero phase lag (no time shift) the filter runs forward first then backwards.

WFILTER performed as a median filter to remove spikes in fluorometer, turbidity meter, transmissometer, and CDOM data. A median value was determined by 49 scans of the window. For CDOM data, an additional box-car filter with a window of 361 scans was applied to remove noise.

SECTIONU (original module, version 1.1) selected a time span of data based on scan number in order to reduce a file size. The minimum number was set to be the start time when the CTD package was beneath the sea-surface after activation of the pump. The maximum number was set to be the end time when the depth of the package was 1 dbar below the surface. The minimum and maximum numbers were automatically calculated in the module.

LOOPEDIT marked scans where the CTD was moving less than the minimum velocity of 0.0 m/s (traveling backwards due to ship roll).

DESPIKE (original module, version 1.0) removed spikes of the data. A median and mean absolute deviation was calculated in 1-dbar pressure bins for both down- and up-cast, excluding the flagged values. Values greater than 4 mean absolute deviations from the median were marked bad for each bin. This process was performed 2 times for temperature, conductivity, SBE 43, and RINKO output.

DERIVE was used to compute oxygen (SBE 43).

BINAVG averaged the data into 1-dbar pressure bins. The center value of the first bin was set equal to the bin size. The bin minimum and maximum values are the center value plus and minus half the bin size. Scans with pressures greater than the minimum and less than or equal to the maximum were averaged. Scans were interpolated so that a data record exist every dbar.

BOTTOMCUT (original module, version 0.1) deleted the deepest pressure bin when the averaged scan number of the deepest bin was smaller than the average scan number of the bin just above.

DERIVE was re-used to compute salinity, potential temperature, and density (□□□.

SPLIT was used to split data into the down cast and the up cast.

Remaining spikes in the CTD data were manually eliminated from the 1-dbar-averaged data. The data gaps resulting from the elimination were linearly interpolated with a quality flag of 6.

(5) Post-cruise calibration

i. Pressure

The CTD pressure sensor offset in the period of the cruise was estimated from the pressure readings on the ship deck. For best results the Paroscientific sensor was powered on for at least 20 minutes before the operation. In order to get the calibration data for the pre- and post-cast pressure sensor drift, the CTD deck pressure was averaged over first and last one minute, respectively. Then the atmospheric pressure deviation from a standard atmospheric pressure (14.7 psi) was subtracted from the CTD deck pressure to check the pressure sensor time drift. The atmospheric pressure was measured at the captain deck (20 m high from the base line) and sub-sampled one-minute interval as a meteorological data.

The pre- and the post-casts deck pressure data showed temperature dependency for the pressure sensor (Fig. 2.4.2). The post-cruise correction of the pressure data is not deemed necessary for the pressure sensor.

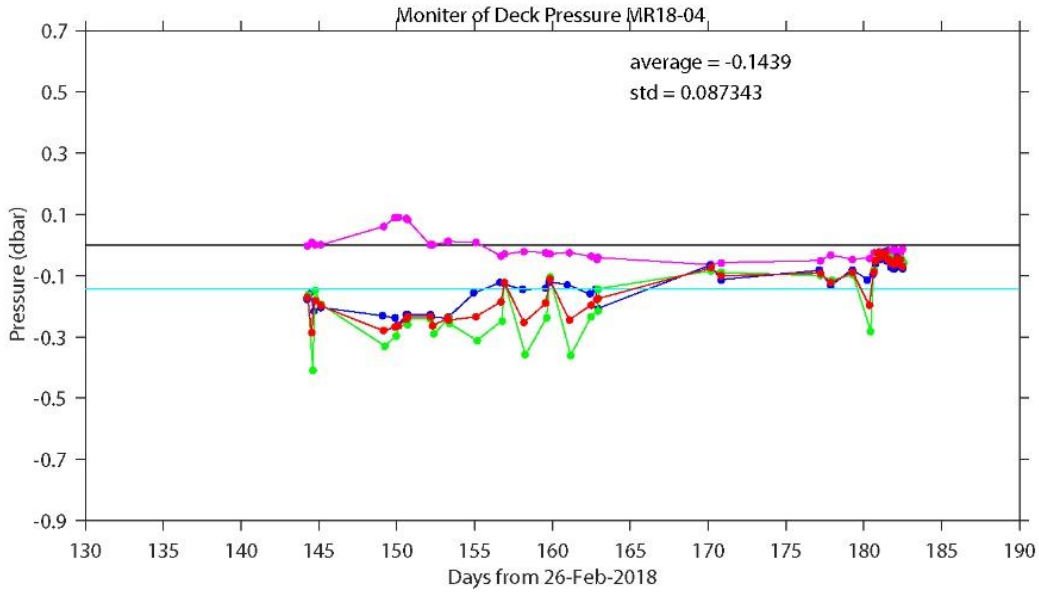

Figure 2.4.2. Time series of the CTD deck pressure for legs 1 and 2. Atmospheric pressure deviation (magenta dots) from a standard atmospheric pressure was subtracted from the CTD deck pressure. Blue and green dots indicate pre- and post-cast deck pressures, respectively. Red dots indicate averages of the pre- and the post-cast deck pressures.

ii. Temperature

The CTD temperature sensors (SBE 3) were calibrated with the SBE 35 according to a method by Uchida et al. (2007). Post-cruise sensor calibration for the SBE 35 will be performed at JAMSTEC in 2019. The CTD temperature was calibrated as

Calibrated temperature = $T - (c_0 \times P + c_1)$

$c_0 = 2.25402901e\text{-}08$

$c_1 = -4.8567e\text{-}04$

where T is CTD temperature in °C, P is pressure in dbar, and c_0 and c_1 are calibration coefficients. The coefficients were determined using the data for the depths deeper than 1950 dbar. The primary temperature data obtained in legs 1 and 2 were used for the post-cruise calibration. The result of the post-cruise calibration is shown in Figs. 2.4.3.

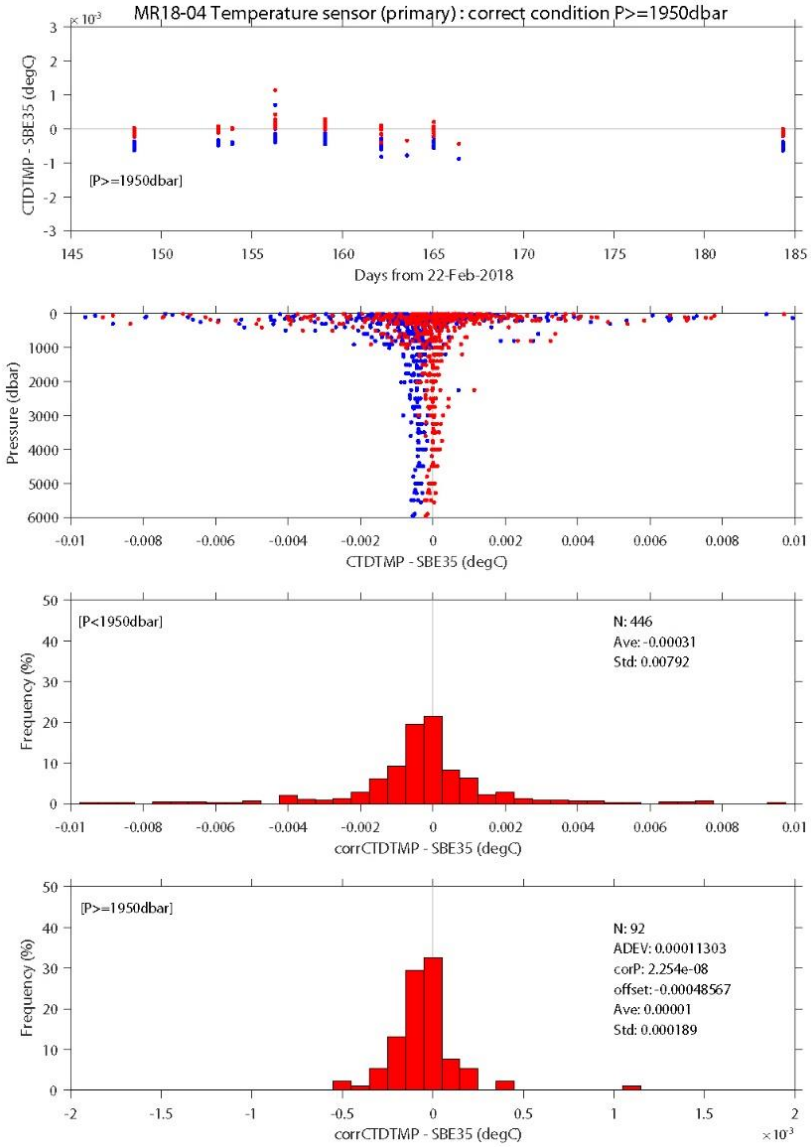

Figure 2.4.3. Difference between the CTD temperature and the SBE 35 for legs 1 and 2. Blue and red dots indicate before and after the post-cruise calibration using the SBE 35 data, respectively. Lower two panels show histogram of the difference after the calibration.

iii. Salinity

The discrepancy between the CTD conductivity and the conductivity calculated from the bottle salinity data with the CTD temperature and pressure data is considered to be a function of conductivity and pressure. The CTD conductivity was calibrated as

Calibrated conductivity =

$C - (c_0 \times C + c_1 \times P + c_2 \times C \times P + c_3 \times P^2 + c_4 \times C \times P^2 + c_5 \times C^2 \times P^2 + c_6$

c_0 = 4.5556205956e-05

c_1 = -6.7291139355e-08

c_2 = 8.3693934158e-08

c_3 = 3.2346035673e-10

c_4 = -3.1376923396e-10

c_5 = 6.3385354039e-11

c_6 = -1.9600475503e-04

where C is CTD conductivity in S/m, P is pressure in dbar, and c_0, c_1, c_2, c_3, c_4, c_5 and c_6 are calibration coefficients. The best fit sets of coefficients were determined by a least square technique to minimize the deviation from the conductivity calculated from the bottle salinity data. The primary conductivity data created by the software module ROSSUM were used after the post-cruise calibration for the temperature data. Data obtained in leg 1 were only used to determine the coefficients. The results of the post-cruise calibration for the CTD salinity is shown in Fig. 2.4.4.

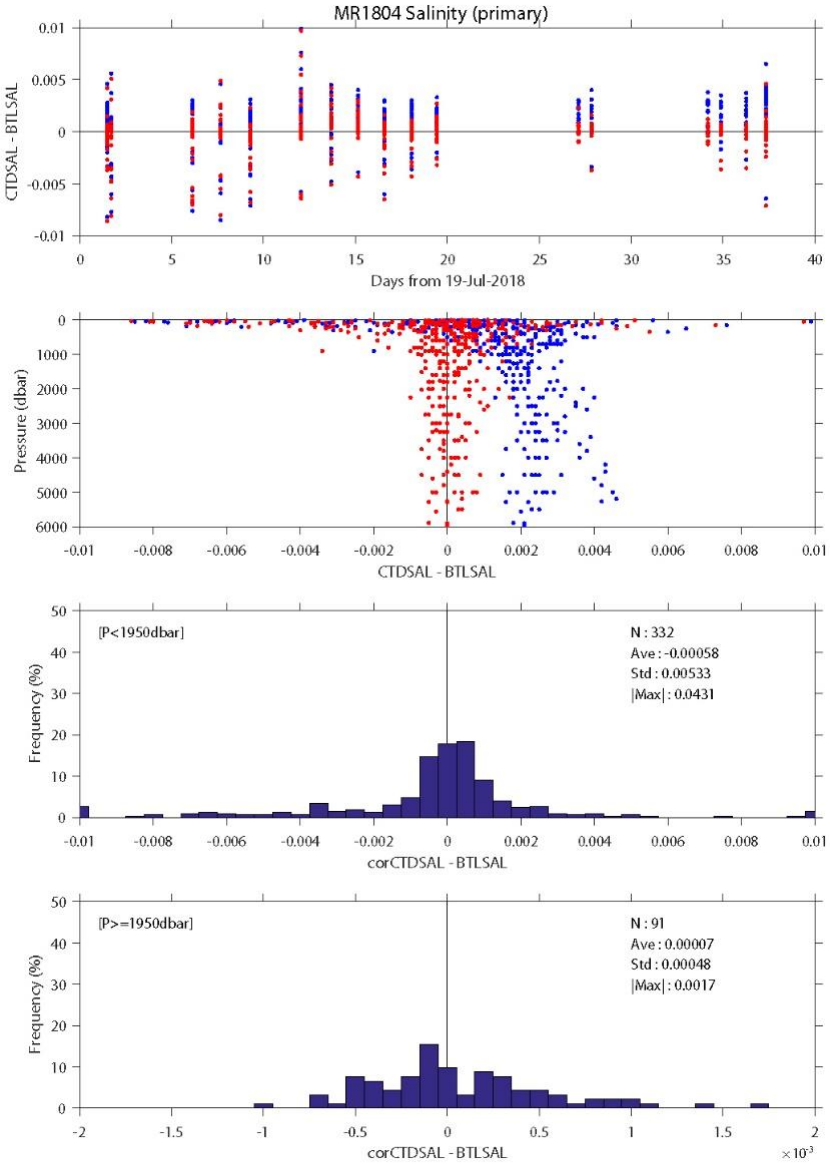

Figure 2.4.4. Difference between the CTD salinity (primary) and the bottle salinity. Blue and red dots indicate before and after the post-cruise calibration, respectively. Lower two panels show histogram of the difference after the calibration.

iv. Dissolved oxygen

The RINKO oxygen sensor was calibrated and used as the CTD oxygen data, since the RINKO has a fast time response. The pressure-hysteresis corrected RINKO data was calibrated by the modified Stern-Volmer equation, basically according to a method by Uchida et al. (2010) with slight modification:

$$[O_2]\ (\mu mol/l) = [(V_0 / V)^{1.2} - 1] / K_{sv} \times (1 + C_p \times P / 1000)$$

and

$$K_{sv} = C_0 + C_1 \times T + C_2 \times T^2$$

$$V_0 = 1 + C_3 \times T$$

$$V = C_4 + C_5 \times V_b + C_6 \times t + C_7 \times t \times V_b$$

C_0 = 4.374745199579160e-03

C_1 = 1.959889948766195e-04

C_2 = 3.299643594882492e-06

C_3 = 3.393174447187830e-05

C_4 = -8.886509933176687e-02

C_5 = 0.3133749584921368

C_6 = 2.122968503551541e-03

C_7 = 9.721622456140531e-06

C_p = 0.026

where V_b is the RINKO output (voltage), V_0 is voltage in the absence of oxygen, T is temperature in °C, P is pressure in dbar, t is exciting time (days) integrated from the first CTD cast, and C0, C1, C2, C3, C4, C5, C6, C7, and Cp are calibration coefficients. The calibration coefficients were determined by minimizing the sum of absolute deviation with a weight from the bottle oxygen data. The revised quasi-Newton method (DMINF1) was used to determine the sets. The post-cruise calibrated temperature and salinity data were used for the calibration. Data obtained in legs 1 and 2 were used to determine the coefficients. The results of the post-cruise calibration for the RINKO oxygen is shown in Fig. 2.4.5.

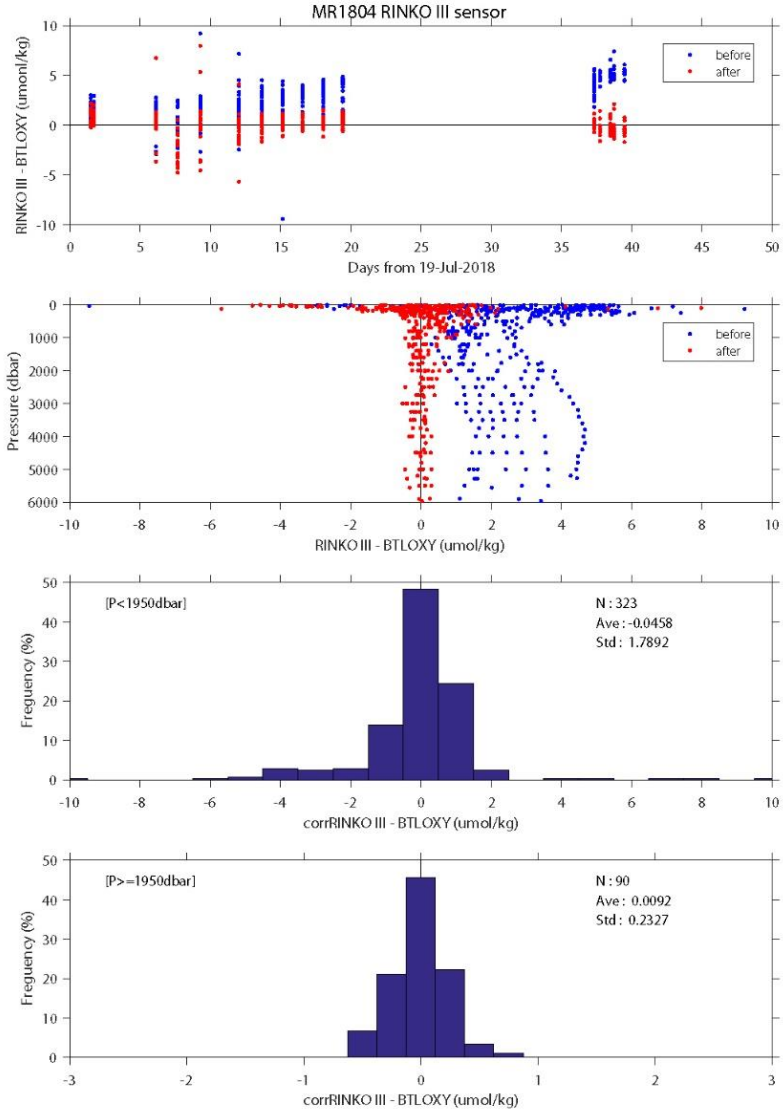

Figure 2.4.5. Difference between the CTD oxygen and the bottle oxygen. Blue and red dots indicate before and after the post-cruise calibration, respectively. Lower two panels show histogram of the difference after the calibration.

v. Fluorescence

The CTD fluorometer (FLUOR in µg/L) was calibrated by comparing with the bottle sampled chlorophyll-a as

$FLUORc = c_0 + c_1 \times FLUOR$

For $FLUOR \leq 0.2$

$c_0 = 0$, $c_1 = 0.756275283551859$

For $FLUOR > 0.2$

$c_0 = 0.0742115780165326$, $c_1 = 0.385217393469197$ (for stations K02 and 001)

$c_0 = 0.0509524615397707$, $c_1 = 0.501512975853006$ (for station 002)

$c_0 = 0.00707774735722697$, $c_1 = 0.720886546765725$ (for stations KEO, 003, 004, 005, 006)

where c_0 and c_1 are calibration coefficients. The bottle sampled data obtained at dark condition [PAR (Photosynthetically Available Radiation) < 50 μE/(m^2 sec)] were used for the calibration, since sensitivity of the fluorometer to chlorophyll *a* is different at nighttime and daytime. The results of the post-cruise calibration for the fluorometer is shown in Fig. 2.4.6.

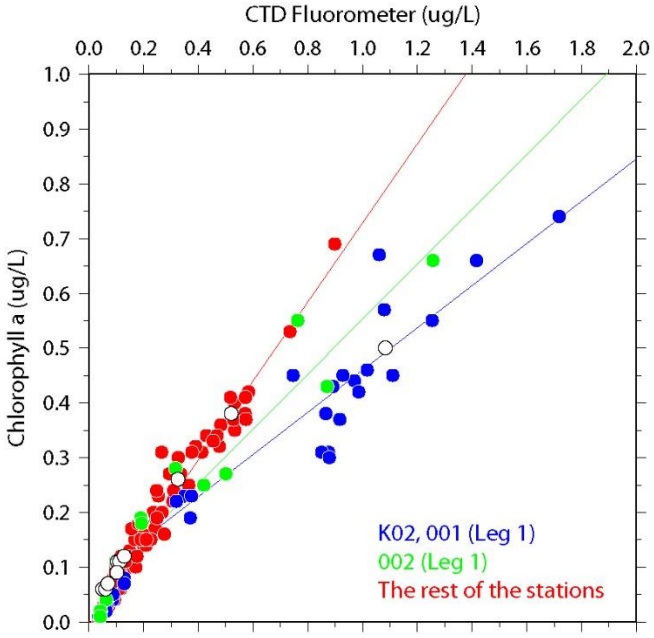

Figure 2.4.6. Comparison of the CTD fluorometer and the bottle sampled chlorophyll-a. The regression lines are also shown.

vi. Transmission

The transmissometer (T_r in %) is calibrated as

$T_r = (V–V_d) / (V_r–V_d) \times 100$

wehre V is the measured signal (voltage), V_d is the dark offset for the instrument, and V_r is the signal for clear water. V_d can be obtained by blocking the light path. V_d and V_{air}, which is the signal for air, were measured on deck before each cast after wiping the optical windows with ethanol. V_d was constant (0.0012) during the cruise. Vr is estimated from the measured maximum signal in the deep ocean at each cast. Since the transmissometer drifted in time, Vr is expressed as

$V_r = c_0 \times \exp(c_1 \times t) + c_2 \times t + c_3$

c_0 = 9.005603350864108e-02

c_1 = -0.1636953646978961

c_2 = 7.157164520392141e-03

c_3 = 4.625489007057624

where t is working time (in days) of the transmissometer from the first cast of leg 1, and c_0, c_1, c_2 and c_3 are calibration coefficients. Maximum signal was extracted for each cast. Data whose depth of the maximum signal was shallower than 1300 dbar were not used to estimate V_r.

vii. Colored dissolved organic material

It is known that output from the CDOM sensor is affected by the temperature change (Yamashita et al., 2015). The temperature effect on the CDOM sensor was evaluated in the laboratory before and after the cruise. The effect of temperature is standardized as:

$CDOM_r = CDOM / [1 + \rho \times (T - T_r)]$

$T_r = 20.0$

$\rho = -0.0062$

where CDOM is the output from the CDOM sensor, T is temperature in °C, Tr is reference temperature, and ρ is the temperature coefficient ($°C^{-1}$). Since output from the CDOM sensor was largely shifted in leg 1, the temperature coefficient evaluated after the cruise is used. In addition, Pressure hysteresis (difference between down- and up-cast profiles) was seen in the output. Therefore, the down-cast profile was corrected to much with up-cast profile as:

$CDOM_c = CDOM_r \times (1 - c_0 \times [P_{max} - P])$

$c_0 = 3.5e\text{-}6$

where P is pressure in dbar, P_{max} is maximum pressure in dbar at the cast, and c_0 is the correction coefficient.

viii. Photosynthetically active radiation

The PAR sensor was calibrated with an offset correction. The offset was estimated from the data measured in the deep ocean during the cruise. The corrected data (PARc) is calculated from the raw data (PAR) as follows:

$PARc\ [\mu E\ m^{-2}\ s^{-1}] = PAR - 0.104.$

(6) References

Edwards, B., D. Murphy, C. Janzen and N. Larson (2010): Calibration, response, and hysteresis in deep-sea dissolved oxygen measurements, J. Atmos. Oceanic Technol., 27, 920–931.

Fukasawa, M., T. Kawano and H. Uchida (2004): Blue Earth Global Expedition collects CTD data aboard Mirai, BEAGLE 2003 conducted using a Dynacon CTD traction winch and motion-compensated crane, Sea Technology, 45, 14–18.

García, H. E. and L. I. Gordon (1992): Oxygen solubility in seawater: Better fitting equations. Limnol. Oceanogr., 37 (6), 1307–1312.

Uchida, H., G. C. Johnson, and K. E. McTaggart (2010): CTD oxygen sensor calibration procedures, The GO-SHIP Repeat Hydrography Manual: A collection of expert reports and guidelines, IOCCP Rep., No. 14, ICPO Pub. Ser. No. 134. Yamashita, Y., C.-J. Liu, H. Ogawa, J. Nishioka, H. Obata, and H. Saito (2015): Application of an in situ fluorometer to determine the distribution of fluorescent organic matter in the open ocean, *Marine Chemistry*, 177, 298–305.

(7) Data archive

These data obtained in this cruise will be submitted to the Data Management Group of JAMSTEC, and will be opened to the public via "Data Research System for Whole Cruise Information in JAMSTEC (DARWIN)" in JAMSTEC web site.

<http://www.godac.jamstec.go.jp/darwin/e>

2.5 Salinity measurement

Masahide WAKITA (JAMSTEC MIO)
Kenichi KATAYAMA (MWJ)

(1) Objective

To measure bottle salinity obtained by CTD casts, bucket sampling, RAS, and the continuous sea surface water monitoring system (TSG).

(2) Methods

a. Salinity Sample Collection

Seawater samples were collected with 12 liter water sampling bottles, bucket, RAS, and TSG. The salinity sample bottles of the 250ml brown glass bottles with screw caps were used for collecting the sample water. Each bottle was rinsed three times with the sample water, and filled with sample water to the bottle shoulder. The salinity sample bottles for TSG were sealed with a plastic cone and screw cap because we took into consideration the possibility of storage for about one month. These caps were rinsed three times with the sample water before use. The bottles were stored for more than 24 hours in the laboratory before the salinity measurement.

The Kind and number of samples taken as shown as follows;

Table 2.5.1. Kind and number of samples

Kind of Samples	Number of samples
Samples for CTD and Bucket	374
Samples for RAS	88
Samples for TSG	21
Total	395

b. Instruments and Method

The salinity measurement on R/V MIRAI was carried out during the cruise of MR18-04 Leg1 using the salinometer (Model 8400B “AUTOSAL”; Guildline Instruments Ltd.: S/N 62556, 62827) with an additional peristaltic-type intake pump (Ocean Scientific International, Ltd.). Three precision digital thermometers (1502A; FLUKE: S/N B78466, B81549 and B81550) were used for monitoring the ambient temperature and the bath temperature of the salinometers.

The specifications of AUTOSAL salinometer and thermometer are shown as follows;

Salinometer (Model 8400B “AUTOSAL”; Guildline Instruments Ltd.)

Measurement Range	: 0.005 to 42 (PSU)
Accuracy	: Better than ±0.002 (PSU) over 24 hours without re-standardization
Maximum Resolution	: Better than ±0.0002 (PSU) at 35 (PSU)

Thermometer (1502A: FLUKE)

Measurement Range	: 16 to 30 deg C (Full accuracy)
Resolution	: 0.001 deg C
Accuracy	: 0.006 deg C (@ 0 deg C)

The measurement system was almost the same as Aoyama *et al.* (2002). The salinometer was operated in the air-conditioned ship's laboratory at a bath temperature of 24 deg C. The ambient temperature varied from approximately 21 deg C to 23 deg C, while the bath temperature was very stable and varied within +/- 0.002 deg C on rare occasion. The measurement for each sample was carried out with the double conductivity ratio and defined as the median of 31 readings of the salinometer. Data collection was started 5 seconds after filling the cell with the sample and it took about 10 seconds to collect 31 readings by the personal computer. Data were taken for the sixth and seventh filling of the cell after rinsing five times. In the case of the difference between the double conductivity ratio of these two fillings being smaller than 0.00002, the average value of the double conductivity ratio was used to calculate the bottle salinity with the algorithm for practical salinity scale, 1978 (UNESCO, 1981). If the difference was greater than or equal to 0.00003, an eighth filling of the cell was done. In the case of the difference between the double conductivity ratio of these two fillings being smaller than 0.00002, the average value of the double conductivity ratio was used to calculate the bottle salinity. In the case of the double conductivity ratio of eighth filling did not satisfy the criteria above, we measured a ninth filling of the cell and calculated the bottle salinity. The measurement was conducted in about 8 hours per day and the cell was cleaned with neutral detergent after the measurement of the day.

(3) Results

a. Standard Seawater

Standardization control of the salinometers were set to 608 (S/N 62556) and 487 (S/N 62827), respectively. All measurements were carried out at this setting. The values of STANDBY were 24+5136-5137 (S/N 62556) and 24+5458-5462 (S/N 62827), respectively, and those of ZERO were 0.0±0000-0001. The conductivity ratio of IAPSO Standard Seawater batch P161 was 0.99987 (the double conductivity ratio was 1.99974) and was used as the standard for salinity. 29 bottles of P161 were measured.

Fig.2.5.1 shows the time series of the double conductivity ratio for the Standard Seawater batch P161 before correction. The average of the double conductivity ratio were 1.99974 (S/N 62556) and 1.99972 (S/N 62827), and those standard deviation were 0.00001, which is equivalent to 0.0002 in salinity.

Fig.2.5.2 shows the time series of the double conductivity ratio for the Standard Seawater batch P161 after correction. The average of the double conductivity ratio after correction was 1.99974 (S/N 62827) and the standard deviation was 0.00001, which is equivalent to 0.0002 in salinity

The specifications of SSW used in this cruise are shown as follows ;

Batch	:	P161
Conductivity ratio	:	0.99987
Salinity	:	34.995
Use by	:	3rd May 2020

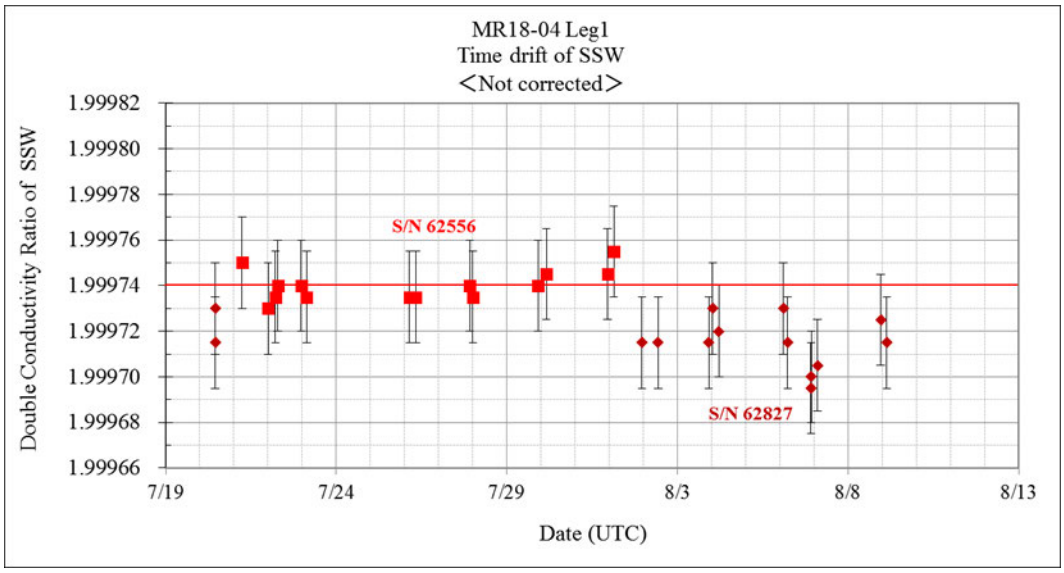

Figure 2.5.1. Time series of the double conductivity ratio for the Standard Seawater batch P161 (Before correction).

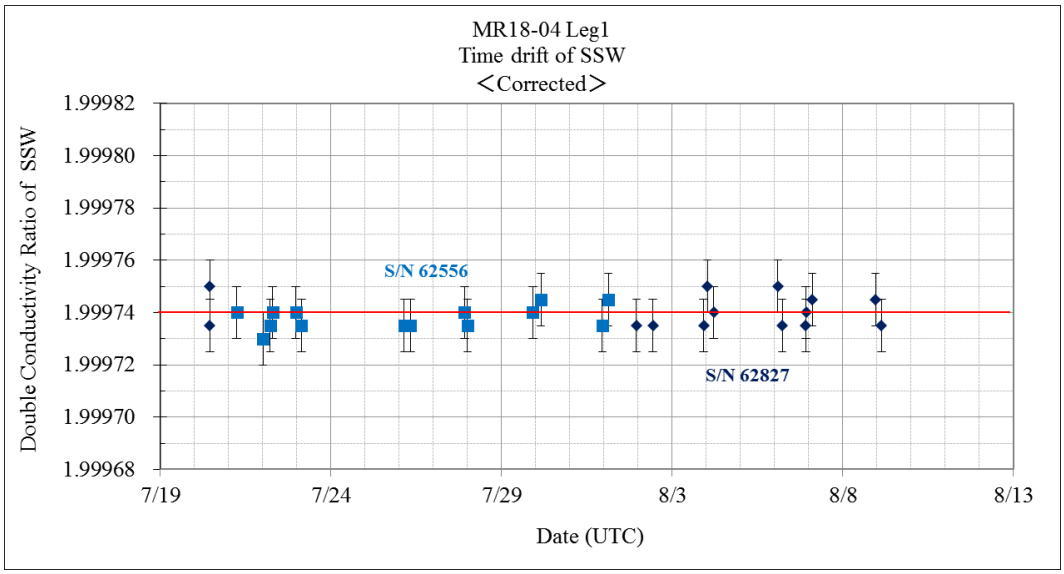

Figure 2.5.2. Time series of the double conductivity ratio for the Standard Seawater batch P161 (After correction).

b. Sub-Standard Seawater

Sub-standard seawater was made from sea water filtered by a pore size of 0.2 micrometer and stored in a 20-liter container made of polyethylene and stirred for at least 24 hours before start measuring. It was measured about every 6 samples in order to check for the possible sudden drifts of the salinometer.

c. Replicate Samples

We estimated the precision of this method using 33 pairs of replicate samples taken from the same water sampling bottle. Fig.2.5.3 shows the histogram of the absolute difference between each pair of the

replicate samples. The average and the standard deviation of absolute difference among 33 pairs of replicate samples were 0.0002 and 0.0002 in salinity, respectively.

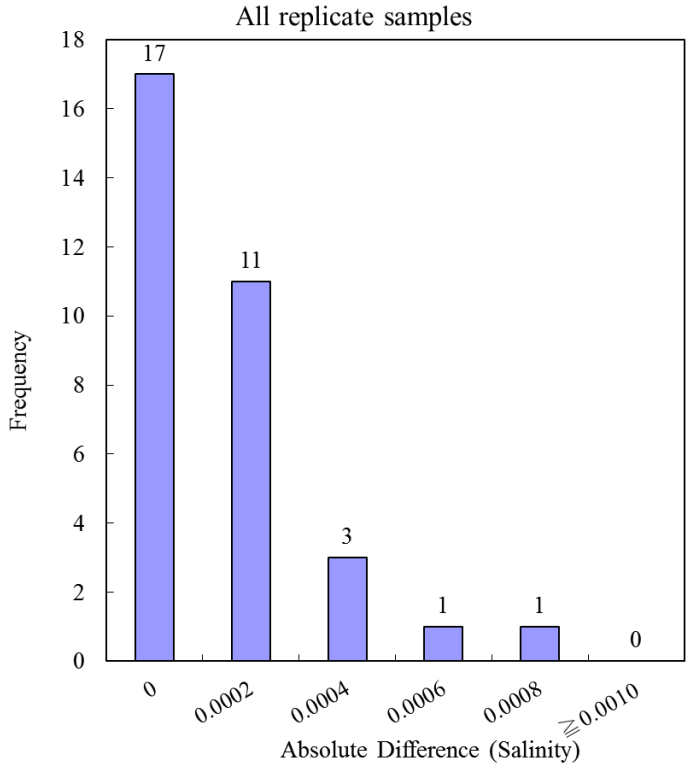

Figure 2.5.3. The histogram of the double conductivity ratio for the absolute difference of replicate samples.

(4) Data archive

These raw datasets will be submitted to JAMSTEC Data Management Group (DMG).

(5) Reference

・Aoyama, M. , T. Joyce, T. Kawano and Y. Takatsuki: Standard seawater comparison up to P129. Deep-Sea Research, I, Vol. 49, 1103～1114, 2002

・UNESCO : Tenth report of the Joint Panel on Oceanographic Tables and Standards. UNESCO Tech. Papers in Mar. Sci., 36, 25 pp., 1981

2.6. Dissolved Oxygen

Masahide WAKITA (JAMSTEC MIO)
Haruka TAMADA (MWJ)
Erii IRIE (MWJ)

(1) Objective

Determination of dissolved oxygen in seawater by Winkler titration.

(2) Parameters

Dissolved Oxygen

(3) Instruments and Methods

Following procedure is based on Winkler method (Dickson, 1996; Culberson, 1991).

i) Instruments

Burette for sodium thiosulfate and potassium iodate;

Automatic piston burette (APB-510 / APB-610 / APB-620) manufactured by Kyoto Electronics Manufacturing Co., Ltd. / 10 cm^3 of titration vessel

Detector;

Automatic photometric titrator (DOT-15X) manufactured by Kimoto Electric Co., Ltd.

Software;

DOT_Terminal Ver. 1.3.1

ii) Reagents

Pickling Reagent I: Manganese(II) chloride solution (3 mol dm^{-3})

Pickling Reagent II:

Sodium hydroxide (8 mol dm^{-3}) / Sodium iodide solution (4 mol dm^{-3})

Sulfuric acid solution (5 mol dm^{-3})

Sodium thiosulfate (0.025 mol dm^{-3})

Potassium iodate (0.001667 mol dm^{-3})

iii) Sampling

Seawater samples were collected with Niskin bottle attached to the CTD/Carousel Water Sampling System (CTD system). Seawater for oxygen measurement was transferred from the bottle to a volume calibrated flask (ca. 100 cm^3), and three times volume of the flask was overflowed. Temperature was simultaneously measured by digital thermometer during the overflowing. After transferring the sample, two reagent solutions (Reagent I and II) of 1 cm^3 each were added immediately and the stopper was inserted carefully into the flask. The sample flask was then shaken vigorously to mix the contents and to disperse the precipitate finely throughout. After the precipitate has settled at least halfway down the flask, the flask was shaken again vigorously to disperse the precipitate. The sample flasks containing pickled samples were stored in a laboratory until they were titrated.

iv) Sample measurement

For over two hours after the re-shaking, the pickled samples were measured on board. Sulfuric acid solution with its volume of 1 cm^3 and a magnetic stirrer bar were put into the sample flask and the sample was stirred. The samples were titrated by sodium thiosulfate solution whose morality was determined by potassium iodate solution. Temperature of sodium thiosulfate during titration was recorded by a digital thermometer. Dissolved oxygen concentration (μmol kg^{-1}) was calculated by sample temperature during seawater sampling, salinity of the sensor on CTD system, flask volume, and titrated volume of sodium thiosulfate solution without the blank. During this cruise, 2 sets of the titration apparatus were used.

v) Standardization and determination of the blank

Concentration of sodium thiosulfate titrant was determined by potassium iodate solution. Pure potassium iodate was dried in an oven at 130 ºC, and 1.7835 g of it was dissolved in deionized water and diluted to final weight of 5 kg in a flask. After 10 cm^3 of the standard potassium iodate solution was added to an another flask using a volume-calibrated dispenser, 90 cm^3 of deionized water, 1 cm^3 of sulfuric acid solution, and 1 cm^3 of pickling reagent solution II and I were added in order. Amount of titrated volume of sodium thiosulfate for this diluted standard potassium iodate solution (usually 5 times measurements average) gave the morality of sodium thiosulfate titrant.

The oxygen in the pickling reagents I (1 cm^3) and II (1 cm^3) was assumed to be 7.6×10^{-8} mol (Murray et al., 1968). The blank due to other than oxygen was determined as follows. First, 1 and 2 cm^3 of the standard potassium iodate solution were added to each flask using a calibrated dispenser. Then 100 cm^3 of deionized water, 1 cm^3 of sulfuric acid solution, 1 cm^3 of pickling II reagent solution, and same volume of pickling I reagent solution were added into the flask in order. The blank was determined by difference between the first (1 cm^3 of potassium iodate) titrated volume of the sodium thiosulfate and the second (2 cm^3 of potassium iodate) one. The titrations were conducted for 3 times and their average was used as the blank value.

(4) Observation log

i) Standardization and determination of the blank

Table 2.6.1 shows results of the standardization and the blank determination during this cruise.

Table 2.6.1. Results of the standardization and the blank determinations during cruise

Date (yyyy/mm/dd)	Potassium iodate ID	Sodium thiosulfate ID	DOT-15X (No.9)		DOT-15X (No.10)		Stations
			E.P. (cm^3)	Blank (cm^3)	E.P. (cm^3)	Blank (cm^3)	
2018/07/19	K1805B01	T1806A	3.960	0.000	3.960	-0.001	KEOM002, KEOM003
2018/07/24	K1805B03	T1806A	3.958	0.001	3.959	0.002	K02M002, K02M005
2018/07/28	K1805B04	T1806A	3.956	0.002	3.959	0.001	K02M007, 001M001
2018/08/01	K1805B05	T1806A	3.956	0.003	3.958	0.000	002M001, 003M001, 004M001
2018/08/06	K1805B06	T1806A	3.960	0.004	3.961	0.002	005M001, 006M001

ii) Repeatability of sample measurement

Replicate samples were taken at every CTD casts. The standard deviation of the replicate measurement (Dickson et al., 2007) was 0.12 μmol kg^{-1} (n=35).

(5) Data archives

These data obtained in this cruise will be submitted to the Data Management Group (DMG) of JAMSTEC, and will opened to the public via "Data Research System for Whole Cruise Information in JAMSTEC (DARWIN)" in JAMSTEC web site.
<http://www.godac.jamstec.go.jp/darwin/e>

(6) References

Culberson, C. H. (1991). *Dissolved Oxygen.* WHPO Publication 91-1.

Dickson, A. G. (1996). Determination of dissolved oxygen in sea water by Winkler titration. In *WOCE Operations Manual*, Part 3.1.3 Operations & Methods, WHP Office Report WHPO 91-1.

Dickson, A. G., Sabine, C. L., & Christian, J. R.(Eds.), (2007). *Guide to best practices for ocean CO_2 measurements, PICES Special Publication 3*: North Pacific Marine Science Organization.

Murray, C. N., Riley, J. P., & Wilson, T. R. S. (1968). The solubility of oxygen in Winklerreagents used for the determination of dissolved oxygen. *Deep Sea Res.*, 15, 237-238.

2.7 Nutrients

Masahide WAKITA (JAMSTEC MIO)
Shinichiro YOKOGAWA (MWJ)
Elena HAYASHI (MWJ)

(1) Objectives

The objectives of nutrients analyses during the R/V Mirai MR18-04 Leg1 cruise in the Western Pacific Ocean, of which EXPOCODE is 49NZ20180719, is as follows:

- Describe the present status of nutrients concentration with excellent comparability using certified reference material of nutrient in seawater.

(2) Parameters

The determinants are nitrate, nitrite, silicate, phosphate and ammonia in the Western Pacific Ocean

(3) Instruments and methods

(3.1) Analytical detail using QuAAtro 2-HR systems (BL TEC K.K.)

Nitrate + nitrite and nitrite are analyzed following a modification of the method of Grasshoff (1976). The sample nitrate is reduced to nitrite in a cadmium tube the inside of which is coated with metallic copper. The sample stream after reduction is treated with an acidic, sulfanilamide reagent to produce a diazonium ion. N-1-Naphthylethylenediamine Dihydrochloride added to the sample stream to produce a red azo dye. With reduction of the nitrate to nitrite, both nitrate and nitrite react and are measured; without reduction, only nitrite reacts. Thus, for the nitrite analysis, no reduction is performed and the alkaline buffer is not necessary. Nitrate is computed by difference.

The silicate method is analogous to that described for phosphate. The method used is essentially that of Grasshoff et al. (1999). Silicomolybdic acid is first formed from the silicate in the sample and molybdic acid. The silicomolybdic acid is reduced to silicomolybdous acid, or "molybdenum blue," using ascorbic acid.

The phosphate analysis is a modification of the procedure of Murphy and Riley (1962). Molybdic acid is added to the seawater sample to form phosphomolybdic acid which is in turn reduced to phosphomolybdous acid using L-ascorbic acid as the reductant.

The ammonia in seawater is mixed with an alkaline containing EDTA, ammonia as gas state is formed from seawater. The ammonia (gas) is absorbed in sulfuric acid by way of 0.5 μm pore size membrane filter (ADVANTEC PTFE) at the dialyzer attached to analytical system. The ammonia absorbed in sulfuric acid is determined by coupling with phenol and hypochlorite to form indophenols blue. Wavelength using ammonia analysis is 630 nm, which is absorbance of indophenols blue.

The details of modification of analytical methods for four parameters, Nitrate, Nitrite, Silicate and Phosphate, used in this cruise are also compatible with the methods described in nutrients section in GO-SHIP repeat hydrography manual (Hydes et al., 2010), while an analytical method of ammonium is compatible with Determination of ammonia in seawater using a vaporization membrane

permeability method (Kimura, 2000). The flow diagrams and reagents for each parameter are shown in Figures 2.7.1 to 2.7.5.

(3.2) Nitrate + Nitrite Reagents

50 % Triton solution

50 mL Triton™ X-100 provided by Sigma-Ardrich Japan G. K. (CAS No. 9002-93-1), were mixed with 50 mL Ethanol (99.5 %).

Imidazole (buffer), 0.06 M (0.4 % w/v)

Dissolve 4 g Imidazole (CAS No. 288-32-4), in 1000 mL Ultra-pure water, add 2 mL Hydrogen chloride (CAS No. 7647-01-0). After mixing, 1 mL 50 % Triton solution is added.

Sulfanilamide, 0.06 M (1 % w/v) in 1.2 M HCl

Dissolve 10 g 4-Aminobenzenesulfonamide (CAS No. 63-74-1), in 900 mL of Ultra-pure water, add 100 mL Hydrogen chloride (CAS No. 7647-01-0). After mixing, 2 mL 50 % Triton solution is added.

NED, 0.004 M (0.1 % w/v)

Dissolve 1 g N-(1-Naphthalenyl)-1,2-ethanediamine, dihydrochloride (CAS No. 1465-25-4), in 1000 mL of Ultra-pure water and add 10 mL Hydrogen chloride (CAS No. 7647-01-0). After mixing, 1 mL 50 % Triton solution is added. This reagent was stored in a dark bottle.

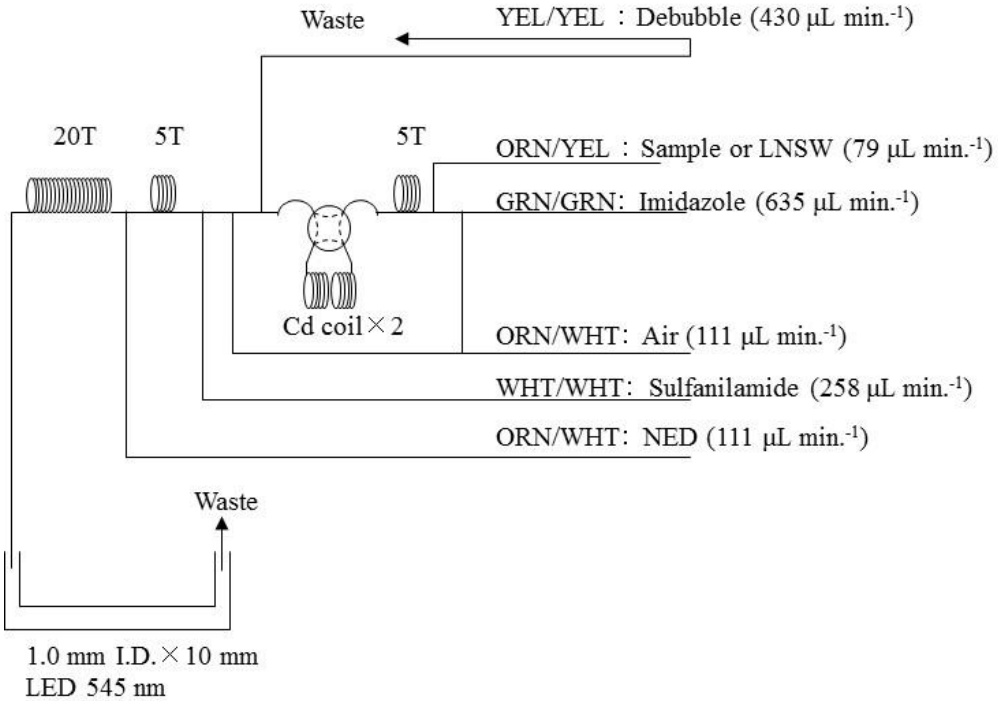

Figure 2.7.1. NO_3+NO_2 (1ch.) Flow diagram.

(3.3) Nitrite Reagents

50 % Triton solution

50 mL Triton™ X-100 provided by Sigma-Ardrich Japan G. K. (CAS No. 9002-93-1), were mixed with 50 mL Ethanol (99.5 %).

Sulfanilamide, 0.06 M (1 % w/v) in 1.2 M HCl

Dissolve 10 g 4-Aminobenzenesulfonamide (CAS No. 63-74-1), in 900 mL of Ultra-pure water, add 100 mL Hydrogen chloride (CAS No. 7647-01-0). After mixing, 2 mL 50 % Triton solution is added.

NED, 0.004 M (0.1 % w/v)

Dissolve 1 g N-(1-Naphthalenyl)-1,2-ethanediamine, dihydrochloride (CAS No. 1465-25-4), in 1000 mL of Ultra-pure water and add 10 mL Hydrogen chloride (CAS No. 7647-01-0). After mixing, 1 mL 50 % Triton solution is added. This reagent was stored in a dark bottle.

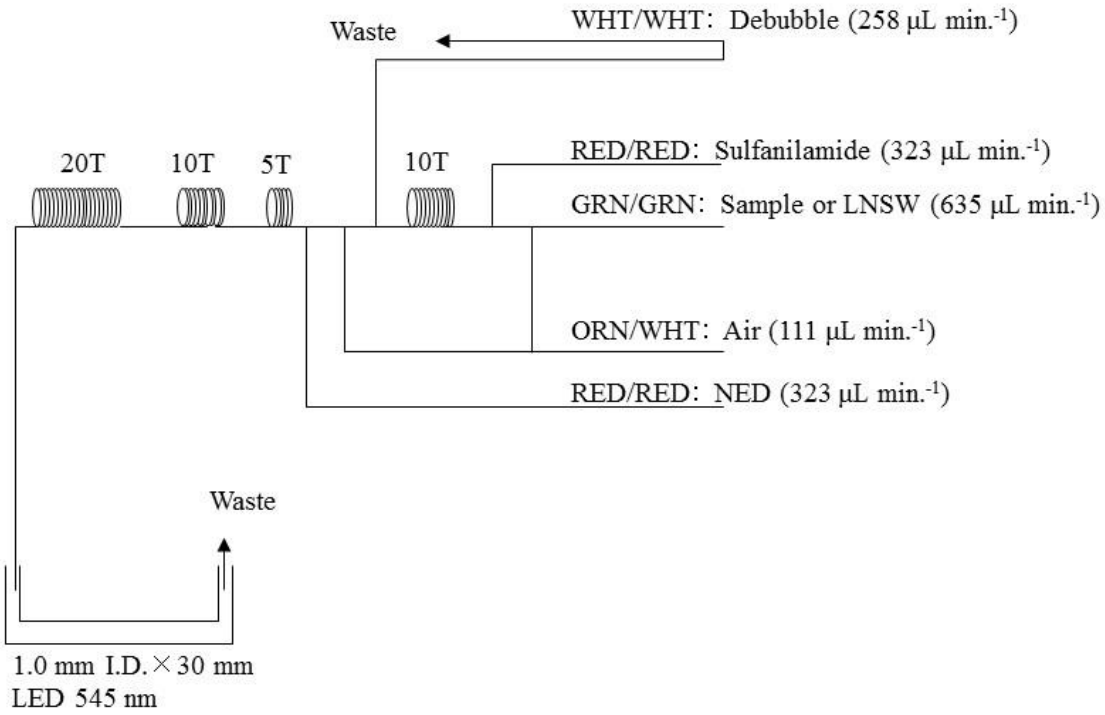

Figure 2.7.2. NO_2 (2ch.) Flow diagram.

(3.4) Silicate Reagents

15 % Sodium dodecyl sulfate solution

75 g Sodium dodecyl sulfate (CAS No. 151-21-3) were mixed with 425 mL Ultra-pure water.

Molybdic acid, 0.06 M (2 % w/v)

Dissolve 15 g Sodium molybdate dihydrate (CAS No. 10102-40-6), in 980 mL Ultra-pure water, add 8 mL Sulfuric acid (CAS No. 7664-93-9). After mixing, 20 mL 15 % Sodium dodecyl sulfate solution is added.

Oxalic acid, 0.6 M (5 % w/v)

Dissolve 50 g Oxalic acid (CAS No. 144-62-7), in 950 mL of Ultra-pure water.

Ascorbic acid, 0.01 M (3 % w/v)

Dissolve 2.5 g L-Ascorbic acid (CAS No. 50-81-7), in 100 mL of Ultra-pure water. This reagent was freshly prepared at every day.

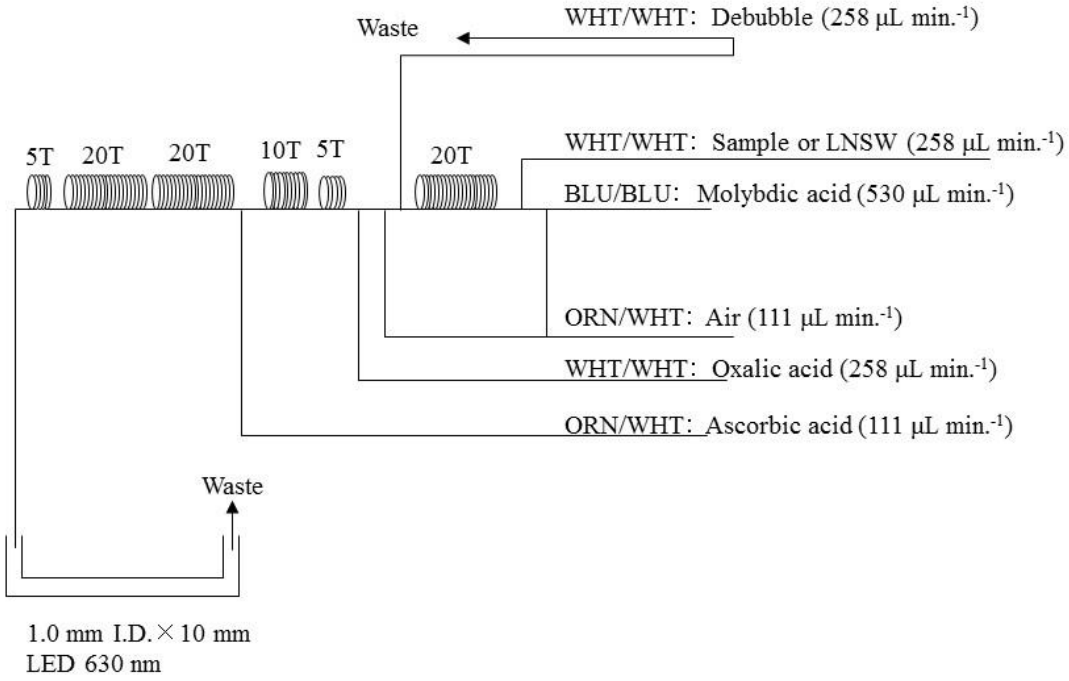

Figure 2.7.3. SiO_2 (3ch.) Flow diagram.

(4.5) Phosphate Reagents

15 % Sodium dodecyl sulfate solution

75 g Sodium dodecyl sulfate (CAS No. 151-21-3) were mixed with 425 mL Ultra-pure water.

Stock molybdate solution, 0.03 M (0.8 % w/v)

Dissolve 8 g Sodium molybdate dihydrate (CAS No. 10102-40-6), and 0.17 g Antimony potassium tartrate trihydrate (CAS No. 28300-74-5), in 950 mL of Ultra-pure water and added 50 mL Sulfuric acid (CAS No. 7664-93-9).

PO_4 color reagent

Dissolve 1.2 g L-Ascorbic acid (CAS No. 50-81-7), in 150 mL of stock molybdate solution. After mixing, 3 mL 15 % Sodium dodecyl sulfate solution is added. This reagent was freshly prepared before every measurement.

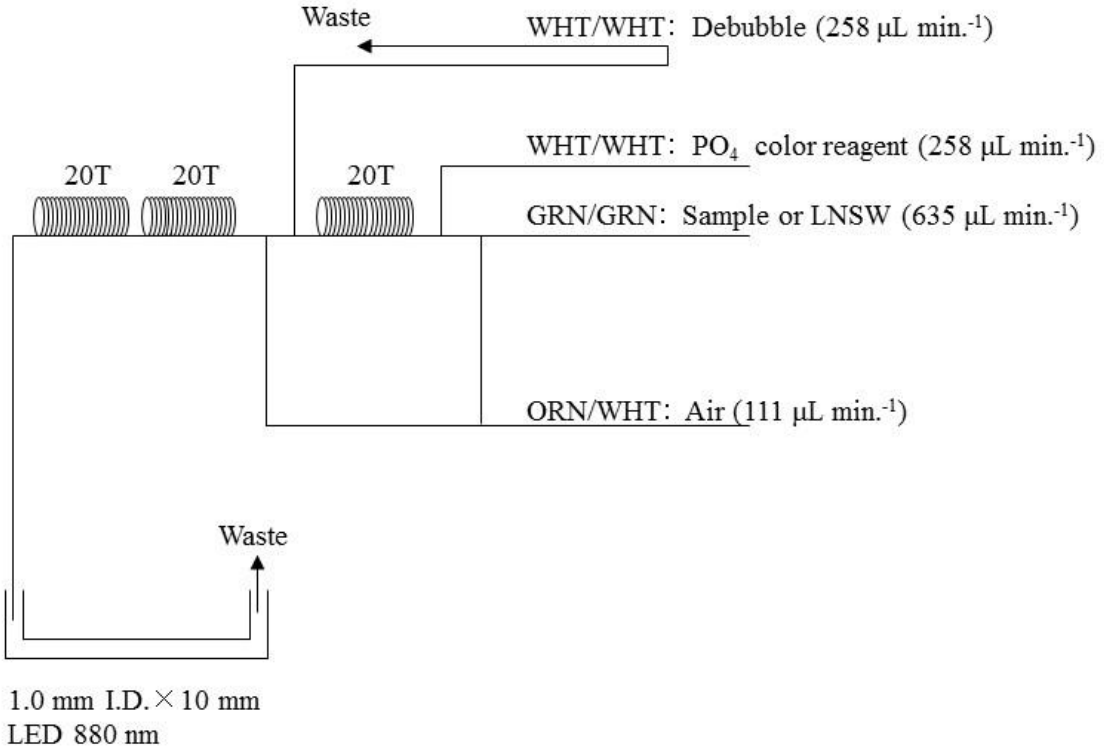

Figure 2.7.4. PO_4 (4ch.) Flow diagram.

(3.6) Ammonia Reagents

30 % Triton solution

30 mL Triton™ X-100 provided by Sigma-Ardrich Japan G. K. (CAS No. 9002-93-1), were mixed with 70 mL Ultra-pure water.

EDTA

Dissolve 41 g tetrasodium;2-[2-[bis(carboxylatomethyl)amino]ethyl-(carboxylatemethyl)amino]acetate;tetrahydrate (CAS No. 13235-36-4), and 2 g Boric acid (CAS No. 10043-35-3), in 200 mL of Ultra-pure water. After mixing, 1 mL 30 % Triton solution is added. This reagent is prepared at a week about.

NaOH liquid

Dissolve 5 g Sodium hydroxide (CAS No. 1310-73-2), and 16 g tetrasodium;2-[2-[bis(carboxylatomethyl)amino]ethyl-(carboxylatomethyl)amino]acetate;tetrahydrate (CAS No. 13235-36-4) in 100 mL of Ultra-pure water. This reagent is prepared at a week about.

Stock nitroprusside

Dissolve 0.25 g Sodium nitroferricyanide dihydrate (CAS No. 13755-38-9) in 100 mL of Ultra-pure water and add 0.2 mL 1M Sulfuric acid. Stored in a dark bottle and prepared at a month about.

Nitroprusside solution

Mix 4 mL stock nitroprusside and 5 mL 1M Sulfuric acid in 500 mL of Ultra-pure water. After mixing, 2 mL 30 % Triton solution is added. This reagent is stored in a dark bottle and prepared at every 2 or 3 days.

Alkaline phenol

Dissolve 10 g Phenol (CAS No. 108-95-2), 5 g Sodium hydroxide (CAS No. 1310-73-2) and 2 g Sodium citrate dihydrate (CAS No. 6132-04-3), in 200 mL Ultra-pure water. Stored in a dark bottle and prepared at a week about.

NaClO solution

Mix 5 mL Sodium hypochlorite (CAS No. 7681-52-9) in 45 mL Ultra-pure water. Stored in a dark bottle and fleshly prepared before every measurement. This reagent is prepared 0.3 % available chlorine.

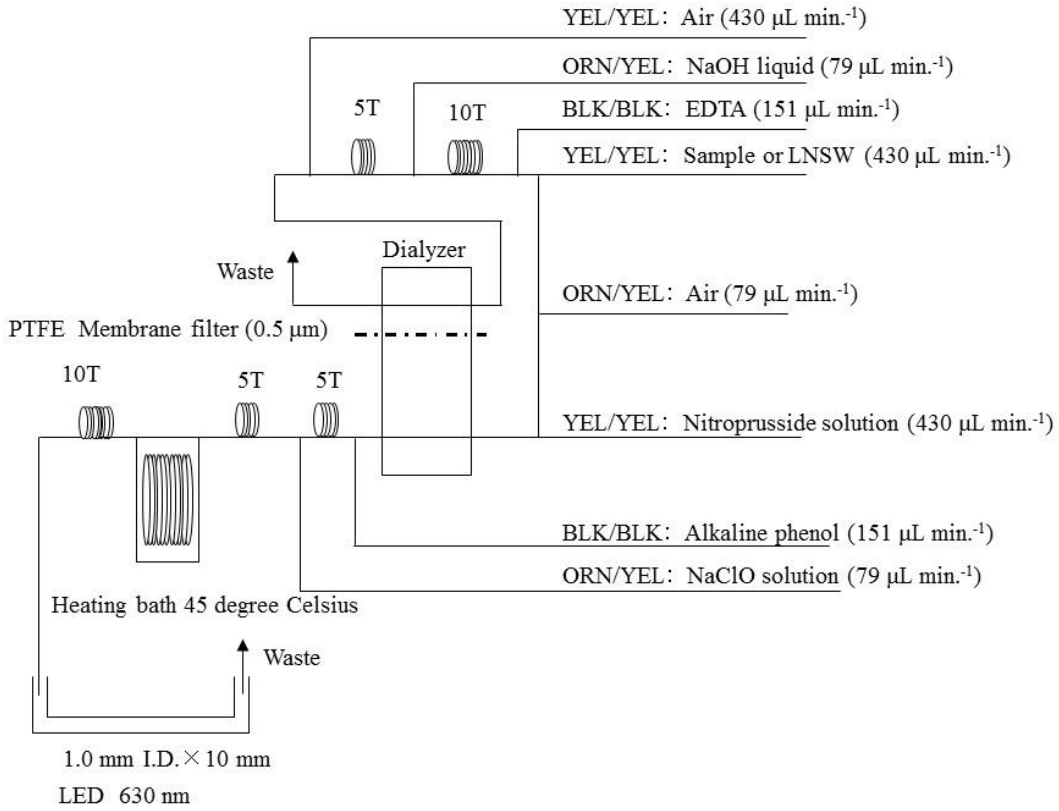

Figure 2.7.5. NH_4 (5ch.) Flow diagram.

(3.7) Sampling procedures

Sampling of nutrients followed that oxygen, salinity and trace gases. Samples were drawn into a virgin 10 mL polyacrylates vials without sample drawing tubes. These were rinsed three times before filling and vials were capped immediately after the drawing. The vials are put into water bath adjusted to ambient temperature, 22.0 ± 0.4 degree Celsius, in about 30 minutes before use to stabilize the temperature of samples.

No transfer was made and the vials were set an auto sampler tray directly. Samples were analyzed after collection within 24 hours.

(3.8) Data processing

Raw data from QuAAtro 2-HR were treated as follows:

- Check baseline shift.
- Check the shape of each peak and positions of peak values taken, and then change the positions of peak values taken if necessary.
- Carry-over correction and baseline drift correction were applied to peak heights of each samples followed by sensitivity correction.
- Baseline correction and sensitivity correction were done basically using liner regression.
- Load pressure and salinity from uncalibrate CTD data to calculate density of seawater tentatively. To calculate the final nutrients concentration we used salinity obtained bottle samples for 374 and salinity from uncalibrate CTD data for 36 samples.
- Calibration curves to get nutrients concentration were assumed second order equations.

(3.9) Summary of nutrients analysis

We made 11 QuAAtro runs for the water columns sample collected by 11 casts at 8 stations during this cruise. The total amount of layers of the seawater sample reached to 682. We made basically duplicate measurement. The station locations for nutrients measurement is shown in Fig. 2.7.6.

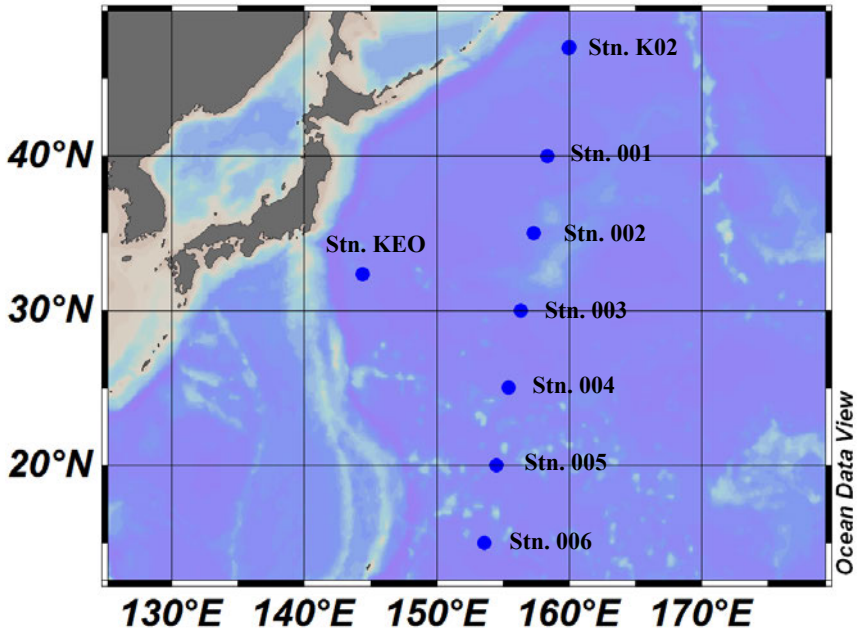

Figure 2.7.6. Sampling positions of nutrients sample.

(4) Station list

The sampling station list for nutrients is shown in Table 2.7.1.

Table 2.7.1. List of stations.

Station	Cast	Date (UTC)	Position*		Depth (m)
		(mmddyy)	Latitude	Longitude	
KEO	2	072018	32.3565N	144.3986E	5771.8
KEO	3	072018	32.3725N	144.4064E	299.8
K02	1	072518	47.0032N	160.0142E	5182.3
K02	5	072618	47.0087N	160.0115E	299.6
K02	7	072818	47.0047N	159.9981E	5176.1
001	1	073118	40.0036N	158.3363E	5446.1
002	1	080118	35.0116N	157.3259E	2003.5
003	1	080318	29.9996N	156.3278E	5785.2
004	1	080418	25.0027N	155.4019E	2001.2
005	1	080618	20.0095N	154.4791E	5851.2
006	1	080718	15.0027N	153.6008E	2000.4

*: Position indicates latitude and longitude where CTD reached maximum depth at the cast.

(5) Certified Reference Material of nutrients in seawater

KANSO CRMs (Lot: CK, CD, CJ, CB, BZ) were used to ensure the comparability and traceability of nutrient measurements during this cruise. The details of CRMs are shown below.

Production

KANSO CRMs are certified reference material (CRM) for inorganic nutrients in seawater. These were produced by KANSO Co.,Ltd. This certified reference material has been produced using autoclaved natural seawater on the basis of quality control system under ISO Guide 34 (JIS Q 0034).

KANSO Co.,Ltd. has been accredited under the Accreditation System of National Institute of Technology and Evaluation (ASNITE) as a CRM producer since 2011. (Accreditation No.: ASNITE 0052 R)

Property value assignment

The certified values are arithmetic means of the results of 30 bottles from each batch (measured in duplicates) analysed by KANSO Co.,Ltd. and Japan Agency for Marine-Earth Science and Technology (JAMSTEC) using the colorimetric method (continuous flow analysis, CFA, method). The salinity of calibration solutions were adjusted to the salinity of this CRM ± 0.5.

Metrological Traceability

Each certified value of nitrate, nitrite, and phosphate of KANSO CRMs were calibrated versus one of Japan Calibration Service System (JCSS) standard solutions for each nitrate ions, nitrite ions, and phosphate ions. JCSS standard solutions are calibrated versus the secondary solution of JCSS for each of these ions. The secondary solution of JCSS is calibrated versus the specified primary solution produced by Chemicals Evaluation and Research Institute (CERI), Japan. CERI specified primary solutionsare calibrated versus the National Metrology Institute of Japan (NMIJ) primary standards solution of nitrate ions, nitrite ions and phosphate ions, respectively.

For a certified value of silicate of KANSO CRM was determined by one of Merck KGaA silicon standard solution 1000 mg L^{-1} Si traceable to National Institute of Standards and Technology (NIST) SRM of silicon standard solution (SRM 3150).

The certified values of nitrate, nitrite, and phosphate of KASNO CRM are thus traceable to the International System of Units (SI) through an unbroken chain of calibrations, JCSS, CERI and NMIJ solutions as stated above, each having stated uncertainties. The certified values of silicate of KANSO CRM are traceable to the International System of Units (SI) through an unbroken chain of calibrations, Merck KGaA and NIST SRM 3150 solutions, each having stated uncertainties.

As stated in the certificate of NMIJ CRMs each certified value of dissolved silica, nitrate ions, and nitrite ions was determined by more than one method using one of NIST (National Institute of Standards and Technology) SRM of silicon standard solution and NMIJ primary standards solution of nitrate ions and nitrite ions. The concentration of phosphate ions as stated information value in the certificate was determined NMIJ primary standards solution of phosphate ions. Those values in the certificate of NMIJ CRMs are traceable to the International System of Units (SI).

One of analytical methods used for certification of NMIJ CRM for nitrate ions, nitrite ions, phosphate ions and dissolved silica was colorimetric method (continuous mode and batch one). The colorimetric method is same as the analytical method (continuous mode only) used for certification of KANSO CRM. For certification of dissolved silica, exclusion chromatography/isotope dilution-inductively coupled plasma mass spectrometry and Ion exclusion chromatography with post-column detection were used. For certification of nitrate ions, Ion chromatography by direct analysis and Ion chromatography after halogen-ion separation were used. For certification of nitrite ions, Ion chromatography by direct analysis was used.

NMIJ CRMs were analysed at the time of certification process for CRM and the results were confirmed within expanded uncertainty stated in the certificate of NMIJ CRMs.

(5.1) CRM for this cruise

CRM lots CK, CD, CJ, CB and BZ, which almost cover range of nutrients concentrations in the Western Pacific Ocean are prepared 7 sets.

These CRM assignments were completely done based on random number. The CRM bottles were stored at a room in the ship, REAGENT STORE, where the temperature was maintained around 20.9 degree Celsius - 25.7 degree Celsius.

(5.2) CRM concentration

We used nutrients concentrations for CRM lots CK, CD, CJ, CB and BZ as shown in Table 2.7.2.

Table 2.7.2. Certified concentration and uncertainty (k=2) of CRMs.

unit: μmol kg^{-1}

Lot	Nitrate	Nitrite	Silicate	Phosphate	Ammonia*
CK	0.02 ± 0.03	0.01 ± 0.01	0.73 ± 0.08	0.048 ± 0.012	0.84
CD	5.50 ± 0.05	0.02 ± 0.00	13.93 ± 0.10	0.446 ± 0.008	1.11
CJ	16.20 ± 0.20	0.03 ± 0.01	38.50 ± 0.40	1.190 ± 0.020	0.77
CB	35.79 ± 0.27	0.12 ± 0.01	109.20 ± 0.62	2.520 ± 0.022	0.77

BZ	43.35 ± 0.33	0.22 ± 0.01	161.00 ± 0.93	3.056 ± 0.033	0.49

*For ammonia values are references

(6) Nutrients standards

(6.1) Volumetric laboratory ware of in-house standards

All volumetric glass ware and polymethylpentene (PMP) ware used were gravimetrically calibrated. Plastic volumetric flasks were gravimetrically calibrated at the temperature of use within 4 K.

(6.1.1) Volumetric flasks

Volumetric flasks of Class quality (Class A) are used because their nominal tolerances are 0.05 % or less over the size ranges likely to be used in this work. Class A flasks are made of borosilicate glass, and the standard solutions were transferred to plastic bottles as quickly as possible after they are made up to volume and well mixed in order to prevent excessive dissolution of silicate from the glass. PMP volumetric flasks were gravimetrically calibrated and used only within 4 K of the calibration temperature.

The computation of volume contained by glass flasks at various temperatures other than the calibration temperatures were done by using the coefficient of linear expansion of borosilicate crown glass.

Because of their larger temperature coefficients of cubical expansion and lack of tables constructed for these materials, the plastic volumetric flasks were gravimetrically calibrated over the temperature range of intended use and used at the temperature of calibration within 4 K. The weights obtained in the calibration weightings were corrected for the density of water and air buoyancy.

(6.1.2) Pipettes

All pipettes have nominal calibration tolerances of 0.1 % or better. These were gravimetrically calibrated in order to verify and improve upon this nominal tolerance.

(6.2) Reagents, general considerations

(6.2.1) Specifications

For nitrate standard, “potassium nitrate 99.995 suprapur®” provided by Merck, Batch B1452165, CAS No. 7757-79-1, was used.

For nitrite standard solution, we used “nitrite ion standard solution (NO_2^- 1000) provided by Wako, Lot APR5598, Code. No. 140-06451.” This standard solution was certified by Wako using Ion chromatograph method. Calibration result is 1003 mg L^{-1} at 20 degree Celsius. Expanded uncertainty of calibration (k=2) is 0.7 % for the calibration result.

For the silicate standard, we use “Silicon standard solution SiO_2 in NaOH 0.5 M CertiPUR®” provided by Merck, Code. No. 170236, of which lot number is HC73014836 are used. The silicate concentration is certified by NIST-SRM3150 with the uncertainty of 0.7 %. HC73014836 is certified as 1000 mg L^{-1}.

For phosphate standard, “potassium dihydrogen phosphate anhydrous 99.995 suprapur®” provided by Merck, Batch B1144508, CAS No.: 7778-77-0, was used.

For ammonia standard, “Ammonium Chloride” provided by NMIJ, CAS No. 12125-02-9. We used NMIJ CRM 3011-a. The purity of this standard was greater than 99.9 %. Expanded uncertainty of calibration (k=2) is 0.065 %.

(6.2.2) Ultra-pure water

Ultra-pure water (Milli-Q water) freshly drawn was used for preparation of reagent, standard solutions and for measurement of reagent and system blanks.

(6.2.3) Low nutrients seawater (LNSW)

Surface water having low nutrient concentration was taken and filtered using 0.20 μm pore capsule cartridge filter at MR16-09 cruise on March, 2017. This water is stored in 20 L cubitainer with cardboard box.
LNSW concentrations were assigned to February, 2018 in Yokosuka JAMSTEC Head Quarters.

(6.2.4) Concentrations of nutrients for A, D, B and C standards

Concentrations of nutrients for A, D, B and C standards are set as shown in Table 2.7.3. The C standard is prepared according recipes as shown in Table 2.7.4. All volumetric laboratory tools were calibrated prior the cruise as stated in chapter (6.1) Then the actual concentration of nutrients in each fresh standard was calculated based on the ambient, solution temperature and determined factors of volumetric laboratory wares.
The calibration curves for each run were obtained using 5 levels, C-1, C-2, C-3, C-4, C-5.

Table 2.7.3. Nominal concentrations of nutrients for A, D, B and C standards.

	A	D	B	C-1	C-2	C-3	C-4	C-5
NO_3 (μM)	45000	1800	900	LNSW	9.0	18	36	54
NO_2 (μM)	21900	870	26	LNSW	0.2	0.5	1.0	1.6
SiO_2 (μM)	35800		2840	LNSW	29	58	115	171
PO_4 (μM)	6000		60	LNSW	0.6	1.2	2.4	3.6
NH_4 (μM)	4000		160	LNSW	1.6	3.2	6.4	9.6

Table 2.7.4. Working calibration standard recipes.

C Std.	B Std.
C-5	30 mL

(6.2.5) Renewal of in-house standard solutions

In-house standard solutions as stated in paragraph (6.2) were renewed as shown in Table 2.7.5 to 2.7.7.

Table 2.7.5. Timing of renewal of in-house standards.

NO_3, NO_2, SiO_2, PO_4, NH_4	Renewal
A-1 Std. (NO_3)	maximum a month
A-2 Std. (NO_2)	commercial prepared solution
A-3 Std. (SiO_2)	commercial prepared solution

A-4 Std. (PO_4)	maximum a month
A-5 Std. (NH_4)	maximum a month
D-1 Std.	maximum 8 days
D-2 Std.	maximum 8 days
B Std. (mixture of A-1, D-2, A-3, A-4 and A-5 std.)	maximum 8 days

Table 2.7.6. Timing of renewal of working calibration standards.

Working standards	Renewal
C Std. (dilute B Std.)	every 24 hours

Table 2.7.7. Timing of renewal of in-house standards for reduction estimation.

Reduction estimation	Renewal
36 μM NO_3 (dilute D-1 Std.)	when C Std. renewed
35 μM NO_2 (dilute D-2 Std.)	when C Std. renewed

(7) Quality control

(7.1) Precision of nutrients analyses during the cruise

Precision of nutrients analyses during this cruise was evaluated based on the 9 to 18 measurements, which are measured every 5 to 14 samples, during a run at the concentration of C-5 std. Summary of precisions are shown in Table 2.7.8 and Figs 2.7.7 to 2.7.11. The precisions for each parameter are generally good considering the analytical precisions during the R/V Mirai cruses conducted in 2009 - 2017. During in this cruise, analytical precisions were 0.12 % for nitrate, 0.11 % for nitrite, 0.07 % for silicate, 0.11 % for phosphate and 0.20 % for ammonia in terms of median of precision, respectively. Then we can conclude that the analytical precisions for nitrate, nitrite, silicate, phosphate and ammonia were maintained throughout this cruise.

Table 2.7.8. Summary of precision based on the replicate analyses.

	Nitrate CV %	Nitrite CV %	Silicate CV %	Phosphate CV %	Ammonia CV %
Median	0.10	0.11	0.07	0.11	0.23
Mean	0.11	0.11	0.08	0.10	0.24
Maximum	0.19	0.18	0.14	0.14	0.36
Minimum	0.06	0.08	0.04	0.05	0.09
N	10	10	10	10	10

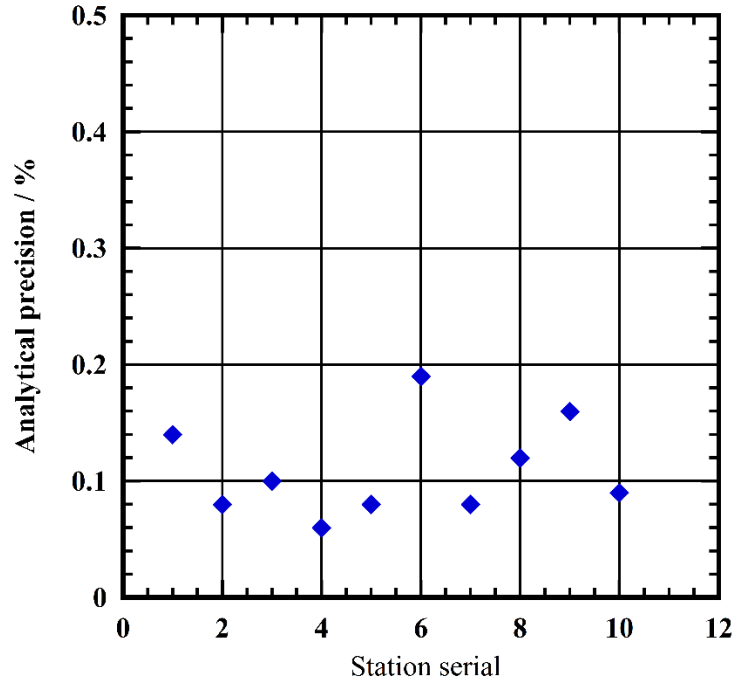

Figure 2.7.7. Time series of precision of nitrate in this cruise.

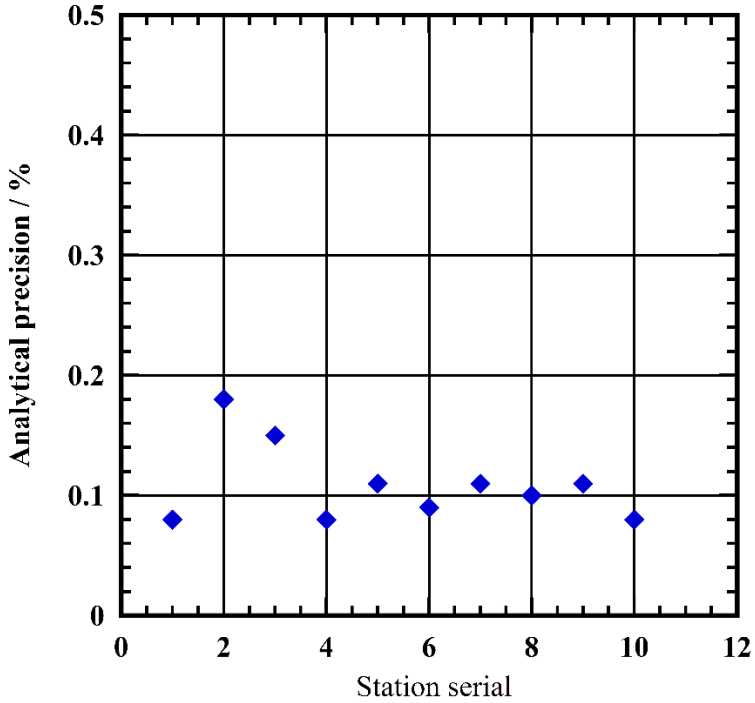

Figure 2.7.8. Time series of precision of nitrite in this cruise.

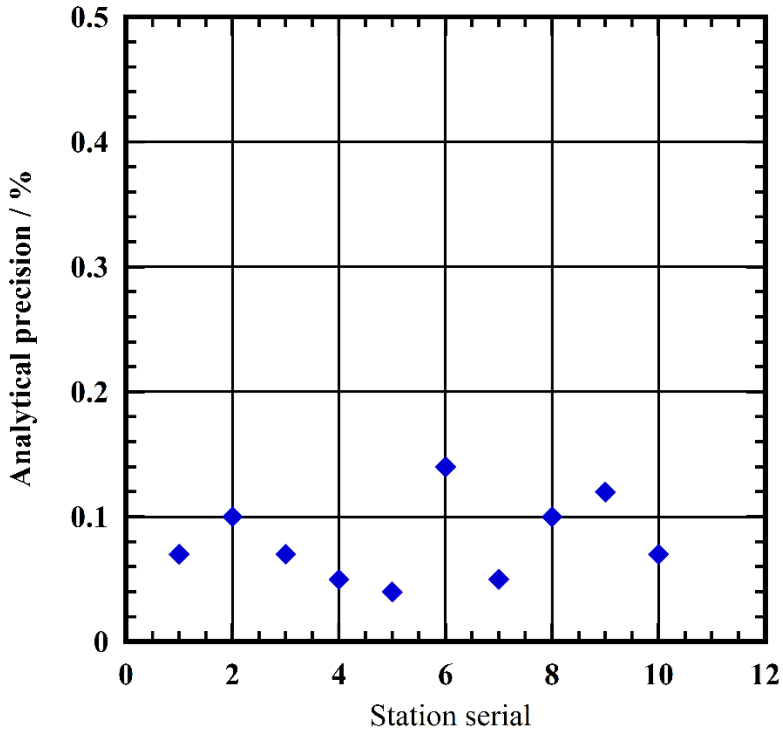

Figure 2.7.9. Time series of precision of silicate in this cruise.

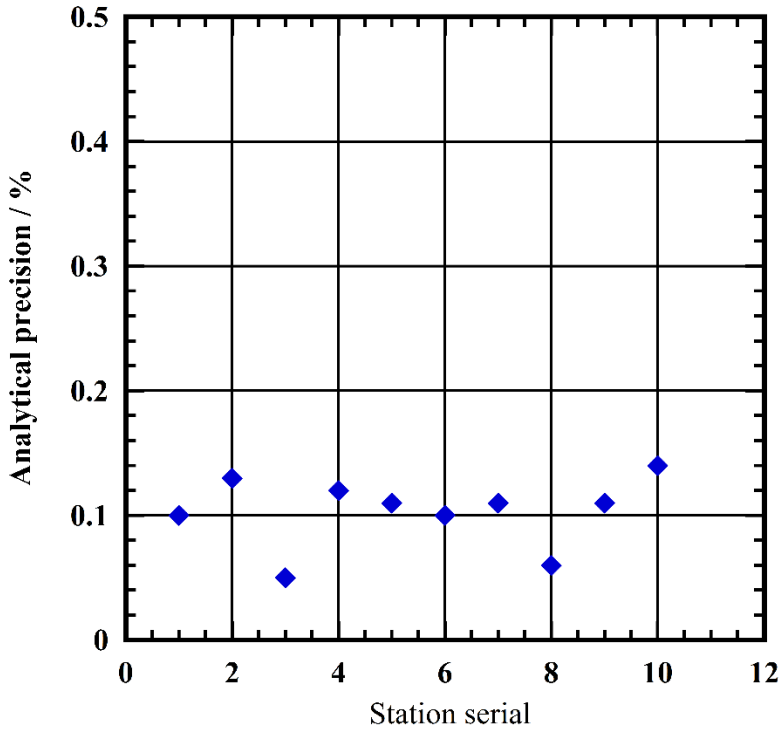

Figure 2.7.10. Time series of precision of phosphate in this cruise.

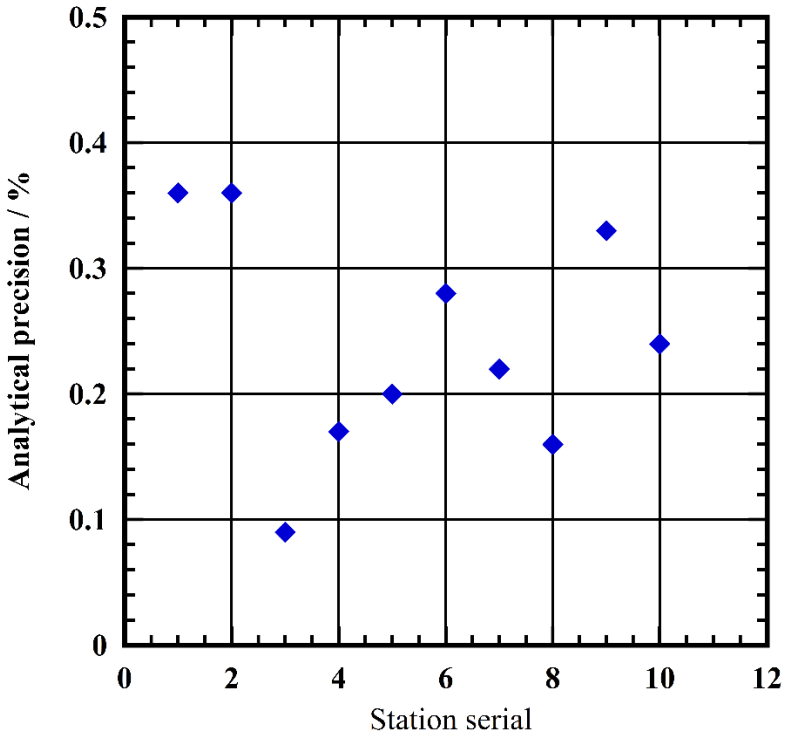

Figure 2.7.11. Time series of precision of ammonia in this cruise.

(7.2) CRM lot. BZ measurement during this cruise

CRM lot. BZ was measured every run to keep the comparability. The results of lot. BZ during this cruise are shown as 2.7.12 to 2.7.16.

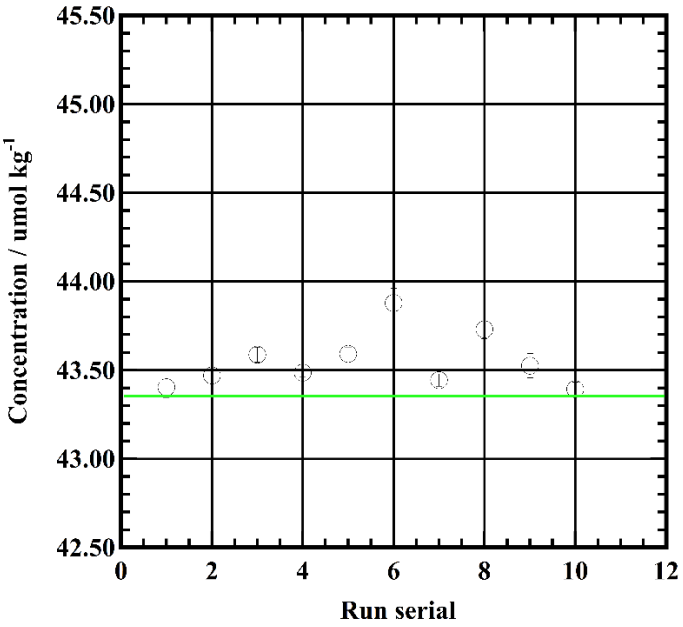

Figure 2.7.12. Time series of CRM- BZ of nitrate in this cruise.
Green line is certified nitrate concentration of CRM.

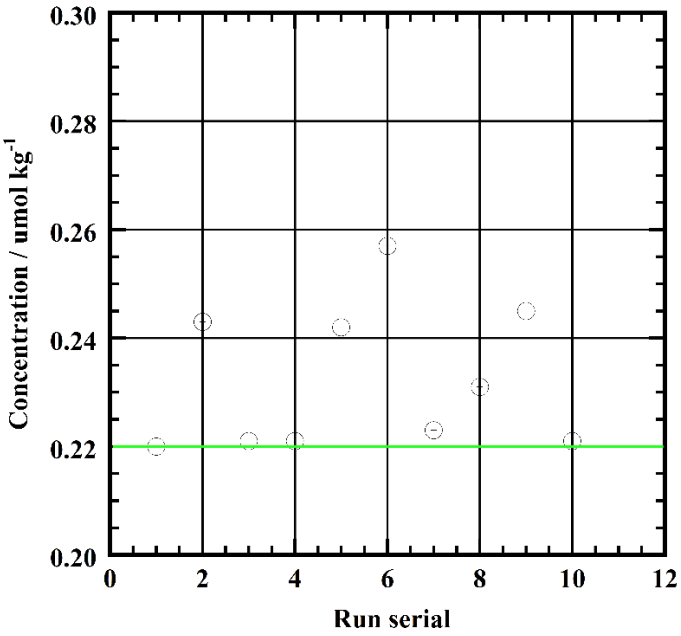

Figure 2.7.13. Time series of CRM- BZ of nitrite in this cruise. Green line is certified nitrite concentration of CRM.

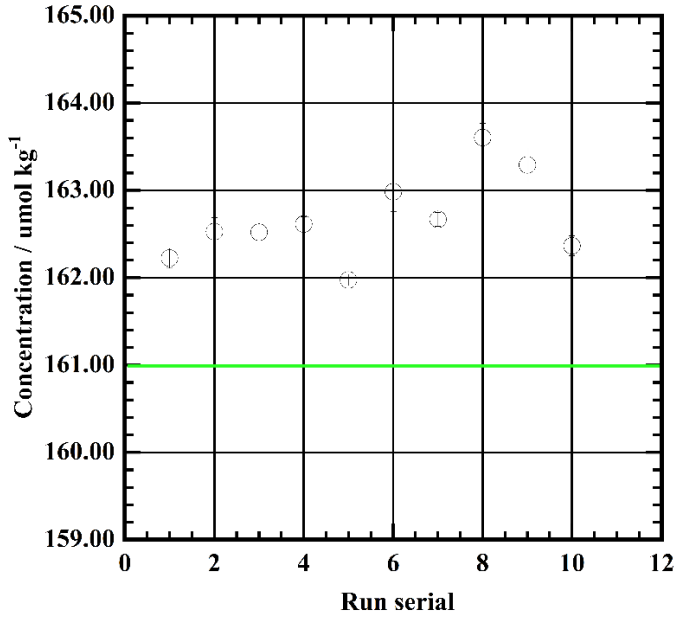

Figure 2.7.14. Time series of CRM- BZ of silicate in this cruise. Green line is certified silicate concentration of CRM.

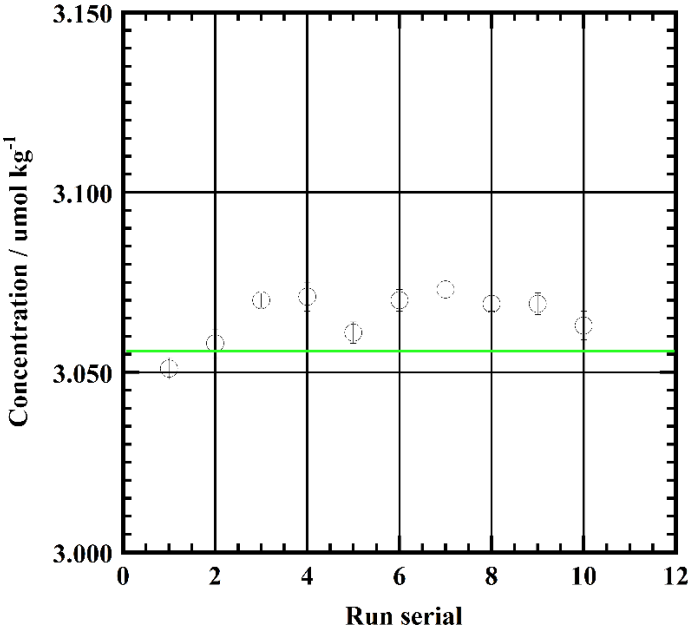

Figure 2.7.15. Time series of CRM- BZ of phosphate in this cruise.
Green line is certified phosphate concentration of CRM.

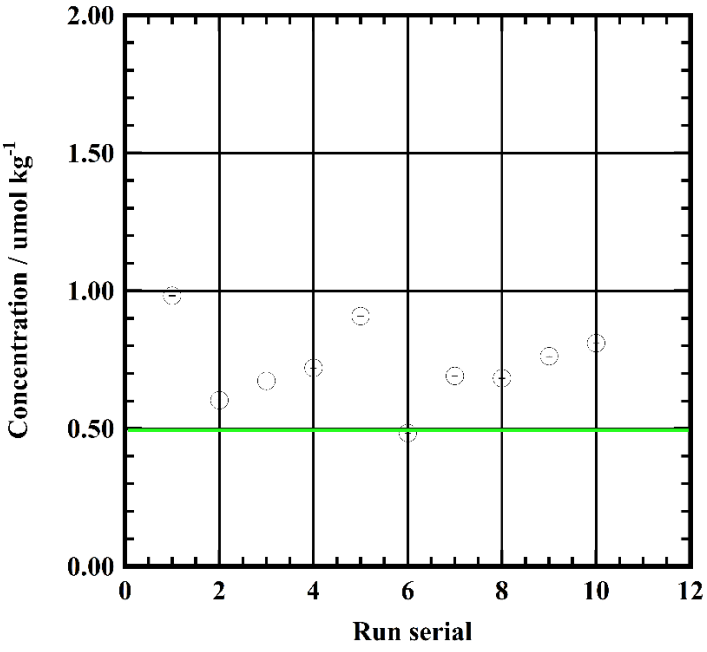

Figure 2.7.16. Time series of CRM- BZ of ammonia in this cruise.
Green line is reference value for ammonia concentration of CRM.

(7.3) Carry over

We can also summarize the magnitudes of carry over throughout the cruise. These are small enough within acceptable levels as shown in Table 2.7.9 and Figs 2.7.17 to 2.7.21.

Table 2.7.9. Summary of carry over throughout this cruise.

	Nitrate %	Nitrite %	Silicate %	Phosphate %	Ammonia %
Median	0.18	0.09	0.17	0.14	0.54
Mean	0.17	0.09	0.17	0.12	0.54
Maximum	0.22	0.15	0.21	0.20	0.68
Minimum	0.11	0.05	0.13	0.00	0.38
N	10	10	10	10	10

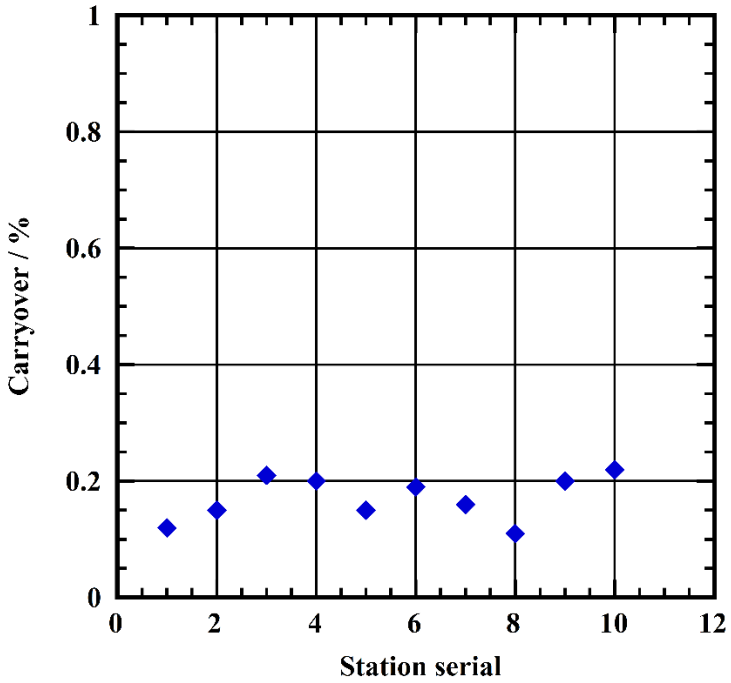

Figure 2.7.17. Time series of carry over of nitrate in this cruise.

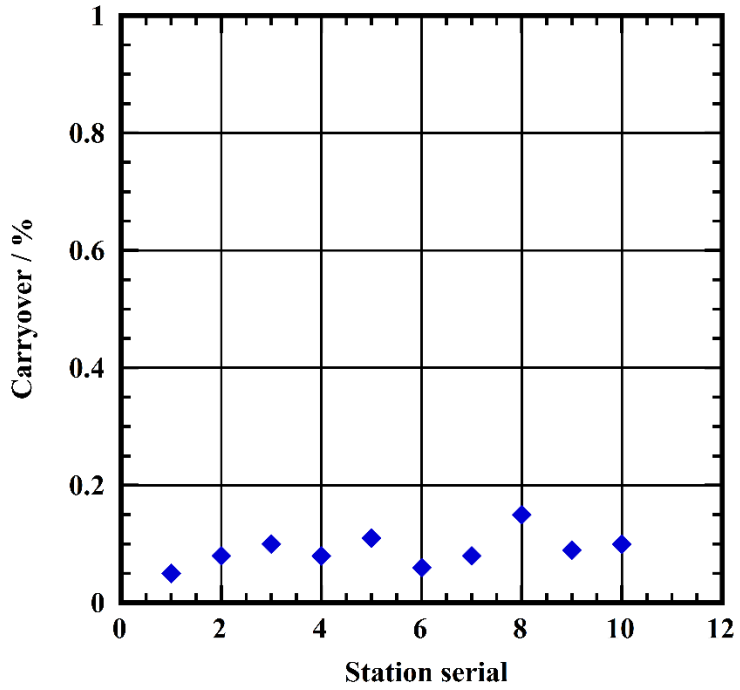

Figure 2.7.18. Time series of carry over of nitrite in this cruise.

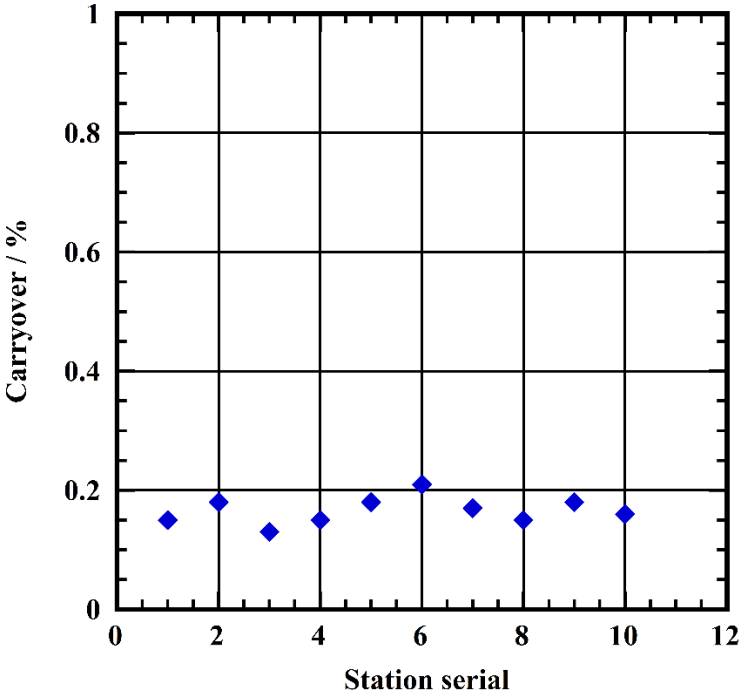

Figure 2.7.19. Time series of carry over of silicate in this cruise.

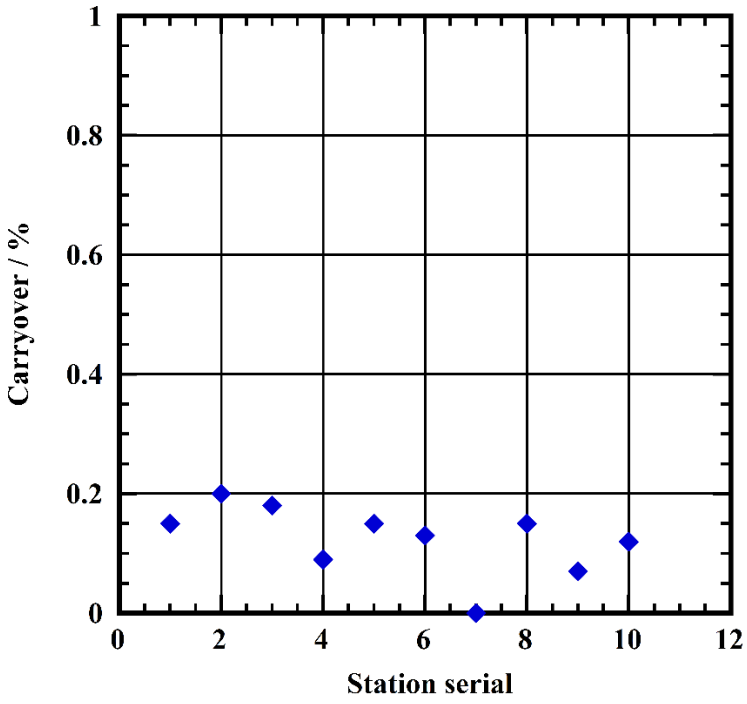

Figure 2.7.20. Time series of carry over of phosphate in this cruise.

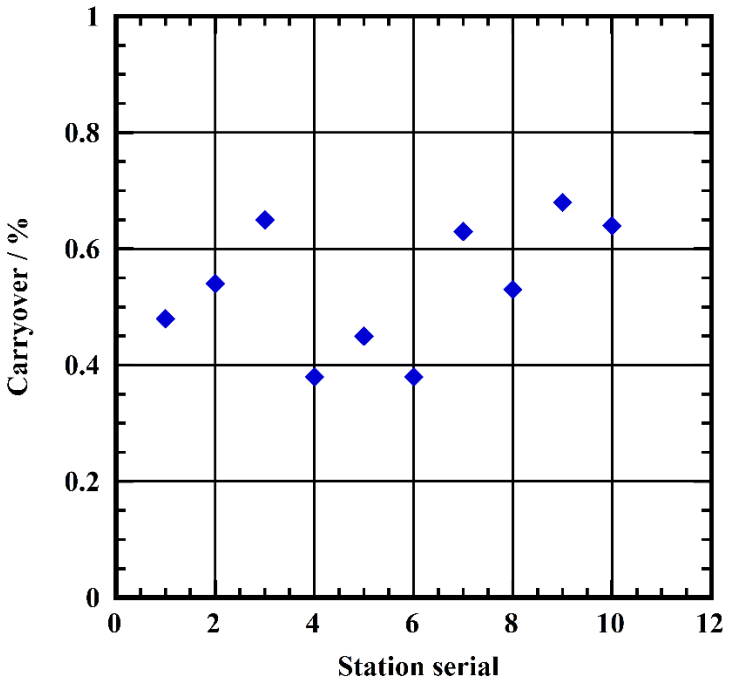

Figure 2.7.21. Time series of carry over of ammonia in this cruise.

(7.4) Estimation of uncertainty of nitrate, silicate, phosphate, nitrite and ammonia concentrations

Empirical equations, eq. (1), (2) and (3) to estimate uncertainty of measurement of nitrate, silicate and phosphate are used based on 14 measurements of 7sets of CRMs (Table 2.7.2) during this cruise. These empirical equations are as follows, respectively.

Nitrate Concentration C_{NO3} in μmol kg^{-1}:
Uncertainty of measurement of nitrate (%) =
$0.42 + 1.3241 * (1 / C_{NO3})$ --- (1)
where C_{NO3} is nitrate concentration of sample.

Silicate Concentration C_{SiO2} in μmol kg^{-1}:
Uncertainty of measurement of silicate (%) =
$0.21 + 2.6035 * (1/ C_{SiO2})$ --- (2)
where C_{SiO2} is silicate concentration of sample.

Phosphate Concentration C_{PO4} in μmol kg^{-1}:
Uncertainty of measurement of phosphate (%) =
$0.001 + 0.4987 * (1/ C_{PO4}) + 0.013361*(1/ C_{PO4})*(1/ C_{PO4})$ --- (3)
where C_{PO4} is phosphate concentration of sample.

Empirical equations, eq. (4) and (5) to estimate uncertainty of measurement of nitrite and ammonia are used based on duplicate measurements of the samples.

Nitrite Concentration C_{NO2} in μmol kg^{-1}:
Uncertainty of measurement of nitrite (%) =
$-0.07 + 0.1533 * (1 / C_{NO2}) + 0.000560*(1 / C_{NO2})*(1 / C_{NO2})$ -- (4)
where C_{NO2} is nitrite concentration of sample.

Ammonia Concentration C_{NH4} in μmol kg^{-1}:
Uncertainty of measurement of ammonia (%) =
$1.58+ 3.2224 * (1 / C_{NH4}) -0.138975 *(1 / C_{NH4})* (1 / C_{NH4})$ --- (5)
where C_{NH4} is ammonia concentration of sample.

(7.5) Detection limit and limit of quantitation of nutrients analyses during the cruise

Detection limit of nutrients analyses is 3 sigma of standard deviation of repeated measurement of LNSW, which is approximated by the following equation.

Detection limit = 10 * standard deviation of repeated measurement of LNSW

The concentration of LNSW was measured 8 to 17 times, every 5 to 14 samples during a measurement. Summary of detection limit are shown in Table 2.7.10. During in this cruise, detection limit were 0.12 μmol kg^{-1} for nitrate, 0.01 μmol kg^{-1} for nitrite, 0.21 μmol kg^{-1} for silicate, 0.009 μmol kg^{-1} for phosphate and 0.14 μmol kg^{-1} for ammonia, respectively.

Limit of quantitation of nutrients analyses is the concentration of which uncertainty is 33 % in the empirical equations, eq. (1) to (5) in 8.4. Summary of detection limit are shown in Table 2.7.10. During in this cruise, limit of quantitation were 0.04 μmol kg^{-1} for nitrate, 0.01 μmol kg^{-1} for nitrite, 0.08 μmol kg^{-1} for silicate, 0.029 μmol kg^{-1} for phosphate and 0.07 μmol kg^{-1} for ammonia, respectively.

Table 2.7.10. Summary of detection limit and limit of quantitation.

	Nitrate μmol kg^{-1}	Nitrite μmol kg^{-1}	Silicate μmol kg^{-1}	Phosphate μmol kg^{-1}	Ammonia μmol kg^{-1}
Detection limit	0.12	0.01	0.21	0.009	0.14
Limit of quantitation	0.04	0.01	0.08	0.029	0.07

(8) Problems / improvements occurred and solutions.

We found that the SiO_2 concentration of K02cast1 a few samples were higher than that of in-house standard, C-5. There was no problem in measurement, but please be careful when using this data.

The initial analytical precision for Stn.K02cast5 samples was poor/low/insufficient due to bad condition of the Cd-coil. We measured these samples again and the analytical precision was improved. The NO_3 concentrations of the second measurement were adopted.

The NH_4 measurement for Stn.005cast1 showed poor analytical precision. Due to the bad condition of the flow cell, the NH_4 concentrations for these samples are not reliable.

(9) List of reagent

List of reagent is shown in Table 2.7.11.

Table 2.7.11. List of reagents in this cruise.

IUPAC name	CAS Number	Formula	Compound Name	Manufacture	Grade
4-Aminobenzenesulfonamide	63-74-1	$C_6H_8N_2O_2S$	Sulfanilamide	Wako Pure Chemical Industries, Ltd.	JIS Special Grade
Ammonium sulfate	7783-20-2	$(NH_4)_2SO_4$	Ammonium Sulfate	National Metrology Institute of Japan	Certified Reference Material
Antimony potassium tartrate trihydrate	28300-74-5	$K_2(SbC_4H_2O_6)_2 \cdot 3H_2O$	Bis[(+)-tartrato]diantimonate(III) Dipotassium Trihydrate	Wako Pure Chemical Industries, Ltd.	JIS Special Grade
Boric acid	10043-35-3	H_3BO_3	Boric Acid	Wako Pure Chemical Industries, Ltd.	JIS Special Grade
Hydrogen chloride	7647-01-0	HCl	Hydrochloric Acid	Wako Pure Chemical Industries, Ltd.	JIS Special Grade
Imidazole	288-32-4	$C_3H_4N_2$	Imidazole	Wako Pure Chemical Industries, Ltd.	JIS Special Grade
L-Ascorbic acid	50-81-7	$C_6H_8O_6$	L-Ascorbic Acid	Wako Pure Chemical Industries, Ltd.	JIS Special Grade
N-(1-Naphthalenyl)-1,2-ethanediamine, dihydrochloride	1465-25-4	$C_{12}H_{16}Cl_2N_2$	N-1-Naphthylethylenediamine Dihydrochloride	Wako Pure Chemical Industries, Ltd.	for Nitrogen Oxides Analysis
Oxalic acid	144-62-7	$C_2H_2O_4$	Oxalic Acid	Wako Pure Chemical Industries, Ltd.	Wako Special Grade
Phenol	108-95-2	C_6H_6O	Phenol	Wako Pure Chemical Industries, Ltd.	JIS Special Grade
Potassium nitrate	7757-79-1	KNO_3	Potassium Nitrate	Merck KGaA	Suprapur®
Potassium dihydrogen phosphate	7778-77-0	KH_2PO_4	Potassium dihydrogen phosphate anhydrous	Merck KGaA	Suprapur®
Sodium citrate dihydrate	6132-04-3	$Na_3C_6H_5O_7 \cdot 2H_2O$	Trisodium Citrate Dihydrate	Wako Pure Chemical Industries, Ltd.	JIS Special Grade
Sodium dodecyl sulfate	151-21-3	$C_{12}H_{25}NaO_4S$	Sodium Dodecyl Sulfate	Wako Pure Chemical Industries, Ltd.	for Biochemistry
Sodium hydroxide	1310-73-2	NaOH	Sodium Hydroxide for Nitrogen Compounds Analysis	Wako Pure Chemical Industries, Ltd.	for Nitrogen Analysis
Sodium hypochlorite	7681-52-9	NaClO	Sodium Hypochlorite Solution	Kanto Chemical co., Inc.	Extra pure
Sodium molybdate dihydrate	10102-40-6	$Na_2MoO_4 \cdot 2H_2O$	Disodium Molybdate(VI) Dihydrate	Wako Pure Chemical Industries, Ltd.	JIS Special Grade
Sodium nitroferricyanide dihydrate	13755-38-9	$Na_2[Fe(CN)_5NO] \cdot 2H_2O$	Sodium Pentacyanonitrosylferrate(III) Dihydrate	Wako Pure Chemical Industries, Ltd.	JIS Special Grade
Sulfuric acid	7664-93-9	H_2SO_4	Sulfuric Acid	Wako Pure Chemical Industries, Ltd.	JIS Special Grade
tetrasodium;2-[2-[bis(carboxylatomethyl)amino]ethyl-(carboxylatomethyl)amino]acetate;tetrahydrate	13235-36-4	$C_{10}H_{12}N_2Na_4O_8 \cdot 4H_2O$	Ethylenediamine-N,N,N',N'-tetraacetic Acid Tetrasodium Salt Tetrahydrate (4NA)	Dojindo Molecular Technologies, Inc.	-
Synonyms: t-Octylphenoxypolyethoxyethanol 4-(1,1,3,3-Tetramethylbutyl)phenyl-polyethylene glycol Polyethylene glycol tert-octylphenyl ether	9002-93-1	$(C_2H_4O)_nC_{14}H_{22}O$	Triton™ X-100	Sigma-Aldrich Japan G.K.	-

(10) Data archives

These data obtained in this cruise will be submitted to the Data Management Group of JAMSTEC, and will be opened to the public via “Data Research System for Whole Cruise Information in JAMSTEC (DARWIN)” in JAMSTEC web site.
<http://www.godac.jamstec.go.jp/darwin/e>

(11) References

Grasshoff, K. 1976. Automated chemical analysis (Chapter 13) in Methods of Seawater Analysis. With contribution by Almgreen T., Dawson R., Ehrhardt M., Fonselius S. H., Josefsson B., Koroleff F., Kremling K. Weinheim, New York: Verlag Chemie.

Grasshoff, K., Kremling K., Ehrhardt, M. et al. 1999. Methods of Seawater Analysis. Third, Completely Revised and Extended Edition. WILEY-VCH Verlag GmbH, D-69469 Weinheim (Federal Republic of Germany).

Hydes, D.J., Aoyama, M., Aminot, A., Bakker, K., Becker, S., Coverly, S., Daniel, A., Dickson, A.G., Grosso, O., Kerouel, R., Ooijen, J. van, Sato, K., Tanhua, T., Woodward, E.M.S., Zhang, J.Z., 2010. Determination of Dissolved Nutrients (N, P, Si) in Seawater with High Precision and Inter-Comparability Using Gas-Segmented Continuous Flow Analysers, In: GO-SHIP Repeat Hydrography Manual: A Collection of Expert Reports and Guidelines. IOCCP Report No. 14, ICPO Publication Series No 134.

Kimura, 2000. Determination of ammonia in seawater using a vaporization membrane permeability method. 7th auto analyzer Study Group, 39-41.

Murphy, J., and Riley, J.P. 1962. Analytica chimica Acta 27, 31-36.

2.8. Total Alkalinity

Masahide WAKITA (JAMSTEC MIO)
Nagisa FUJIKI (MWJ)
Masahiro ORUI (MWJ)
Atsushi ONO (MWJ)

(1) Objective

Onboard total alkalinity measurement of seawater corrected in sampling bottles

(2) Methods, Apparatus and Performance

(2)-1 Seawater sampling

Seawater samples were collected by 12 L water sampling bottles mounted on the CTD/Carousel Water Sampling System and a bucket at 8 stations. The seawater from the water sampling bottle was filled into the 100 mL borosilicate glass bottles (SHOTT DURAN) using a sampling silicone rubber tube with PFA tip. The water was filled into the bottle from the bottom smoothly, without rinsing, and overflowed for 2 times bottle volume (10 seconds). These bottles were pre-washed in advance by soaking in 5 % alkaline detergent (decon90, Decon Laboratories Limited) for more than 3 hours, and then rinsed 5 times with tap water and 3 times with Milli-Q deionized water. The samples were stored in a refrigerator at approximately 5 °C before the analysis, and were put in the water bath with its temperature of about 25 °C for one hour just before analysis.

(2)-2 Seawater analyses

The total alkalinity was measured using a spectrophotometric system (Nihon ANS, Inc.) using a scheme of Yao and Byrne (1998). The calibrated volume of sample seawater (ca. 42 mL) was transferred from a sample bottle into the titration cell with its light path length of 4 cm long via dispensing unit. The TA is calculated by measuring two sets of absorbance at three wavelengths (730, 616, and 444) nm applied by the spectrometer (TM-UV/VIS C10082CAH, Hamamatsu Photonics). One is the absorbance of seawater sample before injecting an acid with indicator solution (bromocresol green sodium salt) and another the one after the injection. For mixing the acid with indicator solution and the seawater sufficiently, they are circulated through the line by a peristaltic pump equipped with periodically renewed TYGON tube 5 minutes before the measurement. Nitrogen bubble were introduced into the titration cell for degassing CO_2 from the mixed solution sufficiently.

The TA is calculated based on the following equation:

$$pH_T = 4.2699 + 0.002578 \times (35 - S) + \log((R(25) - 0.00131) / (2.3148 - 0.1299 \times R(25))) - \log(1 - 0.001005 \times S), \quad (1)$$

$$A_T = (N_A \times V_A - 10^{pHT} \times DensSW(T, S) \times (V_S + V_A)) \times (DensSW(T, S) \times V_S)^{-1}, \quad (2)$$

where R(25) represents the difference of absorbance at 616 nm and 444 nm between before and after the injection. The absorbance of wavelength at 730 nm is used to subtract the variation of absorbance caused by the system. DensSW (T, S) is the density of seawater at temperature (T) and salinity (S), N_A the concentration of the added acid, V_A and V_S the volume of added acid and seawater, respectively.

(3) Preliminary result

The repeatability of this system was provisionally 2.77 μmol kg^{-1} (n = 19) which was estimated from standard deviation of measured RM (KANSO CO., LTD) value during this cruise. A few replicate samples were taken at most of stations and the difference between each pair of analyses was plotted on a range control chart (see Fig. 2.8.1). The average of the difference was provisionally 1.44 μmol kg^{-1} (n = 34) with its standard deviation of 1.24 μmol kg^{-1}.

(4) Data archive

These data obtained in this cruise will be submitted to the Data Management Group (DMG) of JAMSTEC, and will opened to the public via "Data Research System for Whole Cruise Information in JAMSTEC (DARWIN)" in JAMSTEC web site.
<http://www.godac.jamstec.go.jp/darwin/e>

(5) References

Dickson, A. G., Sabine, C. L. & Christian, J. R. (Eds.). (2007). *Guide to best practices for ocean CO2 measurements, PICES Special Publication 3*: North Pacific Marine Science Organization.

Yao, W. and Byrne, R. H. (1998). Simplified seawater alkalinity analysis: Use of linear array spectrometers. *Deep-Sea Research I*, 45, 1383-1392.

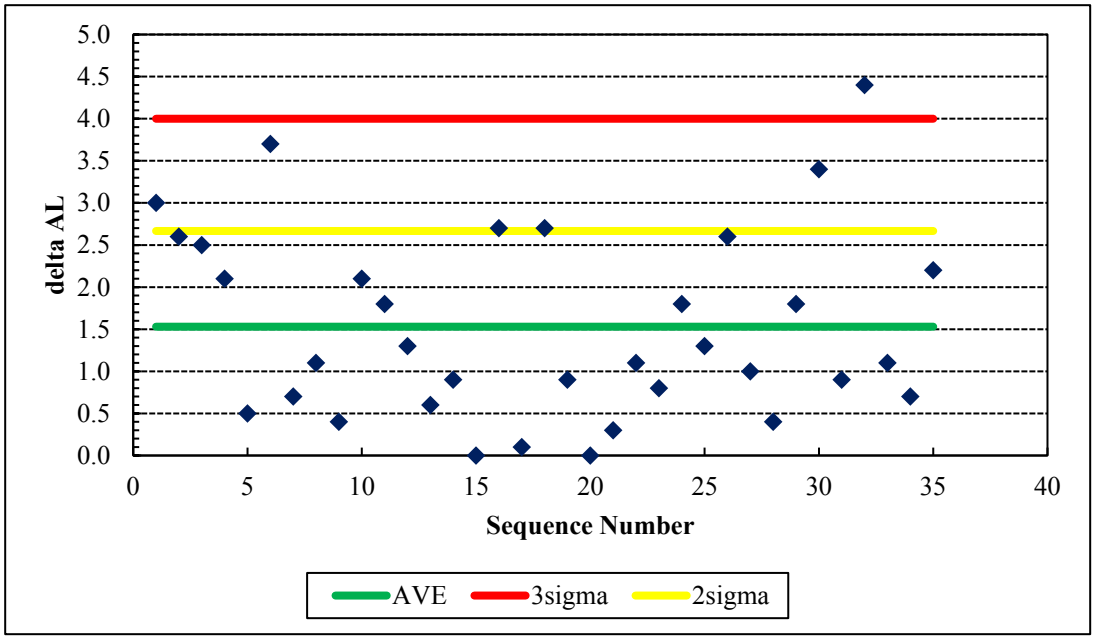

Figure 2.8.1. Range control chart of the absolute differences of replicate measurements of TA carried out during this cruise. AVE represents the average of absolute difference, 3σ the upper control limit (standard deviation of AVE × 3), and 2σ upper warning limit (standard deviation of AVE × 2).

2.9. Dissolved inorganic carbon

Masahide WAKITA (JAMSTEC MIO)
Atsushi ONO (MWJ)
Nagisa FUJIKI (MWJ)
Masahiro ORUI (MWJ)

(1) Objective

Onboard total dissolved inorganic carbon (DIC) concentration measurement of seawater collected in sampling bottles

(2) Methods, Apparatus and Performance

(2)-1 Seawater sampling

Seawater samples were collected by 12 liter water sampling bottles mounted on the CTD/Carousel Water Sampling System and a bucket at 8 stations. Seawater was sampled in a 250 mL glass bottle (SCHOTT DURAN) that was previously soaked in 5 % alkaline detergent solution (decon 90, Decon Laboratories Limited) at least 3 hours and was cleaned by fresh water for 5 times and Milli-Q deionized water for 3 times. A sampling silicone rubber tube with PFA tip was connected to the water sampling bottle when sampling was carried out. The glass bottles were filled from its bottom gently, without rinsing, and were overflowed for 20 seconds. They were sealed using the polyethylene inner lids with its diameter of 29 mm with care not to leave any bubbles in the bottle. Within about one hour after collecting the samples on the deck, the glass bottles were carried to the laboratory to be poisoned. Small volume (3 mL) of the sample (1 % of the bottle volume) was removed from the bottle and 100 μL of over saturated solution of mercury (II) chloride was added. Then the samples were sealed by the polyethylene inner lids with its diameter of 31.9 mm and stored in a refrigerator at approximately 5 °C. About one hour before the analysis, the samples were taken from refrigerator and put in the water bath kept about 20 °C.

(2)-2 Seawater analysis

Measurements of DIC were made with total CO_2 measuring system (Nihon ANS Inc.). The system comprise of seawater dispensing unit, a CO_2 extraction unit, and a coulometer (Model 3000, Nihon ANS Inc.)

The seawater dispensing unit has an auto-sampler (6 ports), which dispenses the seawater from a glass bottle to a pipette of nominal 15 mL volume. The pipette was kept at 20.00 °C ± 0.05 °C by a water jacket, in which water circulated through a thermostatic water bath (NESLAB RTE10, Thermo Fisher Scientific).

The CO_2 dissolved in a seawater sample is extracted in a stripping chamber of the CO_2 extraction unit by adding 10 % phosphoric acid solution. The stripping chamber is made approx. 25 cm long and has a fine frit at the bottom. First, a constant volume of acid is added to the stripping chamber from its bottom by pressurizing an acid bottle with nitrogen gas (99.9999 %). Second, a seawater sample kept in a pipette is introduced to the stripping chamber by the same method. The seawater and phosphoric acid are stirred by the nitrogen bubbles through a fine frit at the bottom of the stripping chamber. The stripped CO_2 is carried to the coulometer through two electric dehumidifiers

(kept at 2 °C) and a chemical desiccant (magnesium perchlorate) by the nitrogen gas (flow rate of 140 mL min^{-1}).

Measurements of system blank (phosphoric acid blank), 1.5 % CO_2 standard gas in a nitrogen base, and seawater samples (6 samples) were programmed to repeat. The variation of our own made JAMSTEC DIC reference material was used to correct the signal drift results from chemical alternation of coulometer solutions.

(3) Preliminary result

A few replicate samples were taken at most of the stations and difference between each pair of analyses was plotted on a range control chart (Fig. 2.9.1). The average of the differences was provisionally 1.13 µmol kg^{-1}, with its standard deviation of 1.01 µmol kg^{-1} (n = 32), which indicate the analysis was sufficiently accurate (< 1.5 µmol kg^{-1}) according to Dickson et al. (2007).

(4) Data archive

These data obtained in this cruise will be submitted to the Data Management Group (DMG) of JAMSTEC, and will opened to the public via "Data Research System for Whole Cruise Information in JAMSTEC (DARWIN)" in JAMSTEC web site.
<http://www.godac.jamstec.go.jp/darwin/e>

(5) Reference

Dickson, A. G., Sabine, C. L. & Christian, J. R. (Eds.). (2007). *Guide to best practices for ocean CO2 measurements, PICES Special Publication 3*: North Pacific Marine Science Organization.

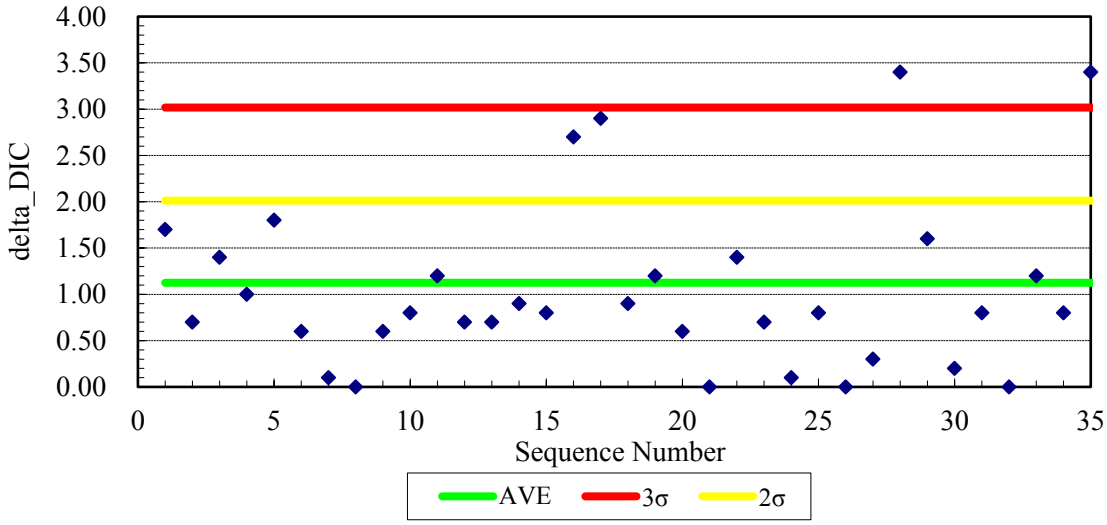

Figure 2.9.1. Range control chart of the absolute differences of replicate measurements of DIC carried out during this cruise. AVE represents the average of absolute difference, 3σ the upper control limit (standard deviation of AVE × 3), and 2σ upper warning limit (standard deviation of AVE × 2).

2.10 Dissolved organic carbon and total dissolved nitrogen

Masahide WAKITA (JAMSTEC MIO)

(1) Objectives

Variabilities in the concentration of dissolved organic carbon (DOC) in seawater have a potentially great impact on the carbon cycle in the marine system, because DOC is a major global carbon reservoir. A change by < 10% in the size of the oceanic DOC pool, estimated to be ~ 700 GtC (IPCC, 2013), would be comparable to the annual primary productivity in the whole ocean. In fact, it was generally concluded that the bulk DOC in oceanic water, especially in the deep ocean, is quite inert based upon ^{14}C-age measurements. Nevertheless, it is widely observed that in the ocean DOC accumulates in surface waters at levels above the more constant concentration in deep water, suggesting the presence of DOC associated with biological production in the surface ocean. This study presents the distribution of DOC in the western subarctic North Pacific.

(2) Sampling

Seawater samples of DOC and TDN were collected by 10 liter Niskin bottles mounted on the CTD/Carousel Water Sampling System and a bucket and brought the total to ~400. Seawater from each Niskin bottle was transferred into 60 ml High Density Polyethylene bottle (HDPE) rinsed with same water three times. Water taken from the surface to bottom is filtered using precombusted (450°C) GF/F inline filters as they are being collected from the Niskin bottle. After collection, samples are frozen upright and preserved at ~ -20 °C cold until analysis in our land laboratory. Before use, all glassware was muffled at 550 °C for 5 hrs.

(3) Analysis

Prior to analysis, samples are returned to room temperature and acidified to pH < 2 with concentrated hydrochloric acid. DOC/TDN analysis was basically made with a high-temperature catalytic oxidation (HTCO) system improved a commercial unit, the Shimadzu TOC-L with a TNM-L units (Shimadzu Co.). In this system, the non-dispersive infrared was used for carbon dioxide produced from DOC during the HTCO process (temperature: 720 °C, catalyst: 0.5% Pt-Al_2O_3). Non-purgeable dissolved nitrogen compounds are combusted and converted to NO which, when mixed with ozone, chemiluminesces for detection by a photomultiplier. The consensus reference material for DOC and TDN (Hansell 2005) was analyzed during the sample measurements.

(3) Preliminary result

The distributions of DOC and TDN will be determined as soon as possible after this cruise.

(4) Data archive

These obtained data will be submitted to JAMSTEC Data Management Group (DMG).

2.11 Particle organic matters

Yoshihisa MINO (Nagoya University)

(1) Objective

Carbon and nitrogen stable isotope ratios ($\delta^{13}C$ and $\delta^{15}N$) of particulate organic matters in the ocean can provide insights into biogeochemical processes, formation and microbial transformation of particles since a mass-dependent isotopic fractionation occurs in each pathway. In this study we examined the vertical distribution of $\delta^{13}C$ and $\delta^{15}N$ of suspended particles to elucidate particle dynamics in the upper ocean of the western subarctic North Pacific.

(2) Sampling

About 20 to 80 liters of seawater were collected by CTD-RMS at the depths from surface to 3,000 m depths, and filtered through pre-combusted GF/F filters (Whatman) and the filters were kept frozen until analysis on shore.

(3) Analysis

The filter samples of suspended particles are exposed to HCl fumes overnight to remove carbonates, dried in vacuum, and then pelletized with a tin disk. Amount of particulate organic carbon and nitrogen (POC, PN) and both isotopes of particles in the pellets are measured with an elemental analyzer combined with a continuous flow isotope-ratio mass spectrometer (Thermo Fisher Scientific).

(4) Data archive

Data will be submitted to JAMSTEC Data Data Management Group (DMG) within 2 years.

2.12 Sea surface water monitoring

Hiroshi UCHIDA (JAMSTEC RCGC)
Haruka TAMADA (MWJ)
Erii IRIE (MWJ)

(1) Objective

Our purpose is to obtain temperature, salinity, dissolved oxygen, fluorescence, and total dissolved gas pressure data continuously in near-sea surface water.

(2) Parameters

Temperature
Salinity
Dissolved oxygen
Fluorescence
Turbidity
Total dissolved gas pressure

(3) Instruments and Methods

The Continuous Sea Surface Water Monitoring System (Marine Works Japan Co. Ltd.) has four sensors and automatically measures temperature, salinity, dissolved oxygen, fluorescence, turbidity and total dissolved gas pressure in near-sea surface water every one minute. This system is located in the "sea surface monitoring laboratory" and connected to shipboard LAN-system. Measured data, time, and location of the ship were stored in a data management PC. Sea water was continuously pumped up to the laboratory from an intake placed at the approximately 4.5 m below the sea surface and flowed into the system through a vinyl-chloride pipe. The flow rate of the surface seawater was adjusted to 10 dm^3 min^{-1}.

i) Instruments

Software

Seamoni Ver.1.0.0.0

Sensors

Specifications of the each sensor in this system are listed below.

Temperature and Conductivity sensor

Model:	SBE-45, SEA-BIRD ELECTRONICS, INC.
Serial number:	4557820-0319
Measurement range:	Temperature -5 ºC - +35 ºC
	Conductivity 0 S m^{-1} - 7 S m^{-1}
Initial accuracy:	Temperature 0.002 ºC
	Conductivity 0.0003 S m^{-1}
Typical stability (per month):	Temperature 0.0002 ºC
	Conductivity 0.0003 S m^{-1}

Resolution: Temperature 0.0001 °C
Conductivity 0.00001 S m^{-1}

Bottom of ship thermometer
Model: SBE 38, SEA-BIRD ELECTRONICS, INC.
Serial number: 3857820-0540
Measurement range: -5 °C - +35 °C
Initial accuracy: ±0.001 °C
Typical stability (per 6 month): 0.001 °C
Resolution: 0.00025 °C

Dissolved oxygen sensor
Model: RINKO II, JFE ADVANTECH CO. LTD.
Serial number: 0013
Measuring range: 0 mg L^{-1} - 20 mg L^{-1}
Resolution: 0.001 mg L^{-1} - 0.004 mg L^{-1} (25 °C)
Accuracy: Saturation ± 2 % F.S. (non-linear) (1 atm, 25 °C)

Fluorescence & Turbidity sensor
Model: C3, TURNER DESIGNS
Serial number: 2300384
Measuring range: Chlorophyll in vivo 0 µg L^{-1} – 500 µg L^{-1}
Minimum Detection Limit: Chlorophyll in vivo 0.03 µg L^{-1}
Measuring range: Turbidity 0 NTU - 1500 NTU
Minimum Detection Limit: Turbidity 0.05 NTU

Total dissolved gas pressure sensor
Model: HGTD-Pro, PRO OCEANUS
Serial number: 37-394-10
Temperature range: -2 °C - 50 °C
Resolution: 0.0001 %
Accuracy: 0.01 % (Temperature Compensated)
Sensor Drift: 0.02 % per year max (0.001 % typical)

(4) Observation log

Periods of measurement, maintenance, and problems during this cruise are listed in Table 2.12.1.

Table 2.12.1. Events list of the Sea surface water monitoring during MR18-04

System Date [UTC]	System Time [UTC]	Events	Remarks
2018/07/19	07:05	All the measurements started and data was available.	Start
2018/07/24	05:01-05:17	Filter Cleaning	

2018/07/27	02:54-03:03	Filter Cleaning	
2018/07/29	04:00	All the measurements stopped.	C3 Maintenance
2018/07/29	05:30	All the measurements started.	Logging restart
2018/07/30	11:25-12:19	Invalid data has monitored.	Flow point is 0.
2018/07/31	02:07	All the measurements stopped.	Maintenance
2018/07/31	03:52	All the measurements started.	Logging restart
2018/08/03	02:14	All the measurements stopped.	Maintenance
2018/08/03	03:24	All the measurements started.	Logging restart

We took the surface water samples from this system once a day to compare sensor data with bottle data of salinity, dissolved oxygen, and twice a day to compare sensor data with bottle data of chlorophyll a. The results are shown in Fig. 2.12.1. All the salinity samples were analyzed by the Model 8400B “AUTOSAL” manufactured by Guildline Instruments Ltd. (see 2.5), and dissolve oxygen samples were analyzed by Winkler method (see 2.6), chlorophyll a were analyzed by 10-AU manufactured by Turner Designs. (see 2.14).

(a)

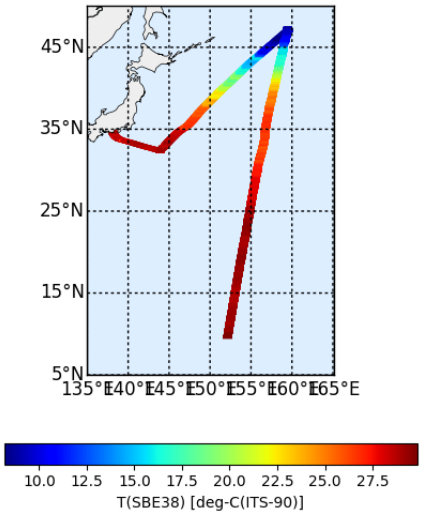

(b)

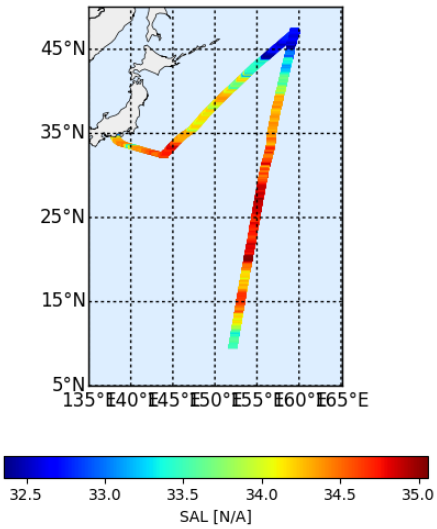
45°N
35°N
25°N
15°N
5°N
135°E
40°E
45°E
50°E
55°E
60°E
65°E
32.5
33.0
33.5
34.0
34.5
35.0
SAL [N/A]

(c)

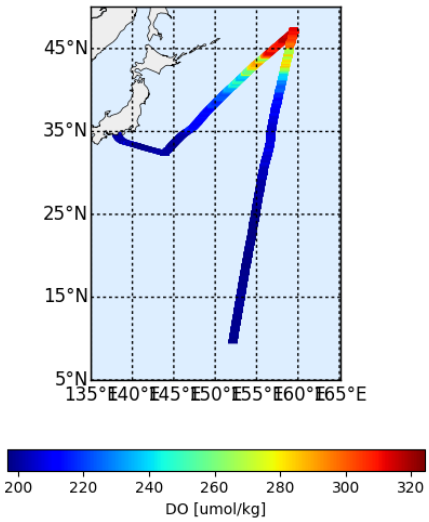
45°N
35°N
25°N
15°N
5°N
135°E
40°E
45°E
50°E
55°E
60°E
65°E
200
220
240
260
280
300
320
DO [umol/kg]

(d)

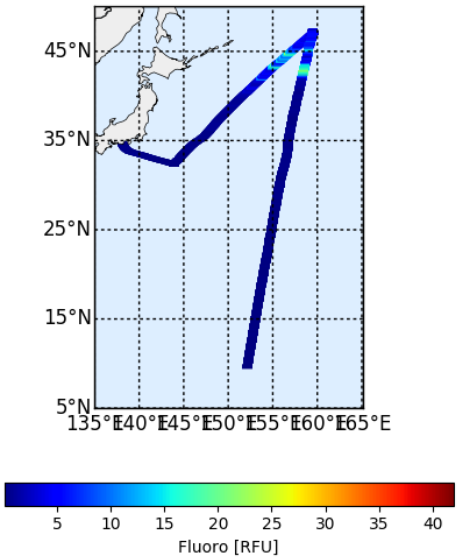

(e)

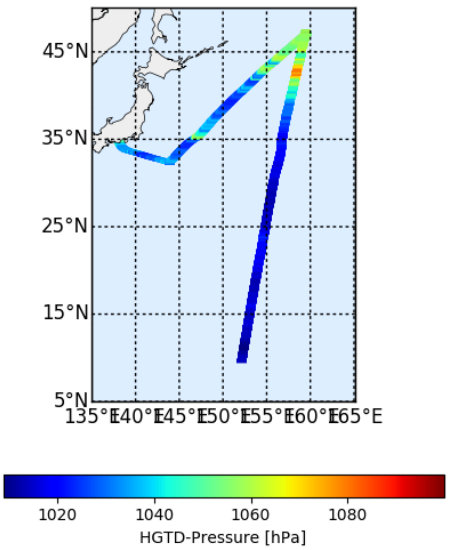

Figure 2.12.1. Spatial and temporal distribution of (a) temperature, (b) salinity, (c) dissolved oxygen, (d) fluorescence and (e) total dissolved gas pressure in MR18-04 cruise.

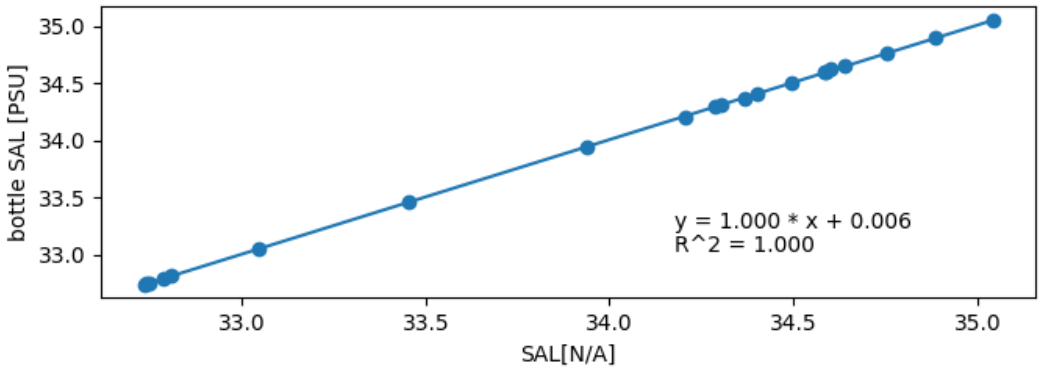

Figure 2.12.2. Correlation of salinity between sensor data and bottle data.

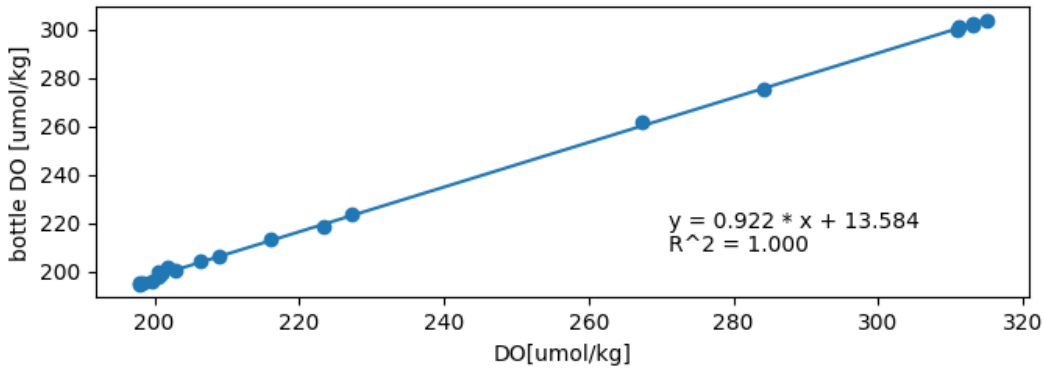

Figure 2.12.3. Correlation of dissolved oxygen between sensor data and bottle data.

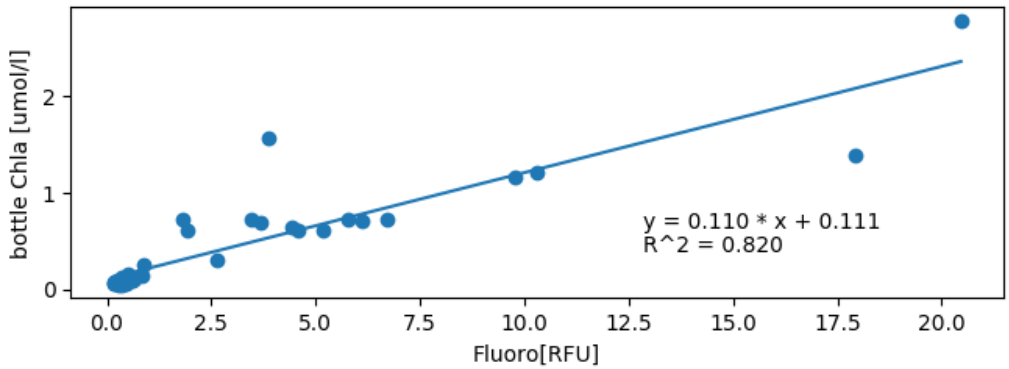

Figure 2.12.4. Correlation of fluorescence between sensor data and bottle data.

(6) Data archives

These data obtained in this cruise will be submitted to the Data Management Group (DMG) of JAMSTEC, and will opened to the public via “Data Research System for Whole Cruise Information in JAMSTEC (DARWIN)” in JAMSTEC web site.
<http://www.godac.jamstec.go.jp/darwin/e>

2.13 In situ filtration system

Yoshihisa MINO (Nagoya University)
Tetsuichi FUJIKI (JAMSTEC RCGC)
Katsunori KIMOTO (JAMSTEC RCGC)
Minoru KITAMURA (JAMSTEC RCGC)
Makio HONDA (JAMSTEC RCGC)
Yoshiyuki NAKANO (JAMSTEC MARITEC)
Kana NAGASHIMA (JAMSTEC RCGC)
Takuhei SHIOZAKI (JAMSTEC RCGC)

(1) Objective

Suspended particulate matter (SPM) in the ocean plays a vital role in the cycling of trace elements and isotopes. Even microanalyses of SPM, however, require filtering hundreds liters of seawater to collect samples. In this cruise, we deployed in situ large volume filtration system at station K2 to measure pigment, DNA, mineral and isotopic compositions as well as foraminifera shells in the suspended particles.

(2) Sampling

At K2, McLane WTS-LV samplers (with a customized battery) were deployed at eight layers for in situ pump filtration (Table 2.13.1), but some filtrations failed due to system troubles particularly during the second deployment. After fixing them on board with helps of MARITEC scientists, we conducted a test deployment at station S4, in which all pumps worked successfully.

Table 2.13.1. Setting for in situ filtration. *Pumps did not work due to system troubles.

Date & station	Depth (m)	Filtration rate (L)	Filters	Measurements	PIC
2018/07/27 K2	10	766	GF/F, 300 μm mesh	HPLC, DNA, Isotopes	Fujiki, Shiozaki, Mino
	50	859	GF/F, 300 μm mesh		
	100	0*	GF/F, 300 μm mesh		
	200	0*	GF/F, 300 μm mesh		
	500	722	GF/F, 300 μm mesh		
	1000	0*	GF/F, 300 μm mesh		
	2000	749	GF/F, 300 μm mesh		
	3000	760	GF/F, 300 μm mesh		
2017/07/28 K2	50	511	GF/F, 45 μm mesh	Carbonate particle, Mineral dust	Kimoto, Nagashima
	100	0*	GF/F, 45 μm mesh		
	150	0*	GF/F, 45 μm mesh		
	250	0*	GF/F, 45 μm mesh		
	350	0*	GF/F, 45 μm mesh		
	500	0*	GF/F, 45 μm mesh		
	600	0*	GF/F, 45 μm mesh		
	700	0*	GF/F, 45 μm mesh		

2017/08/05 S4	10 50 100 150 200 300 -- 500	210 212 195 213 169 199 -- 201	GF/F, 45 μm mesh GF/F, 45 μm mesh GF/F, 45 μm mesh GF/F, 45 μm mesh GF/F, 45 μm mesh GF/F, 45 μm mesh -- GF/F, 45 μm mesh	Carbonate particle, Isotopes	Kimoto, Mino

(3) Analysis

Particles larger than 45 μm were rinsed by fresh water and fixed by the ethanol (99.5 %). Carbonate shelled foraminifera was picked up by the brush under the stereomicroscope and dried on the assemblage slide at room temperature. Their shell density will be measured by Micro-focus X-ray CT (MXCT, ScanXmate-DF160TS105, Comscan Tecno, Co.Ltd) installed in JAMSTEC HQ.
For mineral analyses, filter samples were stored frozen. Mineral compositions will be measured for particles less than 45 μm using a X-ray diffractometer (X'Pert Pro, PANalytical) at JAMSTEC HQ. In addition, shape, size, and trace elements for each mineral grain will be measured using SEM (Quanta 450 FEG, FEI)-EDS (Octane Elite Plus 30, EDAX) and Cathodoluminescence (Mono CL4 Swift, Gatan) at JAMSTEC.

Phytoplankton pigments in the SPM on GF/F were extracted with *N,N*-dimethylformamide for at least 24 h at –20 °C in the dark and then analyzed with an HPLC modular system (Agilent Technologies) on the sea.

For DNA analysis, filter SPM samples were put in the vial including 1 ml of DNA-degradation inhibitor (0.25 M EDTA, 20 % DMSO, and saturated NaCl liquid). The samples will be analyzed at Tsukuba University.

For isotope analysis, filter samples were stored frozen, and their $\delta^{13}C$ and $\delta^{15}N$ will be measured by using EA-IRMS at Nagoya University.

(4) Data archive

Data will be submitted to JAMSTEC Data Data Management Group (DMG) within 2 years.

2.14 Phytoplankton

2.14(a) Chlorophyll *a* measurements by fluorometric determination

Tetsuichi FUJIKI (JAMSTEC RCGC)
Tomomi SONE (MWJ)
Hiroshi HOSHINO (MWJ)
Masanori ENOKI (MWJ)
Yoshiaki SATO (MWJ)

(1) Objective

Phytoplankton biomass can estimate as the concentration of chlorophyll *a*, because all oxygenic photosynthetic plankton contain chlorophyll *a*. Phytoplankton exist various species in the ocean, but the species are roughly characterized by their cell size. The objective of this study is to investigate the vertical distribution of phytoplankton and their size fractionations as chlorophyll *a* by using the fluorometric determination.

(2) Parameters

Total chlorophyll *a*
Size-fractionated chlorophyll *a*

(3) Instruments and Methods

We collected samples for total chlorophyll a from 10 to 19 depths and size-fractionated chlorophyll *a* from 8 depths between the surface and 300 m depth including a chlorophyll *a* maximum layer. The chlorophyll *a* maximum layer was determined by a Chlorophyll Fluorometer (Seapoint Sensors, Inc.) attached to the CTD system.

Seawater samples for total chlorophyll *a* were vacuum-filtrated (< 0.02 MPa) through glass microfiber filter (Whatman GF/F, 25mm-in diameter). Seawater samples for size-fractionated chlorophyll *a* were passed through 10 μm, 3 μm and 1 μm polycarbonate filters (Nuclepore filter, 47-mm in diameter) and glass microfiber filter (Whatman GF/F, 25mm-in diameter) under gentle vacuum (< 0.02 MPa). Phytoplankton pigments retained on the filters were immediately extracted in a polypropylene tube with 7 ml of N,N-dimethylformamide (FUJIFILM Wako Pure Chemical Corporation Ltd.) (Suzuki and Ishimaru, 1990). The tubes were stored at -20 °C under the dark condition to extract chlorophyll *a* at least for 24 hours.

Chlorophyll *a* concentrations were measured by the fluorometer (10-AU, TURNER DESIGNS), which was previously calibrated against a pure chlorophyll *a* (Sigma-Aldrich Co., LLC). To estimate the chlorophyll *a* concentrations, we applied to the fluorometric “Non-acidification method” (Welschmeyer, 1994).

(4) Station list

The number of samples, stations and the sampling positions were shown in Table 2.14(a).2 and Fig. 2.14(a).1.

(5) Preliminary Results

The results of total chlorophyll *a* at station KEO, K02 and 001 to 006 were shown in Fig. 2.14(a).2 to Fig. 2.14(a).5. The results of size fractionated chlorophyll *a* at station KEO, K02, 002,004 and 006 were shown in Fig. 2.14(a).6 to Fig. 2.14(a).10. At each station, water samples were taken in replicate for water of chlorophyll *a* maximum layer. Results of replicate samples were shown in table 2.14(a).1.

(6) Data archives

These data obtained in this cruise will be submitted to the Data Management Group of JAMSTEC, and will be opened to the public via "Data Research System for Whole Cruise Information in JAMSTEC (DARWIN)" in JAMSTEC web site.
http://www.godac.jamstec.go.jp/darwin/e

(7) Reference

Suzuki, R., and T. Ishimaru (1990), An improved method for the determination of phytoplankton chlorophyll using N, N-dimethylformamide, *J. Oceanogr. Soc. Japan*, 46, 190-194.

Welschmeyer, N. A. (1994), Fluorometric analysis of chlrophyll *a* in the presence of chlorophyll *b* and pheopigments. *Limnol. Oceanogr.* 39, 1985-1992.

Table 2.14(a).1. Results of the replicate sample measurements.

	All samples
Number of replicate sample pairs	21
Standard deviation ($\mu g\ L^{-1}$)	0.01

Table 2.14(a).2. Number of samples and casts.

	Number of samples	Number of casts
Total chlorophyll *a*	186	11
size-fractionated chlorophyll *a*	40	5

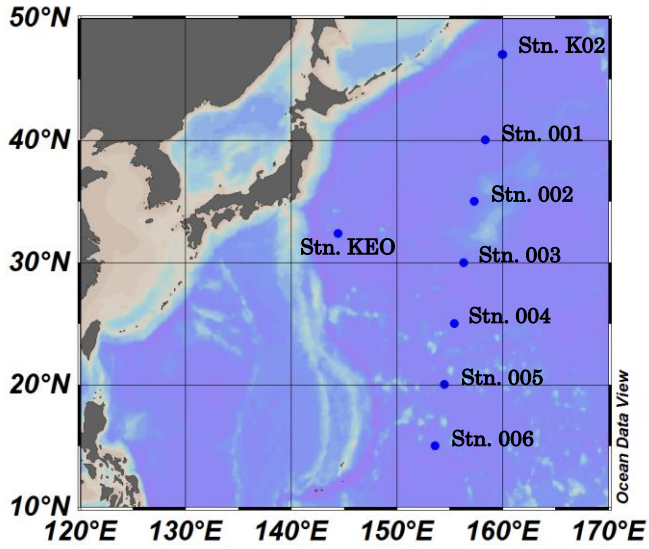

Figure 2.14(a).1. Sampling position of chlorophyll *a* samples in MR18-04Leg1.

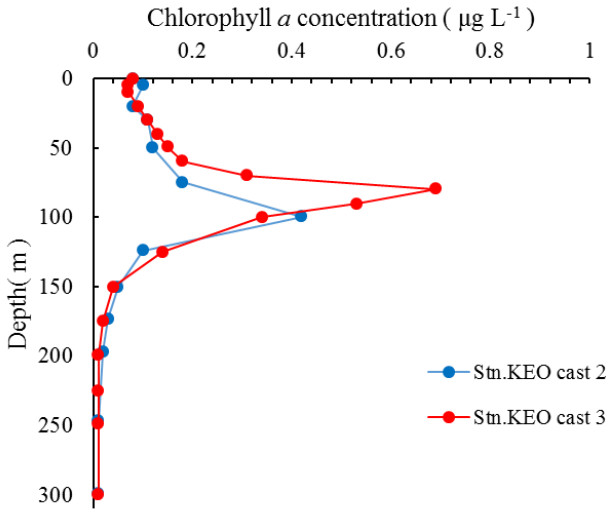

Figure 2.14(a).2. Vertical distribution of chlorophyll *a* at Stn.KEO cast 2 and 3.

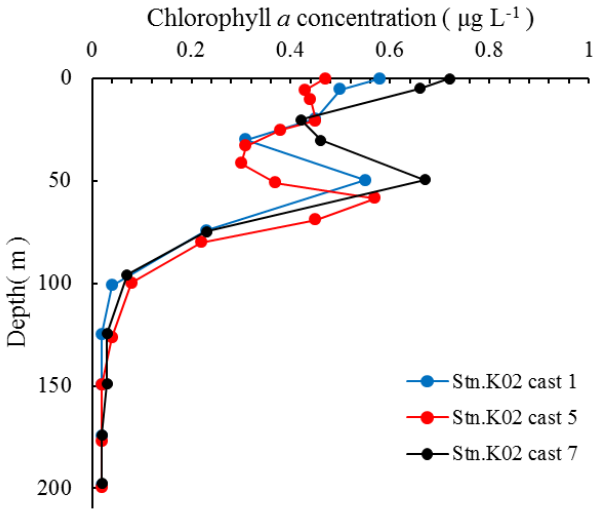

Figure 2.14(a).3. Vertical distribution of chlorophyll *a* at Stn.K02 cast 1, 5, and 7.

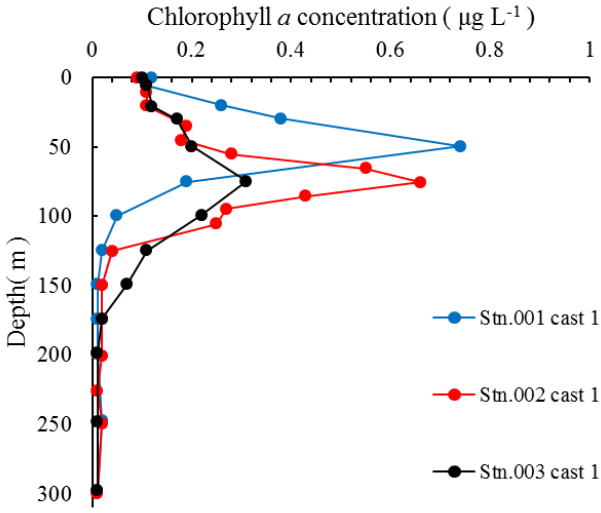

Figure 2.14(a).4. Vertical distribution of chlorophyll *a* at Stn.001, 002 and 003.

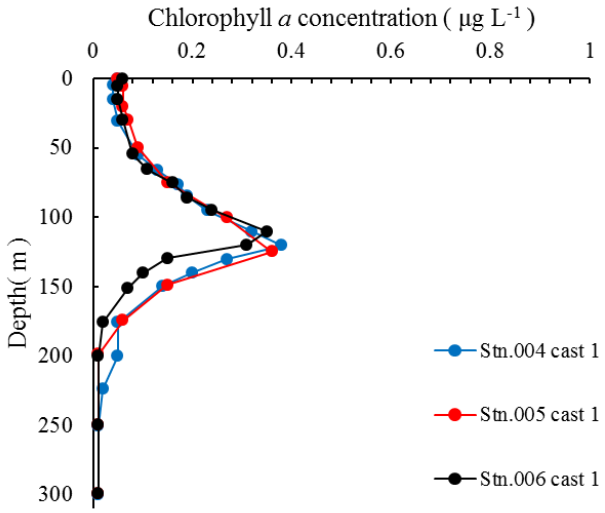

Figure 2.14(a).5. Vertical distribution of chlorophyll *a* at Stn.004, 005 and 006.

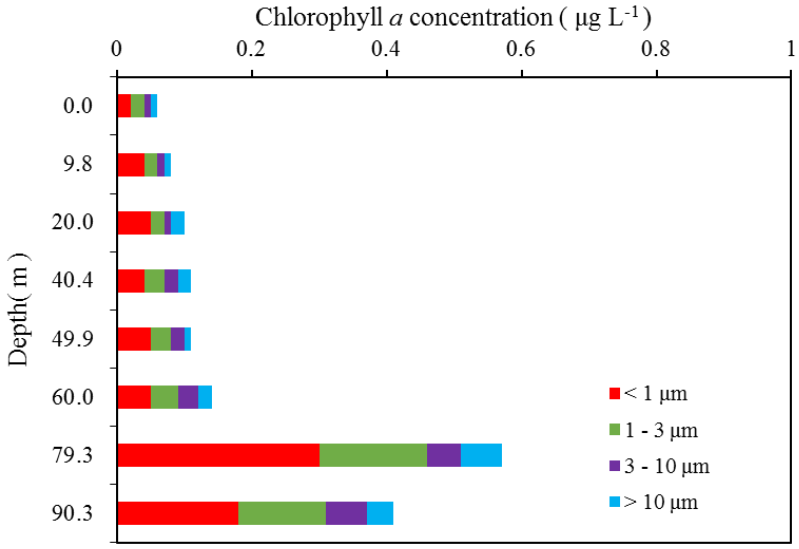

Figure 2.14(a).6. Vertical distribution of size-fractionated chlorophyll *a* at Stn.KEO cast3.

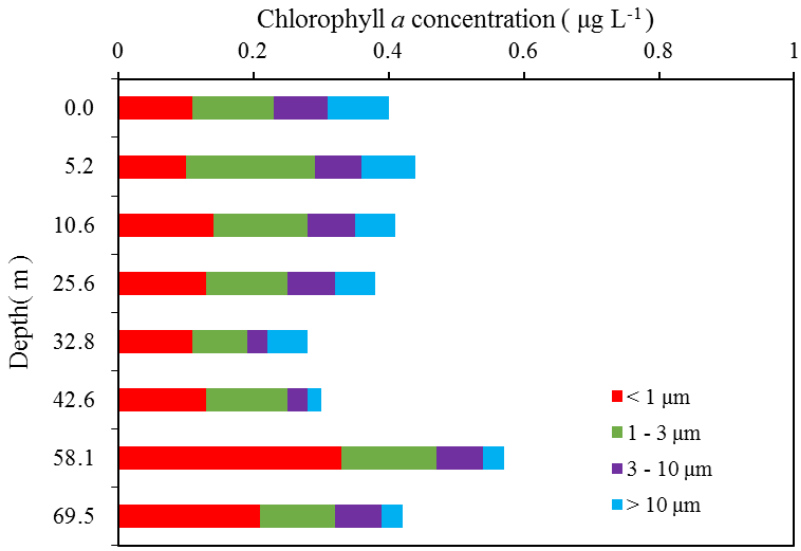

Figure 2.14(a).7. Vertical distribution of size-fractionated chlorophyll *a* at Stn.K02 cast5.

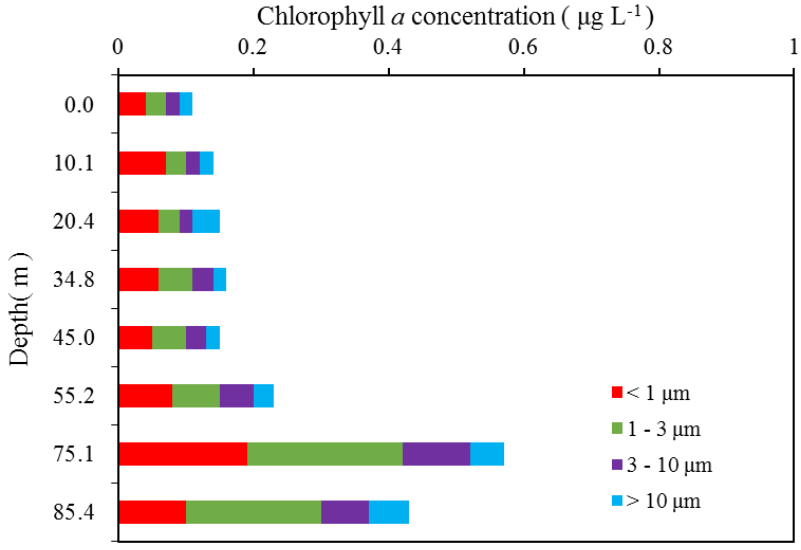

Figure 2.14(a).8. Vertical distribution of size-fractionated chlorophyll *a* at Stn.002 cast1.

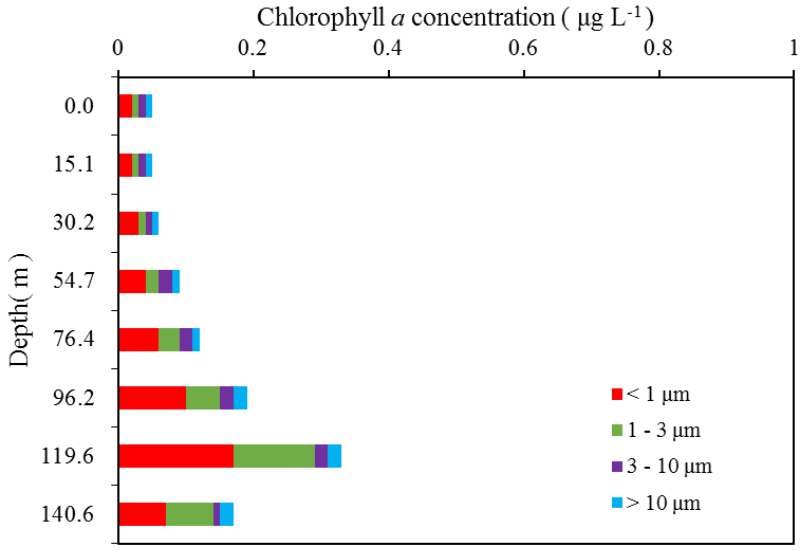

Figure 2.14(a).9. Vertical distribution of size-fractionated chlorophyll *a* at Stn.004 cast1.

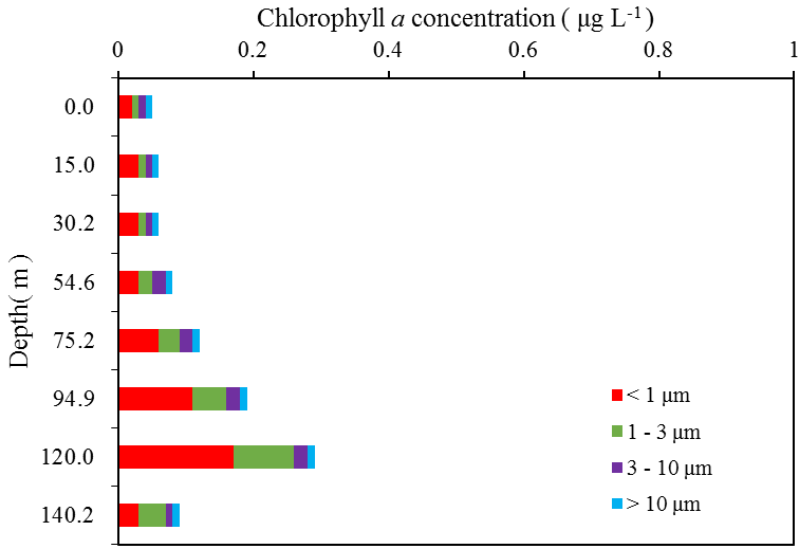

Figure 2.14(a).10. Vertical distribution of size-fractionated chlorophyll *a* at Stn.006 cast1.

2.14(b) HPLC measurements of marine phytoplankton pigments

Tetsuichi FUJIKI (JAMSTEC RCGC)
Hiroshi HOSHINO (MWJ)

(1) Objectives

The chemotaxonomic assessment of phytoplankton populations present in natural seawater requires taxon-specific algal pigments as good biochemical markers. A high-performance liquid chromatography (HPLC) measurement is an optimum method for separating and quantifying phytoplankton pigments in natural seawater. In this cruise, we measured the marine phytoplankton pigments by HPLC to investigate the marine phytoplankton community structure in the western Pacific.

(2) Instruments and Methods

i) Sample collection and treatment

Seawater samples were collected from 8 depths between the surface and 140 m at the cast for the primary production. Seawater samples were collected using Niskin bottles, except for the surface water, which was taken by a bucket. 2 or 3 L of seawater samples were filtered through the 47 mm diameter Whatman GF/F filter under the vacuum condition (approx. -0.02 MPa(G)). To remove retaining seawater in the sample filters, GF/F filters were vacuum-dried in a freezer (0 °C) within 17 hours. Subsequently, phytoplankton pigments retained on a filter were extracted in a glass vial with 4 ml of N,N-dimethylformamide (HPLC-grade) for at least 24 hours in a freezer (-20 °C), and analyzed by HPLC system within a few days.

Residua cells and filter debris were removed through PTFE syringe filter (pore size: 0.2 μm) before the analysis. 125 μl of pigment extract was mixed with 125 μl of 28 mmol L^{-1} tetrabutylazanium;acetate (tetrabutylammonium acetate) buffer (pH 6.5), and then injected into HPLC system. These process were conducted by the autosampler. Phytoplankton pigments were quantified based on C_8 column method (Heukelem & Thomas, 2001).

ii) HPLC System

HPLC System was composed by Agilent 1200 modular system, G1311A quaternary pump (low-pressure mixing system), G1329A autosampler and G7115A photodiode array detector.

iii) Stationary phase

Analytical separation was performed using a ZORBAX Eclipse XDB-C_8 column (150×4.6 mm). The column was maintained at 60 °C in the column heater box.

iv) Mobile phases

The eluant A was the 7:3 (v:v) mixture of methanol and 28 mmol L^{-1} tetrabutyl ammonium acetate buffer (pH 6.5). The eluant B was a methanol. Methanol was the HPLC-grade.

v) Calibrations

HPLC was calibrated using the standard pigments (Table 2.14(b).1).

vi) Internal standard

Internal standard was not added into the both standard samples and pigment extracts.

vii) Working standard

514 μg L^{-1} of chlolophyll *a* standard solution was measured with both standard samples and sea water samples as the working standard. The mean and coefficient of variation (CV) of chromatogram area shown below (Fig. 2.14(b).1):

234.4 ± 1.4 (n = 26), CV=0.6 %

viii) Pigment detection and identification

Chlorophylls and carotenoids were detected by photodiode array spectroscopy (350 nm - 750 nm). Pigment concentrations were calculated from the chromatogram area at the different two channels (Table 2.14(b).1). First channel was allocated at 450 nm of wavelength for the carotenoids and chlorophyll *b*. Second channel was allocated at 667 nm for the chlorophyll *a* and its metabolites.

(3) Preliminary result

Vertical profiles of major pigments at station KEO, K2, 002, 004 and 006 were shown in Figs. 2.14(b).2 to 2.14(b).6.

(4) Data archive

The processed data file of pigments will be submitted to the JAMSTEC Data Management Group (DMG) within a restricted period. Please ask PI for the latest information.

(5) References

Heukelem, L. V. & Thomas, C. S. (2001). Computer-assisted high-performance liquid chromatography method development with applications to the isolation and analysis of phytoplankton pigments. *J. Chromatogr. A* 910, 31-49

Jeffrey S. W., Mantoura R. F. C. & Wright S. W. (Eds.). (1997) *Phytoplankton pigments in oceanography: guidelines to modern methods*, 7 place de Fontenoy, Paris, United Nations Educational, Scientific and Cultural Organization.

Table 2.14(b).1. Retention time and wavelength of identification for pigment standards.

ID	Pigment[1]	Productions	Retention Time (minute)	Wavelength of identification (nm)
1	Chlorophyll *c*3	DHI Laboratory Products	4.095	450
2	Chlorophyllide *a*	DHI Laboratory Products	6.816	667
3	Mg-2,4-divinyl pheoporphyrin *a*5 monomethyl ester	DHI Laboratory Products	6.412	450

4	Chlorophyll *c*2	DHI Laboratory Products	6.351	450
5	Peridinin	DHI Laboratory Products	10.427	450
6	Pheophorbide *a*	DHI Laboratory Products	8.946	667
7	19'-Butanoyloxyfucoxanthin	DHI Laboratory Products	13.480	450
8	Fucoxanthin	DHI Laboratory Products	13.755	450
9	9'-*cis*-Neoxanthin	DHI Laboratory Products	14.361	450
10	Prasinoxanthin	DHI Laboratory Products	14.880	450
11	19'-Hexanoyloxyfucoxanthin	DHI Laboratory Products	15.281	450
12	Violaxanthin	DHI Laboratory Products	15.205	450
13	Diadinoxanthin	DHI Laboratory Products	16.423	450
16	Alloxanthin	DHI Laboratory Products	17.635	450
17	Diatoxanthin	DHI Laboratory Products	18.317	450
18	Zeaxanthin	DHI Laboratory Products	18.868	450
19	Lutein	DHI Laboratory Products	19.046	450
22	Chlorophyll *b*	DHI Laboratory Products	23.082	450
23	Divinyl Chlorophyll *a*	DHI Laboratory Products	24.703	667
24	Chlorophyll *a* from *Anacystis nidulans* algae	Sigma-Aldrich Co., LCC	24.754	667
25	Pheophytin *a*	DHI Laboratory Products	26.439	667
26	Alpha-carotene	DHI Laboratory Products	27.880	450
27	Beta-carotene	DHI Laboratory Products	27.968	450

[1]IUPAC names of the pigments; see Jeffrey et al., 1997.

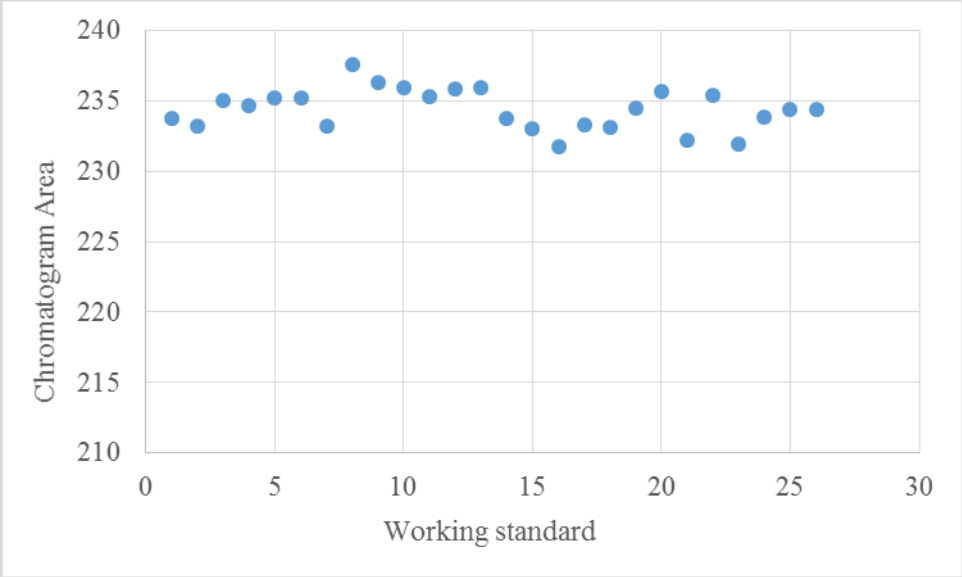

Figure 2.14(b).1. Variability of chromatogram area for working standard.

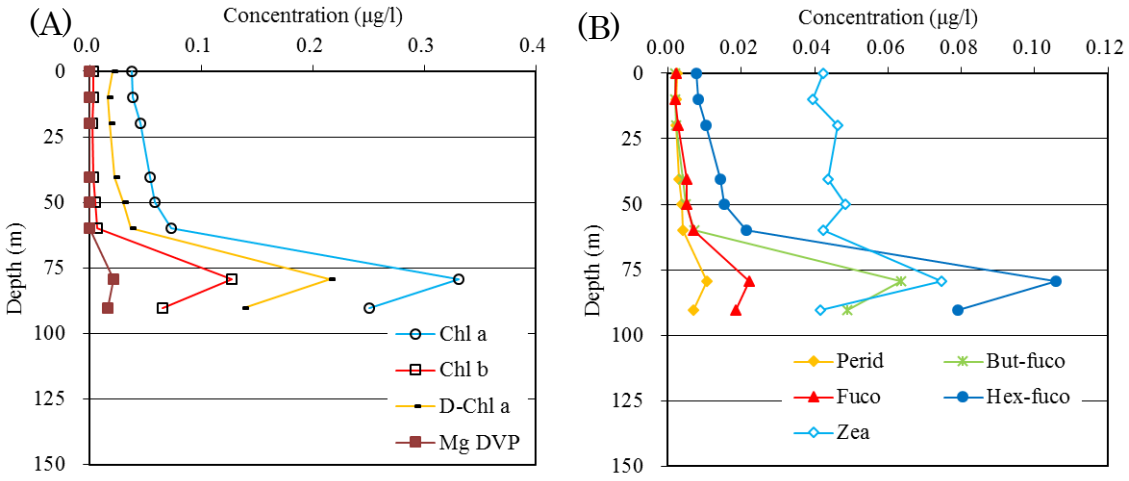

Figure 2.14(b).2.-(A). Vertical distributions of major phytoplankton pigments (chlorophyll *a*, chlorophyll *b*, Divinyl Chlorophyll *a*, and Mg-2,4-divinyl pheoporphyrin *a*5 monomethyl ester) at Stn. KEO, cast 3.

Figure 2.14(b).2.-(B). Vertical distributions of major phytoplankton pigments (peridinin, 19'-butanoyloxyfucoxanthin, fucoxanthin, 19'-hexanoyloxyfucoxanthin, and zeaxanthin) at Stn. KEO, cast 3.

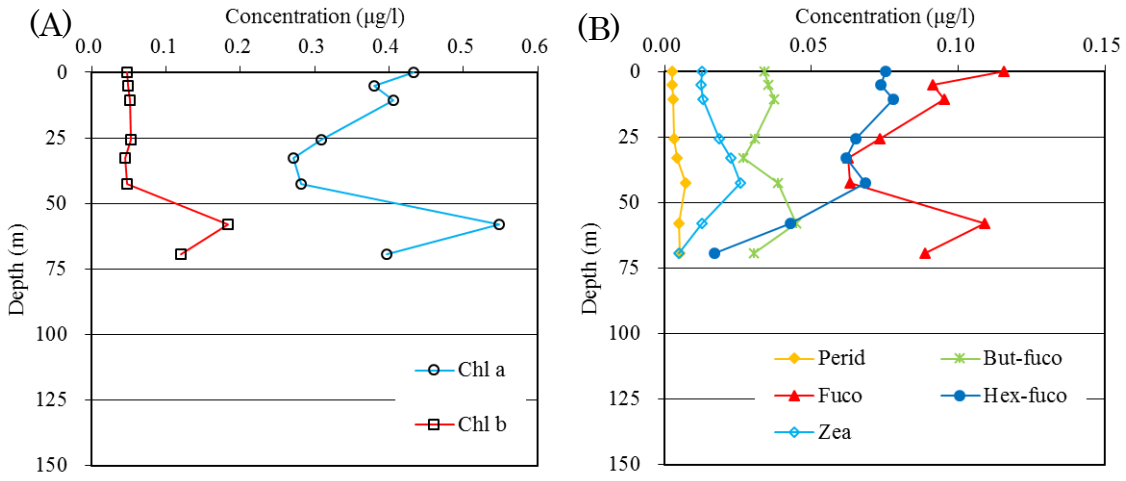

Figure 2.14(b).3.-(A). Vertical distributions of major phytoplankton pigments (chlorophyll *a* and chlorophyll *b*) at Stn. K2, cast 5.
Figure 2.14(b).3.-(B). Vertical distributions of major phytoplankton pigments (peridinin, 19'-butanoyloxyfucoxanthin, fucoxanthin, 19'-hexanoyloxyfucoxanthin, and zeaxanthin) at Stn. K2, cast 5.

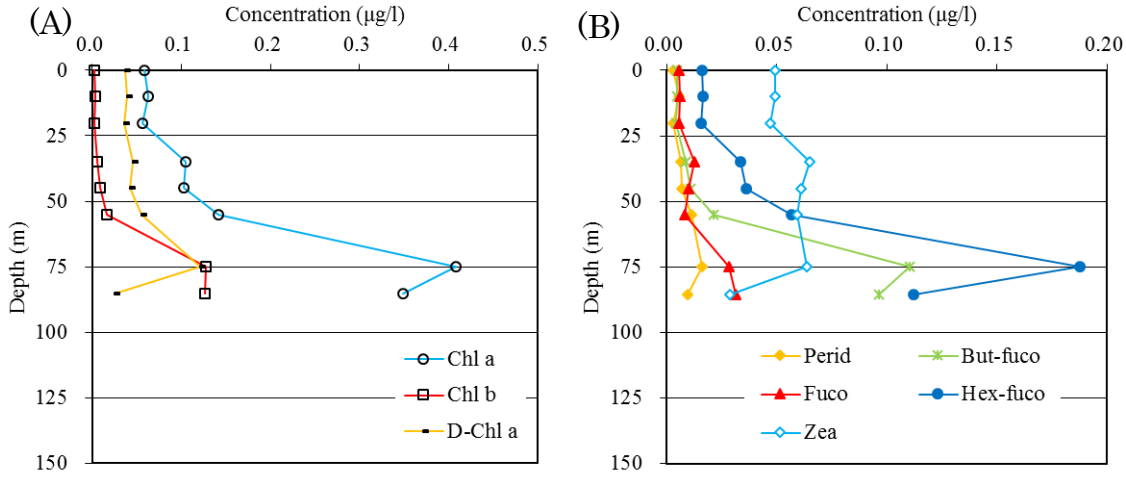

Figure 2.14(b).4.-(A). Vertical distributions of major phytoplankton pigments (chlorophyll *a*, chlorophyll *b* and Divinyl Chlorophyll *a*) at Stn. 002, cast 1.
Figure 2.14(b).4.-(B). Vertical distributions of major phytoplankton pigments (peridinin, 19'-butanoyloxyfucoxanthin, fucoxanthin, 19'-hexanoyloxyfucoxanthin, and zeaxanthin) at Stn. 002, cast 1.

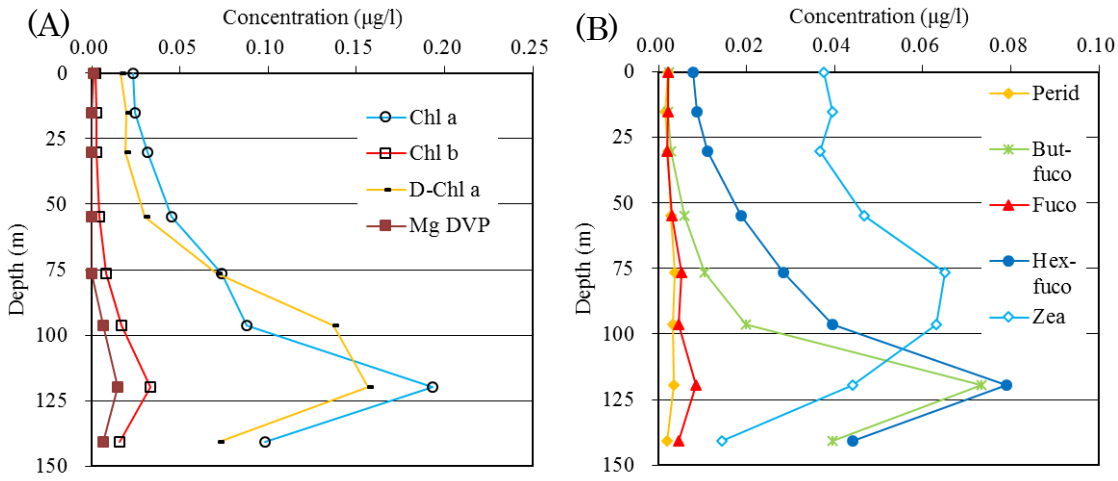

Figure 2.14(b).5.-(A). Vertical distributions of major phytoplankton pigments (chlorophyll *a*, chlorophyll *b*, Divinyl Chlorophyll *a*, and Mg-2,4-divinyl pheoporphyrin *a*5 monomethyl ester) at Stn. 004, cast 1.

Figure 2.14(b).5.-(B). Vertical distributions of major phytoplankton pigments (peridinin, 19'-butanoyloxyfucoxanthin, fucoxanthin, 19'-hexanoyloxyfucoxanthin, and zeaxanthin) at Stn. 004, cast 1.

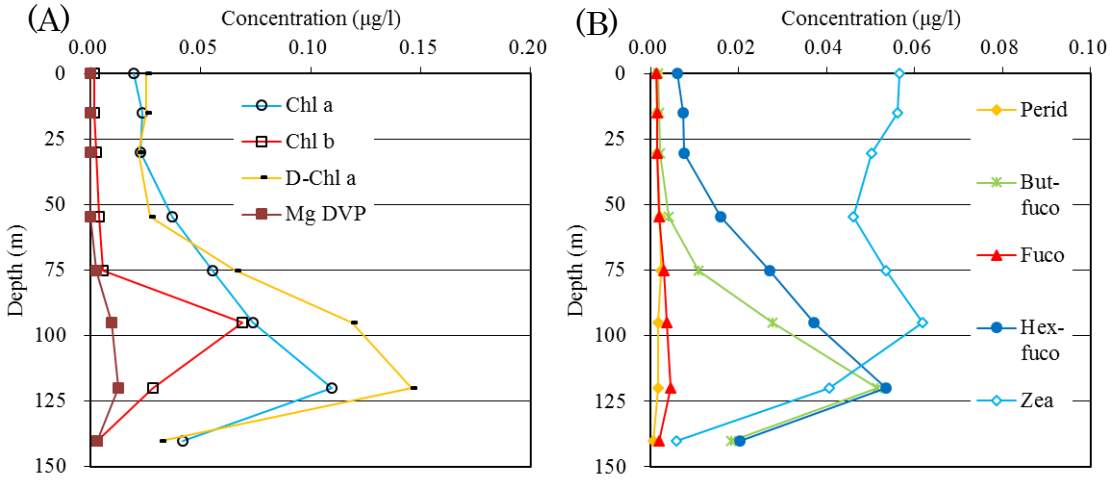

Figure 2.14(b).6.-(A). Vertical distributions of major phytoplankton pigments (chlorophyll *a*, chlorophyll *b*, Divinyl Chlorophyll *a*, and Mg-2,4-divinyl pheoporphyrin *a*5 monomethyl ester) at Stn. 006, cast 1.

Figure 2.14(b).6.-(B). Vertical distributions of major phytoplankton pigments (peridinin, 19'-butanoyloxyfucoxanthin, fucoxanthin, 19'-hexanoyloxyfucoxanthin, and zeaxanthin) at Stn. 006, cast 1.

2.14 (c) Primary Production

Kazuhiko MATSUMOTO (JAMSTEC RCGC)
Keitaro MATSUMOTO (MWJ)
Jun MATSUOKA (MWJ)
Masanori ENOKI (MWJ)

(1) Objectives

Total primary production can be divided into particulate primary production and dissolved primary production. Dissolved organic matter (DOM) release by phytoplankton is a ubiquitous process, and it can self-assemble and form transparent microgels. Such marine gel particles are a fundamental bridge in the DOM-POM continuum in the ocean. To understand the processes of biogeochemical cycles, oceanic total primary production and marine gel particles are estimated at the stations of KEO, K2, S2, S4 and S6.

(2) Methods and Instruments

i. Sampling

Seawater samples were collected at three depths within the euphotic layer using Teflon-coated and acid-cleaned Niskin bottles, except for the surface water, which was taken by a bucket. Seawater samples were transferred into acid-cleaned, transparent bottles. Just before the incubation, $NaH^{13}CO_3$ was added to each bottle at a final concentration of 0.2 mM, sufficient to enrich the bicarbonate concentration by about 10%.

ii. Incubation

(a) On-deck incubation

The bottles were placed in containers, the light levels within which were adjusted with blue acrylic plates. The containers were placed in a water bath cooled by running surface seawater or by immersion cooler. Incubations were started from early morning for 24 h. To estimate the incorporation rate of nitrate, another experiments were conducted during noon and midnight for 2 h with adding $K^{15}NO_3$, respectively.

(b) P vs. E curve experiment

To investigate the relationship between phytoplankton photosynthetic rate (P) and scalar irradiance (E), incubations for the P vs. E curve experiment were conducted in the laboratory. Three incubators were filled with water, and water temperature was controlled appropriately by circulating water coolers, respectively. Each incubator was illuminated at one end by a 500W halogen lamp, and bottles were arranged linearly against the lamp and controlled light intensity by shielding with a neutral density filter on lamp side. Incubations for the P vs. E curve experiment were conducted around noon for 3 h.

iii. Measurement

(a) Particulate fraction

After the incubation, water samples were immediately filtered through a pre-combusted GF/F filter, then the filters were dehydrated in a dry oven (45 ºC), and the remained inorganic carbon in the filter was removed by fuming HCl. The ^{13}C and ^{15}N content of the particulate fraction will be measured with a stable isotope ratio mass spectrometer (Sercon, Ltd.) based on the method of Hama et al. (1983) on land. The analytical function and parameter values used to describe the relationship between the photosynthetic rate (P) and scalar irradiance (E) are best determined using a least-squares procedure from the following equation (Platt et al., 1980).

$$P = P_{max}(1-e^{-\alpha E/Pmax})e^{-b \alpha E/Pmax}$$

where, P_{max} is the light-saturated maximum photosynthetic rate, α is the initial slope of the P vs. E curve, b is a dimensionless photoinhibition parameter.

(b) Dissolved fraction

The filtrate of the on-deck 24 h incubation samples were desalinated using an electro dialyzer equipped with AC-220-550 cartridge (Micro Acilyzer S3, ASTOM Corp.). The frozen desalinated seawater samples, which are brought back to land, are concentrated to 5 mL with a rotary evaporator at 45 ºC, and the dissolved inorganic carbon is removed by adding HCl and subsequent degassing. The samples are further concentrated to about 500 μL and absorbed onto pre-combusted GF/F filter in a tin capsule, and dehydrated in a dry oven (45 ºC). The ^{13}C content of the dissolved fraction (extracellular release of phytoplankton) were measured as described above.

iv. Marine gel particles

(a) Transparent exopolymer particle (TEP)

TEP is very sticky, and it aggregates with other suspended particles, resulting in the formation of sinking marine snow. TEP is formed by coagulation of colloidal TEP precursors present in the phytoplankton released dissolved organic matter. The water samples of 200 mL were filtered onto 0.4-μm polycarbonate filters, and the filters were stained with 1 mL alcian blue solution, and rinsed thrice with 1 mL of Milli-Q water. Stained filter samples were stored in freezer until analysis. Each filter will be soaked for 2 h in 6 mL of 80% sulfuric acid (H_2SO_4) to elute the dye and then the absorbance of the solution is measured at 787 nm in a 1 cm cuvette.

(b) Coomassie stainable particles (CSP)

CSP is protein-containing transparent particle that can be stained with Coomassie brilliant blue (CBB). The water samples of 200 mL were filtered onto 0.4-μm polycarbonate filters, and the filters were stained with 1 mL CBB solution, and rinsed thrice with 1 mL of Milli-Q water. Stained filter samples were stored in freezer until analysis. Each filter will be soaked for 2 h in 4 mL of 3% sodium dodecyl sulfate (SDS) in 50% isopropyl alcohol with sonication to elute the dye and then the absorbance of the solution is measured at 615 nm in a 1 cm cuvette.

(3) Data archive

The data obtained during this cruise will be submitted to the JAMSTEC Data Management Group (DMG).

(4) References

Hama T, Miyazaki T, Ogawa Y, Iwakuma T, Takahashi M, Otsuki A, Ichimura S (1983) Measurement of photosynthetic production of a marine phytoplankton population using a stable 13C isotope. Marine Biology 73: 31-36.

Platt T, Gallegos CL, Harrison WG (1980) Photoinhibition of photosynthesis in natural assemblages of marine phytoplankton. Journal of Marine Research 38: 687-701.

2.15 Zooplankton

2.15(a) Planktic foraminifers and Thecosomatous pteropods

Katsunori KIMOTO (JAMSTEC RCGC)
Minoru KITAMURA (JAMSTEC RCGC)
Keisuke SHIMIZU (Exeter University, UK (Onshore Proponent))

(1) Objectives

The ocean has already absorbed about 30% of the total anthropogenic CO_2 (approximately 155 GtC) since the industrial revolution (IPCC AR5, 2013). This reduces ocean pH (Ocean acidification, OA) and causes wholescale shift in seawater carbonate chemistry. OA also give several impacts to the biological processes; one well-known effect is the lowering of calcium carbonate saturation state, which give negative impact to shell-forming marine organisms such as pteropods and planktic foraminifers etc. OA also affect zooplankton other than the shell-forming organisms, and characteristics of the zooplankton community will be changed. So, we are observing long-term change of zooplankton biomass at K2 by using the plankton collecting apparatus and performing some biological/geochemical analysis to evaluate the biological impact to OA.

In this cruise, for better understanding of biological responses to carbonate saturation status, we aimed for following themes,

a) understanding vertical distributions of pteropods and planktonic foraminifer communities, and change of their shell densities with water depths,
b) clarifying genetic diversities of planktic foraminifers with water depth in the North Pacific,
c) understanding phenotypic and genetic variabilities in the mixed layer for pteropods, and their population structure.

(2) Methods

All plankton samplings were conducted at Sta K2, and their halfway stations of Leg1 (See Table 2.15(a).1). For the purpose (a), we collected specimens by using the Vertical Multi-depth Plankton Sampler (VMPS-3K, Tsurumi Seiki co., Ltd, Fig. 2.15(a).1). VMPS-3K equipped 3 or 4 plankton nets (63 μm mesh, NXX25), magnetic flow-meter, fluorometer (Wet Lab) and CTD sensors (Sea-bird Electrics), and was hauled vertically at a speed of 0.5 m/sec. Opening/closing of each net is electrically controlled from the lab on the ship, we can collect vertically stratified sample sets together with the environmental sensing data. Collected samples were immediately fixed by the ethanol (99.5 %) and stored at the room temperature (~23 °C). For the purpose of (b), planktic foraminifers were picked under the stereomicroscope and transported to the microslides with ethanol (99.5 %) and stored in the refrigerator (~ 4 °C).

For the purposes of (c), a twin-NORPAC net (63 μm mesh, NXX25, Fig. 2.15(a).1) with a large cod end (2,000 ml polypropylene bottles) was vertically hauled. Living pteropods were immediately sorted under the stereomicroscope and fixed by 99.5 % EtOH, and then stored in the refrigerator at the 4 °C temperature.

(3) Onshore study in the future

Pteropod and planktonic foraminiferal shells will be analyzed by the Micro-focus X-ray CT (MXCT) equipped in JAMSTEC HQ in order to elucidate relationships between oceanic carbonate chemistry and individual shell density. The preserved samples of planktic foraminifers will be extracted all DNA and then perform SSU rDNA analysis for genetic diversity analysis. For the population analysis of pteropods, DNA extraction from the preserved specimens and amplifying of gene sequences for the COI region of mtDNA will be performed. After the sequence alignments, population genetic analysis will be performed.

(4) Data Archive

All data will be submitted to JAMSTEC Data Management Group (DMG).

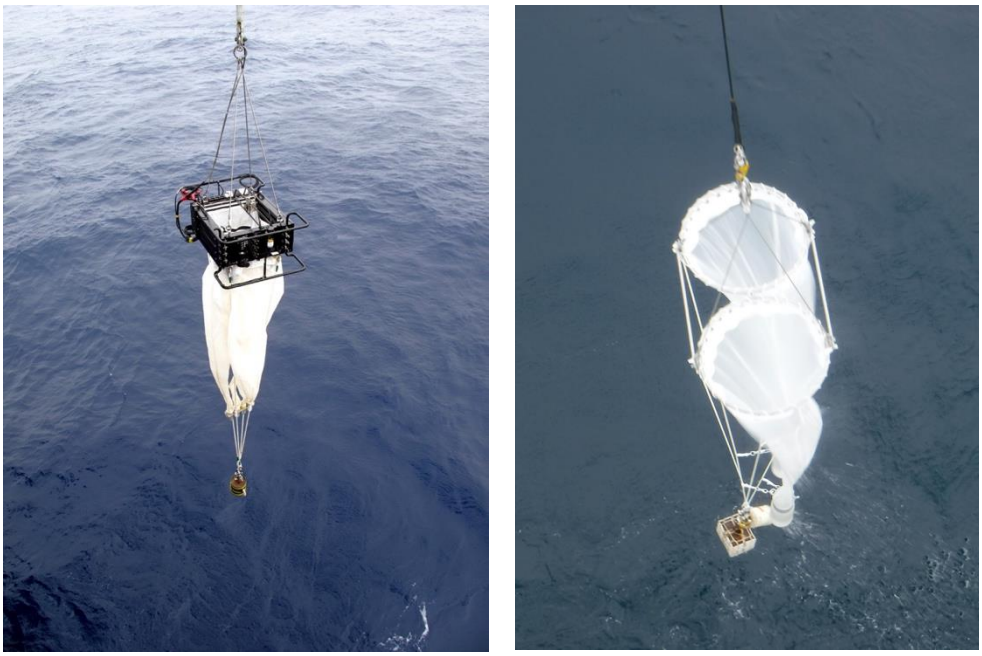

Figure 2.15(a).1 The overview of VMPS (Vertical Multi-depth Plankton Sampler, left) and twin NORPAC net (right).

Table 2.15(a).1. Sampled locations during MR18-04 Leg1.

No.	Sample ID#	species	Fixiation	Station	Latitude			Longitude			water depth m	Date yy/mm/dd			Time	
1	KEO_VMPS-1	Planktic forams, Pteropods	99% Ethernol	Sta. KEO	32	23	N	144	23.5	E	300-500	2018	7	21	2:00	JST
2	KEO_VMPS-2	Planktic forams, Pteropods	99% Ethernol	Sta. KEO	32	23	N	144	23.5	E	200-300	2018	7	21	2:10	JST
3	KEO_VMPS-3	Planktic forams, Pteropods	99% Ethernol	Sta. KEO	32	23	N	144	23.5	E	150-200	2018	7	21	2:20	JST
4	KEO_VMPS-4	Planktic forams, Pteropods	99% Ethernol	Sta. KEO	32	23	N	144	23.5	E	100-150	2018	7	21	2:40	JST
5	KEO_VMPS-5	Planktic forams, Pteropods	99% Ethernol	Sta. KEO	32	23	N	144	23.5	E	50-100	2018	7	21	2:50	JST
6	KEO_VMPS-6	Planktic forams, Pteropods	99% Ethernol	Sta. KEO	32	23	N	144	23.5	E	0-50	2018	7	21	3:00	JST
7	KEO_NORPAC-1	Planktic forams, Pteropods	99% Ethernol	Sta. KEO	32	23	N	144	23.5	E	0-150	2018	7	21	3:20	JST
8	KEO_NORPAC-2	Planktic forams, Pteropods	99% Ethernol	Sta. KEO	32	23	N	144	23.5	E	0-150	2018	7	21	3:35	JST
9	KEO_NORPAC-3	Planktic forams, Pteropods	99% Ethernol	Sta. KEO	32	23	N	144	23.5	E	0-150	2018	7	21	3:55	JST
10	KEO_NORPAC-4	Planktic forams, Pteropods	99% Ethernol	Sta. KEO	32	23	N	144	23.5	E	0-150	2018	7	21	4:15	JST
11	KEO_NORPAC-5	Planktic forams, Pteropods	99% Ethernol	Sta. KEO	32	23	N	144	23.5	E	0-150	2018	7	21	4:30	JST
12	K2_NORPAC-1	Planktic forams, Pteropods	99% Ethernol	Sta. K2	47	00	N	165	00	E	0-150	2018	7	25	18:40	JST
13	K2_NORPAC-2	Planktic forams, Pteropods	99% Ethernol	Sta. K2	47	00	N	165	00	E	0-150	2018	7	25	18:50	JST
14	K2_NORPAC-3	Planktic forams, Pteropods	99% Ethernol	Sta. K2	47	00	N	165	00	E	0-50	2018	7	25	19:00	JST
15	K2_NORPAC-4	Planktic forams, Pteropods	99% Ethernol	Sta. K2	47	00	N	165	00	E	0-50	2018	7	25	19:10	JST
16	K2_NORPAC-5	Planktic forams, Pteropods	99% Ethernol	Sta. K2	47	00	N	165	00	E	0-50	2018	7	25	19:20	JST
17	K2_NORPAC-6	Planktic forams, Pteropods	99% Ethernol	Sta. K2	47	00	N	165	00	E	0-50	2018	7	25	19:30	JST
18	K2_NORPAC-7	Planktic forams, Pteropods	99% Ethernol	Sta. K2	47	00	N	165	00	E	0-150	2018	7	27	16:45	JST
19	K2_NORPAC-8	Planktic forams, Pteropods	99% Ethernol	Sta. K2	47	00	N	165	00	E	0-150	2018	7	27	17:00	JST
20	K2_NORPAC-9	Planktic forams, Pteropods	99% Ethernol	Sta. K2	47	00	N	165	00	E	0-150	2018	7	27	17:15	JST
21	K2_NORPAC-10	Planktic forams, Pteropods	99% Ethernol	Sta. K2	47	00	N	165	00	E	0-150	2018	7	27	17:30	JST
22	K2_VMPS-1	Planktic forams, Pteropods	99% Ethernol	Sta. K2	47	00	N	165	00	E	500-300	2018	7	29	18:50	JST
23	K2_VMPS-2	Planktic forams, Pteropods	99% Ethernol	Sta. K2	47	00	N	165	00	E	300-200	2018	7	29	19:00	JST
24	K2_VMPS-3	Planktic forams, Pteropods	99% Ethernol	Sta. K2	47	00	N	165	00	E	200-150	2018	7	29	19:10	JST
25	K2_VMPS-4	Planktic forams, Pteropods	99% Ethernol	Sta. K2	47	00	N	165	00	E	150-100	2018	7	29	19:30	JST
26	K2_VMPS-5	Planktic forams, Pteropods	99% Ethernol	Sta. K2	47	00	N	165	00	E	100-50	2018	7	29	19:40	JST
27	K2_VMPS-6	Planktic forams, Pteropods	99% Ethernol	Sta. K2	47	00	N	165	00	E	50-0	2018	7	29	19:50	JST
28	S1_VMPS-1	Planktic forams, Pteropods	99% Ethernol	Sta S1	40	00	N	158	20	E	1100-1360	2018	7	31	13:30	JST
29	S1_VMPS-2	Planktic forams, Pteropods	99% Ethernol	Sta S1	40	00	N	158	20	E	900-1100	2018	7	31	13:40	JST
30	S1_VMPS-3	Planktic forams, Pteropods	99% Ethernol	Sta S1	40	00	N	158	20	E	780-900	2018	7	31	13:50	JST
31	S1_VMPS-4	Planktic forams, Pteropods	99% Ethernol	Sta S1	40	00	N	158	20	E	670-780	2018	7	31	14:20	JST
32	S1_VMPS-5	Planktic forams, Pteropods	99% Ethernol	Sta S1	40	00	N	158	20	E	590-670	2018	7	31	14:30	JST
33	S1_VMPS-6	Planktic forams, Pteropods	99% Ethernol	Sta S1	40	00	N	158	20	E	520-590	2018	7	31	14:40	JST
34	S1_VMPS-7	Planktic forams, Pteropods	99% Ethernol	Sta S1	40	00	N	158	20	E	470-520	2018	7	31	15:10	JST
35	S1_VMPS-8	Planktic forams, Pteropods	99% Ethernol	Sta S1	40	00	N	158	20	E	420-470	2018	7	31	15:20	JST
36	S1_VMPS-9	Planktic forams, Pteropods	99% Ethernol	Sta S1	40	00	N	158	20	E	370-420	2018	7	31	15:40	JST
37	S1_VMPS-10	Planktic forams, Pteropods	99% Ethernol	Sta S1	40	00	N	158	20	E	205-420	2018	7	31	15:50	JST
38	S1_VMPS-11	Planktic forams, Pteropods	99% Ethernol	Sta S1	40	00	N	158	20	E	0-205	2018	7	31	16:00	JST
39	S2_VMPS-1	Planktic forams, Pteropods	99% Ethernol	Sta S2	35	0	N	157	19.5	E	690-827	2018	8	2	3:50	JST
40	S2_VMPS-2	Planktic forams, Pteropods	99% Ethernol	Sta S2	35	0	N	157	19.5	E	610-690	2018	8	2	4:00	JST
41	S2_VMPS-3	Planktic forams, Pteropods	99% Ethernol	Sta S2	35	0	N	157	19.5	E	0-610	2018	8	2	4:10	JST
42	S2_VMPS-4	Planktic forams, Pteropods	99% Ethernol	Sta S2	35	0	N	157	19.5	E	480-540	2018	8	2	4:40	JST
43	S2_VMPS-5	Planktic forams, Pteropods	99% Ethernol	Sta S2	35	0	N	157	19.5	E	540-610	2018	8	2	4:50	JST
44	S2_VMPS-6	Planktic forams, Pteropods	99% Ethernol	Sta S2	35	0	N	157	19.5	E	480-540	2018	8	2	5:00	JST
45	S2_VMPS-7	Planktic forams, Pteropods	99% Ethernol	Sta S2	35	0	N	157	19.5	E	410-480	2018	8	2	5:30	JST
46	S2_VMPS-8	Planktic forams, Pteropods	99% Ethernol	Sta S2	35	0	N	157	19.5	E	370-410	2018	8	2	5:45	JST
47	S2_VMPS-9	Planktic forams, Pteropods	99% Ethernol	Sta S2	35	0	N	157	19.5	E	280-370	2018	8	2	6:00	JST
48	S2_VMPS-10	Planktic forams, Pteropods	99% Ethernol	Sta S2	35	0	N	157	19.5	E	0-280	2018	8	2	6:20	JST
49	S3_VMPS-1	Planktic forams, Pteropods	99% Ethernol	Sta S3	30	0	N	156	19.5	E	700-1000	2018	8	3	15:30	JST
50	S3_VMPS-2	Planktic forams, Pteropods	99% Ethernol	Sta S3	30	0	N	156	19.5	E	500-700	2018	8	3	15:40	JST
51	S3_VMPS-3	Planktic forams, Pteropods	99% Ethernol	Sta S3	30	0	N	156	19.5	E	300-500	2018	8	3	15:50	JST
52	S3_VMPS-4	Planktic forams, Pteropods	99% Ethernol	Sta S3	30	0	N	156	19.5	E	150-300	2018	8	3	16:20	JST
53	S3_VMPS-5	Planktic forams, Pteropods	99% Ethernol	Sta S3	30	0	N	156	19.5	E	50-150	2018	8	3	16:25	JST
54	S3_VMPS-6	Planktic forams, Pteropods	99% Ethernol	Sta S3	30	0	N	156	19.5	E	0-50	2018	8	3	16:30	JST
55	S3_NORPAC-1	Planktic forams, Pteropods	99% Ethernol	Sta S3	30	0	N	156	19.5	E	0-300	2018	8	3	16:50	JST
56	S3_NORPAC-2	Planktic forams, Pteropods	99% Ethernol	Sta S3	30	0	N	156	19.5	E	0-150	2018	8	3	17:10	JST
57	S3_NORPAC-3	Planktic forams, Pteropods	99% Ethernol	Sta S3	30	0	N	156	19.5	E	0-150	2018	8	3	17:25	JST
58	S4_VMPS-1	Planktic forams, Pteropods	99% Ethernol	Sta.S4	25	0	N	155	23	E	700-1000	2018	8	4	16:30	JST
59	S4_VMPS-2	Planktic forams, Pteropods	99% Ethernol	Sta.S4	25	0	N	155	23	E	500-700	2018	8	4	16:50	JST
60	S4_VMPS-3	Planktic forams, Pteropods	99% Ethernol	Sta.S4	25	0	N	155	23	E	0-500	2018	8	4	17:00	JST
61	S4_VMPS-4	Planktic forams, Pteropods	99% Ethernol	Sta.S4	25	0	N	155	23	E	150-300	2018	8	4	17:10	JST
62	S4_VMPS-5	Planktic forams, Pteropods	99% Ethernol	Sta.S4	25	0	N	155	23	E	50-150	2018	8	4	17:20	JST
63	S4_VMPS-6	Planktic forams, Pteropods	99% Ethernol	Sta.S4	25	0	N	155	23	E	0-50	2018	8	4	17:30	JST
64	S4_NORPAC-1	Planktic forams, Pteropods	99% Ethernol	Sta.S4	25	0	N	155	23	E	0-150	2018	8	4	20:10	JST
65	S4_NORPAC-2	Planktic forams, Pteropods	99% Ethernol	Sta.S4	25	0	N	155	23	E	0-150	2018	8	4	20:25	JST
66	S4_NORPAC-3	Planktic forams, Pteropods	99% Ethernol	Sta.S4	25	0	N	155	23	E	0-150	2018	8	4	20:40	JST
67	S5_VMPS-1	Planktic forams, Pteropods	99% Ethernol	Sta.S5	20	2	N	154	29	E	1000-700	2018	8	6	12:30	JST
68	S5_VMPS-2	Planktic forams, Pteropods	99% Ethernol	Sta.S5	20	2	N	154	29	E	500-700	2018	8	6	12:40	JST
69	S5_VMPS-3	Planktic forams, Pteropods	99% Ethernol	Sta.S5	20	2	N	154	29	E	300-500	2018	8	6	12:50	JST
70	S5_VMPS-4	Planktic forams, Pteropods	99% Ethernol	Sta.S5	20	2	N	154	29	E	150-300	2018	8	6	13:10	JST

Table 2.15(a).1 (continued) Sampled locations during MR18-04 Leg1.

No.	Sample ID#	species	Fixiation	Station	Latitude			Longitude			water depth m	Date yy/mm/dd			Time	
71	S5_VMPS-5	Planktic forams, Pteropods	99% Ethernol	Sta.S5	20	2	N	154	29	E	50-150	2018	8	6	13:20	JST
72	S5_VMPS-6	Planktic forams, Pteropods	99% Ethernol	Sta.S5	20	2	N	154	29	E	0-50	2018	8	6	13:30	JST
73	S5_NORPAC-1	Planktic forams, Pteropods	99% Ethernol	Sta.S5	20	2	N	154	29	E	0-200	2018	8	6	14:00	JST
74	S5_NORPAC-2	Planktic forams, Pteropods	99% Ethernol	Sta.S5	20	2	N	154	29	E	0-50	2018	8	6	14:10	JST
75	S5_NORPAC-3	Planktic forams, Pteropods	99% Ethernol	Sta.S5	20	2	N	154	29	E	0-50	2018	8	6	14:20	JST
76	S6_VMPS-1	Planktic forams, Pteropods	99% Ethernol	Sta.S6	15	0	N	153	35.5	E	1000-700	2018	8	8	21:30	JST
77	S6_VMPS-2	Planktic forams, Pteropods	99% Ethernol	Sta.S6	15	0	N	153	35.5	E	500-700	2018	8	8	21:40	JST
78	S6_VMPS-3	Planktic forams, Pteropods	99% Ethernol	Sta.S6	15	0	N	153	35.5	E	300-500	2018	8	8	21:50	JST
79	S6_VMPS-4	Planktic forams, Pteropods	99% Ethernol	Sta.S6	15	0	N	153	35.5	E	150-300	2018	8	8	22:10	JST
80	S6_VMPS-5	Planktic forams, Pteropods	99% Ethernol	Sta.S6	15	0	N	153	35.5	E	50-150	2018	8	8	22:20	JST
81	S6_VMPS-6	Planktic forams, Pteropods	99% Ethernol	Sta.S6	15	0	N	153	35.5	E	0-50	2018	8	8	22:30	JST
82	S6_NORPAC-1	Planktic forams, Pteropods	99% Ethernol	Sta.S6	15	0	N	153	35.5	E	0-50	2018	8	8	22:50	JST
83	S6_NORPAC-2	Planktic forams, Pteropods	99% Ethernol	Sta.S6	15	0	N	153	35.5	E	0-50	2018	8	9	23:00	JST

2.15(b) Mesozooplankton

Minoru KITAMURA (JAMSTEC RCGC)

(1) Objective

To understand/discuss influences of environmental changes on plankton community is one of our research themes for MR18-04 cruise. Recent researches suggested that ocean acidification may influence not only maintaining of $CaCO_3$ test but also larval development of crustacean zooplankton such as copepods and euphausiids which are dominated in the zooplankton community. Long-term increasing trends of zooplankton biomasses were detected in the two time-series stations, BATS and ALOHA. Thus, accurate understanding on long-term dynamics of zooplankton biomass is important as one of the basic information when we detect biological responses against environmental changes. In this study, we will analyze zooplankton dynamics by using time-series of backscatter intensities obtained by moored ADCPs at K2. To validate acoustically estimated zooplankton biomass, actual biomass data based on the zooplankton samples obtained from the net tows is needed. Thus, we conducted zooplankton samplings at K2.

Additionally, zooplankton samplings to understand species diversity in the subtropical zooplankton communities were conducted. Comparing with the subarctic zooplankton communities, researches on the subtropical ones are still scarce in the western Pacific. In general, species diversity of the subtropical zooplankton communities is higher than the subarctic ones. Thus, I started ecological study on the subtropical zooplankton focused on their species diversity.

(2) Methods

To reduce net avoidance of larger zooplankton such as euphausiids, the ORI net (1.6 m in mouth diameter, 8m long, and 0.33 mm in mesh) was obliquely towed at an average ship speed of 2 knots. Target layers of the zooplankton samplings were 0-50 and 0-400 m. Filtering volume of water was estimated using a flow meter (S/N: 2370) mounted in the net mouth. Maximum sampling depth of each trawl was recorded using a depth sensor (DEFI-D50, JFE-Advantec Co. Ltd; S/N 081N005) attached in the net frame. Sampling information were summarized in Table 2.15(b).1. Collected zooplankton samples were quantitatively divided onboard, a subsample (1/8, 1/16 or 1/32) was preserved in –20 ºC for biomass measurement and another subsample (1/16, 1/32 or 1/64) was fixed and preserved in 5% buffered formalin seawater for community structure analysis.

For the subtropical zooplankton diversity study, twin NORPAC net (45 cm in mouth diameter, 0.33 and 0.1 mm in mesh) was vertically hauled in the stations from S3 to S6. Maximum depth of each sampling was 150 m, and rewind speed of wire was 1.0 m/sec. To estimate filtering volume, a flow-meter was mounted in each net mouth. Collected zooplankton samples were immediately fixed using 5% buffered formalin seawater.

Table 2.15(b).1. Summary of ORI net hauls.

Zooplankton samplings by using ORI net

Sampling gear: ORI net (2-m^2 net with 0.33-mm mesh). Flow meter ID: 2370. Sampling layer was recorded using DEFI-D50 (S/N AZ6003).

Stn.	Date & Time				Position		Wire out	Sampling layer	F-meter read	Filtering vol.	Subsamples	Filter No.	Remarks
	LST	net in	UTC	net in	Lat.	Long.							
		out		out	(N)	(E)	(m)	(m)		(m^3)			
K2	2018/7/27	15:40	2018/7/27	4:40	46° 59.90'	160° 00.30'	800	0~400	17,791	2908.8	15/16Frozen	E-29, 30, 31, 32	Day
		16:10		5:10							1/16Formalin		
K2	2018/7/27	16:33	2018/7/27	5:33	46° 58.97'	160° 00.51'	100	0~60	2,568	419.9	3/4 Frozen	E-28	Day
		16:47		5:47							1/4 Formalin		
K2	2018/7/27	22:02	2018/7/27	11:02	47° 01.02'	159° 59.62'	800	0~490	16,243	2655.7	7/8 Frozen	E-33, 34, 35, 36	Night
		22:30		11:30							1/32 Formalin		
K2	2018/7/27	22:46	2018/7/27	11:46	47° 00.34'	159° 59.92'	100	0~80	2,083	340.6	1/4 Frozen	E-37	Night
		22:57		11:57							1/4 Formalin		
K2	2018/7/28	13:17	2018/7/28	2:18	47° 00.28'	160° 00.10'	800	0~420	18,062	2953.1	3/8 Frozen	E-38, 39, 40, 41	Day
		13:45		2:45							1/16Formalin		
K2	2018/7/28	14:01	2018/7/28	3:01	46° 59.96'	159° 58.85'	100	0~42	2,704	442.1	3/16 Frozen	E-42	Day
		14:10		3:10							1/8Formalin		

Table 2.15(b).2. Summary of NORPAC net hauls.

Ship's speed: 1.0 kt (1sec.

Stn.	Cast ID	Date (yyyy/mm/dd) and Time				Position		Wire out	Wire angle	Flow-meter revolution		Filtering vol. (m^3)	
		LST		UTC		Lat.	Long.	(m)	(°)	XX13	GG52	XX13	GG52
S3	S3-1	2018/8/3	20:30	2017/8/3	9:30	29° 58.38'	156° 16.95'	150	0	1625	1578	22.8	22.1
	S3-2		20:42		9:42	29° 58.25'	156° 16.85'	150	0	1608	1645	22.5	23.0
S4	S4-1	2018/8/4	21:45	2018/8/4	10:45	25° 00.70'	155° 25.02'	150	0	1480	1611	20.7	22.6
	S4-2		21:59		10:59	25° 00.67'	155° 24.92'	150	0	1422	1585	19.9	22.2
S5	S5-1	2018/8/6	19:16	2018/8/6	8:16	20° 02.18'	154° 28.85'	150	0	1500	1578	21.0	22.1
	S5-2		19:29		8:29	20° 02.26'	154° 28.85'	150	0	1421	1520	19.9	21.3
S6	S6-1	2018/8/8	1:53	2018/8/7	14:53	15° 00.61'	153° 35.87'	150	0	1581	1640	22.1	23.0
	S6-2		2:08		15:08	15° 00.68'	153° 35.89'	150	0	1527	1648	21.4	23.1

(3) Sample archive

All formalin fixed or frozen subsamples are stored under Kitamura until analyzing.

2.15(c) Heterotrophic Protist

Onboard participants:
Yoshiyuki ISHITANI (Center for Computational Sciences, University of Tsukuba)
Euki YAZAKI (School of Life and Environmental Sciences, University of Tsukuba)

On-land collaborators:
Tetsuo HASHIMOTO (Faculty of Life and Environmental Sciences, University of Tsukuba)
Yuji INAGAKI (Center for Computional Sciences, University of Tsukuba)
Yurika UJIIÉ (Center for Advanced Marine Core Research, Kochi University)

(1) Objectives

Our aim was to collect genetic diversity of marine heterotrophic protists (e.g., planktic foraminifera and radiolarians) and to measure the photosynthetic activity of radiolarians during the cruise. Plankton-net samples were obtained from multiple layers corresponding to the hydrography of each station. These samples will be utilized to assess the biodiversity of marine tested planktons: planktic foraminifera, radiolarians, which secrete calcareous or siliceous shells preserved in marine sediment as fossils, and of marine heterotrophic protists.

Marine tested planktons have wide habitat ranges in geography and depth of the world oceans. In particular, the depth habitat of radiolarians reaches to the deep layer around 3000 m water depth. The biodiversity of these planktons have been influenced by oceanic environmental changes throughout long geological period. The fossil archives are powerful indexes to reconstruct the paleoceanographic change and leads us to presume the future climate transition. However, the molecular phylogenetic studies recently unveiled the complex biodiversity in these planktons. Although the morphological characters of the shells have classified the species, those morphospecies contained multi genetic types, which have own biogeographic distribution according to water mass structure. Therefore, the combination of genetic and morphological analyses should be required to understand the biodiversity of marine tested organisms.

Some radiolarians and planktic foraminifers have various photosynthetic symbionts (dinoflagellates, pelagophytes, haptophytes, and cyanobacterias), and their abundances are extremely higher than those in natural environments. Their rich photosynthetic symbionts are supposed to sustain primary production in the oligotrophic conditions where most algae are restricted their survivals. Intriguingly, some radiolarians and foraminifers are known to have symbionts-specificity, and each symbiotic alga prefer certain light conditions. Because the light conditions in the ocean vertically change through the surface waters, symbionts-specificity may control the distribution patterns of hosts. Our aim of this study is evaluating the importance of photosynthetic activity of radiolarian symbionts for primary production in the oligotrophic conditions, and revealing the relationship between the host's distribution pattern and symbionts-specificity.

The other aim was to establish cultures of novel hetero or osmotrophic protist (mono cellular eukaryotic organism) from the subarctic North Pacific and to resolve several evolutionary events of eukaryote using various information from the protists (e.g. morphological data, genome data and transcriptome data), especially whole eukaryotic relationship. It was still undescribed that the diversity of eukaryotic organisms and the relationship among whole eukaryotic linages as it could not be

revealed in previous studies. Especially, there is no conclusion on the evolutionary relationship between major linages in eukaryotes and we are still examining many hypotheses (e.g. Burki et al. 2016, *Proc. R. Soc.*). Most of the diversity of each major linage in eukaryotes is consisted by protist and it is difficult to grasp the whole protist diversity because it was suggested that there are many protists not belonging to known species in various natural environments by metagenomic analysis (de Vargas et al. 2015, *Science*). It is highly likely that such novel protists will include important strains that elucidate the deep relationship among eukaryotic large lineages. In this cruise, we aim for the elucidation of the eukaryotic large lineage by establishing cultures of novel protist not belonging to the known to date and estimating the phylogenetic position of the protist by phylogenetic analysis.

(2) Sampling equipments

i) VMPS

VMPS system (supplied by Dr. Kimoto, JAMSTEC) with 63 μm mesh, was produced to collect planktons at multi layers (four layers) by vertical towing (Terazaki, 1991). The first net normally keeps open a mouth during taking down the net frame until the bottom depth. Many users have suggested the first net always has contamination then. In this cruise, we preserved the sample of the first net as an archive of a water column for each cast and used only three net samples for our study.

ii) Twin NORPAC net

Twin NORPAC net was equipped with 63 μm mesh and the 2 litter bottle sampler (supplied by Dr. Kimoto, JAMSTEC).

(3) Operation schedule

At stations operated VMPS, the CTD observation over 1000 m water depth was firstly done to check the hydrographic condition and decide the depth range for net-towing. The operation schedule is shown in Appendix 1.

St. KEO: We obtained VMPS net samples between 950 and 0 m water depth.
St. K2: We obtained VMPS net samples between 950 and 0 m water depth.
St. 1: We obtained VMPS net samples between 200 and 0 m water depth after picked planktic foraminifers by Dr. Kimoto. Because radiolarians seemed to be weakened due to taking too much time after sampling, we combined different net samples (samples collected from different layers) and picked radiolarian cells promptly.
St. 3: We obtained Twin NORPAC net samples between 300 and 0 m water depth.
St. 5: We obtained VMPS net samples between 950 and 0 m water depth.

(4) Hydrography

Three out of five stations (KEO, 3, and 5) were located in the North Pacific Subtropical Gyre. Station KEO and 3 placed in the southern edge of the Kuroshio Current and St. 5 was northern edge of the Pacific Warm Water Pool (Fig. 2.15(c).1b). St. KEO was almost in the basement of the Kuroshio Oyashio Extension (KOE), and St. 3 was located in the middle of KOE. Both St. K2 and 1 were located in the Oyashio Current in the Western Subarctic Gyre. Surface mixing layer was observed shallower than 15, 25, and 50 m water depth at St. KEO, K2, and 5, respectively. Chlorophyll maximum layer was distributed 40-120 m (maxima at 80 m water depth), 25-95 m (maxima at 45 m

water depth), and 50-180 m (maxima at 120 m water depth) water depth at St. KEO, K2, and 5, respectively.

(5) Materials and research plan

We collected single- and multi-cell samples of planktic foraminifera and radiolarians and sea water samples from five observation points.

i) Genetic diversity of planktic foraminifers

Responsibility: Y. Ishitani, Y. Inagaki, Y. Ujiié

Each single-cell sample of planktic foraminifera was brushed and cleaned in filtered sea-water and preserved in the PCR-tube with the genomic DNA extraction buffer. A total of 259 planktic foraminifers were obtained: 15, 129, 66, and 49 specimens from St. KEO, K2, 3, and 5, respectively. Nine morphospecies of planktic foraminifers were identified in these samples.

Globorotalia menardii (Parker, Jones & Brady)
Truncorotalia truncatulinoides (d'Orbigny) (=*Globorotalia truncatulinoides*)
Turborotalia hirsuta (d'Orbigny) (=*Globorotalia hirsuta*)
Globigerinoides ruber (d'Orbigny)
Globigerinoides sacculifer (Brady)
Neogloboquadrina dutertrei (d'Orbigny)
Neogloboquadrina incompta (Cifelli)
Orbulina universa (d'Orbigny)
Globigerina quinqueloba (Natland)

Rich genetic diversity of planktic foraminifers has been reported by the molecular phylogenetic studies (e.g., Ujiié and Lipps, 2009). The morphometric analyses have successfully assessed the morphological differences between genetic types (Morard et al., 2009). Moreover, the ecological characters of each genetic type can be traced by isotopic analyses (de Garidel-Thoron et al., unpublished). The combined studies of genetic, morphological, and geochemical analyses on same specimens have revealed the biogeographic distribution of the genetic types and their geochemical features in the worldwide scale (Morad et al., 2015). However, recent molecular marker for planktic foraminifers still has low resolution for some species (e.g., *Globigerinoides sacculifer*). To resolve this problem, we are developing new molecular marker in mitochondrial genome. We will reevaluate the biogeographic distribution of planktic foraminifers with this novel molecular marker.

ii) Genetic diversity of radiolarians

Responsibility: Y. Ishitani, Y. Inagaki

Each single-cell sample of radiolarian was brushed and cleaned in filtered sea-water and preserved in the PCR-tube with the genomic DNA extraction buffer. A total of 480 radiolarian specimens were obtained: 62, 143, 24, 131, and 120 specimens from St. KEO, K2, 1, 3, and 5, respectively. Eighty four morphospecies of radiolarians were identified in these samples.

Acanthostaurus sp.
Actinomma sp.
Amphisphaera sp.
Anthocyrtidium ophirense
Lamprocyclas maritalis
Litharachnium circumtexta
Litharachnium tentorium
Lithopera bacca

Arthlacanthida sp.
Astrolithidae sp.
Axoprunum stauraxonium
Botryostrobus aquilonarius
Chaunacanthida sp.
Circodiscus sp.
Clathromitra circumtexta
Cycladophora davisiana
Cycladophora bicornis
Clathrocorys murrayi
Cyrtopera languncula
Cornutella profunda
Corocalyptra cervus
Carpocanistrum coronatum
Conarachnium parabolicum
Disolenia sp.
Dorydruppa bensoni
Dictyocoryne profunda
Dictyocoryne truncatum
Dictyophimus crisiae
Dictyophimus infabricatus
Dictyocodon elegans
Didymocyrtis tetrathalumus
Druppatructus ostracion
Eucecryphalus gegenbauri
Eucyrtidium hexagonatum
Eucyrtidium acuminatum
Eucyrtidium dictyopodium
Ellipsoxiphium palliatum
Euchitonia elegans
Hexacontium hostile
Hexacontium elegans
Hexalonche amphisiphon
Hexapyle dodecantha
Hexastylus triaxonius
Heliodiscus asteriscus
Holacanthida sp.
Lipmanella xiphephorum
Liriospyris thorax
Lophophaena hispida
Lophospyris pentagona
Lychnaspis sp.
Myelastrum trinibrachium
Myelastrum quandrifolium
Nephrospyris renilla
Octopyle stenozona
Phorticium pylonium
Pterocanium praetextum
Pterocanium trilobum
Pterocorys zancleus
Pterocorys campanula
Pseudodictyophimus gracilipes
Phormospyris stabilis
Rhizoplegma boreale
Sethoconus myxobrachia
Spongotrochus gracialis
Spongodiscus resurgens
Spongodiscus biconcavus
Spongopyle osculosa
Staurolithium sp.
Stylochlamidium venustum
Stylodictya validispina
Spongaster tetras
Spongaster pentas
Spongoliva ellipsoides
Stichocorys seriata
Spirocyrtis scalaris
Stichopilium bicorne
Spongurus pylomaticus
Tetrapyle octacantha
Tetraphormis rotula
Theophormis callipilium
Theocorythium veneris
Verticillata hexacantha

Larcospira quandranguls *Xiphatractus pluto*

We collected 84 morphospecies from each station. Most of them are common at all station. Most of the morphospecies will firstly be sequenced in this study and supply the phylogenetic information to the radiolarian phylogeny at species, genus, or family level. Accumulating the molecular information will complete the radiolarian phylogeny and evolution.

We also collected the species having specific geographic distribution. This morphospecies, which is called "Tropical submergence", is surface dweller in high latitude whereas same species is deep dweller in low latitude area. These taxa have broad distribution and high standing stocks in each water mass (Ishitani et al., 2008), though this specific pattern is observed in the morphospecies. We will confirm whether this phenomenon is happen within same species (molecular genomic level) or not. If these are composed of same genetic species, they could submerge to deferent water mass across the barriers of the surface currents. In a case of a complex of different species, their distribution is represented by different genetic species.

iii) Phylogenetic relationship of radiolarians
Responsibility: Y. Ishitani, Y. Inagaki

Multiple-cell sample of radiolarians was brushed and cleaned in filtered sea-water and (1) preserved in Trizol or (2) amplified cDNA library with SMART-seq v4 kit. For radiolarian species belonging to Spumellaria and Acatharia are used for this study.

Hexaconus sp.	6 cells (Trizol)	
Lychnapsis sp.	10 cells (Trizol)	3 cells (SMART-seq)
Rhizoplegma boreale	4 cells (Trizol)	
Spongodiscus biconcavus	10 cells (Trizol)	3 cells (SMART-seq)

We will analyze RNA of *Hexaconus* sp., *Lychnapsis* sp., *Rhizoplegma boreale* and *Spongodiscus biconcavus*, which were dominant species in the radiolarian collection of this cruise. We will use their protein-coding genes represented as house keeping genes with low evolutionary rate. The phylogeny of the protein-coding gene is available to reveal the phylogenetic relationship at the Radiolarian order level. Moreover, these taxa have specific pseudopodia characterized by thicker and quickly motility rather than the other species. These characters of the pseudopodia are similar to that of foraminiferal reticulopodia. Concerning the sister group relationship between Radiolaria and Foraminifera in the crown of Rhizaria, this fact leads two hypotheses; one is lateral gene transfer from Foraminifera, and another one is express of ancestral character, which is common between Radiolaria and Foraminifera. This study will supply a powerful evidence to understand phylogenetic relationship between Radiolaria and Foraminifera, and also early evolution of Rhizaria.

iv) Diversity of radiolarian symbionts and their photosynthetic activity
Responsibility: Y. Ishitani, Y. Inagaki

Each single-cell sample of radiolarian was brushed and cleaned in filtered sea-water and measured photosynthetic activity by Fast Repetition Rate Fluorometry (FRRF). We measured 39 radiolarians species dwelling in the surface waters above 300m water depth. Also, we extracted pigments from some radiolarians (*Dictyocoryne profunda*, *D. truncatum,* and *Euchitonia elegans*) by dimethylformamide (DMF) overnight at 4˚C, and measured pigment concentration by using High Performance Liquid Chromatography (HPLC).

Fast Repetition Rate Fluorometry is the method measure the fluorescence which is filled in the electron transportation through Photosystem II by a sequence of rapid light flashes. This method can measure minimum fluorescence (F0) and maximum fluorescence (Fm), and high F0 and Fm suggest high photosynthetic activity. Our FRRF can flash two type of light; blue and green, which can measure the photosynthetic activity of chlorophyll-a (most algae and cyanobactera) and phycobilin (cyanobacterias), respectively. Because the absorption wavelength of chlorophyll-a and phycobilin overlapped a little, the FRRF of green light detect chlorophyll-a a bit. Thus, higher F0 and Fm of green light than those of blue light can only maen the presence of phycobilin (cyanobacterias). From the FRRF measurements, we can detect the chlorophyll activity of chlorophyll-a (most algae and cyanobactera) and phycobilin (cyanobacterias).

We measured chlorophyll activity of symbionts in radiolarians by using FRRF (Appendic2). Some radiolarians show high F0 and Fm in blue light (Fig. 2.15(c).1a), and *Sphaerozoum punctatum* and *Sethoconus myxobrachia* showed extremely high value. We also observed their high abundance of algal symbionts under the microscope. *Sethoconus myxobrachia* is rare species, and its ecological information is restricted. This observation shed a light on the ecology of this mysterious radiolarinan. We also measured chlorophyll activity of symbionts in two radiolarians (*Dictyocoryne profunda* and *D. truncatum*) known to have cyanobacterias (Yuasa et al., 2012; Foster et al., 2006). However, these two radiolarians showed higher F0 and Fm of blue light than those of green light (Fig. 2.15(c).1), suggesting symbionts in radiolarians have no phycobilin (cyanobacterias). From the HPLC analysis, we detected zeaxanthin (having in cyanobacetrium) in *D. profunda* and fucoxanthine (having in diatoms) in *D. truncatum* (Table 2.15(c).1). The presence of zeaxanthin (cyanobacetrium) but no chlorophyll-activity in FRRF suggests that cyanobacterium symbionts in *D. profunda* skip Photosystem II and photophosphorylate cyclically, which we cannot detect photosynthetic activity by FRRF. Cyclic photophosphorylation produces less energy than linear photophosphorylation (used by most algae), but it form low destructive reactive oxygen species. We know extremely high abundance of symbionts in radiolarian, and reactive oxygen species from such abundant symbionts is possibly too lethal to survive. Thus, we hypothesize that host radiolarian (*D. profunda*) control photophosphorylation of cyanobacterium symbionts to avoid much destructive reactive oxygen species. While, the absence of zeaxanthin (cyanobacetrium) but no chlorophyll-activity in FRRF suggests that cyanobacterium symbionts in *D. truncatum* have no photosynthesis. Some endosymbiotic cyanobacteria in diatoms, dinoflagellates, and coccolithophores are used for nitrogen fixation but no photosynthesis (e.g., Nakayama et al., 2014). The immunolabeling experiment suggests cyanobacterium symbionts in *D. truncatum* have nitrogenase for nitrogen fixation (Foster et al., 2006). These results suggest cyanobacterium symbionts in *D. truncatum* are used for nitrogen fixation. Intriguingly, fucoxanthine (diatoms) are detected from *D. truncatum*, suggesting the presence of diatom's symbionts. Light microscopic analysis suggested the yellow-brown pigmented microalgae are coexisted with endobionts (Anderson and Matsuoka, 1992). *Dictyocoryne truncatum* possibly possess cyanobacterium for nitrogen fixation and diatoms for photosynthesis.

(a) Blue light

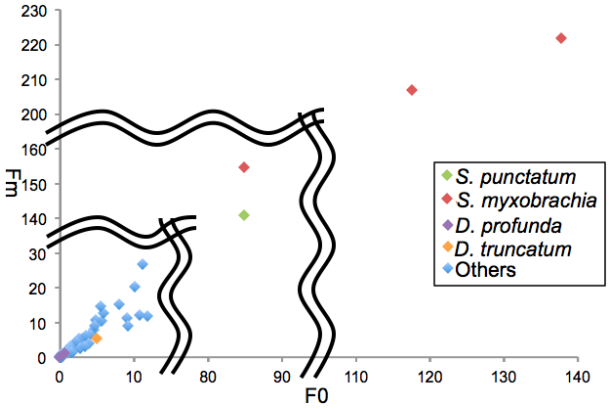

(b) Green light

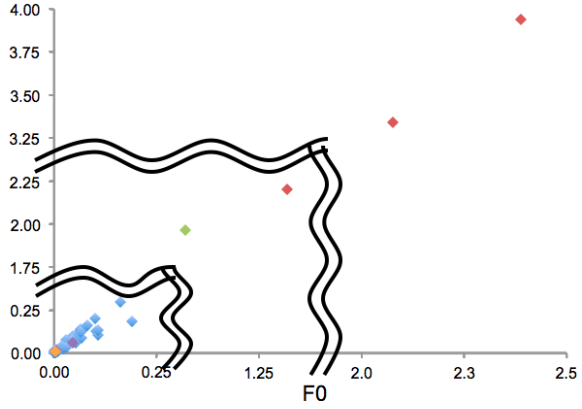

Figure 2.15(c).1. Fm and Fo value of FRRF with (a) blue light and (b) green light.

Table. 2.15(c).1. Pigment type and density of each radiolarian detected by HPLC.

Species	Pigment	Density （μg/L）	Memo
Dictyocoryne profunda	Zeaxanthin	0.37	
	Beta-carotene	0.17	Possibly α-carotene
Dictyocoryne truncatum	19'-hexanoyloxyfucoxanthin	0.41	
Euchitonia elegans	Chlorophyll c2	0.13	Possibly Mgdvp
	Peridinin	0.2	

v) Establish the cultures of novel hetero- or osmotrophic protists

Responsibility: T. Shiratori, E. Yazaki, T. Hashimoto, Y. Inagaki

Each seawater sample was filtered twice with a filter with different pore sizes (8μm and 3 μm). Seawater samples filtered with filters of 3 μm and 8 μm were added to the medium (1/2 ESM + one grain of sterilized rice: total 40ml) in 4 ml each and incubated 20℃. We established 21 cultured strains mixed with various eukaryotes.

We will establish mono cultures from 21 mixed cultures and extract total DNA from the established mono culture strain. Moreover, we will amplify the 18s rDNA sequence as a phylogenetic marker from that DNA and perform using the 18s rDNA sequence to estimate the phylogenetic position of the cultured strain. If the cultured strain is not close to the existing eukaryotic lineage by phylogenetic analysis based on 18s rDNA, we will acquire a large-scale sequence data based on total RNA extracted from the cultured strain and estimated elucidate the phylogenetic position by large scale multiple gene phylogeny.

7. Conclusion

During three weeks cruise in 2018, we succeed to obtain many important samples from the northwestern part of the Pacific area. Each participant has own research project that will yield many useful information for understanding the biodiversity of marine heterotrophic protists.

8. Acknowledgement

We thank the captain and crew of *R/V Mirai* for their technical support and navigation during the cruise. We deeply appreciate for kind organization of chief scientist Dr. T. Fujiki and for big help of all onboard scientists.

References

Anderson, R. and Matsuoka, A., 1992. Endocytoplasmic microalgae and bacteroids within the central capsule of the Radiolarian *Dictyocoryne truncatum*. Symbioses 12, 237–47.

Burki, F., Kaplan, M., Tikhonenkov, D. V., et al., 2016. Untangling the early diversification of eukaryotes: a phylogenomic study of the evolutionary origins of Centrohelida, Haptophyta and Cryptista. Proc. R. Soc. B. Sci., 283, 1823

De Vargas, C., Audic, S., Henry, N., et al. 2015. Eukaryotic plankton diversity in the sunlit ocean. Science 348, 1261605Foster, R., Carpenter, E., Bergman, B., 2006. Unicellular cyanobionts in open ocean dinoflagellates, radiolarians, and tintinnids: ultrastructural characterization and immuno-localization of phycoerythrin and nitrogenase. J. Phycol. 42, 453–463.

Ishitani, Y., Takahashi, K., Okazaki, Y., Tanaka, S., 2008. Vertical and geographic distribution of selected radiolarian species in the North Pacific. Micropaleontology, 54, 27-39.

Morard, R., Quillévéré, F., Escarguel, G., et al., 2009. Morphological recognition of cryptic species in the planktonic foraminifer Orbulina universa. Mar Micropaleontol. 71, 148-165.

Morad R., Darling, K., Mahé, F., et al., 2015. PFR2: a curated database of planktonic foraminifera 18S ribosomal DNA as a resource for studies of plankton ecology, biogeography, and evolution. Mol. Ecol. Res. 15, 1472-1485.

Nakayama, T., Kamikawa, R., Tanifuji, et al., 2014. Complete genome of a nonphotosynthetic cyanobacterium in a diatom reveals recent adaptations to an intracellular lifestyle. Proc. Natl. Acad. Sci. USA. 111, 11407-11412.

Terazaki, M., 1991. Study on Deep-Sea Plankton. Pro. Adv. Mar.Tech. Conf. 4, 25-31.

Ujiié, Y., Lipps, J.H., 2009. Cryptic diversity in planktonic foraminifera in the northwestern Pacific Ocean. J. Foramin. Res. 39 (3), 145–154.

Yuasa Y., Horiguchi, T., Mayama, S., Matsuoka, S., Takahashi, O., 2012. Ultrastructural and molecular characterization of cyanobacterium symbionts in *Dictypcoryne profunda* (polycystine radiolarian). Symbiosis 57, 51-55.

2.15(d) Respiration experiments of pelagic copepods

Tatsuki Toda (Soka University)
Noriaki Natori (Soka University)

(1) Objectives

Copepods (Crustacea: Copepoda) are the most abundant group on earth and the major link between primary production and higher trophic levels in aquatic food webs (Mauchline 1998). These free-living calanoid copepods present all marine regions and usually make up 70% more of all net collected plankton (Lalli and Parsons 1993). The aim of this study is to determine the oxygen consumption of pelagic calanoid copepods by using a recently developed fiberoptic oxygen meter with their high sensitivity, their ability to measure low oxygen concentrations with a high precision, their driftless signals and their application to microscales (Köster *et al.* 2008). Direct measurements of oxygen consumption of copepods in a controlled system provide a robust estimate of the organisms' metabolic demand and energy expenditure (Brown *et al.* 2004; Ikeda 1985).

(2) Instruments and methods

i) Oxygen measurements using an oxygen-dependent luminescence

Respiration rates of copepods were estimated from reduction rates of dissolved oxygen (DO) concentration measured with a 4-channel fiberoptic oxygen meter (FireSting O_2, PyroScience GmbH, Aachen, Germany). Three 5-mL DO glass vials were used to rear copepods, and another DO glass vial was used for control. Planar oxygen sensor spots (5 mm diameter, PyroScience GmbH) were pasted onto the inner walls of the DO glass vials with double sticky tape. The sensor spots are coated with the REDFLASH indicators which use red light excitation and lifetime detection in the near infrared, with PET foil as carrier material. The measuring principle of the optical oxygen meter is based on the quenching of the REDFLASH indicator luminescence caused by collision between oxygen molecules and the REDFLASH indicator. The REDFLASH indicators are excitable with red light and show an oxygen-dependent luminescence. The sensor signal was read out using a fiber spot sensor connecting via the channel of the FireSting O_2 to PC.

ii) Rearing of copepods

Copepods were collected with a plankton net (60 cm diameter, 180-μm mesh size, with a plastic bottle at the bottom) from four stations located on the western Pacific; KEO, K2, S1 and S4. The copepods were immediately transferred into seawater collected at the site and kept in a cold room at temperature about 4 °C. The sample was inspected with a dissecting microscope (WILD M10, Leica) to sort target species. As representative species occurring the western Pacific, we selected 11 species on board; *Candacia* sp., *Euchaeta* sp., *Gaetanus simplex*, *Gaidius* sp., *Metridia pacifica*, *Neocalanus cristatus*, *Neocalanus gracilis*, *Phaenna* sp., *Pleuromamma xyphais*, *Pleuromamma* sp.1 and *Pleuromamma* sp.2. Copepods collected were transferred to DO glass vials and reared in an incubator. DO concentration of each DO glass vial was continuously measured by 4-channel fiberoptic oxygen meter. Respiration rate (R, nmol O_2 ind^{-1} h^{-1}) was estimated from the slope of the linear regression line of oxygen concentration in both experimental and control DO glass vials against incubation time using the following equation:

$$R = (\Delta O_{exp} - \Delta O_c) V/N$$

where ΔO_{exp} and ΔO_c are the coefficients of oxygen consumption (μmol O_2 L^{-1} h^{-1}) estimated as the slope of the regression lines in the three experimental vials and slope in the control vials, respectively, using the least-square method, and V and N are volume of the DO glass vial and number of copepods in the control vial (Liu and Ban 2016).

(3) Preliminary result

Estimated respiration rates of copepod collected were shown in Table 2.1.1. The oxygen measurements were carried out at several temperatures or densities on each species. The conditions of measurements were shown in Table 2.1.1.

Table 2.1.1. Individual respiration rates of copepods collected by a plankton net (nmol O_2 ind^{-1} h^{-1})

Species	Vial 1	Vial 2	Vial 3	Mean	SD
KEO_*Phaenna* sp._10°C	1.13	1.68	1.91	1.57	0.40
KEO_*Phaenna* sp._15°C	3.27	3.58	3.23	3.36	0.19
KEO_*Phaenna* sp._20°C	5.02	4.45	5.14	4.87	0.37
K2-1_*Gaetanus simplex*_4°C	0.993	1.35	0.976	1.11	0.21
K2-1_*Gaetanus simplex*_6°C	1.38	1.56	1.43	1.46	0.09
K2-1_*Gaetanus simplex*_8°C	1.60	2.21	2.03	1.95	0.31
K2-1_*Candacia* sp._4°C	4.95	5.68	5.14	5.26	0.38
K2-1_*Candacia* sp._6°C	3.29	3.46	6.02	4.26	1.53
K2-1_*Candacia* sp._8°C	2.69	3.28	6.67	4.21	2.15
K2-1_*Gaidius* sp._4°C	2.52	3.50	2.11	2.71	0.72
K2-1_*Gaidius* sp._6°C	2.04	3.89	2.59	2.84	0.95
K2-1_*Gaidius* sp._8°C	3.83	4.64	3.28	3.91	0.68
K2-1_*Neocalanus cristatus*_4°C	4.79	4.23	4.89	4.63	0.36
K2-1_*Neocalanus cristatus*_6°C	5.52	6.72	5.99	6.07	0.60
K2-1_*Neocalanus cristatus*_8°C	8.34	-	7.63	-	-
K2-2_*Metridia pacifica*_4°C	0.709	1.18	0.760	0.884	0.26
K2-2_*Metridia pacifica*_6°C	0.814	1.38	0.842	1.01	0.32
K2-2_*Metridia pacifica*_8°C	0.958	1.48	1.04	1.16	0.28
K2-2_*Pleuromamma* sp.1_4°C_3ind	2.46	2.90	2.52	2.63	0.24
K2-2_*Pleuromamma* sp.1_6°C_3ind	2.81	3.23	2.95	3.00	0.21
K2-2_*Pleuromamma* sp.1_8°C_3ind	3.08	3.73	3.20	3.34	0.34
K2-2_*Pleuromamma* sp.1_6°C_5ind	2.88	3.10	2.68	2.89	0.21
S1_*Pleuromamma* sp.2_4°C	2.00	1.48	2.67	2.05	0.60
S1_*Pleuromamma* sp.2_6°C	2.05	2.20	2.77	2.34	0.38
S1_*Pleuromamma* sp.2_8°C	2.10	2.28	3.17	2.52	0.57
S1_*Pleuromamma* sp.2_10°C	2.63	2.85	3.73	3.07	0.58
S1_*Pleuromamma xyphais*_4°C	1.39	2.56	2.79	2.25	0.75
S1_*Pleuromamma xyphais*_6°C	1.63	2.16	2.25	2.01	0.33
S1_*Pleuromamma xyphais*_8°C	1.93	3.38	3.05	2.79	0.76

S1_*Pleuromamma xyphais*_10°C	2.18	3.40	3.86	3.14	0.87
S4_*Neocalanus gracilis*_15°C	4.40	5.40	1.72	3.84	1.90
S4_*Neocalanus gracilis*_20°C	4.60	6.82	4.21	5.21	1.41
S4_*Neocalanus gracilis*_25°C	6.19	7.27	6.95	6.80	0.55
S4_*Euchaeta* sp._10°C	3.60	3.84	1.74	3.06	1.15
S4_*Euchaeta* sp._15°C	6.85	5.67	3.87	5.46	1.50
S4_*Euchaeta* sp._20°C	9.97	8.01	6.68	8.22	1.66

(4) Data archive

These obtained data will be submitted to JAMSTEC Data Management Group (DMG).

(5) References

Brown, J. H., J. F. Gillooly, A. P. Allen, V. M. Savage and G. B. West (2004) Toward a metabolic theory of ecology. *Ecology*, 85, 1771–1789.

Ikeda, T. (1985) Metabolic rates of epipelagic marine zooplankton as a function of body mass and temperature. *Mar. Biol.*, 85, 1–11.

Köster, M., C. Karause and G. A. Paffenhöfer (2008) Time-series measurements of oxygen consumption of copepod nauplii. *Mar. Ecol. Prog. Ser.*, 353, 157–164.

Lalli, C. M. and T. R. Parsons (1993) Biological oceanography: An introduction. Butterworth Heinemann Ltd, Oxford.

Liu, X. and S. Ban (2016) Effects of acclimatization on metabolic plasticity of *Eodiaptomus japonicus* (Copepoda: Calanoida) determined using an optical oxygen meter. *J. Plankton Res.*, 39, 111–121.

Mauchline, J. (1998) The biology of calanoid copepods. *Adv. Mar. Biol.*, 33, 1–710.

2.16 Distribution patterns of microbial abundance, activity and diversity

Taichi YOKOKAWA (JAMSTEC)
Akinori YABUKI (JAMSTEC)
Masahito SHIGEMITSU (JAMSTEC)
Takashi SHIRATORI (JAMSTEC)

(1) Introduction

Microbes (prokaryotes and pico-eukaryotes) play a major role in marine biogeochemical fluxes. Biogeochemical transformation rates and functional diversity of microbes are representative major topics in marine microbial ecology. However, the link between microbes properties and biogeochemistry in the epi- meso- and bathypelagic layers has not been explained systematically despite of the recent studies that highlight the role of microbes in the cycling of organic and inorganic matter. (Herndl and Reinthaler 2013; Yokokawa et al. 2013; Nunoura et al. 2015). Moreover, microbial diversity and biogeography in the meso- and bathypelagic ocean and its relationship with upper layers and deep-water circulation have also not been well studied.

The objectives of this study, which analyze the water columns from sea surface to just above the bottom of western North Pacific, were 1) to determine the abundance of microbes; 2) to study the heterotrophic/autotrophic production of prokaryotes; 3) to assess the community composition of microbes; 4) to know microbial diversity through water columns in the both subarctic and subtropical regions.

(2) Methods

Microbial abundance

Samples for microbial abundances (prokaryotes, pico-eukaryotes and viruses) were collected in every routine cast and depth, and the bucket samplings. Samples were fixed with glutaraldehyde (final concentration 0.5%) and frozen at -80°C. The abundance and relative size of microbes and viruses will be measured by a flow cytometry in after nucleic acid staining with SYBR-Green I.

Microbial activity measurements

Heterotrophic microbial production was determined based on ^{3}H-leucine incorporation rate. ^{3}H-leucine incorporation rate was determined as a proxy for heterotrophic or mixotrophic prokaryotic production. Triplicate subsamples (1.5 mL) dispensed into screw-capped centrifuge tubes amended with 10 nmol L^{-1} (final concentration) of [^{3}H]-leucine (NET1166, PerkinElmer) and incubated at in situ temperature (± 2°C) in the dark. One trichloroacetic acid (TCA) killed blank was prepared for each sample. Incubation periods were 1 hour and 24 hours for the upper (0 – 250 m) and deeper (300 – bottom) water layers, respectively. After the incubation, proteins were TCA (final conc. 5%) extracted twice by centrifugation (15000 rpm, 10 min, Kubota 3615-sigma), followed by the extraction with ice-cold 80% ethanol.

The samples will be radioassayed with a liquid scintillation counter using Ultima-GOLD (Packard) as scintillation cocktail. Quenching is corrected by external standard channel ratio. The disintegrations per minute (DPM) of the TCA-killed blank is subtracted from the average DPM of the samples, and the resulting DPM is converted into leucine incorporation rates.

Samples for leucine incorporation activity measurements were taken at stations KEO, K2, S1, S3, S5 in the routine “Deep” casts.

Autotrophic microbial production was determined based on ^{14}C-bicarbonate incorporation rate. ^{14}C-bicarbonate incorporation rate was determined as a proxy for autotrophic or mixotrophic prokaryotic production. Triplicate subsamples (20 mL) dispensed into screw-capped centrifuge tubes were inoculated with 1480 kBq (final concentration) of $NaH^{14}CO_3$ (NEC086H, PerkinElmer) and incubated at in situ temperature (± 2°C) in the dark for 72-144 hours. One glutaraldehyde-killed blank was prepared for each sample. Incubations were terminated by adding glutaraldehyde (2% final concentration) to the samples, and the samples were filtered onto 0.2-μm polycarbonate filters.

The samples will be radioassayed with a liquid scintillation counter using Filter-Count (PerkinElmer) as scintillation cocktail, after the filters are fumed with concentrated HCl for 12 hours. Quenching is corrected by external standard channel ratio. The DPM of the glutaraldehyde-killed blank is subtracted from the average DPM of the samples and the resulting DPM is converted into bicarbonate incorporation rates.

Samples for ^{14}C-bicarbonate incorporation activity measurements were taken at stations KEO, K2, S1, S3, and S5 in the routine "Deep" casts.

Microbial diversity

Microbial cells in water samples were filtrated on cellulose acetate filter (0.2μm) and stored at -80˚C. Environmental DNA or RNA will be extracted from the filtrated cells and used for 16S/18S rRNA gene tag sequencing using MiSeq, quantitative PCR for genes for 16S rRNA, and/or metatranscriptomics. Samples for microbial diversity were taken at stations KEO, K2, S1, S3, and S5 in the routine “Deep” cast, and the bucket samplings.

Cultivation of eukaryote

Water samples were collected from KEO, K2, S1, S3, and S5. Samples were filtered through polycarbonate filter (10μm) and precultured with culture media at 20 °C under a 12h/12h light/dark cycle. Precultured protists were isolated by micropipetting method or serial dilution method and incubated in the same condition as precultures. Cultures will be identified by light microscopy and 18S rRNA gene sequences.

References

Herndl GJ, Reinthaler T (2013) Microbial control of the dark end of the biological pump. Nature geoscience, 6:718-724

Yokokawa T, Yang Y, Motegi C, Nagata T (2013) Large-scale geographical variation in prokaryotic abundance and production in meso- and bathypelagic zones of the central Pacific and Southern Ocean. Limnology and Oceanography, 58:61-73

Nunoura T, Takaki Y, Hirai M, Shimamura S, Makabe A, Koide O, Kikuchi T, Miyazaki J, Koba K, Yoshida N, Sunamura M, Takai K (2015) Hadal biosphere: Insight into the microbial ecosystem in the deepest ocean on Earth. Proceedings of the Natioanl Academy of Sciences 112:1230-1236

2.17 Fluorescent dissolved organic matter (FDOM)

Masahito Shigemitsu (JAMSTEC RCGC)

(1) Objectives

Marine dissolved organic matter (DOM) is known to be one of the largest reservoirs of reduced carbon on Earth, and most of the carbon exists as refractory DOM (RDOM) (Hansell et al., 2009). RDOM is thought to be generated by microbial mineralization of organic matter produced in the sunlit surface ocean, and play an important role in carbon sequestration (Jiao et al., 2010). Some components of the RDOM can be detected as fluorescent DOM (FDOM).

In this cruise, we try to gain insights into interactions between RDOM and microbial abundance, activity and diversity in the western North Pacific.

(2) Methods

Seawater samples were obtained from Niskin bottles on a CTD-rosette system at 5 stations (stations KEO, K2, S1, S3, and S5). Each sample taken in the upper 250 m was filtered using a pre-combusted (450 ^{o}C for 4 hours) 47-mm Whatman GF/F filter. The filtration was carried out by connecting a spigot of the Niskin bottle through silicone tube to an inline plastic filter holder. Filtrates were collected in pre-combusted borosilicate glass vials, and were immediately stored frozen until analysis. Other samples taken below 250 m were unfiltered and stored in the same way.

The frozen samples will be thawed at room temperature, and excitation-emission matrix (EEM) fluorescence will be measured using a fluorometer (Aqualog, Horiba). Fluorescence intensities will be normalized to Raman area. In order to separate discrete fluorescent fractions from the measured EEMs, we will apply parallel factor analysis (PARAFAC) with the DOMFluor toolbox (Stedmon and Bro, 2008). The EEMs of the excitation wavelengths from 240 nm to 450 nm and emission wavelengths from 300 nm to 560 nm will be used for PARAFAC modeling, and several components model will be used.

(3) References

Hansell, D. A., C. A. Carlson, D. J., Repeta, and R. Schlitzer, Dissolved organic matter in the ocean: A controversy stimulates new insights, Oceanogr. 22, 202-211, 2009

Jiao, N. et al., Microbial production of recalcitrant dissolved organic matter: long-term carbon storage in the global ocean, Nat. Rev. Microbiol. 8, 593-599, 2010.

Stedmon, C. A. and R. Bro, Characterizing dissolved organic matter fluorescence with parallel factor analysis: a tutorial, Limnol. Oceanogr. Methods 6, 572-579, 2008.

2.18 Seawater density

Hiroshi UCHIDA (JAMSTEC RCGC)

(1) Objectives

The objective of this study is to collect Absolute Salinity (also called “density salinity”) data and to evaluate the algorithm to estimate Absolute Salinity provided along with TEOS-10 (the International Thermodynamic Equation of Seawater 2010) (IOC et al., 2010).

(2) Instruments and methods

i) Seawater density by an oscillation-type density meter

Seawater densities will be measured after the cruise with an oscillation-type density meter (DMA 5000M, Anton-Paar GmbH, Graz, Austria) with a sample changer (Xsample 122, Anton-Paar GmbH). The sample changer is used to load samples automatically from up to ninety-six 12-mL glass vials.

The water samples were collected in 100-mL aluminum bottles (Mini Bottle Can, Daiwa Can Company, Japan) at stations KEO_2, K02_7, 001_1, 003_1 and 005_1. The bottles were stored upside down in a warehouse of the ship. Densities of the samples will be measured at 20 ºC by the density meter and density salinity can be back calculated from measured density and temperature (20 ºC) with TEOS-10.

ii) Seawater density by a developing refractive index density meter

Seawater densities will also be measured after the cruise with a developing refractive index density meter. The water samples for this measurement were collected in 200-mL borosilicate glass bottles used for the IAPSO Standard Seawater at station K02_7.

(3) Data archive

These obtained data will be submitted to JAMSTEC Data Management Group (DMG).

(4) References

IOC, SCOR and IAPSO (2010) The international thermodynamic equation of seawater – 2010: Calculation and use of thermodynamic properties. Intergovernmental Oceanographic Commission, Manuals and Guides No. 56, United Nations Educational, Scientific and Cultural Organization (English), 196 pp.

2.19 Sound velocity

Hiroshi UCHIDA (JAMSTEC RCGC)
Shinsuke TOYODA (MWJ)
Tomohide NOGUCHI (MWJ)
Keisuke TAKEDA (MWJ)
Rio KOBAYASHI (MWJ)
Tomokazu CHIBA (MWJ)

(1) Objectives

The objective of this measurement is to estimate Absolute Salinity profiles from sound velocity data with temperature and pressure data from CTD, and to evaluate the algorithm to estimate Absolute Salinity provided along with TEOS-10 (the International Thermodynamic Equation of Seawater 2010) (IOC et al., 2010).

(2) Instruments and methods

Sound velocity profiles were measured at the CTD casts by using two velocimeter (MiniSVS OEM [serial no. 24001] and MiniSVP [serial no. 49618], Valeport Ltd., Devon, United Kingdom). The sound velocity sensing elements are a ceramic transducer (signal sound pulse of 2.5 MHz frequency), a signal reflector, and spacer rods to control the sound path length (5 cm for MiniSVS and 10 cm for MiniSVP), providing a measurement at depths up to 6000 m. The velocimeters were attached to the CTD frame and level of the sound path of the velocimeter was same as that of the CTD temperature sensors. Sound velocity data were obtained through serial uplink port of the CTD at a sampling rate of 12 Hz for MiniSVS and stored in the velocimeter at a sampling rate of 8 Hz for MiniSVP. Although temperature and pressure data were also measured by the MiniSVP, only sound velocity data from MiniSVS and MiniSVP will be combined with the CTD temperature and pressure data measured at a sampling rate of 24 Hz to estimate Absolute Salinity.

Absolute Salinity can be back calculated from measured sound velocity, temperature and pressure and will be calibrated in situ referred to the Absolute Salinity measured by a density meter for water samples.

(3) Data archive

These obtained data will be submitted to JAMSTEC Data Management Group (DMG).

(4) References

IOC, SCOR and IAPSO (2010) The international thermodynamic equation of seawater – 2010: Calculation and use of thermodynamic properties. Intergovernmental Oceanographic Commission, Manuals and Guides No. 56, United Nations Educational, Scientific and Cultural Organization (English), 196 pp.

2.20 LADCP

Hiroshi UCHIDA (JAMSTEC RCGC)
Shinya KOUKETSU (JAMSTEC RCGC)
Kensuke WATARI (JAMSTEC MARITEC)
Masahiro KAKU (JAMSTEC MARITEC)
Shinsuke TOYODA (MWJ)
Tomohide NOGUCHI (MWJ)
Keisuke TAKEDA (MWJ)
Rio KOBAYASHI (MWJ)
Tomokazu CHIBA (MWJ)

(1) Objectives

The objective of this measurement is to obtain oceanic current profiles from sea surface to seafloor.

(2) Instruments and methods

Current profiles were measured by acoustic Doppler current profilers (ADCP) (Workhorse Monitor WHM300, Teledyne RD Instruments, Inc., Poway, California, USA, serial no. 22900 [downward looking] and 22899 [upward looking]) attached to the CTD/water sampling frame. The ADCP has four acoustic transducers with 20-degree beam angles, rated in water depths up to 6000 m. The lowered ADCPs (LADCP) makes direct current measurements at the depths of the CTD, thus providing a full profile of current velocity. The LADCPs were powered during the CTD casts by a 48 volts battery pack. By combining the measured seawater velocity and seafloor velocity relative to the CTD frame, and shipboard navigation data during the CTD cast, the absolute velocity profile can be obtained (e.g. Visbeck, 2002; Kouketsu, 2016).

In this cruise, the LADCP data were collected with the following configuration.

Bin size: 4.0 m
Number of bins: 25
Pings per ensemble: 1
Ping interval: 1.0 second

To estimate absolute velocity of the CTD frame accurately, an inertial measurement unit (DMU-30, Silicon Sensing Systems Japan, Hyogo, Japan) was tested with the LADCPs. Three-axis angular increment, angular acceleration, speed increment and acceleration data were obtained with a sampling rate of 200 Hz at station KEO_2, K02_1, K02_7, 001_1, 003_1 and 005_1.

(3) Data archive

These obtained data will be submitted to JAMSTEC Data Management Group (DMG).

(4) Reference

Kouketsu, S. (2016): Lowered Acoustic Doppler Current Profiler (LADCP). *Guideline of ocean observations*, 8, G809EN:001-007.

Visbeck, M. (2002): Deep velocity profiling using Lowered Acoustic Doppler Current Profiler: Bottom track and inverse solutions. *J. Atmos. Oceanic Technol.*, 19, 794–807.

2.21 Micro-Rider

Hiroshi UCHIDA (JAMSTEC RCGC)
Shinya KOUKETSU (JAMSTEC RCGC)

(1) Objectives

The objective of this study is to to evaluate vertical mixing by measuring microstructure of temperature profiles.

(2) Instruments and methods

Microstructure observations were carried out by using Micro-Rider 6000 (MR6000, Rockland Scientific International, Inc., Victoria, British Colombia, Canada, serial no. 154). The MR6000 was mounted on the CTD/water sampling frame with the temperature sensors directed downward and the power was supplied through the CTD. Two thermistors (FP07) were used to obtain high-frequency changes in temperature (Table 2.21.1). Pressure and acceleration were also obtained by the MR6000 with high-frequency. Temperature profile obtained by the CTD secondary temperature sensor with low-frequency were also stored in the MR6000. These data will be processed by using a similar method to that of Goto et al. (2018).

Table 2.21.1. List of serial number of the temperature sensor used in this cruise.

Station no.	Primary	Secondary	Note
KEO_1	T1112	T1510	Bad data for T1112
KEO_2 ~ KEO_3	T1337	T1510	Bad data for T1337
KEO_4 ~ 006_2	T1320	T1510	

(3) Data archive

These obtained data will be submitted to JAMSTEC Data Management Group (DMG).

(4) Reference

Goto, Y., I. Yasuda and M. Nagasawa (2018): Comparison of turbulence intensity from CTD-attached and free-fall microstructure profiles. *J. Atmos. Oceanic Technol.*, 35, 147–162.

2.22 RBR CTD testing

Hiroshi UCHIDA (JAMSTEC RCGC)

(1) Objectives

The objective this measurement is to to evaluate the RBR CTDs by comparing with the Sea-Bird CTD.

(2) Instruments and methods

RBR Ltd. (Ottawa, Canada) designs and manufacturers self-contained CTDs and OEM sensors, and over the last few years has been developing instruments for deep applications (e.g., Argo and Deep Argo floats). Making accurate measurements of conductivity requires a careful examination of how the sensor behaves at increasingly high pressures. A few years ago, the RBR conductivity sensor was redesigned, and this means that the pressure effect needs to be revisited because the new sensors respond in a different way to pressure.

Six RBR CTDs (RBR Concerto) were tested (Table 2.22.1). Slow descent and ascent rate profiles without water sampling were obtained at K02_3 (rate of 0.2 m/s and without heave motion of the crane) and 006_2 (rate of 0.1 m/s with heave motion of the crane for depths deeper than 100 m), to evaluate the dynamic corrections made to conductivity, such as the thermal inertia effect on conductivity, depend on profiling rate. The RBR CTD with oxygen sensors was used in the deep in situ filtration observation. The RBR CTD was attached to the frame of the in situ filtration device (conductivity sensor upward) and 4 hours long data were obtained at 3000 m depths.

Table 2.22.1. List of serial number of the RBR CTDs used in this cruise.

Station no.	Rated pressure (dbar)	Station_cast no. tested
066094*	6000	All CTD stations and the deep in situ filtration (3000 m) (conductivity sensor downward for KEO_1~4, K02_1~2)
060661	6000	All CTD stations (conductivity sensor downward for KEO_1~4, K02_1)
060669, 060671	2000	KEO_3~4, K02_3~6, K02_8~9, 002_1~2, 004_1~2, 006_1~2
066127, 066128	1300	K02_3, 006_2~3

*with two optical dissolved oxygen sensors (RBRcoda ODO fast, serial no. 93143 and 93146)

(3) Data archive

These obtained data will be submitted to JAMSTEC Data Management Group (DMG).

2.23 Spectral absorption and attenuation meter testing

Hiroshi UCHIDA (JAMSTEC RCGC)
Haruka TAMADA (MWJ)
Erii IRIE (MWJ)

(1) Objectives

The objective of this test is to estimate sea surface chlorophyll concentration from beam absorption and attenuation coefficients measured continuously along the cruise track.

(2) Instruments and methods

Beam absorption and attenuation coefficients were measured by spectral absorption and attenuation meter (ACS, Sea-Bird Scientific, Philomath, Oregon, USA, serial no. ACS035). The ACS measures absorption (m-1) and attenuation (m-1) at 5 Hz and their pathlengths of the beams are 25 cm. The ACS was used with the continuous Sea Surface Water Monitoring system in the sea surface monitoring laboratory. Measured data were recorded by using the Compass Software (Sea-Bird Scientific).

The ACS frequently stopped and required to restart. Therefore, the data were fragmentary.

(3) Data archive

These obtained data will be submitted to JAMSTEC Data Management Group (DMG).

(4) Reference

Roesler, C.S. and A.H. Barnard (2013): Optical proxy for phytoplankton biomass in the absence of photophysiology: Rethinking the absorption line height. *Methods in Oceanography*, 7, 79–94.

3.1 KEO Sediment trap experiment

Makio HONDA (JAMSTEC RCGC)

(1) Purpose

Based on the comparison study of biogeochemistry in the northwestern North Pacific eutrophic subarctic region and oligotrophic subtropical region ("K2S1 project" in 2010 - 2013), it was clarified that biological activity in the subtropical region is comparable to or slightly larger than that in the subarctic region (Special issue of Journal of Oceanography vol.72 no.3 2016; Honda et al. 2017). In order to verify the support mechanism of biological activity, that is the mechanism of nutrient supply, time-series sediment trap experiment was initiated in 2014 at about 4900 m of the station KEO. This station is the time-series station maintained by National Ocean and Atmosphere Administration (NOAA) Pacific Marine Environmental Laboratory (PMEL) (URL: https://www.pmel.noaa.gov/ocs/data/disdel/). Surface buoy with meteorological sensors and physical oceanographic sensors have been deployed at station KEO since 2004. Therefore, these time-series data of meteorology and physical oceanography can be utilized to interpret time-series variability in sediment trap data. Owing to simultaneous analysis of time-series data obtained by NOAA surface buoy and JAMSTEC sediment trap between 2014 and 2016, it was verified that mesoscale cyclonic eddy potentially plays a role in nutrient supplier (Honda et al. in press). In order to evaluate other potential mechanisms such as typhoon and aeolian dust input, sediment trap experiment has been continued at station KEO. Last year KEO sediment trap mooring system was turn around in November during T/S Hakuho-maru KH-17-05 cruise.

(2) Recovery

In the evening on 20 July 2018, thanks to great efforts by marine technicians from Marine Works Japan ltd. and ship crews, sediment trap mooring system was successfully recovered. Although several grass floats were broken, time-series sediment trap sample since November 2017 was successfully collected.

(3) Preliminary result: total mass flux

Onboard, heights of collected samples (settling particles) in collecting cups were measured roughly with scale. Characteristic of variability of total mass flux of sediment trap samples are as follows:

(i) 2017 – 2018

After deployment in November 2017, total mass flux gradually increased and peaked in January 2018 (Fig. 3.1.1 upper). However, this peak was very small compared with large peak in April 2018. Small increase in winter and large increase in spring is typical seasonal variability at station KEO (Honda et al. in press).

(ii) History of total mass flux

Observed seasonal variability during the last deployment was compared with previous data (Fig. 3.1.2 lower). As a result, increase of total mass flux observed in April 2018 was the largest and average of total mass flux during last deployment tended to be larger than previous one.

(4) Future analysis

Above preliminary result is qualitative one. In order to evaluate settling particles quantitatively, on land laboratory, sediment trap sample will be pretreated (splitting, filtration, dry-up, pulverization) and major chemical components such as organic carbon, inorganic carbon, biogenic opal, $CaCO_3$ and Al will be analyzed.

(4) Data archive

Obtained data will be submitted to KEO sediment trap database (URL: https://ebcrpa.jamstec.go.jp/egcr/e/oal/oceansites_keo/).

(5) References

Honda MC, Matsumoto K, Fujiki T, Siswanto E, Sasaoka K, Kawakami H, Wakita M, Mino Y, Sukigara C, Kitamura M, Sasai Y, Smith SL, Hashioka T, Yoshikawa C, Kimoto K, Watanabe S, Kobari T, Nagata T, Hamasaki K, Kaneko R, Uchimiya M, Fukuda H, Abe O, Saino T (2017) Comparison of carbon cycle between the western Pacific subarctic and subtropical time-series stations: highlights of the K2S1 project. *J Oceanogr* 73:647-667. doi:10.1007/s10872-017-0423-3.

Honda MC, Sasai Y, Siswanto E, Kuwano-Yoshida A, Aiki H, Cronin MF (in press) Impact of cyclonic eddies and typhoons on biogeochemistry in the oligotrophic ocean based on biogeochemical/physical/meteorological time-series at station KEO. *Progress in Earth and Planetary Science*.

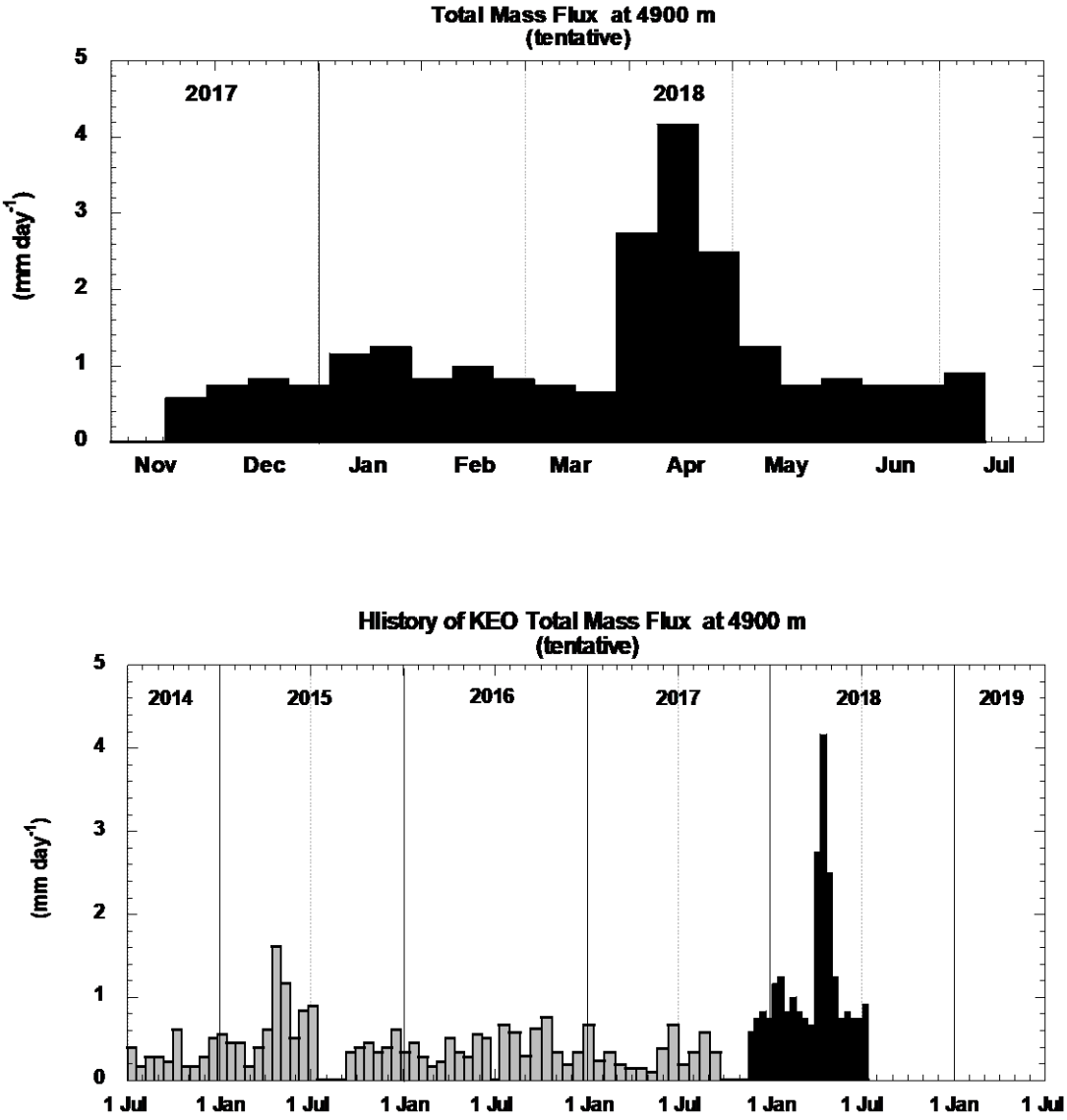

Figure 3.1.1 Seasonal variability in quantitative total mass flux (height day^{-1}) during November 2017 and July 2018 (upper) and since July 2014 (lower)

(6) Redeployment

After retrieving sample / data, replacement of new battery and initialization of schedule (Table 3.1.1), sediment trap mooring system was deployed on 21 July 2018. Designs of mooring system are shown in Fig. 3.1.2. Based on “positioning” with SSBL, determined anchor position is

32°21.9922’N

144°24.9694’E

Water depth 5786 m

It is planned that this mooring system will be recovered in summer 2019.

Table 3.1.1 Schedule (opening day of each cup)

Int （days）	17
1	2018/7/23 0:00
2	2018/8/9 0:00
3	2018/8/26 0:00
4	2018/9/12 0:00
5	2018/9/29 0:00
6	2018/10/16 0:00
7	2018/11/2 0:00
8	2018/11/19 0:00
9	2018/12/6 0:00
10	2018/12/23 0:00
11	2019/1/9 0:00
12	2019/1/26 0:00
13	2019/2/12 0:00
14	2019/3/1 0:00
15	2019/3/18 0:00
16	2019/4/4 0:00
17	2019/4/21 0:00
18	2019/5/8 0:00
19	2019/5/25 0:00
20	2019/6/11 0:00
21	2019/6/28 0:00
22	2019/7/15 0:00

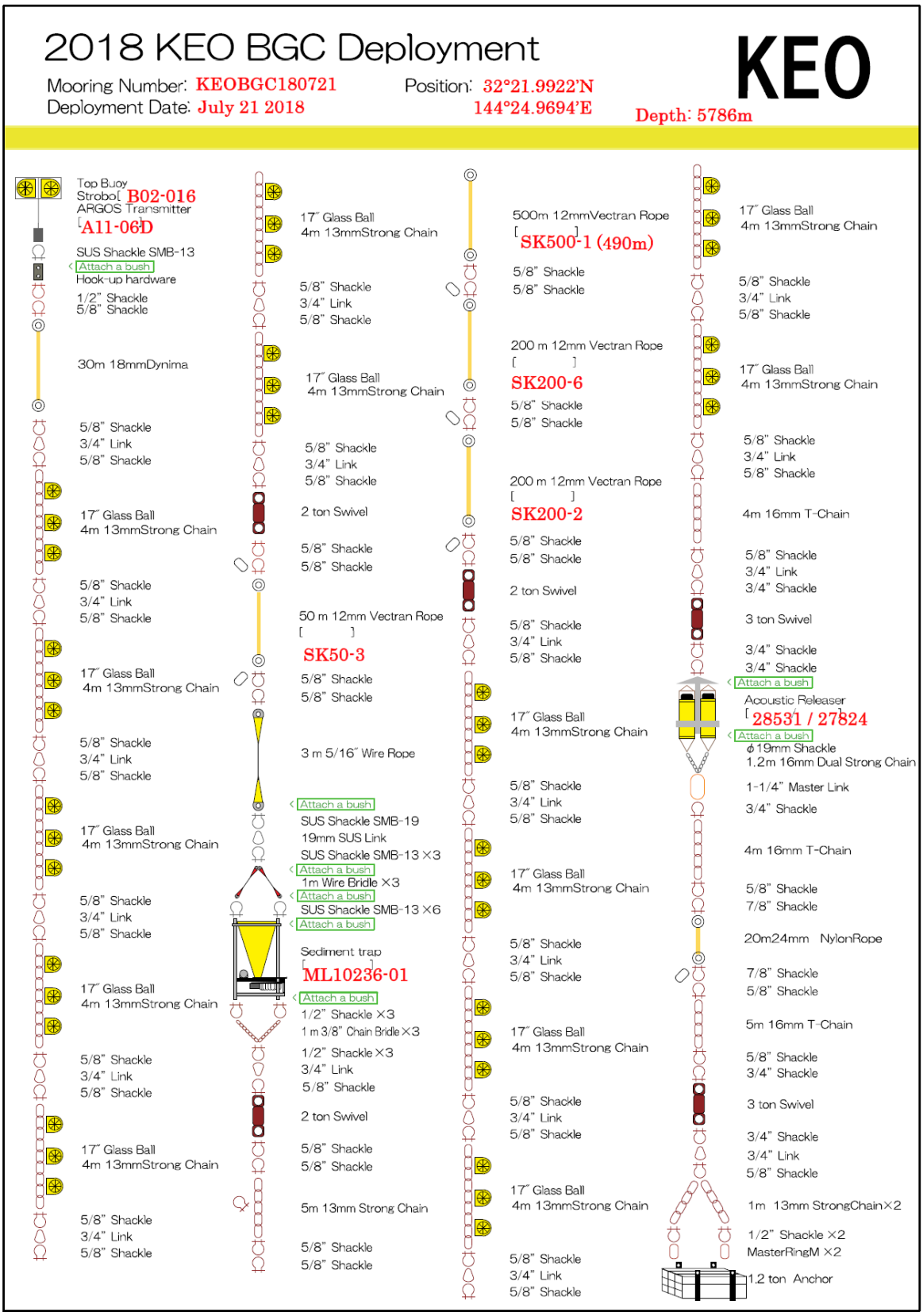

Figure 3.1.2 Design of 2018 KEO sediment trap mooring system

3.2 Hybrid profiling buoy system

3.2(a) Recovery and deployment

Tetsuichi FUJIKI (JAMSTEC RCGC)
Minoru KITAMURA (JAMSTEC RCGC)
Masahide WAKITA (JAMSTEC MIO)
Yoshiyuki NAKANO (JAMSTEC MARITEC)
Hiroshi UCHIDA (JAMSTEC RCGC)
Hiroki USHIROMURA (MWJ)
Tomohide NOGUCHI (MWJ)
Kenichi KATAYAMA (MWJ)
Keisuke TAKEDA (MWJ)

Hybrid profiling buoy is combined two moorings, BGC mooring(biogeochemistry) and POPPS mooring (ocean productivity profiling system). We recovered Hybrid profiling buoy system at Station K-2 which were deployed at MR17-04Leg1 and deployed Hybrid profiling buoy system at Station K-2. Deployment operation took approximately 6 hours. After sinker was dropped, we positioned the mooring systems by measuring the slant ranges between research vessel and the acoustic releaser. The position of the mooring is finally determined as follow:

Table 3.2(a).1. Mooring positions of respective mooring systems.

	Recovery	Deployment
Mooring Number	K2H170721	K2H180729
Working Date	Jul. 21 2017	Jul. 29 2018
Latitude	47 ° 00.35 N	47 ° 00.46 N
Longitude	159 ° 58.25 E	159 ° 58.40 E
Sea Beam Depth	5,218 m	5,220 m

The deployment Hybrid profiling buoy consists of a top buoy with 24lbs(11kg) buoyancy, underwater winch, instruments, wire and ropes, recovery buoy with 496lbs(225kg) buoyancy, glass floats (Benthos 17” glass ball), dual releasers (Edgetech) and 4,911lbs (2,228kg) sinker. An ARGOS compact mooring locator was mounted on underwater winch, and a submersible recovery strobe was mounted on the top buoy. This mooring system was planned to keep the following time-series observational instruments are mounted approximately 130 m below sea surface. On the Hybrid profiling buoy, two Sediment Traps are installed on the 1,000 m and 4,800 m. three auto sampling systems(RAS) are installed on the 200 m, 300m and 3,000 m. Extra CTD (SBE-37) and Do Sensor (RINKO and Optode) are mounted on the dual acoustic releaser and inline wire rope, inline SUS frame(250 m and 2,000 m), Sediment Trap, RAS, underwater winch, top buoy. Details for each instrument are described below (section 3.2(c), 3.2(d), 3.2(e), 3.2(f), 3.2(g), 3.2(h)). Serial number of instruments are as follows:

Table 3.2(a).2. Serial numbers of instruments.

	Recover	Deployment
Station and type	K2	K2
Mooring Number	K2H170721	K2H180729
Top Buoy(130m)	-	-
Iridium Transmiter	-	-
Storobo	E10-024	G02-009
FRRF	780263009	780263011
PAR	0277	20554
RINKO	20526	0264
CTD (SBE19plusV2)	7763	7681
AFP07	179,180	187,189
Winch(150m)	-	-
Argos Transmitter	F01-038	C01-081
SBE37	1893	1893
OPTODE	03	03
HpHS (HPS-14)	505163002	-
(175m)	Wire	Wire
SBE37	1892	1892
OPTODE	6	6
RAS (200m)	ML11241-09	ML11241-09
SBE37	2239	2239
OPTODE	50	50
HpHS(HPS-14)	505061002	60100265002
SUNA V2	NTR-1016	NTR-1004
SUNA Battery	BAT-1013	BAT-1049
(250m)	SUS frame	SUS frame
SBE37	2756	2756
RINKO	0092	0004
RAS (300m)	ML11241-07	ML11241-10
SBE37	2289	2289
RINKO	051	051
ADCP(370m)	1434	1533
SBE37	2288	2288
OPTODE	9	9
(475m)	Wire	Wire
SBE37	10737	10737
OPTODE	10	10
Sediment Trap(1000m)	26S001	ML10236-02
SBE37	2285	2285
RINKO	0007	0007
(2000m)	SUS frame	SUS frame

SBE37 RINKO	2748 0006	2748 0006
RAS(3000m) SBE37 RINKO	SUS frame 2738 0005	ML11241-11 2738 0005
Sediment Trap(4800m)	ML11241-22	ML10558-01
Releaser Releaser SBE-37 SBE26	28509 27809 2731 0262	28533 27868 2731 -

Table 3.2(a).3. Recovery Hybrid profiling buoy system record.

Mooring Number K2H170721

Project	Time-Series	Depth	5,218.0	m
Area	North Pacific	Planned Depth	5,206.2	m
Station	K2	Length	5,088.3	m
Target Position	**47°00.35 N**	Depth of Buoy	120	m
	159°58.32 E	Period	1	year

ACOUCTIC RELEASERS			
Type	Edgetech	Edgetech	
Serial Number	28509	27809	
Receive F.	11.0 kHz	11.0 kHz	
Transmit F.	14.0 kHz	14.0 kHz	
RELEASE C.	**335704**	**344535**	
Enable C.	377142	360320	
Disable C.	377161	360366	
Battery	2 years	2 years	
Release Test	OK	OK	

RECOVERY				
Recorder	Hiroki Ushiromura	Work Distance	2.3	Nmile
Ship	R/V MIRAI	Send Enable C.	4:22	
Cruise No.	MR18-04Leg1	Slant Renge	-	msec
Date	2018/7/26	Send Release C.	4:26	
Weather	m	Discovery Buoy	4:29	
Wave Hight	2.3 m	Pos. of Top Buoy	47°00.89	N
Seabeam Depth	- m		159°58.25	E
Ship Heading	185 deg	Pos. of Start	47°00.71	N
Ship Ave.Speed	- knot		159°58.17	E
Wind	<170> 10.7 m/s	Pos. of Finish	46°58.48	N
Current	<025> 0.2 cm/s		159°56.85	E

Table 3.2(a).4. Deployment Hybrid profiling buoy system record.

Mooring Number K2H180729

Project	Time-Series	Depth	5,220.0	m
Area	North Pacific	Planned Depth	5,218.0	m
Station	K2	Length	5,088.9	m
Target Position	**47°00.35 N**	Depth of Buoy	130	m
	159°58.32 E	Period	1	year
ACOUCTIC RELEASERS				
Type	Edgetech	Edgetech		
Serial Number	28533	27868		
Receive F.	11.0 kHz	11.0 kHz		
Transmit F.	14.0 kHz	14.0 kHz		
RELEASE C.	**223307**	**335534**		
Enable C.	201054	322710		
Disable C.	201077	322756		
Battery	2 years	2 years		
Release Test	OK	OK		
DEPLOYMENT				
Recorder	Hiroki Ushiromura	Start	11.5	Nmile
Ship	R/V MIRAI	Overrun	600	m
Cruise No.	MR18-04Leg1	Let go Top Buoy	21:12	
Date	2018/07/28-29	Let go Anchor	3:06	
Weather	f	Sink Top Buoy	3:49	
Wave Hight	1.6 m	Pos. of Start	47°05.74	N
PDR Depth	5,212 m		160°13.38	E
Ship Heading	242 deg	Pos. of Drop. Anc.	47°00.17	N
Ship Ave.Speed	- knot		159°57.92	E
Wind	<284> 4.7 m/s	Pos. of Mooring	47°00.46	N
Current	<278> 0.1 cm/s		159°58.40	E

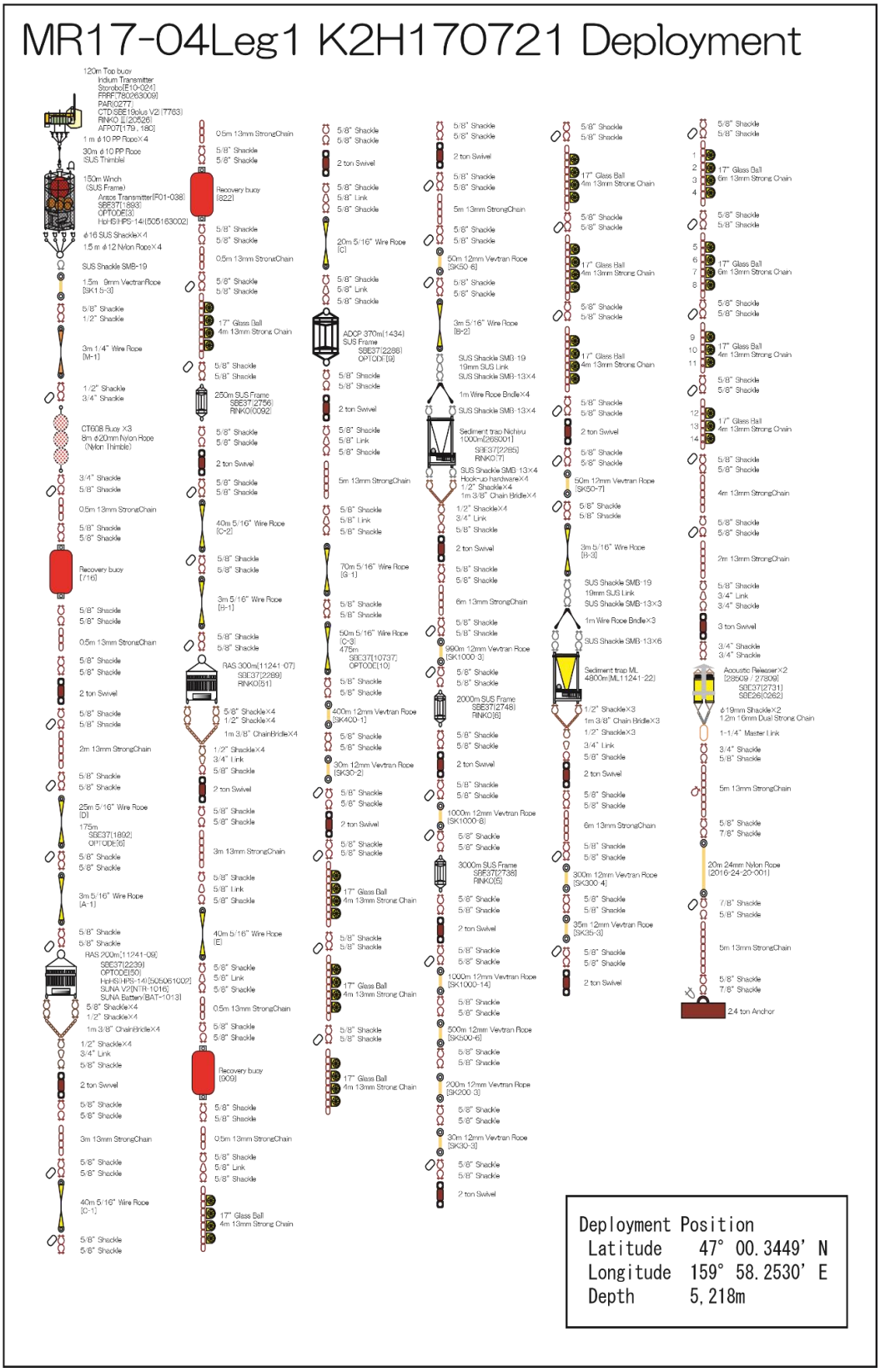

Figure 3.2(a).1. Hybrid profiling buoy system recovered.

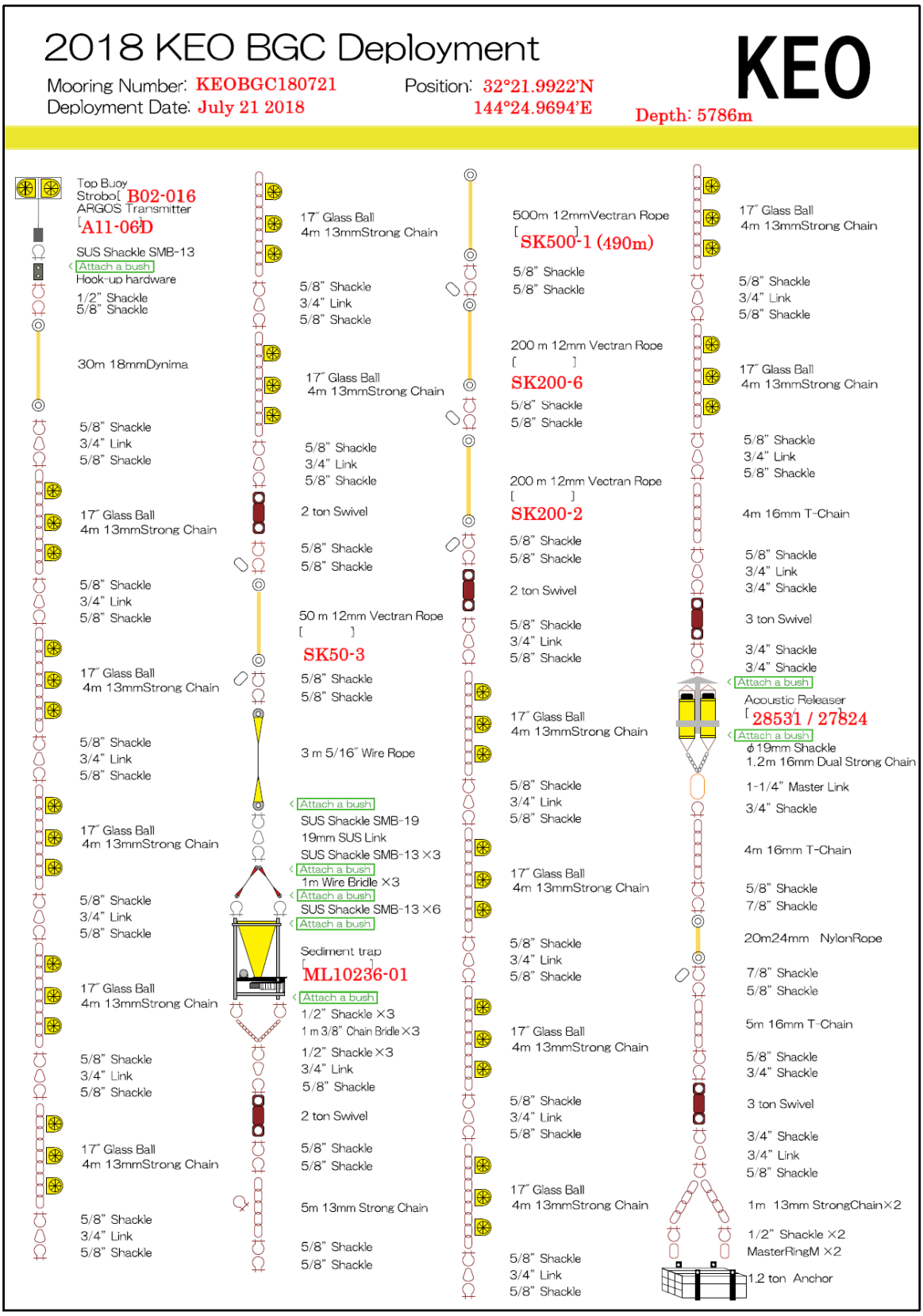

Figure 3.2(a).2. Hybrid profiling buoy system deployed.

3.2(b) Instruments

Tetsuichi FUJIKI (JAMSTEC RCGC)
Minoru KITAMURA (JAMSTEC RCGC)
Hiroki USHIROMURA (MWJ)
Tomohide NOGUCHI (MWJ)
Kenichi KATAYAMA (MWJ)
Keisuke TAKEDA (MWJ)

On mooring systems, instruments for details are as follows:

*Top buoy and underwater winch, RAS, Hybrid pH sensor, ADCP, Sediment trap, CTD, DO and Pressure sensor are described below

(section 3.2(c), 3.2(d), 3.2(e),3.2(f),3.2(g), 3.2(h)).

(1) ARGOS Beacon

The NOVATECH MMA-7500 ARGOS Beacon contains an ARGOS satellite transmitter designed as a ruggedized incident alerting system for oceanographic applications deployed anywhere in the world. It may be submerged for long periods in ocean depths to 7,500 m (24,000feet).

The device can be turned ON or OFF by triggering the internal reed switch with a magnet. The activation of the MMA-7500 is completely automatic and water sensor controlled. The water sensor is located in the antenna base – when submerged, the beacon goes into low-power hibernation mode.

The water sensor hysteresis is approx. 90 seconds. The beacon will continue to transmit for up to 90 seconds when submerged and will begin transmitting within 90 seconds of surfacing. At the surface the beacon transmits an ARGOS position data massage for 90 days.

(Specifications)

Transmitter Output:	1 watt
Harmonics:	-40 db minimum
Batteries:	8 CR123A Lithium cells
Battery Life:	90days at the surface
Operating Temp:	-40 ºC to +60ºC
Transmit Freq:	401.6300 MHz - 401.6800 MHz
Antenna:	Field replaceable 1/4 wave whip
Max Depth:	7,500 m
Weight:	In air 1.25lbs (0.56kg), In water 0.75lbs (0.34kg)
Dimensions:	16.5"long (420mm),1.0"diameter (250mm)

(2) Submersible Recovery Strobe

The NOVATECH MMF-7500 Mini-Flasher is intended to aid in the marking or recovery of oceanographic instruments, manned vehicles, remotely operated vehicles, buoys or structures. Due to the occulting (firing closely spaced bursts of light) nature of this design, it is much more visible than conventional marker strobes, particularly in poor sea conditions.

(Specifications)

Flash Rate:	Double burst 4 second delay.
Visible Range:	Up to 5 Nm
Battery Type:	7×CR123A Lithinm
Life:	Approximately 6 days, standard configuration (Double burst every 4s @ 170 lm)
Max. Depth:	7,500m
Switch:	Water conductivity
Weight:	air 1.44lbs(0.66kg) water 0.96lbs(0.44kg)
Dimensions:	Length 15.00” (381mm) Diameter 1.44” (29mm)

(3) SUNA V2

The SUNA V2 is the ultimate solution for real-time nutrient monitoring. This sensor measures nitrate with industry leading accuracy and stability over a wide range of environmental conditions (including extremely turbid and high CDOM conditions), from blue-ocean nitraclines to storm runoff in rivers and streams. The SUNA V2 incorporates the proven MBARI-ISUS nitrate measurement technology, which is based on the absorption characteristics of nitrate in the UV light spectrum.

(Specifications)

Limit of Detection:	0.5 / 0.2μM
Range of Detection:	3000 / 4000μM
Accuracy:	2 / N/AμM
Precision:	0.3 / 2.4μM
Drift:	0.3 / 1μM
Turbidity Range:	625NTU / 1250NTU
PathLength:	10nm & 5nm
Wavelength Range:	190-370nm
Lamp Type:	Continuous Wave, Deuterium Lamp
Lamp Lifetime:	900h
Input Voltage:	8-18V
Power Consumption:	7.5W (0.625A or 12V) nominal
Material:	Titanium
Depth Rating:	500m
Weight:	5.1kg
Displacement:	1749 cm^3

3.2(c) Underwater profiling buoy system (POPPS)

Tetsuichi FUJIKI (JAMSTEC RCGC)

(1) Objective

An understanding of the variability in phytoplankton productivity provides a basic knowledge of how aquatic ecosystems are structured and functioning. The primary productivity of the world oceans has been measured mostly by the radiocarbon tracer method or the oxygen evolution method. As these traditional methods use the uptake of radiocarbon into particulate matter or changes in oxygen concentration in the bulk fluid, measurements require bottle incubations for periods ranging from hours to a day. This methodological limitation has hindered our understanding of the variability of oceanic primary productivity. To overcome these problems, algorithms for estimating primary productivity by using satellite ocean color imagery have been developed and improved. However, one of the major obstacles to the development and improvement of these algorithms is a lack of *in situ* primary productivity data to verify the satellite estimates.

During the past decade, the utilization of active fluorescence techniques in biological oceanography has brought marked progress in our understanding of phytoplankton photosynthesis in the oceans. Above all, fast repetition rate (FRR) fluorometry reduces the primary electron acceptor (Q_a) in photosystem (PS) II by a series of subsaturating flashlets and can measure a single turnover fluorescence induction curve in PSII. The PSII parameters derived from the fluorescence induction curve provide information on the physiological state related to photosynthesis and can be used to estimate gross primary productivity. FRR fluorometry has several advantages over the above-mentioned traditional methods. Most importantly, because measurements made by FRR fluorometry can be carried out without the need for time-consuming bottle incubations, this method enables real-time high-frequency measurements of primary productivity. In addition, the FRR fluorometer can be used in platform systems such as moorings, drifters, and floats.

The current study aimed to assess the vertical and temporal variations in PSII parameters and primary productivity in the western Pacific, by using an underwater profiling buoy system that uses the FRR fluorometer (system name: POPPS)

(2) Methods

a) Primary productivity profiler

The POPPS consisted mainly of an observation buoy equipped with a submersible FRR fluorometer (DF-14, Kimoto Electric), a scalar irradiance sensor (QSP-2200, Biospherical Instruments), a CTD sensor (SBE19plusV2, Sea-Bird Scientific) and a dissolved oxygen sensor (RINKO III, JFE Advantech) and an underwater winch (Fig. 3.2(a).1, 2). The observation buoy moved between the winch depth and the surface at a rate of 0.2 m s^{-1} and measured the vertical profiles of phytoplankton fluorescence, irradiance, temperature, salinity and dissolved oxygen. The profiling rate of the observation buoy was set to 0.2 m s^{-1} to detect small-scale variations (approx. 1 m) in the vertical profile. To minimize biofouling of instruments, the underwater winch was placed below the euphotic layer so that the observation buoy was exposed to light only during the measurement period. In addition, the vertical migration of observation buoy reduced biofouling of instruments.

b) Measurement principle of FRR fluorometer

The FRR fluorometer consists of closed dark and open light chambers that measure the fluorescence induction curves of phytoplankton samples in darkness and under actinic illumination. To allow relaxation of photochemical quenching of fluorescence, the FRR fluorometer allows samples in the dark chamber to dark adapt for about 1 s before measurements. To achieve cumulative saturation of PSII within 150 μs — i.e., a single photochemical turnover — the instrument generates a series of subsaturating blue flashes at a light intensity of 30 mmol quanta m^{-2} s^{-1} and a repetition rate of about 250 kHz. The PSII parameters are derived from the single-turnover-type fluorescence induction curve by using the numerical fitting procedure described by Kolber et al. (1998). Analysis of fluorescence induction curves measured in the dark and light chambers provides PSII parameters such as fluorescence yields, photochemical efficiency and effective absorption cross section of PSII, which are indicators of the physiological state related to photosynthesis. Using the PSII parameters, the rate of photosynthetic electron transport and the gross primary productivity can be estimated.

c) Site description and observations

The POPPS deployed at station K2 during the Mirai cruise (MR17-04 Leg1, July – August 2017) was recovered on 26 July 2018 (LT). Unfortunately, because of a problem with the underwater winch, the recovered POPPS did not work between July 2017 and July 2018.

The POPPS was newly-deployed on 29 July 2018 (LT). Measurements with the POPPS were made at 3:00 local time (UTC+11h) and 12:00 local time (UTC+11h) every 5 days from 29 July 2018. In addition, to gain a better understanding of observational data from the POPPS, separately from the POPPS, we moved up and down a submersible FRR fluorometer between surface and ~100 m at the station K2 using a ship winch, and measured the vertical and spatial variation in PSII parameters.

Measurement schedule at station K2 (UTC, YY/MM/DD HH:MM)

1. 18/07/29 16:00	2. 18/07/30 01:00	3. 18/07/30 16:00	4. 18/07/31 01:00
5. 18/07/31 16:00	6. 18/08/01 01:00	7. 18/08/01 16:00	8. 18/08/02 01:00
9. 18/08/02 16:00	10. 18/08/03 01:00	11. 18/08/07 16:00	12. 18/08/08 01:00
13. 18/08/12 16:00	14. 18/08/13 01:00	15. 18/08/17 16:00	16. 18/08/18 01:00
17. 18/08/22 16:00	18. 18/08/23 01:00	19. 18/08/27 16:00	20. 18/08/28 01:00
21. 18/09/01 16:00	22. 18/09/02 01:00	23. 18/09/06 16:00	24. 18/09/07 01:00
25. 18/09/11 16:00	26. 18/09/12 01:00	27. 18/09/16 16:00	28. 18/09/17 01:00
29. 18/09/21 16:00	30. 18/09/22 01:00	31. 18/09/26 16:00	32. 18/09/27 01:00
33. 18/10/01 16:00	34. 18/10/02 01:00	35. 18/10/06 16:00	36. 18/10/07 01:00
37. 18/10/11 16:00	38. 18/10/12 01:00	39. 18/10/16 16:00	40. 18/10/17 01:00
41. 18/10/21 16:00	42. 18/10/22 01:00	43. 18/10/26 16:00	44. 18/10/27 01:00
45. 18/10/31 16:00	46. 18/11/01 01:00	47. 18/11/05 16:00	48. 18/11/06 01:00
49. 18/11/10 16:00	50. 18/11/11 01:00	51. 18/11/15 16:00	52. 18/11/16 01:00
53. 18/11/20 16:00	54. 18/11/21 01:00	55. 18/11/25 16:00	56. 18/11/26 01:00
57. 18/11/30 16:00	58. 18/12/01 01:00	59. 18/12/05 16:00	60. 18/12/06 01:00
61. 18/12/10 16:00	62. 18/12/11 01:00	63. 18/12/15 16:00	64. 18/12/16 01:00
65. 18/12/20 16:00	66. 18/12/21 01:00	67. 18/12/25 16:00	68. 18/12/26 01:00
69. 18/12/30 16:00	70. 18/12/31 01:00	71. 19/01/04 16:00	72. 19/01/05 01:00
73. 19/01/09 16:00	74. 19/01/10 01:00	75. 19/01/14 16:00	76. 19/01/15 01:00

77. 19/01/19 16:00	78. 19/01/20 01:00	79. 19/01/24 16:00	80. 19/01/25 01:00
81. 19/01/29 16:00	82. 19/01/30 01:00	83. 19/02/03 16:00	84. 19/02/04 01:00
85. 19/02/08 16:00	86. 19/02/09 01:00	87. 19/02/13 16:00	88. 19/02/14 01:00
89. 19/02/18 16:00	90. 19/02/19 01:00	91. 19/02/23 16:00	92. 19/02/24 01:00
93. 19/02/28 16:00	94. 19/03/01 01:00	95. 19/03/05 16:00	96. 19/03/06 01:00
97. 19/03/10 16:00	98. 19/03/11 01:00	99. 19/03/15 16:00	100. 19/03/16 01:00
101. 19/03/20 16:00	102. 19/03/21 01:00	103. 19/03/25 16:00	104. 19/03/26 01:00
105. 19/03/30 16:00	106. 19/03/31 01:00	107. 19/04/04 16:00	108. 19/04/05 01:00
109. 19/04/09 16:00	110. 19/04/10 01:00	111. 19/04/14 16:00	112. 19/04/15 01:00
113. 19/04/19 16:00	114. 19/04/20 01:00	115. 19/04/24 16:00	116. 19/04/25 01:00
117. 19/04/29 16:00	118. 19/04/30 01:00	119. 19/05/04 16:00	120. 19/05/05 01:00
121. 19/05/09 16:00	122. 19/05/10 01:00	123. 19/05/14 16:00	124. 19/05/15 01:00
125. 19/05/19 16:00	126. 19/05/20 01:00	127. 19/05/24 16:00	128. 19/05/25 01:00
129. 19/05/29 16:00	130. 19/05/30 01:00	131. 19/06/03 16:00	132. 19/06/04 01:00
133. 19/06/08 16:00	134. 19/06/09 01:00	135. 19/06/13 16:00	136. 19/06/14 01:00
137. 19/06/18 16:00	138. 19/06/19 01:00	139. 19/06/23 16:00	140. 19/06/24 01:00
141. 19/06/28 16:00	142. 19/06/29 01:00	143. 19/07/03 16:00	144. 19/07/04 01:00
145. 19/07/08 16:00	146. 19/07/09 01:00	147. 19/07/13 16:00	148. 19/07/14 01:00
149. 19/07/18 16:00	150. 19/07/19 01:00	151. 19/07/23 16:00	152. 19/07/24 01:00
153. 19/07/28 16:00	154. 19/07/29 01:00	155. 19/08/02 16:00	156. 19/08/03 01:00
157. 19/08/07 16:00	158. 19/08/08 01:00	159. 19/08/12 16:00	160. 19/08/13 01:00
161. 19/08/17 16:00	162. 19/08/18 01:00	163. 19/08/22 16:00	164. 19/08/23 01:00
165. 19/08/27 16:00	166. 19/08/28 01:00	167. 19/09/01 16:00	168. 19/09/02 01:00
169. 19/09/06 16:00	170. 19/09/07 01:00	171. 19/09/11 16:00	172. 19/09/12 01:00
173. 19/09/16 16:00	174. 19/09/17 01:00	175. 19/09/21 16:00	176. 19/09/22 01:00
177. 19/09/26 16:00	178. 19/09/27 01:00	179. 19/10/01 16:00	180. 19/10/02 01:00
181. 19/10/06 16:00	182. 19/10/07 01:00	183. 19/10/11 16:00	184. 19/10/12 01:00
185. 19/10/16 16:00	186. 19/10/17 01:00	187. 19/10/21 16:00	188. 19/10/22 01:00
189. 19/10/26 16:00	190. 19/10/27 01:00	191. 19/10/31 16:00	192. 19/11/01 01:00
193. 19/11/05 16:00	194. 19/11/06 01:00	195. 19/11/10 16:00	196. 19/11/11 01:00
197. 19/11/15 16:00	198. 19/11/16 01:00	199. 19/11/20 16:00	

References

Kolber, Z. S., O. Prášil and P. G. Falkowski. 1998. Measurements of variable chlorophyll fluorescence using fast repetition rate techniques: defining methodology and experimental protocols. Biochim. Biophys. Acta. 1367: 88-106.

3.2(d) Remote automatic sampler (RAS)

Masahide WAKITA (JAMSTEC MIO)
Hiroshi UCHIDA (JAMSTEC RCGC)
Yoshihisa MINO (Nagoya University)

In order to investigate the seasonal variation of pH in the intermediate layer, and the vertical gradients of biogeochemical properties which affects vertical diffusion flux across the boundary with the thermocline, RAS on 200m and 300m (Fig. 3.2(d).1) will work following schedule (Table 3.2(d).1) and obtain samples of dissolved inorganic carbon (DIC), total alkalinity (TA), nutrients (Phosphate, Nitrate + Nitrite, Silicate), $^{15}NO_3$ and salinity. We will compare these properties from 10 liter Niskin bottles mounted on the CTD/Carousel Water Sampling System for calibration on RAS samples at K2 in this cruise.

Salinity of RAS seawater samples were measured by salinometer (Model 8400B "AUTOSAL" Guildline Instruments). Salinity of RAS samples should be lower than ambient seawater, because RAS samples were diluted with 20% saturated $HgCl_2$ solution. Salinity measured by salinometer will be slightly lower than that observed by SBE-37 sensor (CTD). RAS samples (~500ml) were diluted with 2.5 ml of 20% saturated $HgCl_2$ solution for preservative. For chemical properties, the dilutions of RAS samples by $HgCl_2$ must be corrected by a ratio of salinity by SBE-37 to that by salinometer. We will correct measurements of DIC, TA and nutrients. We used coulometric and potentiometric techniques to measure DIC and TA, respectively. Nutrient (silicate, phosphate, and nitrate) concentrations were measured with a continuous flow analyzer. $^{15}NO_3$ will be measured by Tokai University.

Figure 3.2(d).1. Remote Automatic Samplers deployed on 200m (left) and 300m (right).

Table 3.2(d).1. Sampling schedule of RAS in 200m and 300m on Hybrid mooring at station K2.

RAS No.	RAS 200m		RAS 300m		Memo	
	Date		Date			
	Interval 10 days		Interval 10 days			
#	mm/dd/yyyy	Time(UTC)	mm/dd/yyyy	Time(UTC)		
1	07/22/2017	16:00:00	07/22/2017	16:00:00	20% Saturated $HgCl_2$ 0.5ml	Interval 1 hour for duplicate sampling
2	07/22/2017	17:00:00	07/22/2017	17:00:00	20% Saturated $HgCl_2$ 0.5ml	
3	08/01/2017	16:00:00	08/01/2017	16:00:00	20% Saturated $HgCl_2$ 0.5ml	
4	08/11/2017	16:00:00	08/11/2017	16:00:00	20% Saturated $HgCl_2$ 0.5ml	
5	08/21/2017	16:00:00	08/21/2017	16:00:00	20% Saturated $HgCl_2$ 0.5ml	
6	08/31/2017	16:00:00	08/31/2017	16:00:00	20% Saturated $HgCl_2$ 0.5ml	
7	09/10/2017	16:00:00	09/10/2017	16:00:00	20% Saturated $HgCl_2$ 0.5ml	
8	09/20/2017	16:00:00	09/20/2017	16:00:00	20% Saturated $HgCl_2$ 0.5ml	
9	09/30/2017	16:00:00	09/30/2017	16:00:00	20% Saturated $HgCl_2$ 0.5ml	
10	10/10/2017	16:00:00	10/10/2017	16:00:00	20% Saturated $HgCl_2$ 0.5ml	
11	10/20/2017	16:00:00	10/20/2017	16:00:00	20% Saturated $HgCl_2$ 0.5ml	Interval 1 hour for duplicate sampling
12	10/20/2017	17:00:00	10/20/2017	17:00:00	20% Saturated HgCl2 0.5ml	
13	10/30/2017	15:00:00	10/30/2017	15:00:00	20% Saturated $HgCl_2$ 0.4ml	
14	11/09/2017	16:00:00	11/09/2017	16:00:00	20% Saturated $HgCl_2$ 0.5ml	
15	11/19/2017	16:00:00	11/19/2017	16:00:00	20% Saturated $HgCl_2$ 0.5ml	
16	11/29/2017	16:00:00	11/29/2017	16:00:00	20% Saturated $HgCl_2$ 0.5ml	
17	12/09/2017	16:00:00	12/09/2017	16:00:00	20% Saturated $HgCl_2$ 0.5ml	
18	12/19/2017	16:00:00	12/19/2017	16:00:00	20% Saturated $HgCl_2$ 0.5ml	
19	12/29/2017	16:00:00	12/29/2017	16:00:00	20% Saturated $HgCl_2$ 0.6ml	
20	01/08/2018	16:00:00	01/08/2018	16:00:00	20% Saturated $HgCl_2$ 0.7ml	
21	01/18/2018	16:00:00	01/18/2018	16:00:00	20% Saturated $HgCl_2$ 0.8ml	
22	01/28/2018	16:00:00	01/28/2018	16:00:00	20% Saturated $HgCl_2$ 0.5ml	
23	02/07/2018	16:00:00	02/07/2018	16:00:00	20% Saturated $HgCl_2$ 0.5ml	Interval 1 hour for duplicate sampling
24	02/07/2018	17:00:00	02/07/2018	17:00:00	20% Saturated HgCl2 0.5ml	
25	02/17/2018	16:00:00	02/17/2018	16:00:00	20% Saturated $HgCl_2$ 0.4ml	
26	02/27/2018	16:00:00	02/27/2018	16:00:00	20% Saturated $HgCl_2$ 0.5ml	
27	03/09/2018	16:00:00	03/09/2018	16:00:00	20% Saturated $HgCl_2$ 0.5ml	
28	03/19/2018	16:00:00	03/19/2018	16:00:00	20% Saturated $HgCl_2$ 0.5ml	
29	03/29/2018	16:00:00	03/29/2018	16:00:00	20% Saturated $HgCl_2$ 0.5ml	
30	04/08/2018	16:00:00	04/08/2018	16:00:00	20% Saturated $HgCl_2$ 0.5ml	
31	04/18/2018	16:00:00	04/18/2018	16:00:00	20% Saturated $HgCl_2$ 0.5ml	
32	04/28/2018	16:00:00	04/28/2018	16:00:00	20% Saturated $HgCl_2$ 0.5ml	
33	05/08/2018	16:00:00	05/08/2018	16:00:00	20% Saturated $HgCl_2$ 0.5ml	
34	05/18/2018	16:00:00	05/18/2018	16:00:00	20% Saturated $HgCl_2$ 0.5ml	
35	05/28/2018	16:00:00	05/28/2018	16:00:00	20% Saturated $HgCl_2$ 0.5ml	Interval 1 hour for duplicate sampling
36	05/28/2018	17:00:00	05/28/2018	17:00:00	20% Saturated $HgCl_2$ 0.5ml	
37			06/02/2018	16:00:00	20% Saturated $HgCl_2$ 0.5ml	Interval 5 days
38	06/07/2018	16:00:00	06/07/2018	16:00:00	20% Saturated $HgCl_2$ 0.5ml	
39			06/12/2018	16:00:00	20% Saturated $HgCl_2$ 0.5ml	
40	06/17/2018	16:00:00	06/17/2018	16:00:00	20% Saturated $HgCl_2$ 0.5ml	
41			06/22/2018	16:00:00	20% Saturated $HgCl_2$ 0.5ml	
42	06/27/2018	16:00:00	06/27/2018	16:00:00	20% Saturated $HgCl_2$ 0.5ml	
43			07/02/2018	16:00:00	20% Saturated $HgCl_2$ 0.5ml	
44	07/07/2018	16:00:00	07/07/2018	16:00:00	20% Saturated $HgCl_2$ 0.5ml	
45			07/12/2018	16:00:00	20% Saturated $HgCl_2$ 0.5ml	
46	07/17/2018	16:00:00	07/17/2018	16:00:00	20% Saturated $HgCl_2$ 0.5ml	
47			07/22/2018	16:00:00	20% Saturated $HgCl_2$ 0.5ml	
48	~~07/27/2018~~	~~16:00:00~~	~~07/27/2018~~	~~16:00:00~~	~~20% Saturated $HgCl_2$ 0.5ml~~	

3.2(e) Hybrid pH sensor

Yoshiyuki NAKANO (JAMSTEC MARITEC)

(1) Objective

We have been developing newly stable and accurate *in situ* system for pH measurement using hybrid technique (potentiometric and spectrophotometric). In this cruise, we aim at testing the new Hybrid pH sensor (HpHS) in the open sea. We recovered HpHS at K2 which was deployed at MR17-04 Leg.1 with Hybrid profiling buoy system (200m). The HpHS was deployed mooring with Hybrid profiling buoy system (200m) in this cruise for about one year.

(2) Method

The HpHS is constituted two types of pH sensors (i.e. potentiometric pH sensor and spectrophotometric pH sensor). The spectrophotometric pH sensor can measure pH correctly and stably, however it needs large power consumption and a lot of reagents in a long period of observation. On the other hand, although the potentiometric pH sensor is low power consumption and high-speed response (within 20 seconds), drifts in the pH of the potentiometric measurements may possibly occur for a long period of observation. The HpHS can measure in situ pH correctly and stably combining advantage of both pH sensors. The HpHS is correcting the value of the potentiometric pH sensor (measuring frequently) by the value of the spectrophotometric pH sensor (measuring less frequently). It is possible to calibrate in situ with standard solution (Tris buffer) on the spectrophotometric pH sensor. Therefore, the drifts in the value of potentiometric pH measurements can be compensated using the pH value obtained from the spectrophotometric pH measurements. Thereby, the sensor can measure accurately the value of pH over a long period of time with low power consumption.

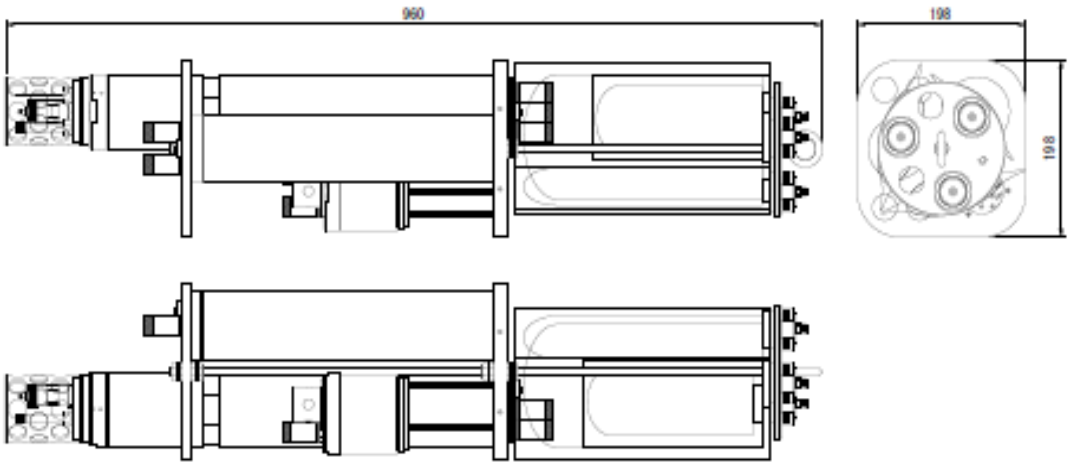

Figure. 3.2(e).1. Side view of HpHS

Table 3.2(e).1. Specification of HpHS

	Potentiometry	Spectrophotometry
Range	6.0 ~ 8.3 pH	7.2 ~ 8.2 pH
Initial Accuracy	0.01 pH	0.002 pH
Analytical Method	Glass Electrode	m-cresol purple
Response speed	20 sec (90%, 25 deg C)	3 min (90%)
Resolution	0.001 pH	
Sample rate	1 sec	
Temperature range	0 ~ 40 deg C (Resolution: 0.01 deg C)	
Dimension	198×198×960 mm	
Weight	10 kg (in air)	
Depth rating	3,000 m	

(3) Results

We succeeded in recovering the HpHS with RAS in Hybrid profiling buoy system and obtaining long term (about one year) pH data every four hours.

(4) Data Archive

All data will be submitted to JAMSTEC Data Management Group (DMG) and is currently under its control.

Reference

DICKSON, A.G., SABINE, C.L. and CHRISTIAN, J.R. (Eds.) (2007) Guide to best practices for ocean CO_2 measurements. PICES Special Publication 3, 191 pp.

LIU, X., PATSAVAS, M.C. and BYRNE, R.H. (2011) Purification and characterization of meta-cresol purple for spectrophoto-metric seawater pH measurements. Environ. Sci. Technol., 45, pp. 4862-4868.

PATSAVAS, M.C., BYRNE, R.H. and LIU, X. (2013) Purification of meta-cresol purple and cresol red by flash chromatography: Procedures for ensuring accurate spectrophotometric seawater pH measurements. Mer. Chem., 150, pp. 19-24.

3.2(f) ADCP

Minoru KITAMURA (JAMSTEC RIGC)

An Acoustic Doppler Current Profiler (ADCP) was installed at a depth of 370 m on the K2 mooring. Purposes of data samplings (and investigators) are as follows;

(1) to observe seasonal current structure fluctuation (A. Nagano and M. Wakita, JAMSTEC),

(2) to understand zooplankton dynamics (M. Kitamura, JAMSTEC)

Using the former data, we will be able to understand mixing/stratifying processes in the surface layer and nutrient supply to the surface layer due to vertical diffusion. On the other hand, ADCP have been used not only physical oceanography but also biological researches. That is, zooplankton biomass can be estimated using acoustic backscattering intensities collected from ADCP. So, we will also analyze zooplankton dynamics at K2.

Specifications

Model: Workhorse LongRanger (Teledyne RD Instruments, Poway, CA, USA)
S/N: 1434 (recovered ADCP), 1533 (deployed ADCP)
Frequency: 75 kHz
Max. depth: 1500m
Dimensions: 1014 mm in length, 550 mm in width
Weights: ADCP; 86 kg in air and 55 kg in water
Frame; 46 kg in water (recovered), 54 kg in air and 47 kg in water (deployed)
Beam angle/width: 20°/4°
DC input: 20-60VDC, four internal alkaline battery packs
Voltage: 42V DC (new), 28V DC (depleted)
Velocity resolution: 1mm/s

Setting parameters for data sampling

Depth cell size: 8 m
Number of depth cells: 60
Ping per ensemble: 30
Intervals: 60 min.
Mode: Broadband mode

3.2 (g) Sediment trap

Minoru KITAMURA (JAMSTEC RIGC)

(1) Objective

To observe long-term trend of the sinking carbon flux at K2, the sediment trap experiment is conducted. Two sediment traps which moored at 1000 m and 4810 m were recovered from the K2H170721 mooring on 26 July, 2018. And two sediment traps were newly installed at 1000 m and 4810 m in the K2H180729 mooring which deployed on 29 July, 2017.

(2) Description of instruments

Two kinds of sediment trap were used in this experiment, MARK78H-21 (McLane Research Laboratories, INC., MA, USA) and SMD26S-6000 (NiGK Corporation, Tokyo, Japan). The former trap which had 21 sampling cups was installed at 4810 m of the recovered mooring, and 1000 and 4810 m of the deployed mooring. Sampling interval of the McLane traps were every 20 days for both the recovered and deployed moorings. The latter model of trap with 26 sampling cups was attached at 1000 m of the recovered mooring. Shorter interval of sampling (10 days) was scheduled during the season of high primary productivity while samplings were conducted every 20 days in other seasons. Specifications and serial numbers of the two traps are summarized in the following tables:

Table 3.2(g).1. Specifications of two sediment traps

	SMD26S-6000 (NiGK Corporation)	MARK78H-21 (McLane Research Lab.)
Max. depth (m)	6000	7000
Dimensions (diameter × height, cm)	104 × 160	91 ×164
Mouth area (m^2)	0.5	0.5
Weights (kg)	86 in air, 46 in water	72 in air, 39 in water
No. of sampling bottles	26	21
Volume of sampling bottles (ml)	270	250
Battery	Alkaline/Lithium pack	14 Alkaline batteries or a Battery pack
Communication cables	RMG4-USB	RMG3-Serial port-USB
Software	N-SMD	Crosscut
OS	Win 7	Win 7

Table 3.2 (g)-2. Serial numbers and battery types

	Model	S/N	Battery
Recovery from			
1000 m	NiGK, SMD26S-6000	26S001	Alkaline/Lithium pack
4810 m	McLane, MARK78H-21	ML11241-22	14 Alkaline batteries
Deployed at			
1000 m	McLane, MARK78H-21	ML10236-02	Battery pack
4810 m	McLane, MARK78H-21	ML10558-01	14 Alkaline batteries

(3) Sampling schedules

Sampling schedules of the recovered and deployed sediment traps were summarized in the following tables. Internal clock of each sediment trap was set in UTC. The deployed mooring systems will be recovered during *Mirai* cruise held in 2019.

Table 3.2(g).3. Sampling schedules of the recovered sediment traps.

NiGK Sediment Trap 1000 m

Bottle No.	Sampling (UTC, yyyy/mm/dd) Start	End	Interval (days)
No.1	2017/07/22 13:00	2017/08/11 13:00	20
No.2	2017/08/11 13:00	2017/08/31 13:00	20
No.3	2017/08/31 13:00	2017/09/20 13:00	20
No.4	2017/09/20 13:00	2017/10/10 13:00	20
No.5	2017/10/10 13:00	2017/10/30 13:00	20
No.6	2017/10/30 13:00	2017/11/19 13:00	20
No.7	2017/11/19 13:00	2017/12/09 13:00	20
No.8	2017/12/09 13:00	2017/12/29 13:00	20
No.9	2017/12/29 13:00	2018/01/18 13:00	20
No.10	2018/01/18 13:00	2018/02/07 13:00	20
No.11	2018/02/07 13:00	2018/02/27 13:00	20
No.12	2018/02/27 13:00	2018/03/19 13:00	20
No.13	2018/03/19 13:00	2018/04/08 13:00	20
No.14	2018/04/08 13:00	2018/04/28 13:00	20
No.15	2018/04/28 13:00	2018/05/08 13:00	10
No.16	2018/05/08 13:00	2018/05/18 13:00	10
No.17	2018/05/18 13:00	2018/05/28 13:00	10
No.18	2018/05/28 13:00	2018/06/07 13:00	10
No.19	2018/06/07 13:00	2018/06/17 13:00	10
No.20	2018/06/17 13:00	2018/06/27 13:00	10
No.21	2018/06/27 13:00	2018/07/07 13:00	10
No.22	2018/07/07 13:00	2018/07/17 13:00	10
No.23	2018/07/17 13:00	2018/07/27 13:00	10
No.24	2018/07/27 13:00	2018/08/06 13:00	10
No.25	2018/08/06 13:00	2018/08/26 13:00	20
No.26	2018/08/26 13:00	2018/09/15 13:00	20

McLane Sediment Trap 4800 m

Bottle No.	Sampling (UTC) Start	End	Interval (days)
No.1	2017/07/22 13:00	2017/08/11 13:00	20
No.2	2017/08/11 13:00	2017/08/31 13:00	20
No.3	2017/08/31 13:00	2017/09/20 13:00	20
No.4	2017/09/20 13:00	2017/10/10 13:00	20
No.5	2017/10/10 13:00	2017/10/30 13:00	20
No.6	2017/10/30 13:00	2017/11/19 13:00	20
No.7	2017/11/19 13:00	2017/12/09 13:00	20
No.8	2017/12/09 13:00	2017/12/29 13:00	20
No.9	2017/12/29 13:00	2018/01/18 13:00	20
No.10	2018/01/18 13:00	2018/02/07 13:00	20
No.11	2018/02/07 13:00	2018/02/27 13:00	20
No.12	2018/02/27 13:00	2018/03/19 13:00	20
No.13	2018/03/19 13:00	2018/04/08 13:00	20
No.14	2018/04/08 13:00	2018/04/28 13:00	20
No.15	2018/04/28 13:00	2018/05/18 13:00	20
No.16	2018/05/18 13:00	2018/06/07 13:00	20
No.17	2018/06/07 13:00	2018/06/27 13:00	20
No.18	2018/06/27 13:00	2018/07/17 13:00	20
No.19	2018/07/17 13:00	2018/08/06 13:00	20
No.20	2018/08/06 13:00	2018/08/26 13:00	20
No.21	2018/08/26 13:00	2018/09/15 13:00	20

Table 3.2(g).4. Sampling schedules of the deployed sediment traps.

McLane Sediment Trap 1000 m

Bottle No.	Sampling (UTC, yyyy/mm/dd) Start	End	Interval (days)
No.1	2018/07/30 13:00	2018/08/19 13:00	20
No.2	2018/08/19 13:00	2018/09/08 13:00	20
No.3	2018/09/08 13:00	2018/09/28 13:00	20
No.4	2018/09/28 13:00	2018/10/18 13:00	20
No.5	2018/10/18 13:00	2018/11/07 13:00	20
No.6	2018/11/07 13:00	2018/11/27 13:00	20
No.7	2018/11/27 13:00	2018/12/17 13:00	20
No.8	2018/12/17 13:00	2019/01/06 13:00	20
No.9	2019/01/06 13:00	2019/01/26 13:00	20
No.10	2019/01/26 13:00	2019/02/15 13:00	20
No.11	2019/02/15 13:00	2019/03/07 13:00	20
No.12	2019/03/07 13:00	2019/03/27 13:00	20
No.13	2019/03/27 13:00	2019/04/16 13:00	20
No.14	2019/04/16 13:00	2019/05/06 13:00	20
No.15	2019/05/06 13:00	2019/05/26 13:00	20
No.16	2019/05/26 13:00	2019/06/15 13:00	20
No.17	2019/06/15 13:00	2019/07/05 13:00	20
No.18	2019/07/05 13:00	2019/07/25 13:00	20
No.19	2019/07/25 13:00	2019/08/14 13:00	20
No.20	2019/08/14 13:00	2019/09/03 13:00	20
No.21	2019/09/03 13:00	2019/09/23 13:00	20

McLane Sediment Trap 4800 m

Bottle No.	Sampling (UTC) Start	End	Interval (days)
No.1	2018/07/30 13:00	2018/08/19 13:00	20
No.2	2018/08/19 13:00	2018/09/08 13:00	20
No.3	2018/09/08 13:00	2018/09/28 13:00	20
No.4	2018/09/28 13:00	2018/10/18 13:00	20
No.5	2018/10/18 13:00	2018/11/07 13:00	20
No.6	2018/11/07 13:00	2018/11/27 13:00	20
No.7	2018/11/27 13:00	2018/12/17 13:00	20
No.8	2018/12/17 13:00	2019/01/06 13:00	20
No.9	2019/01/06 13:00	2019/01/26 13:00	20
No.10	2019/01/26 13:00	2019/02/15 13:00	20
No.11	2019/02/15 13:00	2019/03/07 13:00	20
No.12	2019/03/07 13:00	2019/03/27 13:00	20
No.13	2019/03/27 13:00	2019/04/16 13:00	20
No.14	2019/04/16 13:00	2019/05/06 13:00	20
No.15	2019/05/06 13:00	2019/05/26 13:00	20
No.16	2019/05/26 13:00	2019/06/15 13:00	20
No.17	2019/06/15 13:00	2019/07/05 13:00	20
No.18	2019/07/05 13:00	2019/07/25 13:00	20
No.19	2019/07/25 13:00	2019/08/14 13:00	20
No.20	2019/08/14 13:00	2019/09/03 13:00	20
No.21	2019/09/03 13:00	2019/09/23 13:00	20

(4) Preliminary result

Sequential samples of the sinking particles were collected both from the 500 m and 4810 m recovery traps. Onboard, heights of the particle samples in the collecting cups were measured with scale in order to know general view of their seasonal change. Using base area of collecting cup (18.1 cm^2), we estimated volume flux for each collecting period (18 days). We also measured pH of seawater in collecting cups onboard. The volume flux (cm^3/m^2/day), and pH for each sample were summarized in the table. And seasonal change of the volume fluxes at the two depths were shown in the following figure.

Table 3.2(g).5. Time-series of the volume fluxes.

1000m, NiGK SMD26S-6000

Bottle	Start (local time)	End	Interval (days)	Height (cm)	Flux (cm^3)
#1	2017/07/23 0:00	2017/08/12 0:00	20	8.7	158.0
#2	2017/08/12 0:00	2017/09/01 0:00	20	4.6	83.2
#3	2017/09/01 0:00	2017/09/21 0:00	20	2.1	37.4
#4	2017/09/21 0:00	2017/10/11 0:00	20	2.4	42.8
#5	2017/10/11 0:00	2017/10/31 0:00	20	1.5	27.7
#6	2017/10/31 0:00	2017/11/20 0:00	20	1.5	27.1
#7	2017/11/20 0:00	2017/12/10 0:00	20	0.4	6.6
#8	2017/12/10 0:00	2017/12/30 0:00	20	0.1	1.8
#9	2017/12/30 0:00	2018/01/19 0:00	20	0.0	0.6
#10	2018/01/19 0:00	2018/02/08 0:00	20	0.1	2.4
#11	2018/02/08 0:00	2018/02/28 0:00	20	0.1	1.8
#12	2018/02/28 0:00	2018/03/20 0:00	20	0.1	1.8
#13	2018/03/20 0:00	2018/04/09 0:00	20	0.1	1.8
#14	2018/04/09 0:00	2018/04/29 0:00	20	0.0	0.6
#15	2018/04/29 0:00	2018/05/09 0:00	10	0.1	1.8
#16	2018/05/09 0:00	2018/05/19 0:00	10	0.0	0.0
#17	2018/05/19 0:00	2018/05/29 0:00	10	0.03	0.6
#18	2018/05/29 0:00	2018/06/08 0:00	10	0.1	1.2
#19	2018/06/08 0:00	2018/06/18 0:00	10	0.5	9.6
#20	2018/06/18 0:00	2018/06/28 0:00	10	0.1	1.8
#21	2018/06/28 0:00	2018/07/08 0:00	10	0.0	0.0
#22	2018/07/08 0:00	2018/07/18 0:00	10	0.1	1.2
#23	2018/07/18 0:00	2018/07/28 0:00	10	2.5	44.6
#24	2018/07/28 0:00	2018/08/07 0:00	10	0	0
#25	2018/08/07 0:00	2018/08/27 0:00	20		
#26	2018/08/27 0:00	2018/09/16 0:00	20		

4800m, McLane Mark7

Bottle	Start (local time)	End	Interval (days)	Height (cm)	Flux (cm^3)
#1	2017/07/23 0:00	2017/08/12 0:00	20	4.6	90.3
#2	2017/08/12 0:00	2017/09/01 0:00	20	3.4	66.7
#3	2017/09/01 0:00	2017/09/21 0:00	20	1.9	37.9
#4	2017/09/21 0:00	2017/10/11 0:00	20	5.2	102.7
#5	2017/10/11 0:00	2017/10/31 0:00	20	1.1	20.9
#6	2017/10/31 0:00	2017/11/20 0:00	20	0.8	16.4
#7	2017/11/20 0:00	2017/12/10 0:00	20	1.0	19.6
#8	2017/12/10 0:00	2017/12/30 0:00	20	0.7	13.1
#9	2017/12/30 0:00	2018/01/19 0:00	20	0.8	16.4
#10	2018/01/19 0:00	2018/02/08 0:00	20	0.8	15.0
#11	2018/02/08 0:00	2018/02/28 0:00	20	1.0	19.6
#12	2018/02/28 0:00	2018/03/20 0:00	20	5.5	107.3
#13	2018/03/20 0:00	2018/04/09 0:00	20	1.5	30.1
#14	2018/04/09 0:00	2018/04/29 0:00	20	3.1	61.5
#15	2018/04/29 0:00	2018/05/19 0:00	20	9.0	176.6
#16	2018/05/19 0:00	2018/06/08 0:00	20	4.3	83.7
#17	2018/06/08 0:00	2018/06/28 0:00	20	2.6	50.4
#18	2018/06/28 0:00	2018/07/18 0:00	20	1.7	32.7
#19	2018/07/18 0:00	2018/08/07 0:00	20	no sample	
#20				no sample	
#21				no sample	

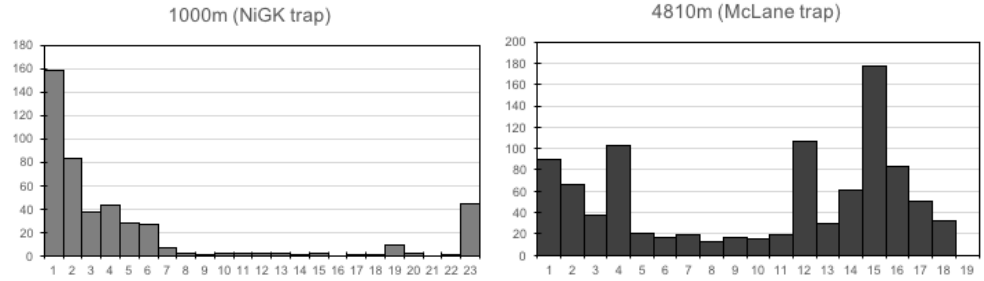

Figure 3.2(g).1. Seasonal changes of volume fluxes at 1000 and 4810 m of the station K2.

(5) Sample archives

All samples are stored in JAMSTEC/Yokosuka. Each sample will be divided into ten aliquots and these subsamples will be distributed to co-researchers for further analysis.

3.2(h) CTD, DO & pressure sensors

Hiroshi UCHIDA (JAMSTEC RCGC)
Masahide WAKITA (JAMSTEC MIO)

(1) Objectives

The objective of this study is to grasp variability of temperature, salinity and oxygen at the K2 mooring site.

(2) Instruments and methods

Pressure, temperature and salinity were measured by CTDs (SBE37SM or SBE37SMP, Sea-Bird Scientific, Bellevue, Washington, USA). Dissolved oxygen was measured by optical oxygen sensors (Oxygen Optode model 3830, Aanderaa Data Instruments AS, Bergen, Norway, and RINKO-I or RINKO-I DSP, JFE Advantech Co. Ltd., Hyogo, Japan). The Oxygen Optode sensor was attached to a datalogger with an internal battery and memory in a titanium housing (Compact-OPTODE, Alec Electronics Co., Ltd., Kobe, Japan). A sampling interval was set to 1 hour for the CTD and oxygen sensors. Sea bottom pressure was also measured accurately by a digiquartz pressure sensor (SBE26, Sea-Bird Scientific). A sampling interval was set to 5 minutes and data were obtained until March 23, 2018.

Sensors used in the K2 mooring observations are summarized in Table 3.2 (h).1, and obtained salinity and potential temperature data are plotted in Figs. 3.2 (h).1, 3.2 (h).2 and 3.2 (h).3.

Table 3.2(h).1 Serial number of the CTD and oxygen sensors recovered from the K2 mooring.

Planned depth	CTD	Oxygen	Note
150 m	1893 (SBE37SM)	0003 (CompactOPTODE)	Winch
175 m	1892 (SBE37SM)	0006 (CompactOPTODE)	Wire
200 m	2239 (SBE37SM)	0050 (CompactOPTODE)	RAS
250 m	2756 (SBE37SM)	0092 (RINKO-I)	SUS frame
300 m	2289 (SBE37SM)	0051 (RINKO-I)	RAS
370 m	2288 (SBE37SM)	0009 (CompactOPTODE)	ADCP
475 m	10737 (SBE37SMP)	0010 (CompactOPTODE)	Wire
1000 m	2285 (SBE37SM)	0007 (RINKO-I DSP)	Trap
2000 m	2748 (SBE37SM)	0006 (RINKO-I DSP)	SUS frame
3000 m	2738 (SBE37SM)	0005 (RINKO-I DSP)	SUS frame
Bottom	2731 (SBE37SM)*	none	Releasers

* with Digiquartz pressure sensor (SBE26, serial no. 75736)

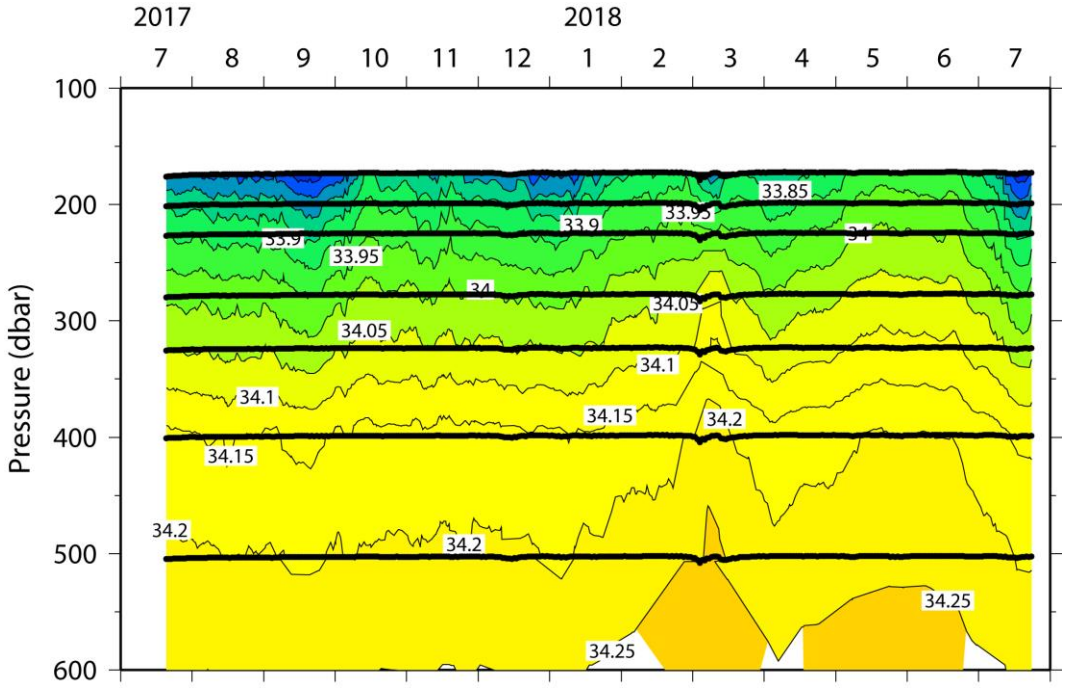

Figure 3.2(h).1 Time series of salinity.

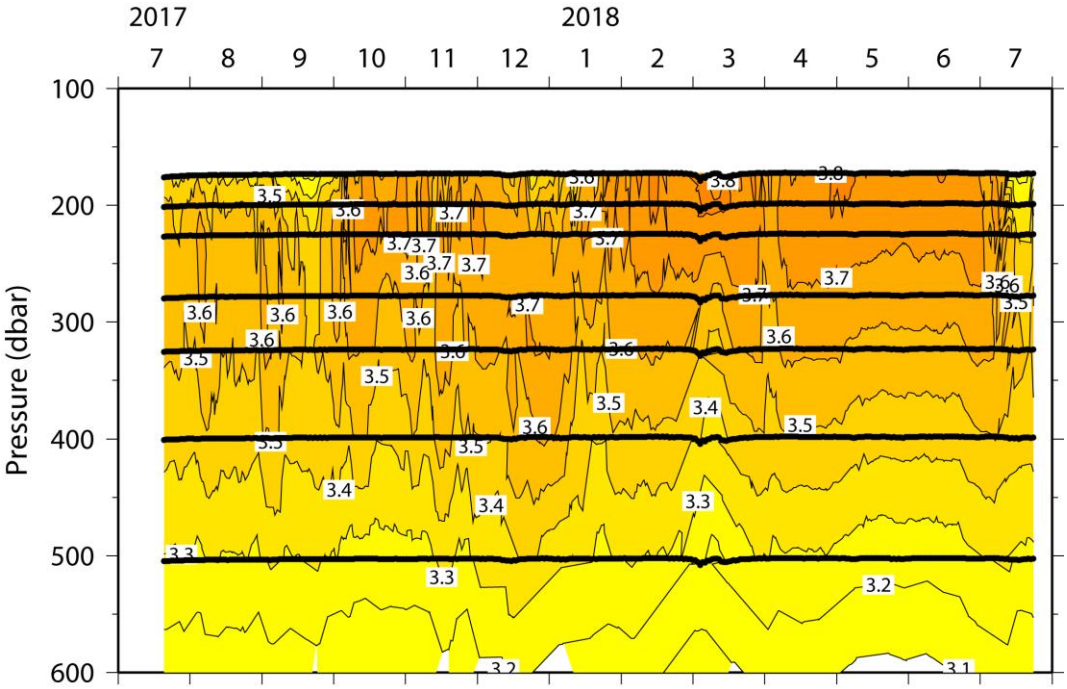

Figure 3.2(h).2. Time series of potential temperature.

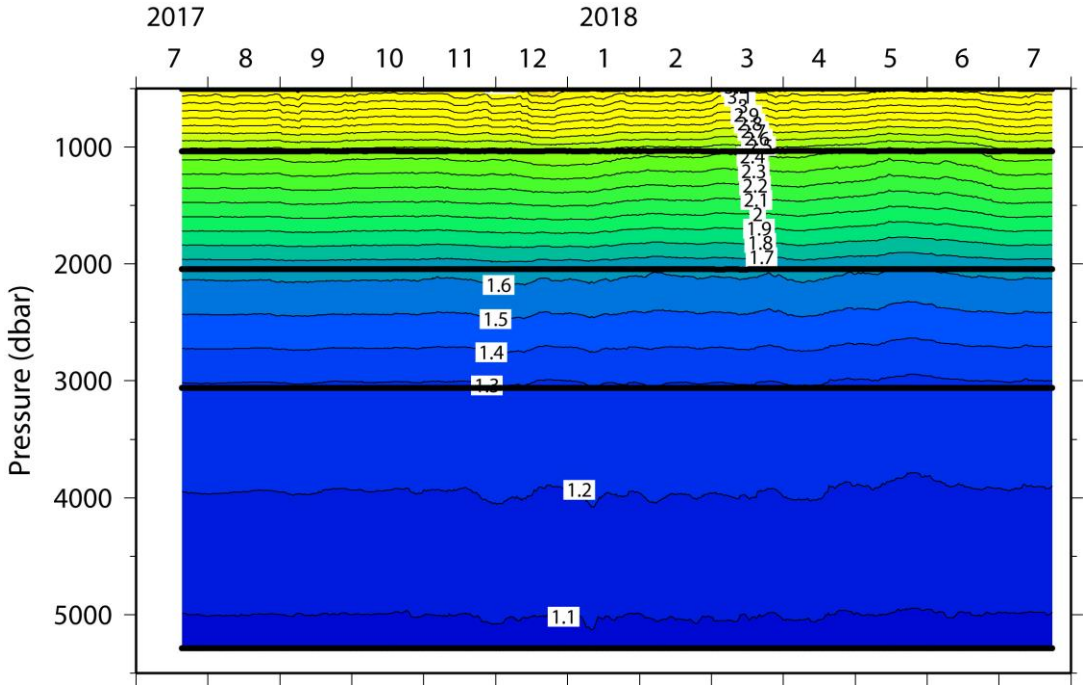

Fig. 3.2(h).3. Time series of potential temperature for depths deeper than 500 dbar.

(3) Data archive

These obtained data will be submitted to JAMSTEC Data Management Group (DMG).

3.3 Multi Observation Glider

Kensuke WATARI (JAMSTEC MARITEC)
Masahiro KAKU (JAMSTEC MARITEC)
Satoshi TSUBONE (Interlink Co. Ltd)
Keisuke TAKEDA (MWJ)

(1) Objective

In the rapidly changing global environment, the problem of the greatest environmental stress is the collapse of the ecosystem. Especially, the influence is remarkable in the Bering Sea from the world's most productive North Pacific Subarctic. Measurement by hanging a sensor from a ship allows precise measurement, while the spatial and temporal degrees of freedom are constrained by ship time. In order to solve this problem, we would like to advance elucidation of the ecological mechanism by collecting wider data by installing FRRF in an autonomous underwater glider and observing the sea area. In this observation, FRRF was mounted on underwater glider and experimental observation was carried out.

(2) Description of instruments deployed

Developed for this observation, the FRRF-mounted underwater glider "MOG" is a testing machine for underwater gliders for observation equipped with a common platform "MOF system" under development by JAMSTEC. It is an underwater glider with a propulsion function equipped with a live primary battery, a buoyancy adjustment mechanism, a pitch adjustment mechanism, and a swing thruster. It has a CTD sensor, depth sensor, acceleration sensor, geomagnetic sensor, gyro sensor, and has a function that can move to any set direction and depth. The main body can transmit and receive data by iridium communication, and the operation period varies depending on the observation sequence and mounted sensors, but the tester assumes observations around 10 days. In this observation, FRRF (manufactured by Kimoto Electronics) was mounted on 1 MOGs and observed. In addition, another tester that evaluated the Do sensor was inserted separately.

In this observation, we set to observe constant water temperature zone (6.3 ℃ ~ 8.3 ℃). In addition, profile observation from water depth 100 m was conducted once every 24 hours. The entry date and observation point are shown in the table below.

Table 3.3.1 MOG deploy

Launch Date	Machine No	Recovery Date	Option Sensor	Deploy point
2018/7/25	1	2017/7/27	Do	47’0201N, 160’0167E
2018/7/25	2	2017/7/27	FRRF	47’0201N, 160’0261E

Deploy of MOG went from "MIRAI". Recovery was done with a rubber boat equipped with "MIRAI". The maximum dive depth is 160 m, profile observation of CTD and FRRF is performed at sedimentation.

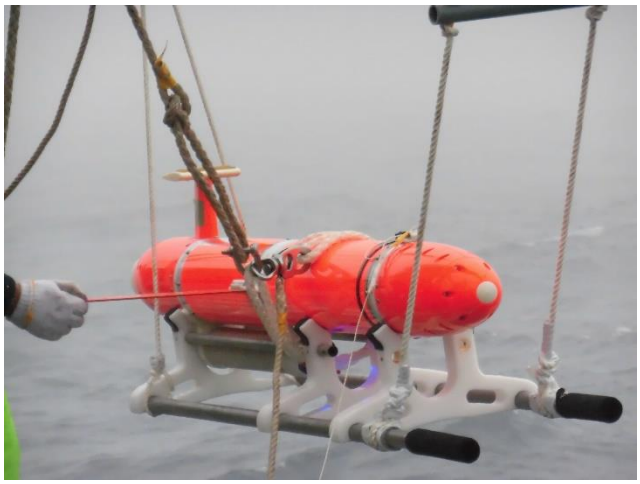

Figure 3.3.1. Deploy of MOG

(3) Preliminary result

Observation data obtained by this observation are as follows.

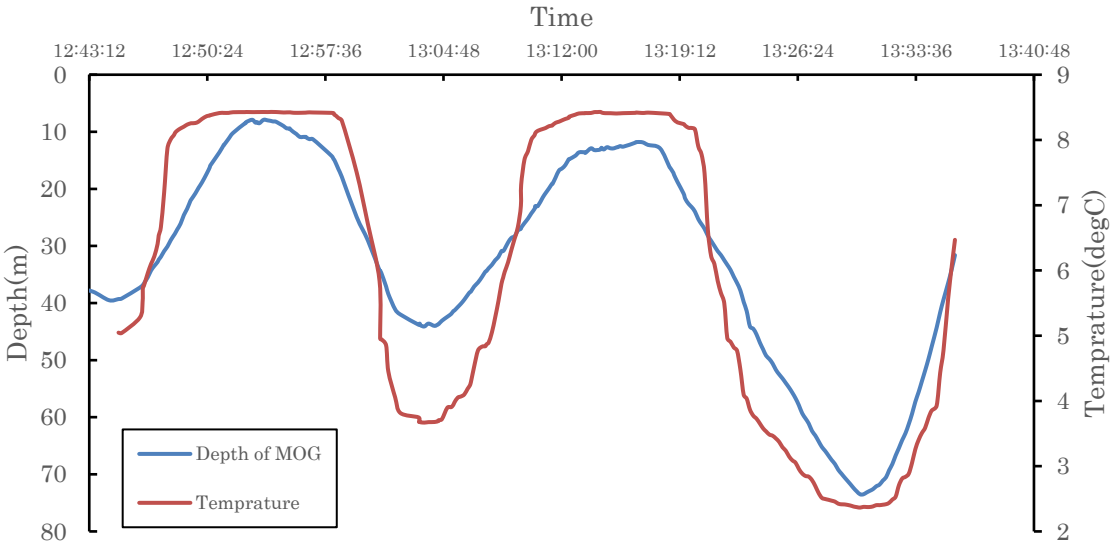

Figure 3.2.2. Observation of isothermal zone by MOG

MOG is introduced into the sea area around K2 and is set to observe its surroundings. Fig. 3.2.2 shows the depth change and the temperature change during dive. It is understood that it follows the temperature change with the value of 6.3 to 8.3 ° C as the center. The data observed by the CTD sensor are shown in Fig. 3.2.3 MOG uses thruster's suction flow to pour seawater into the CTD sensor. Fig. 3.2.4 shows GPS information sent from the MOG when levitated. We observe by submerging to interpolate coordinate points.

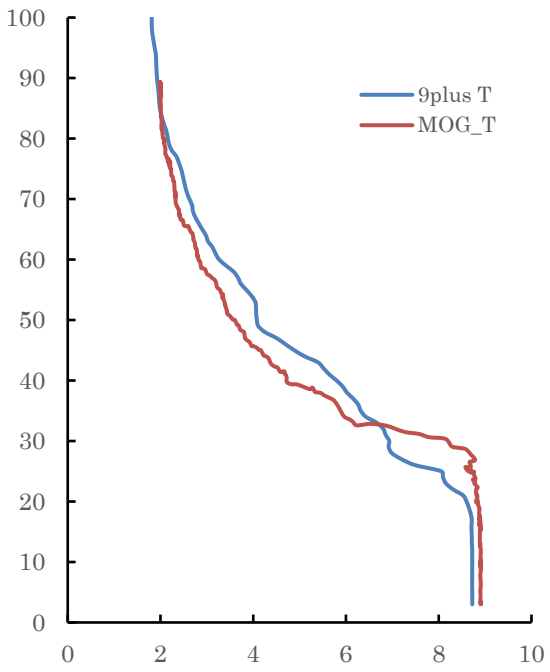

Figure 3.2.3. Temperature profile

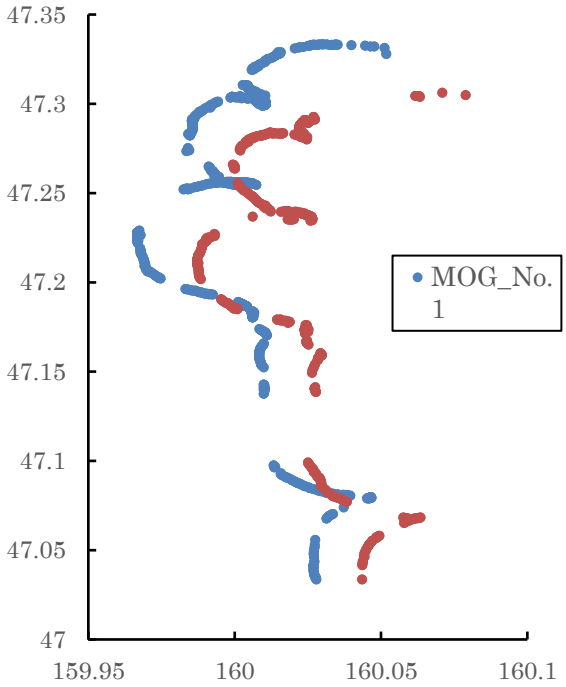

Figure 3.2.4. GPS info from MOG

3.4 Argo floats

Shuhei MASUDA (JAMSTEC RCGC)
Shigeki HOSODA (JAMSTEC RCGC)
Mizue HIRANO (JAMSTEC RCGC)
Kanichi KATAYAMA (MWJ)

(1) Objectives

The objective of this study is to clarify the mechanisms of climate and oceanic environment variability to understand changes of earth system through estimations of heat and material transports, and to improve their long-term forecasts of climate changes, by monitoring in the global ocean. To achieve the objective, automatically long-term measurements of physical and biogeochemical parameters are carried out with deployment of Argo floats at the biogeochemical mooring station K2 (47°N, 160°E) in the western North Pacific Ocean.

One biogeochemical Argo (BGC APEX) float has been deployed, which measures biogeochemical parameters, temperature and salinity down to a depth of 2000dbar. The purpose of the observation is to clarify changes of phytoplankton and dissolved oxygen concentrations related to physical and biological processes. In collaboration with shipboard and mooring observations at K2, long-term and spatial variability of biogeochemical process will be captured in the western subpolar North Pacific region where seasonal variability of primary production is enhanced. The deployed float will also contribute to the international project of biogeochemical (BGC) Argo to construct the global array.

Also, one deep Argo float (Deep APEX) has been deployed, which measures temperature, salinity and dissolved oxygen down to a depth of 6000dbar. The purpose of the deployment is to clarify changes of deep ocean environment, circulation and water mass. Since deep Argo float obtains frequent profiles with fine vertical resolution, accurate variability can be investigated. The deployed deep Argo float will also contribute to construct global deep Argo array for the purpose of detection of changes in heat storage associated with climate changes.

The deep and BGC Argo float data will also apply to the ESTOC, which is 4D-VAR data assimilation system to estimate state of global ocean for climate changes, to investigate whole mechanism of long-term changes in the ocean.

(2) Parameters

・Water temperature, salinity, pressure, dissolved oxygen, back scattering, CDOM and chlorophyll

(3) Methods

i. Biogeochemical Argo Profiling float deployment

We launched APEX Biogeochemical (BGC) float manufactured by Teledyne Webb Research. This float equips SBE41 CTD sensor manufactured by Sea-Bird Electronics Inc., ARO-FT dissolved oxygen sensor manufactured JFE Advantech Co., Ltd. and FLBBCD-AP2 backscattering, CDOM and chlorophyll sensors manufactured by WET Labs.

The float drifts at a depth of 1000 dbar (called the parking depth) until next vertical measurements, then goes upward from a depth of 2000 dbar to the sea surface every 2 days. During the ascent, physical and biogeochemical values are measured every 2 dbar or at depths following depth table. During surfacing for a few ten minutes, the float sends all measured data to the land via the Iridium satellite telecommunication system with Rudics protocol. Those float observations will be sustained for about a few years depending on internal battery lifetime. The status of float and its launching information is shown in Table 3.4.1.

Table 3.4.1 Status of floats and their launches

APEX BGC Float(2000dbar)

Float Type	APEX BGC float manufactured by Teledyne Webb Research.
CTD sensor	SBE41 manufactured by Sea-Bird Electronics Inc.
Oxygen sensor	ARO-FT by JFE Advantech Co., Ltd
Backscatter Fluorescence Chlorophyll	FLBBCD-AP2 manufactured by WET Labs, Inc. Backscattering: wavelength: 700nm CDOM: ex/em→ 370/460nm Chlorophyll: ex/em→ 470/695nm
Cycle	Every day (approximately 30minutes at the sea surface)
Iridium transmit type	Router-Based Unrestricted Digital Internetworking Connectivity Solutions (RUDICS)
Target Parking Pressure	1000 dbar
Sampling layers	2dbar interval from 2000 dbar to surface (approximately 1000 levels)

Launches

Float S/N	WMOID	Date and Time of Launch (UTC)	Location of Launch	CTD St. No.
8507	2903354	2018/07/25 07:17:00	47-0168 [N] 160-0392 [E]	K2

ii. Deep Argo Profiling float deployment

We also launched Deep float (Deep APEX) manufactured by Teledyne Webb Research. This float equips SBE61 CTD for deep sensor manufactured by Sea-Bird Electronics Inc. and RINKO ARO-FT dissolved oxygen sensor by JFE Advantech Co., Ltd.

The float drifts at a depth of 2000 dbar (called the parking depth) during drifting mode, then goes upward from a depth of 6000 dbar to the sea surface every 3 days (later change to 15 days). During the ascent, physical and biogeochemical values are measured at depths listed in depth table. When surfacing for approximately half an hour, the float sends all measured data to the land via through the Iridium telecommunication system. The observation by the float will be continuously conducted for about four years. The status of float and its launching information is shown in Table 3.4.2.

Table 3.4.2 Status of floats and their launches of DeepFloats

DeepFloat(Deep APEX)

Float Type	Deep APEX Teledyne Webb Research
CTD sensor	SBE61 manufactured by Sea-Bird Electronics Inc.
Oxygen sensor	RINKO AROD-FT manufactured by JFE Advantech Co., Ltd.
Cycle	10 days (approximately 30minutes at the sea surface)
Iridium transmit type	RUDICS Service
Target Parking Pressure	2000 dbar
Sampling layers	5dbar interval from 6000 dbar to surface (approximately 1200 layers)

Launches

Float S/N	WMOID	Date and Time of Launch (UTC)	Location of Launch	CTD St. No.
081	2903353	2018/07/25 07:11:00	47.0168 [N] 160.0398 [E]	K2

(4) Data archive

The Argo float data with real-time quality control are provided to meteorological organizations, research institutes, and universities via Global Data Assembly Center (GDAC: http://www.usgodae.org/argo/argo.html, http://www.coriolis.eu.org/) and Global Telecommunication System (GTS) within 24 hours following the procedure decided by Argo data management team. Delayed mode quality control is conducted for the float data within 6 months ~ 1 year, to satisfy their data accuracy for the use of research. Those quality controls of data are freely available via internet and utilized for not only research use but also weather forecasts and any other variable uses. Below figures show vertical profiles of launched BGC APEX (WMO ID: 2903354) and RINKO Deep APEX (WMO ID: 2903353) as samples.

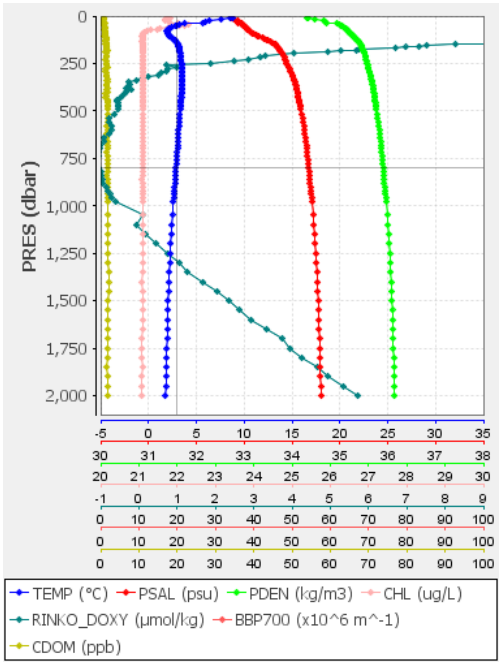

WMO ID: 2903354
DATE: 2018/07/26 22:10:02
POSITION: 47.074N, 160.038E

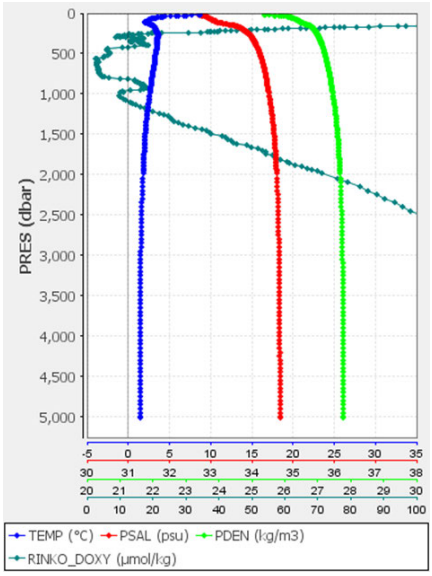

WMO ID: 2903353
DATE: 2018/07/29 0:27:49
POSITION: 47.211N, 159.993E

Fig. 3.4.1. Vertical profiles of first measurements on deployed BGC (upper panel) and deep (lower panel) Argo floats. (Upper) Blue, red, green, dark green, pink and yellow lines mean profiles of temperature, salinity, potential density, dissolved oxygen, backscatter and CDOM. (Lower) Blue, red, green and dark green lines show profiles of temperature, salinity, potential density and dissolved oxygen.

3.5 Satellite image acquisition (MCSST from NOAA/HPRT)

Tetsuichi FUJIKI (JAMSTEC RCGC)
Ryo OYAMA (NME)
Masanori MURAKAMI (NME)
Takehito HATTORI (MIRAI crew)

(1) Objectives

The objectives are to collect cloud data in a high spatial resolution mode from the Advance Very High-Resolution Radiometer (AVHRR) on the NOAA and MetOp polar orbiting satellites.

(2) Methods

We received the down link High Resolution Picture Transmission (HRPT) signal from satellites, which passed over the area around the R/V MIRAI. We processed the HRPT signal with the in-flight calibration and computed the brightness temperature (MCSST). A cloud image map around the R/V MIRAI was made from the data for each pass of satellites.

We received and processed polar orbiting satellites data throughout this cruise.

(3) Preliminary results

Fig.3.5.1 show the MCSST image in area of K2.

(4) Data archives

The raw data obtained during this cruise will be submitted to the Data Management Group (DMG) in JAMSTEC.

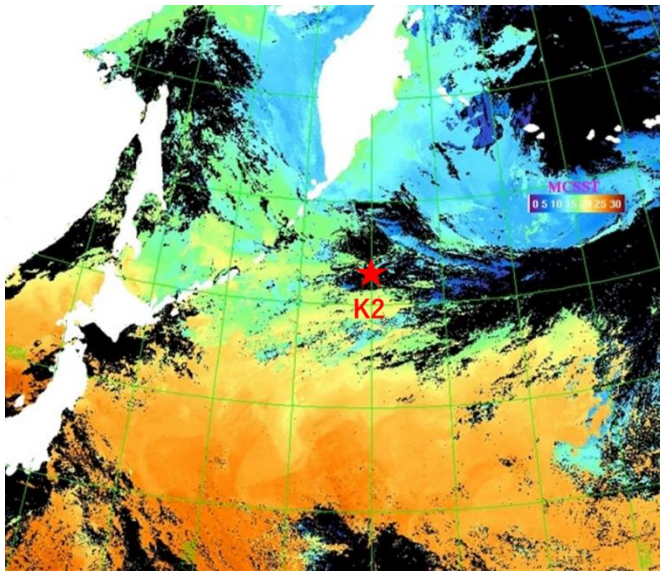

Figure 3.5.1. MCSST image in area of K2 (29th Jul.)